

University of Warwick institutional repository: <http://go.warwick.ac.uk/wrap>

A Thesis Submitted for the Degree of PhD at the University of Warwick

<http://go.warwick.ac.uk/wrap/34638>

This thesis is made available online and is protected by original copyright.

Please scroll down to view the document itself.

Please refer to the repository record for this item for information to help you to cite it. Our policy information is available from the repository home page.

A STUDY OF CARBOHYDRATE STATIONARY
PHASES FOR THE SEPARATION
OF ENANTIOMERS BY HIGH PERFORMANCE
LIQUID CHROMATOGRAPHY

by

ANDREW J. CRAWFORD

A thesis submitted in partial fulfilment of the
requirements for the degree of Doctor of Philosophy
at the University of Warwick

Department of Chemistry,
University of Warwick.

December, 1993



DECLARATION

The observations and recommendations described in this thesis are those of the author, except where acknowledgement has been made to results and ideas previously published. The work was undertaken at the Department of Chemistry, City University and Department of Chemistry, University of Warwick, between December 1st, 1989 and November 30st, 1992 and has not previously been submitted for a degree at any institution.

ABSTRACT

The relationship between the structure and chromatographic properties of silica is discussed and the preparation and properties of chemically-bonded stationary phases based on silica are reviewed. A detailed account is given of the history of the development of carbohydrate-based stationary phases, including microcrystalline cellulose, other polysaccharides and monosaccharides and their ester and carbamate derivatives, with emphasis on their utility for the chromatographic resolution of enantiomers. Mechanisms of chiral discrimination by these and other types of chiral HPLC phases are discussed in terms of the interactions between functionalities in the stationary phase and solute enantiomers. An overview is given of literature methods for the preparation of oligosaccharide derivatives with suitable reactive groups, such as an isothiocyanate function, for linkage to the surface of aminopropylated silica.

In the experimental part, the thesis describes work carried out to study the effects of stationary phase support properties on the chromatographic behaviour and enantiomer resolution capability of carbohydrate carbamate phases. These phases were prepared by the exhaustive reaction of free hydroxyl groups in carbohydrates, such as cellulose and amylose, with aryl isocyanates, such as phenyl isocyanate and 3,5-dimethylphenyl isocyanate. The resulting carbamates were characterised by ^1H nmr and microanalysis and were coated onto aminopropyl silica supports by evaporation from organic solvents. It was shown that the retention of solutes by these phases correlated directly with

the w/w phase loading, whilst both the separation factor and resolution for various enantiomers displayed a more complex relationship. The influence of changing pore diameter of the aminopropylated silica, with concomitant changes in pore volume and surface area, were evaluated for a series of materials at constant w/w phase loading. Whilst it is currently common practice to use very wide pore (up to 4000 Angstrom) silicas as supports for carbohydrate carbamate phases, it was concluded from the present work that there is little or no justification for using such supports and that good chromatographic performance and effective chiral discrimination can be achieved on much smaller pore (e.g. 500 Angstrom), higher surface area materials.

Carbamate derivatives of cellulose were prepared using phenyl, 3,5-dimethylphenyl and 1-naphthyl isocyanates and of amylose using the first two of these reagents and were shown to have close to the theoretical maximum levels of substitution. Their chiral discriminating abilities were investigated using a test panel of five racemic analytes: trans-stilbene oxide, 2,2,2-trifluoro-1-(9'-anthryl)-ethanol, 1-phenylethanol, benzoin and trogers base. The naphthyl carbamate phase showed no resolving ability for any of these racemates and this appeared to correlate with the presence of N-H bands in the ir spectrum which were indicative of severe disruption of the organised, H-bonded 3-dimensional structure necessary for chiral discrimination. The other four carbamate phases all showed resolving ability, each with its own specific pattern of solute selectivity. The difference in behaviour of the corresponding, identically substituted cellulose and amylose phases, differing only in the configuration of the C-O linkage at the

anomeric carbon on each glucose ring, illustrates the importance of long-range stereochemical properties: chiral discrimination must result not only from local interactions with individual carbamate groups and the adjacent chiral centres on the glucose rings, but also from the influence of the organisation of the polymer chains at the macromolecular level, leading to the creation of "chiral ravines" which display an intrinsic shape selectivity.

A series of malto-oligosaccharides with from 2 to 9 glucose units was obtained, the higher members of the series being separated from a commercially available oligosaccharide mixture by preparative HPLC on an aminopropyl silica column. Each oligosaccharide, and also the phenyl carbamate and 3,5-dimethylphenyl carbamate derivatives prepared from glucose, maltose and maltotriose, were characterised by FAB-MS and LSIMS and the fragmentation patterns of the carbamates were analysed in detail and shown to provide considerable structural information. The glucose penta(phenylcarbamate) was converted into the 1-isothiocyanato-tetra(phenylcarbamate) by successive reactions with HBr and a thiocyanate salt. After spectroscopic characterisation to confirm its structure, it was reacted with aminopropyl silica and the conditions for achieving optimum surface coverage established. Use of a longer spacer chain was also investigated, but did not appear to offer advantages over aminopropyl silica. A model reaction with n-propylamine gave the expected N-n-propyl urea. The silica-bonded glucosyl carbamate phase was examined chromatographically using a test panel of racemic solutes and was found to give some resolution of

certain racemates, but only when very low concentrations of polar modifier (isopropanol) were present in the hexane mobile phase.

Some work was carried out to try to extend the above chemistry to enable carbamate derivatives of the malto-oligosaccharides to be linked to silica through the anomeric position of the first glucose ring. A satisfactory procedure has not yet been established, major experimental difficulties encountered being solubility problems with the higher homologues and a lack of reproducibility in the introduction of the anomeric bromine and its displacement by isothiocyanate. Once these problems have been overcome, the methodology developed should provide a novel series of immobilised oligosaccharide carbamates with potential utility for the resolution of enantiomers.

ACKNOWLEDGEMENTS

I would like to express my profound gratitude to my supervisor, Professor S. A. Matlin, who gave me the opportunity to carry out this research. His keenness, dedication, encouragement and positive thinking helped me throughout this work.

In addition, I would like to thank the S.E.R.C. and Rhone Poulenc Rorer for assisting in the financing my research and to Dr. B. Mackenzie from Rhone Poulenc Rorer for his useful suggestions and discussions.

Thanks are also due to Mr. J. Hastings for running the nmr spectra, Mr. I. Katyal at the University of Warwick and V. G. Analytical, Manchester, U.K. for running mass spectra of my compounds.

Finally, I would like to thank Jacqueline McRae for her considerable assistance with the compilation of this thesis.

CONTENTS

	Page
CHAPTER 1: Introduction	
1.1 Brief History of Modern Liquid Chromatography	1
1.1.2 The Modern Liquid Chromatograph	6
1.2 The Silica Support	11
1.2.1 Physical Properties of Silica Gel	11
1.2.2 Preparation of Silica Gel	16
1.2.3 Chemically Bonded Stationary Phases	17
1.2.4 The Liquid Chromatography Column	26
1.3 Chiral Separations by HPLC	31
1.3.1 Introduction	31
1.3.2 History of Cellulose in Chromatography	34
1.3.3 Mechanisms in Chiral Recognition	45
1.3.4 Categories of HPLC Chiral Phases	53
1.4 Carbohydrates	70
1.4.1 Classification of Carbohydrates	70
1.4.2 Oligosaccharides	71
1.4.3 Polysaccharides	73
1.4.4 Reactions of Sugars	78
 CHAPTER 2: Optimisation of the Support for Coated Chiral Stationary Phases in HPLC	
2.1 Influence of the Chiral stationary Phase Loading	88

2.2	Effect of Pore Size on the Chromatographic Behaviour of Chiral Phases	98
2.2.1	Aminopropylation of Silica	100
2.2.2	Variation of the Chromatographic Properties with Pore Size	107
CHAPTER 3: Preparation of CSP's and investigation of their Chiral Recognition Properties		
3.1	Preparation of CSP's	114
3.1.1	Aminopropyl Silica Coating Procedure	119
3.1.2	Phase Packing Procedure	120
3.2	Chiral Recognition by Polysaccharide Carbamate Phases	121
CHAPTER 4: Mass Spectral Analysis of Carbamated Sugars		
4.1	Introduction to the Separation and Mass Spectral Analysis of Sugars	136
4.1.1	Separation of Sugars by HPLC	136
4.1.2	Studies of Underivatised and Derivatised Sugars by Mass Spectrometry	137
4.2	Generation and Purification of Oligosaccharides	145
4.2.1	Oligosaccharides of Cellulose	145
4.2.2	Oligosaccharides of Amylose	145
4.3	Results of the Mass Spectral Analysis of	

Oligosaccharides	147
4.3.1 Mass Spectral Analysis of Underivatised Sugars Separated by Preparative HPLC	147
4.3.2 Analysis of Derivatised Oligosaccharides	149

CHAPTER 5: Preparation of Monosaccharide and Diasaccharide CSP's

5.1 Cellobiose Octa(phenylcarbamate) Coated onto APS Silica (500Å)	165
5.2 Preparation of Chemically Bonded Carbohydrate CSP's	167
5.2.1 Route of Synthesis	169
5.3 Performance of APS Silica reacted with 1-Isothiocyanato-2,3,4,6-Tetra(phenylcarbamate)- glucopyranose	190
5.4 Linkage of Other Carbohydrate Derivatives to APS Silica	194
5.4.1 Attempted Linkage of the Malto-Tris (arylcarbamates)	194

CHAPTER 6: Experimental

6.1 Preparation of Polysaccharide Derivatives	202
6.2 Preparation of CSP's with CSP Loadings of 5%, 10% and 20% (wt% of Silica)	201
6.3 Column Packing Procedure	202

6.4	Modification of the Silica Surface	203
6.5	Evaluation of the CSP Phases by HPLC	205
6.6	Determination of HETP for an Inert Peak for Column Loadings of 5%, 10% and 20% (wt% of Silica)	206
6.7	Preparation of Bonded Phase Chiral HPLC Columns	207
6.8	Preparation of Mono, Di and Trisaccharide Aryl Carbamates	213
6.9	Generation of Cello and Malto-Oligosaccharides	218
	Appendix	224
	References	225

CHAPTER 1

INTRODUCTION

The history of chromatography is one of periodic advances that has followed some major innovations: partition and paper chromatography in the 1940's; gas and thin layer chromatography in the 1950's; and the various gel or size exclusion methods in the early 1960's. A few years later the practice of chromatography was revolutionised by a technique called "modern liquid chromatography" which offered improvements over traditional column chromatography in equipment, materials, techniques and in terms of results, advantages in convenience, accuracy and speed. Undoubtedly the technique had a large impact in chemical analysis and is a major method for separation, quantitation, and identification of chemical substances. Today, the development of new types of stationary phases for modern liquid chromatography is continuously and rapidly growing to improve separation and selectivity. In the search for stereoselective analytical techniques chiral stationary phases have attracted particular attention for their ability to resolve enantiomer mixtures.

1.1 BRIEF HISTORY OF MODERN LIQUID CHROMATOGRAPHY.

The invention of chromatography is generally ascribed to Tswett¹ who in 1903 showed how compounds could be separated by

elution through a bed of absorbent . Tswett recognised that separation arose because of the different affinities of a substance for the absorbent with which the column was packed, and developed the technique we know today as column adsorption chromatography.

However, for twenty years Tswett's method remained obscure and was used only by a few botanists and biochemists for the investigation of leaf pigments, and then was brought back from oblivion by Kuhn² in 1931. Kuhn and Lederer separated xanthophyll and zeoxanthin adopting Tswett's method, using a column packed with calcium carbonate. This work was soon followed by other publications from Kuhn's group and the technique was soon picked up by many other laboratories, thereby starting the rebirth of liquid column chromatography.

Until the early 1940's, chromatography remained an art based on a body of empirical observations. Today chromatography rests on a sound theoretical basis through the quantitative treatment of chromatographic peaks by Martin and Synge³. Four aspects of major importance were presented in their paper. Firstly, a theoretical treatment of the processes involved in a separation was proposed. This was based upon the operating parameters of the column and expressed the efficiency of the separations achieved in terms of the theoretical plate (height equivalent to a theoretical plate, HETP), by analogy with distillation theory. This was a major advance and enabled a quantitative description of separating processes to be made. Secondly, the paper described the new method of performing separations by partition

chromatography (liquid-liquid). The realisation that by immobilising one liquid on a suitable matrix, a separation could be effected by passing the second liquid over the first constituted a major advance. This paper also indicated two further lines of development: firstly, the moving phase could be replaced by a gas; secondly, the smallest HETP should be attainable by using a very small particle size and a high pressure difference across the length of the column.

The complexity of the chromatographic process which deterred early attempts to treat it theoretically is rooted in the interplay of thermodynamic (equilibrium), mass transfer and kinetic (sorption) phenomena. The earliest theories were based on Wilson's (1940) assumptions that there is complete equilibration of the solute between the mobile and stationary phases, consequently reflecting dynamic effects. In 1943 De Vault ⁴ was the first to express concentration profiles for linear and non-linear isotherms at constant flow rate. His rigorous treatment led to the fundamental Equation (1),

$$V_r = V_m + V_s K \quad (1)$$

which established the relationship between retention volume V_r , the equilibrium constant K , and volumes of the mobile and stationary phases V_m and V_s respectively. The relationship between the retention in chromatography and the thermodynamic equilibrium constant which could be related to the molecular structure of the sample components was of great importance in facilitating their identification and received great attention in the

early 1950s. The major contributors in this area were Martin⁵ in 1949, James and Martin⁶ in 1954, Le Rosen⁷ in 1951 and Pierotti⁸, also in 1951.

However, the equilibrium theory was far from being representative of the events in the chromatographic column and was inadequate to account for band spreading. The first rigorous theory to account for mass transfer and longitudinal diffusion in linear chromatography was put forward by Lapidus and Amundson⁹. Their paper, however, was too exacting to be directly useful in chromatography.

It was through the introduction of gas chromatography by James and Martin¹⁰ that chromatographic theories developed. The rapid growth in this technique and the ease of obtaining quantitative results provided a strong stimulus for theoretical work. In 1956 van Deemter et al¹¹ put forward their rate theory, simplifying the formula of Lapidus to a Gaussian distribution function, thus expressing HETP as a function of the flow velocity and the most significant characteristics of the chromatographic system, such as particle diameter and solute diffusivity. Since then the popular "van Deemter plot" has greatly facilitated the optimisation of chromatographic conditions.

Practical experience with gas chromatography coupled with the theoretical ideas established by Martin and Synge³, and elaborated by Giddings¹², showed that there would be no insuperable difficulties in developing systems for liquid chromatography which would possess the advanced features of

gas chromatography. In the ideal high performance liquid chromatography (HPLC) system, eluent would be pumped into the column under high pressure and at a precisely controlled rate; injection of sample into the column would be either by injection valve or by a syringe/septum arrangement, the sample size would be small to optimise resolution; the column itself would be long and narrow and packed with a carefully prepared and well sized material composed of particles at least ten times smaller than those conventionally used in gas chromatography; finally the emerging solution would be passed to a post-column detector which would monitor the concentration of solutes and produce an electrical signal suitable for recording.

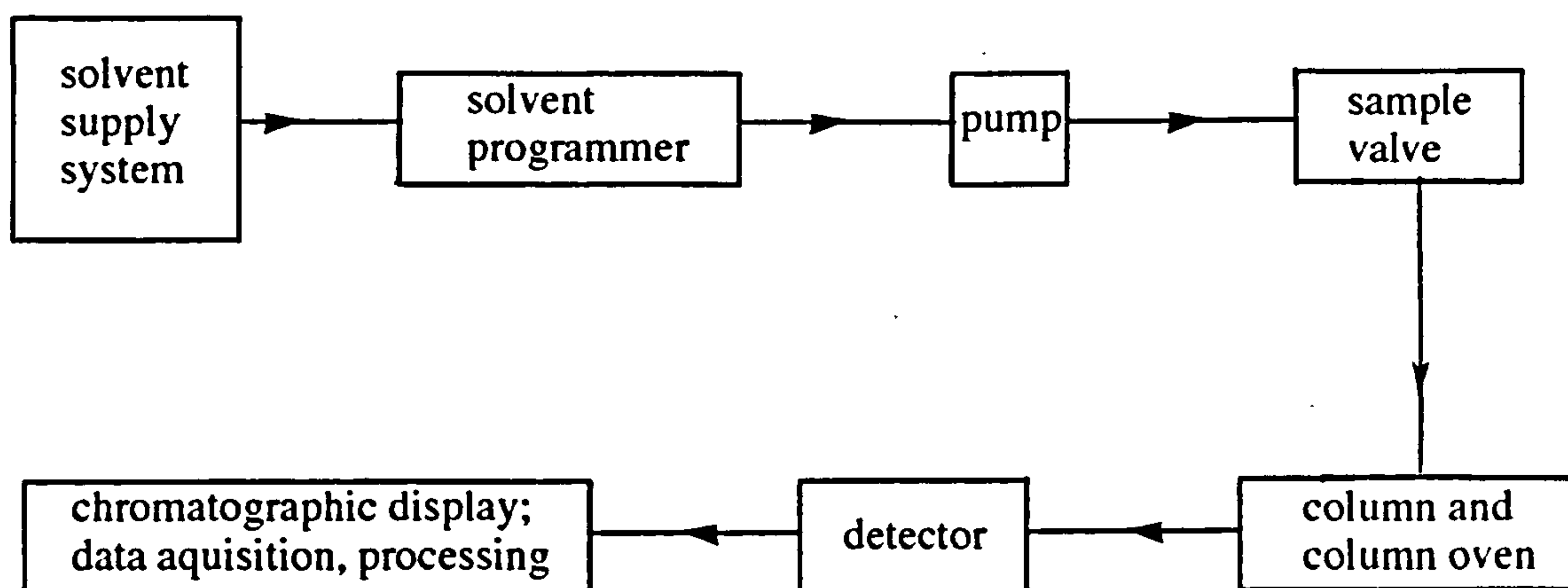
Since the birth of HPLC in 1969, tremendous activity has been aimed at the development of better equipment and columns, and further improvements in the understanding of modern liquid chromatography. In particular, the great potential of small-particle reverse-phase liquid chromatography has been exploited and augmented with gradient elution and by the advent of spectrophotometric detectors operating down to 190nm, making possible the sensitive detection of almost any compound type. Increased use of fluorescence and electrochemical detectors plus off line and on line derivatisation has further pushed detection problems into the background, even for trace analysis.

The development of modern liquid chromatography has provided the analyst with a technique for use where gas liquid chromatography cannot be readily applied: for example, the analysis of thermally unstable, non-volatile or very polar

compounds. It also has the advantage that in liquid chromatography two factors can be changed, the mobile phase and the stationary phase, making the technique more selective and highly specific.

1.1.2 The Modern Liquid Chromatograph

The modern liquid chromatograph is shown in the block diagram in Scheme 1. It consists of 7 major components: solvent supply system; solvent programmer; pump; sample introduction valve; column and optional column oven; detector; data acquisition, processing and display system.



Scheme 1 Modern liquid chromatograph

1.1.2.1 The Solvent Supply System

The solvent supply system consists of a series of solvent reservoirs, usually up to 4 in number, from which one or more

solvents can be selected. They are constructed from glass, have a capacity of at least one litre and sometimes have a de-gassing facility such as a helium gas supply. De-gassing is essential as dissolved air adversely affects the column performance and causes serious detector noise. Off-line degassing of solvents prior to use can be accomplished by ultrasonics, vacuum treatment, micropore filtration or purging with an inert gas.

1.1.2.2 The Solvent Programmer

This is not an essential feature in the arrangement for an isocratic HPLC system if the mobile phase conditions for analysis are previously known. However, it is a very useful time saving feature in optimisation of the mobile phase. The solvent programmer has two functions. Firstly, to select a particular mixture of solvents to be used to develop a separation isocratically and secondly, to arrange the composition of the mobile phase to change regularly, in a pre-defined manner, during the development of the separation of complex mixtures by gradient elution. Thus, most programmers are designed to programme a two- or three-solvent mobile phase over a varying composition ratio.

1.1.2.3 The Solvent Pump

Solvent pumps are usually piston operated and most contain two cylinders, operating alternately in parallel to reduce pressure pulses that can cause detector noise. The parts in contact with the

solvent are made of stainless steel except for non-return valves, seals and gaskets which are made of sapphire or PTFE.

1.1.2.4 Sample Introduction Valves

The sample is introduced reproducibly into a pressurised column via a valve which has either an internal or external loop, filled by a syringe. The loops have a known volume varying from 0.5 μ l to 20 μ l for most analytical purposes. By valve switching, the sample in the loop is displaced by the flow of mobile phase onto the column, with minimal dilution. For most purposes the valve loop is made of stainless steel and best operated at a maximum pressure of 3000 psi to ensure a reasonably long life.

1.1.2.5 The Column and Column Oven

Stainless steel tubing has generally been used to construct high performance liquid chromatography columns in order to withstand high pressure. The tubing must have a smooth precision bore internal diameter, to ensure that a well packed column will not channel near the wall/packing interface because of wall irregularities. This would result in broader peaks and lower efficiency. Connections to the column are made via low dead volume fittings designed to eliminate stagnant pockets of mobile phase. Columns with an internal diameter of 5mm provide a good compromise between sample capacity, the amount of packing used and solvent required, and column efficiency¹³. The column oven thermostats the column to ensure stability and helps dissipate heat generated in the column. The retention time is

linearly related to the distribution coefficient which, in turn, will depend on the operating temperature.

1.1.2.6 Detectors

Ideally, an LC detector must respond to solute concentrations over the range of about 10^{-9} to 10^{-5} g/ml and have a linear response to concentration over at least three orders of magnitude. Unfortunately, there is, at present, no universal detector for HPLC that possesses all the necessary attributes that are required for a completely versatile liquid chromatograph. Therefore, it is necessary to select a detector on the basis of the problem at hand.

Detectors for HPLC can be placed into two categories. Firstly, bulk property detectors, typified by the refractive index (RI) monitor, respond to an overall change in the physical property of the mobile phase due to an eluting solute. Although universal, this type of detector is rather insensitive, having a linear dynamic range from about 5×10^{-7} to 2×10^{-4} g/ml. As RI is very sensitive to temperature changes, the detector should be thermostated. It is also sensitive to mobile phase composition and changes in pressure and flow rate, so is consequently not suitable for use with gradient elution. Despite its disadvantages, RI is frequently used for detecting those solutes that do not absorb in the UV and do not fluoresce. The second class of detectors, the solute property detectors, respond to a physical property of the solute which is not exhibited by the pure mobile phase. Solute property detection is roughly 1000 times more sensitive, giving a detectable signal for a few nanograms of sample.

Ultraviolet/visible absorption, fluorescence and electrochemical detectors have achieved popularity in this category. Pre-column and post-column derivatisation extend their applicability.

The fixed wavelength UV detector, normally operating at 254nm or 280nm (emitted from a mercury lamp) is one of the most widely used detectors for HPLC. The advantages of this detector are its relatively low cost, high sensitivity (nanogram levels) and linearity of response of over 3 orders of magnitude extending from about 3×10^{-8} to 1×10^{-5} g/ml (this will vary somewhat with the extinction coefficient of the solute). If designed correctly it is relatively insensitive to changes in temperature, pressure and flow, and thus can be used with gradient elution. Compounds absorbing ultraviolet radiation include all substances having one or more double bonds and substances having unshared non-bonded electrons. As not all solutes absorb their maximum energy at 254nm, a variable wavelength detector (deuterium lamp source) can be employed which emits energy from 180nm to about 400nm and can take two forms, the dispersive and the diode array detector. The dispersive detector contains a monochromator prior to the detector cell by which the wavelength required is selected. The diode array detector has a diffraction grating subsequent to the cell and disperses the transmitted light across a diode array, the outputs from which are stored in a computer memory bank. Thus, the contents of the detector cell are monitored simultaneously over a wide range of wavelengths and for any retention time the spectrum can be printed out.

1.1.2.7 Data Acquisition, Processing and Display

The results obtained from a chromatographic separation, as depicted by the output from the detector, can be displayed at many levels of sophistication. A simple and widely used way of displaying a chromatogram is on a potentiometric recorder. For quantitative analysis, heights of peaks should be measured and retention distances for peak identification. Many modern chromatographs have A/D converters and the chromatogram is digitised and stored on disc by computer. Using a computer program, retention times, peak heights and areas can be obtained and if previously calibrated, complete quantitative analysis can be performed.

1.2 THE SILICA SUPPORT.

1.2.1 Physical Properties of Silica Gel

The majority of stationary phases employed in LC are based on silica gel. It is not only used on its own as a stationary phase, but also employed as the matrix from which "bonded phases" are made. Silica gel has some unique properties that make it particularly useful in chromatography and these properties arise from the way it is produced.

1.2.1.1 Porosity

The porosity in silica, and in other inorganic oxides, can be fixed either in the course of their formation or by an after-treatment^{14,15}. The pore system is characterised by the width

and size of the pores and their shapes and distribution, all of which can be controlled by the type of chemical reaction and experimental conditions.

1.2.1.1.1 The Mean Pore Diameter D

D may cover a range of several orders of magnitude. Following the recommendation by Dubinin¹⁶, pore sizes are classified as micropores when the pore width is less than 2nm, whilst those exceeding 50nm are termed macropores and those in the intermediate size range ($2 < D < 50\text{nm}$), mesopores. D is expressed as the mean value of a distribution of pore sizes (PSD). When PSD is homogeneous, this resembles a gaussian distribution (see Figure 1a) with its standard deviation being the measure of the width of dispersion. In most instances, heterogeneous distributions are obtained, the simplest being the bimodal, exhibiting two distinct pore maxima (see Figure 1b)

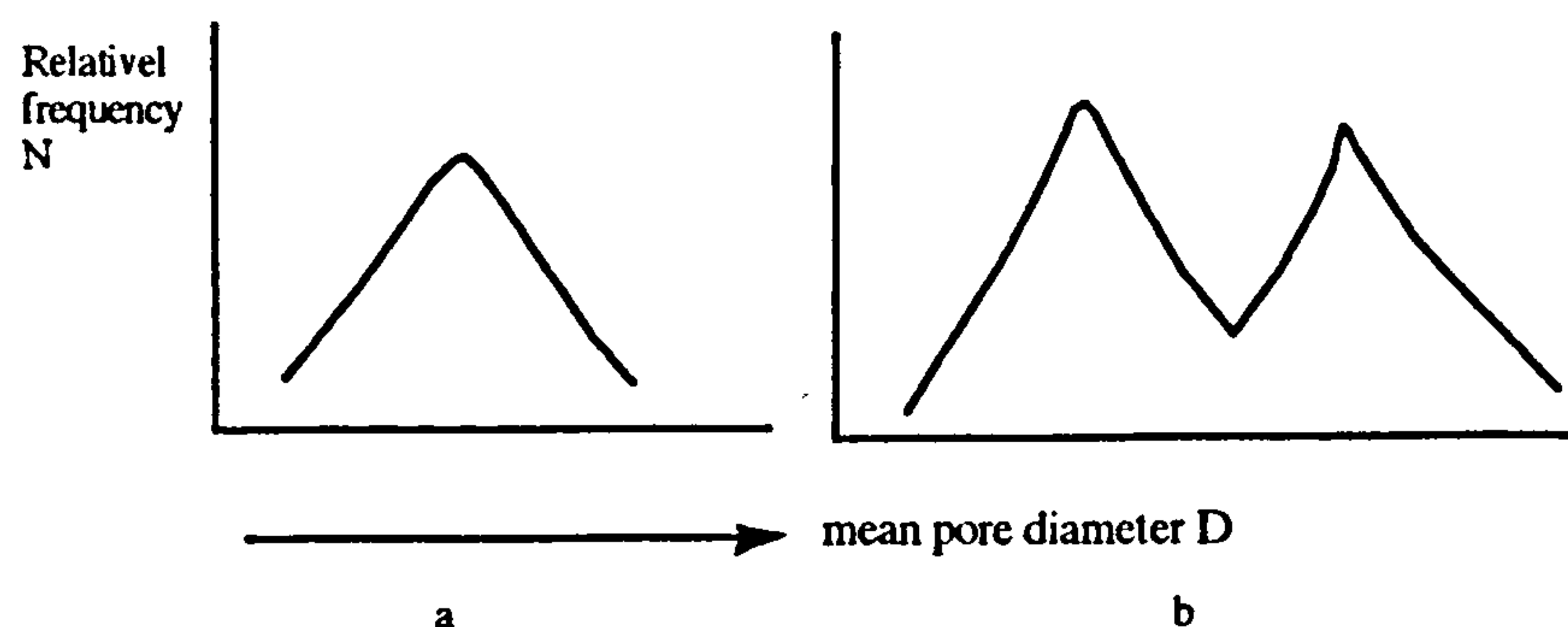


Figure 1 Types of Pore Size Distribution a) homogeneous b) bimodal

As every pore represents a distinct geometric shape, its shape has to be taken into consideration. Because of irregularities in most porous solids, the real shape is known in only a few instances and

models have been employed for approximation (see Figure 2). The most common is that of the cylindrical pores open at one or both ends (a). The ink bottle pores (b) are described by two diameters, the width of the narrow neck (D_n) and the width of the wide body (D_b). A third model is built up of parallel plates (c).

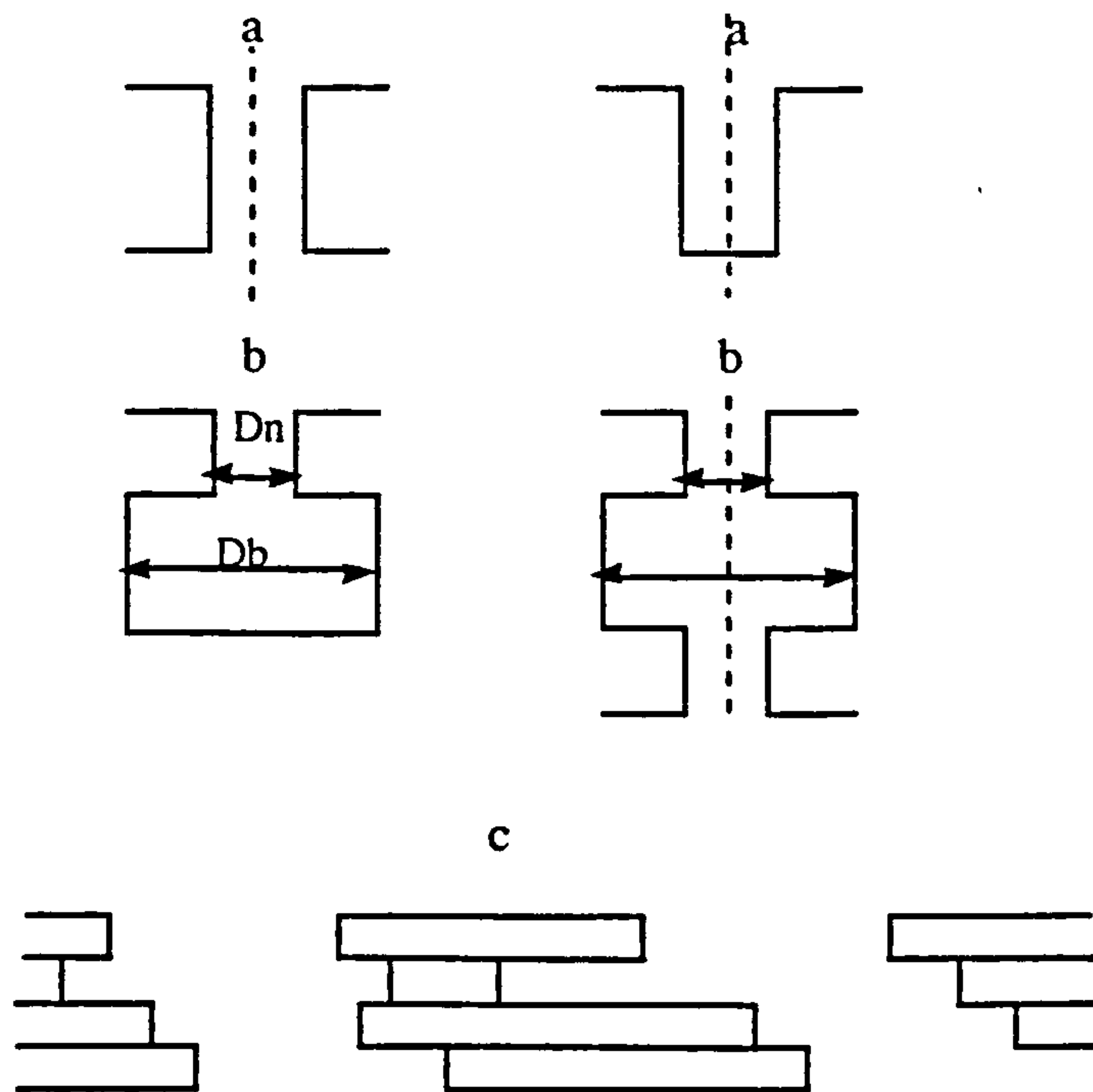


Figure 2 Pore Models; a) cylindrical pores, circular in cross section b) ink-bottle pores having a narrow neck and wide body, D_n = diameter of narrow neck, D_b = diameter of wide body c) slit shaped pores with parallel plates.

1.2.1.1.2 The Specific Surface Area S

The Specific Surface Area (S) of a porous solid is equal to the sum of its internal and external surface areas. The internal surface area originates from the pore walls, as by definition pores have to

be opened to the exterior of the particle. In the case of porous silica the internal surface area is several orders of magnitude larger than the exterior surface area.

1.2.1.1.3 The Specific Pore Volume V_p

V_p is the amount of liquid adsorbate that fills the total volume of pores per gram of adsorbate. The specific surface area and specific pore volume can be attributed to the volumes of micropores, mesopores and macropores. Once V_p is known, the particle porosity, ϵ_p , can be calculated by means of Equation 2, where V_s is the volume of pure solid (mg/g)

$$\epsilon_p\% = \frac{V_p}{V_p + V_s} \times 100 \quad (2)$$

1.2.1.2 Particle Characteristics

It has been shown by a theoretical treatment that column efficiency in liquid chromatography can be considerably improved by employing small particles¹⁷. As a result of a series of studies, 5-10 μm particles have been found to be optimal as packings with respect to column efficiency and practical use¹⁸⁻²¹.

1.2.1.2.1 Particle Size d_p and Shape

For spherical particles, the size can be readily calculated from their diameter d_p . However, many of the silica particles used in

an infinite number of linear dimensions, approximations are needed. One common approach is presented in Figure (3), which gives the projected area diameter d_p of a particle. This value corresponds to the diameter of a circle with the same area as that of the particle resting in a stable position. Other definitions are derived from particle sizing techniques using laser beam diffraction, electro-gradient displacement and sieving, which are useful techniques for establishing particle size changes for coated silica particles.

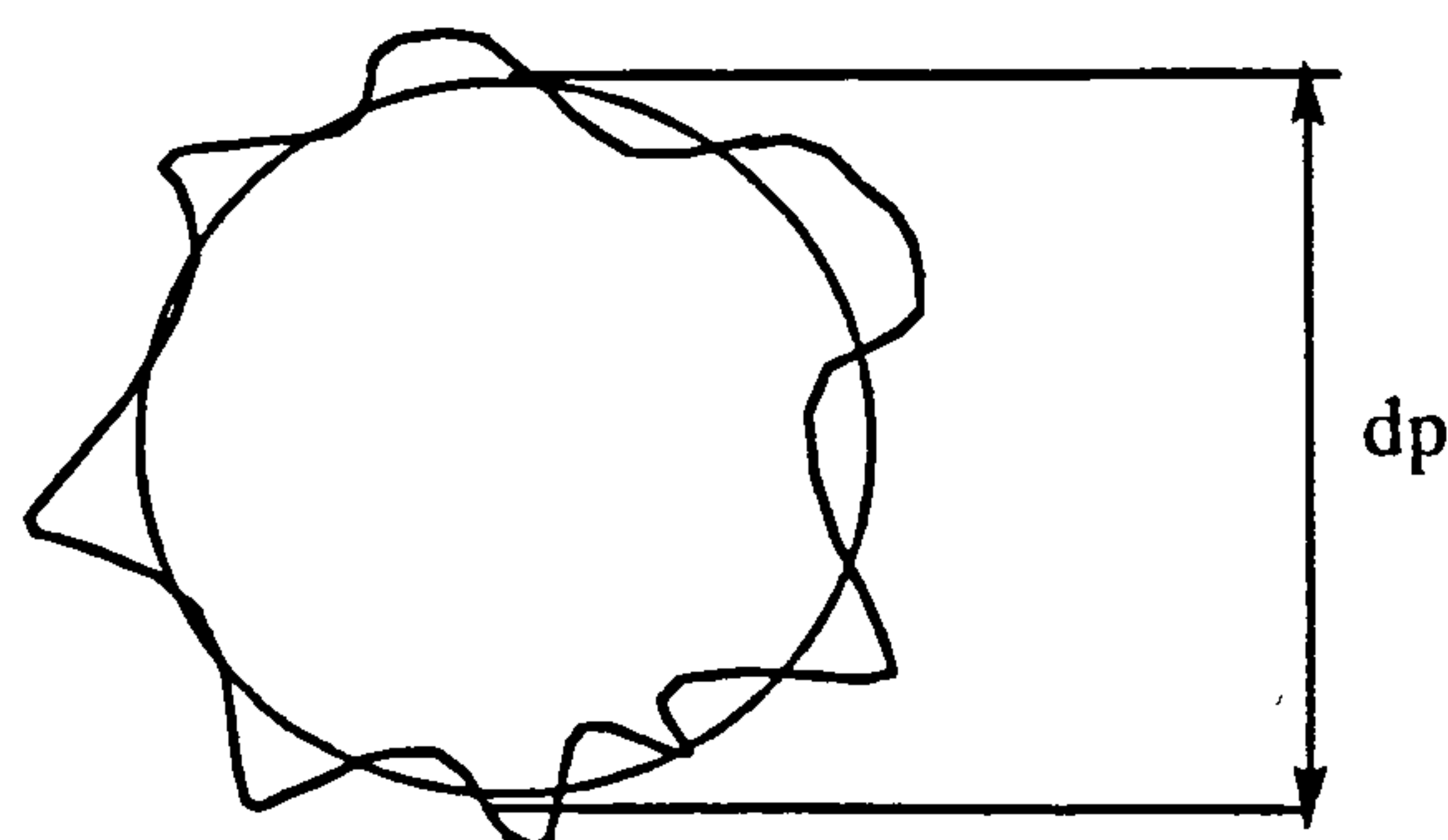


Figure 3 Estimation of the projected area diameter, d_p , of an irregularly shaped particle.

The particle shape influences the packing density of the column bed and the geometry of the interstitial voids between the particles. It is clear that spherical particles of equal size generate a more homogeneous and dense bed than irregular particles, thus giving rise to a more laminar flow profile. When considering coated silica particles for HPLC, one must consider that the surface of the silica particle will no longer be totally smooth and that

surface irregularities could arise from agglomeration processes during preparation of the phase.

1.2.2 Preparation of Silica Gel

Silica gel is made in large batches by adding hydrochloric acid to a solution of sodium metasilicate. Initially, silicic acid is released but quickly starts to condense with itself to form dimers, trimers and eventually polymeric silicic acid. The polymer continues to grow until, at a particular size, the solution begins to gel. As a result of this process, primary particles of silica gel are formed which may have diameters ranging from a few angstroms to many thousands of angstroms. The size of the primary particles depends upon the temperature and pH of the mixture at the time of gelling. It is the formation of these primary particles that confers onto silica gel its high porosity and high surface area, which are so important in its use as a stationary phase or support in LC. Furthermore, it is the condensation between primary particles that causes their adhesion and the onset of gel formation. After the gel has become solid, it is allowed to stand for a few days while condensation between the primary particles continues and the gel shrinks and excludes water. This process is called Sinerisis and the firm gel that is finally produced is called the hydrogel. The hydrogel is then heated for a few hours at 120°C and the resulting product is called the xerogel which, after grinding to an appropriate particle size is the material employed as the stationary phase or support for LC and is called irregular silica gel.

The physical properties of irregular silica gel are difficult to control during manufacture and therefore, appropriate material for LC is selected from the particular batch that provides the desired surface area and porosity. As the pore size is controlled by the primary particles during the gelling process, the pores of the silica gel can range from a few angstroms to many thousands of angstroms.

1.2.3 Chemically Bonded Stationary Phases

In the last 20 years, chemically bonded stationary phases have greatly augmented the versatility of chromatographic separations. Although they were first employed as stationary phases rather than column activity moderators in gas chromatography²² the explosive growth in the utilisation of bonded phases can be linked to the development of High Performance Liquid Chromatography.

The surface of hydrated silica is covered with hydroxyl groups that are attached to silicon atoms. The silica surface is modified by a heterogeneous chemical reaction which takes place at a solid/liquid interface to yield an immobile chemically bonded surface layer. The modification of the silica surface provides an attractive surface for the liquid stationary phases to be coated onto. However, the main advantages of chemically bonded phases are in the areas of column stability and longevity.

1.2.3.1 Bonded Phase Preparation

The first approach to the bonding of stationary phases is attributed to Halasz and Sebastian²³ who popularised such phases. They esterified silica gel with alcohol's which resulted in a "brush-type" or monomeric bonded phase in the form of Si-O-R, R being the bonded moiety. Such bonded phases however, are susceptible to hydrolysis; therefore in liquid chromatography, aqueous solvents could not be used as mobile phases. At present, most bonded phases are prepared by the reaction of organosilane compounds with silica gel, utilised successfully in the mid-60's by Abel and Nickless²⁴. A chloro or alkoxy silane is refluxed with silica gel in dry solvents. Bonded phases prepared from organosilanes are quite resistant to hydrolysis due to the formation of sterically hindered Si-O-Si-R bonds. Figure 4 schematically represents the reactions that take place between mono-, di- and tri-chloro or alkoxyorganosilanes and silica gel. Currently it is accepted²⁵ that the number of accessible hydroxyl groups on the silica surface is between 4 and 5 groups per nm². For steric reasons, only two of the three trichloro or trialkoxy groups can react with the surface silanol, as depicted in Figure 4.

The unreacted groups on the organosilane moiety can be easily hydrolysed to form hydroxyl groups that can react with further

excess reagents to form a polymeric coating. In liquid chromatography, such polymers can lead to deterioration of the efficiency due to stagnant pockets of trapped mobile phase. The free hydroxyl groups can also interfere with the chromatographic separation due to mixed retention mechanisms. To prepare reproducible bonded phases and prevent the formation of free hydroxyl groups on the organosilanes, several precautions should be taken. Firstly, the reaction should be performed in dry solvents, secondly, the water absorbed on the silica gel surface should be removed by heating to 150°C under vacuum for 16 hours and the dried silica then left to stand over saturated lithium chloride solution for 24 hours prior to reaction.

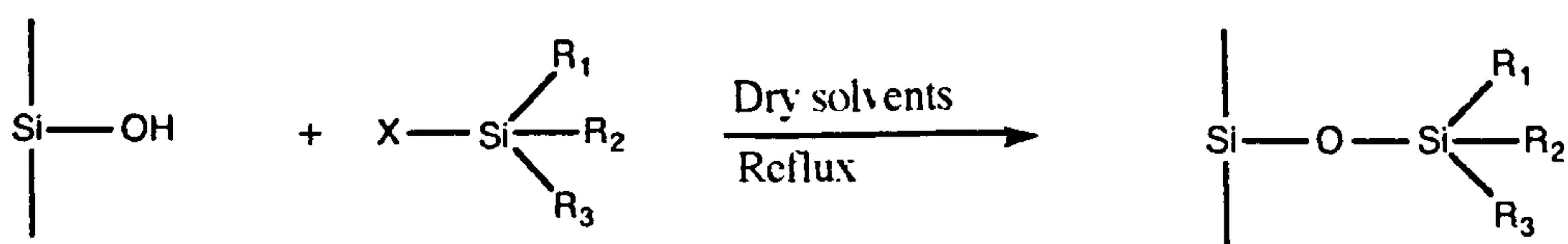
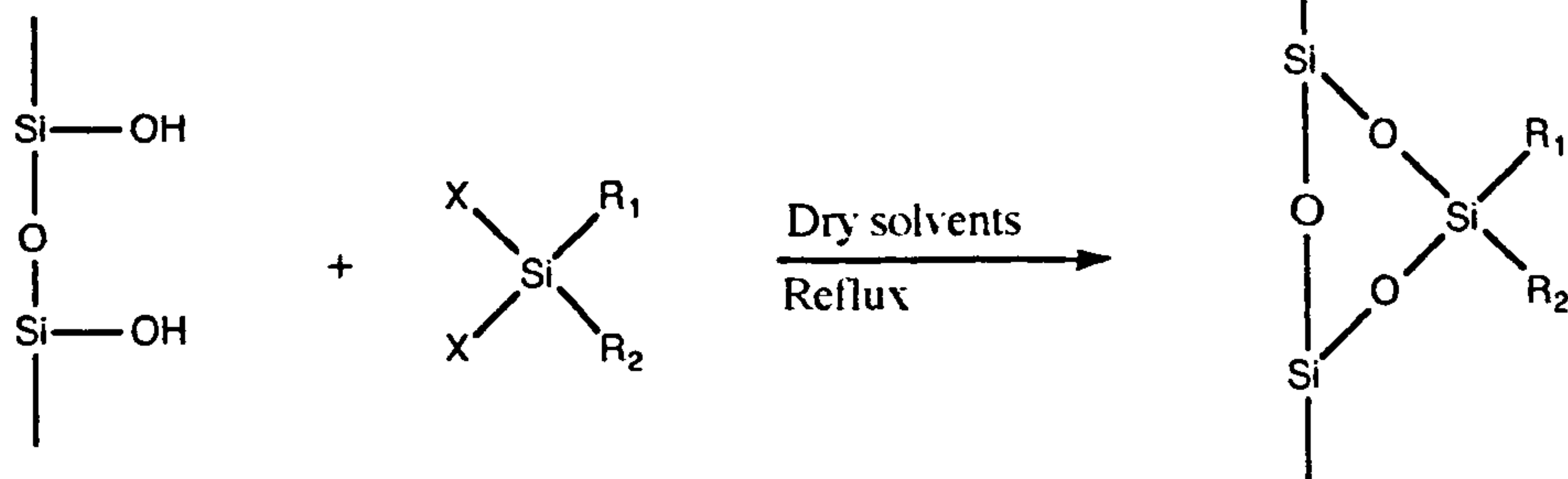
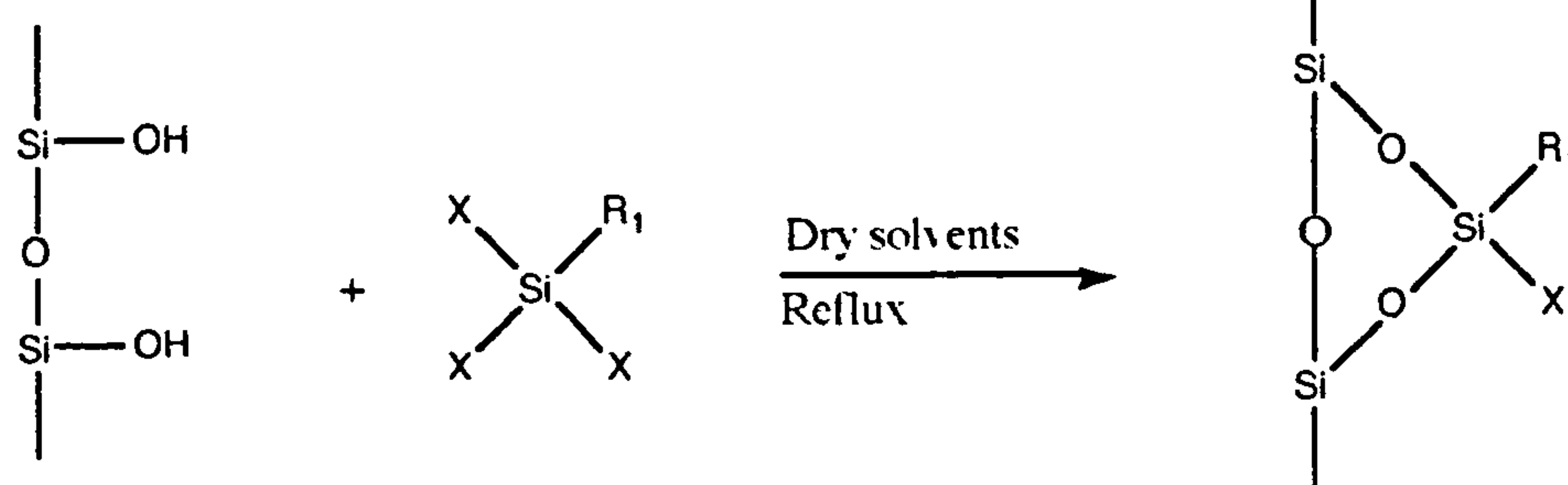
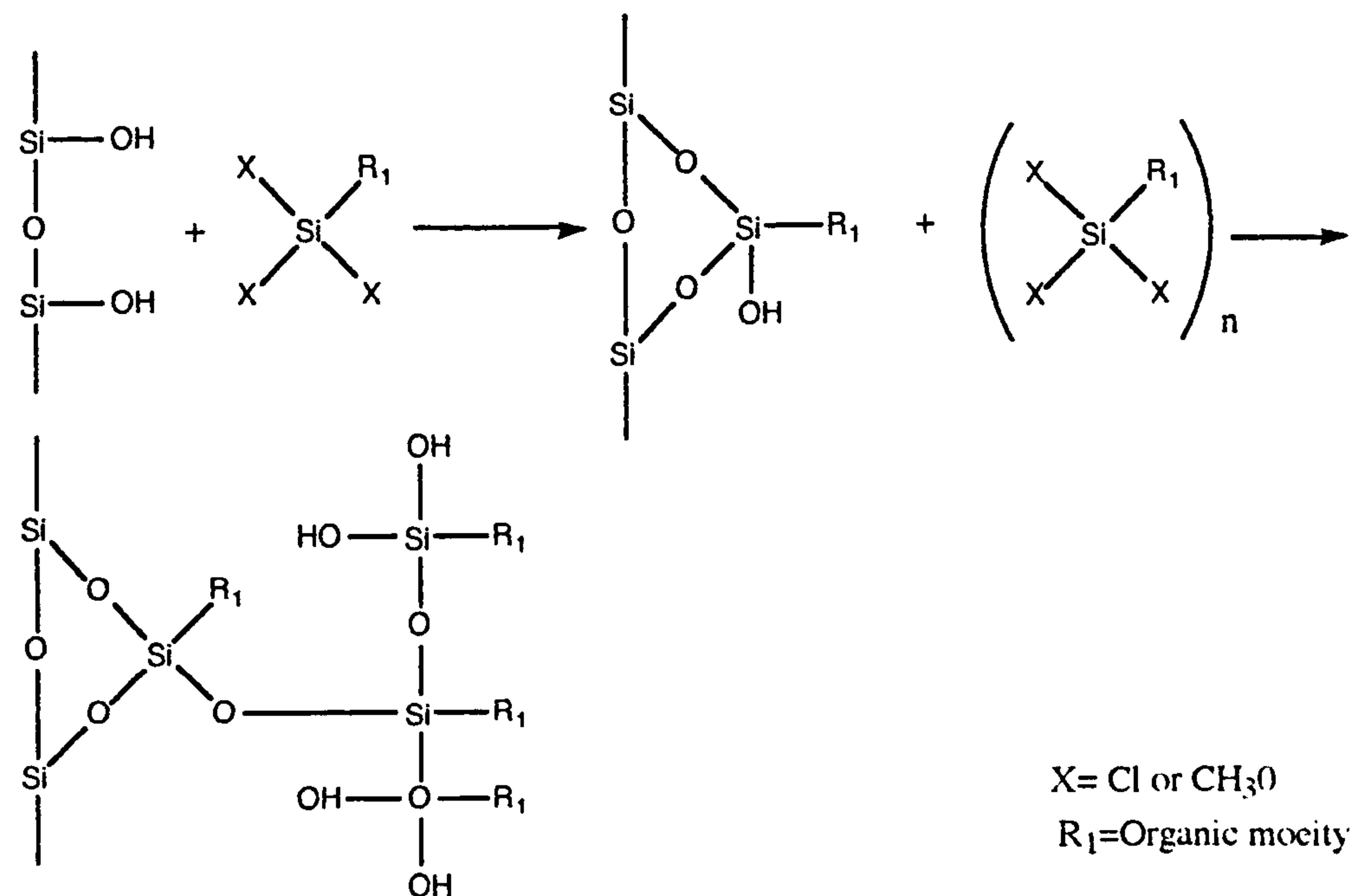
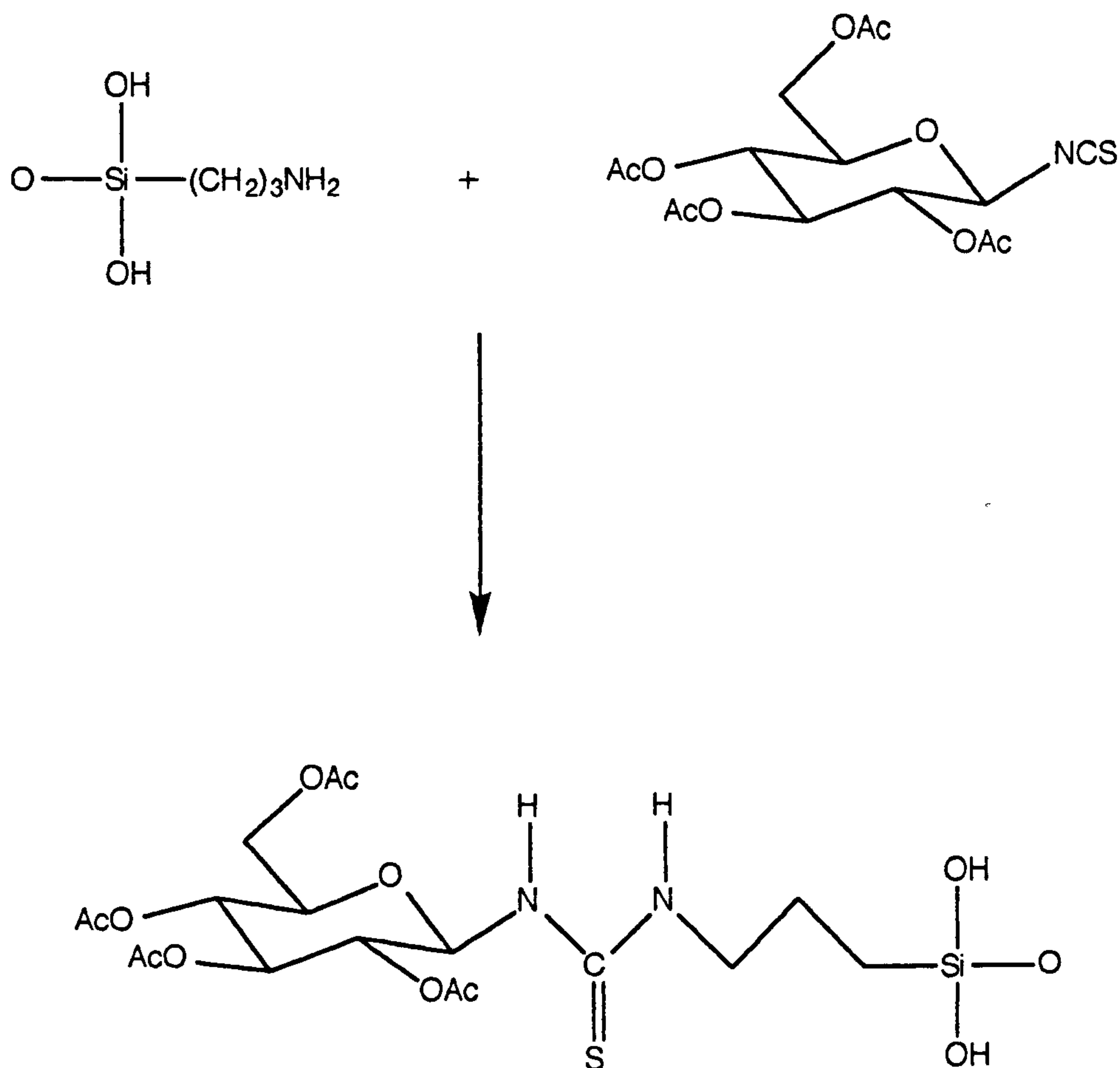
a) Monofunctionalb) Bifunctionalc) Trifunctional (in dry solvent)c) Trifunctional (solvent with protic impurities)

Figure 4 Diagram of the reaction of chloro or alkoxysilanes with silica gel

Jones²⁶ showed the optimum concentration of silica gel to organic modifier (aminopropyltriethoxysilane) was in the ratio of 2:1 and that the reaction proceeds as fruitfully by shaking the reaction mixture gently as by refluxing.

There are several other methods used to bond the stationary phase to the silica surface. For example, Locke et al²⁷ reported the use of Grignard reagents to attach the stationary phase to the solid supports. Gilpin and co-workers²⁸ reported an in situ bonding procedure. However most commercially available bonded phases are prepared with either bi or tri-functional silanes and include amine $(\text{CH}_2)_n\text{NH}_2$; nitrile $(\text{CH}_2)_n\text{CN}$ and phenyl $(\text{CH}_2)_n\text{C}_6\text{H}_5$. The most popular covalently bonded phases are the reverse phases which contain "brush-type" paraffin chains having 4, 8 or 18 carbon atoms attached. These types have been termed C-4; C-8 and C-18 respectively.

Hence, using the appropriate organic chlorosilanes or alkoxy silanes, non-polar or polar groups such as octadecyl chains, amines or aromatic rings can be bonded to silica to provide stationary phases covering a wide range of polarities. The amino function has been shown to be a useful, stable intermediate for preparation of bonded phases that possess a different functionality than the reverse phase type. König²⁹ synthesised chiral supports by coupling the isothiocyanate derivatives of peracetylated D-glucose to aminopropyl silica gel (see Scheme 2)



Scheme 2 Coupling of peracetylated D-glucose to aminopropylated silica gel

A distinct advantage of this strategy involving the reaction of a surface amino group and an isothiocyanate group is that it is possible to fully characterise the reactant prior to bonding.

1.2.3.2 Calculation of Surface Coverage

The amount of the stationary phase bonded to the support is an important parameter frequently used to assess the extent of the reaction between the silica support and the organic chloro or alkoxy silanes. This quantity can be reported in several ways:

a) From the results of elemental analysis, the weight/weight per cent of carbon in the solid is reported. If N and Cl etc are part of the bonded phase, their weight/weight should also be given. Typical values for per cent carbon on silica gel having a surface area of $300\text{-}350\text{m}^2/\text{g}$ is about 3-4% for a methyl silane and about 20% for octadecyl silane. Reporting only the total per cent carbon content is not a satisfactory procedure for characterising the bonded phase as it gives incomplete information.

b) By use of the elemental analysis results, the surface coverage can be reported in terms of weight of bonded phase per unit surface area of support. Along the same lines, Unger *et al*³⁰ recommended that surface coverage should be reported in terms of the moles of bonded phase for specific surface area. This approach has advantages for comparing products of different surface concentrations, irrespective of their origins and their specific surface areas.

The surface concentration is generally cited as $\mu\text{mole m}^{-2}$, and when calculating its value from the elemental analysis figures, one should correct for the weight increase of the support due to modification, to avoid an erroneous result^{31,32}. The following expression (Equation 3) was given by Berendsen *et al*³³ and Hemetsberger³⁴ for calculating the alkylsilane density from carbon content data.

$$N_M = \frac{10^6 \times \%C}{S[(100 \times n \times 12) - (\%C \times Mw)]} = \mu\text{moles m}^{-2} \quad (3)$$

where S is the surface area, S_{BET} m^2g^{-1} of bare silica (where S_{BET} refers to the method devised by Brunauer, Emmett and Teller for surface area determination.); $\%C$ is the carbon percentage as determined by elemental analysis ; n is the number of carbon atoms in the modified chain and Mw is the relative molecular mass of the organic moiety of the bonded organosilane, in the use of APS silica corresponding to $\text{CH}_2\text{CH}_2\text{CH}_2\text{NH}_2 = 58$.

Typical values³⁵ for straight chain alkanes bonded to silica gels vary between $2\text{-}4\mu\text{moles m}^{-2}$ with the surface hydroxyl concentration of about $8\mu\text{ moles m}^{-2}$.

c) The surface coverage can also be reported in terms of the number of organic groups per square nanometer³³, Equation 4.

$$N_G = \frac{6.023 \times 10^5 \times \%C}{S[(100 \times n \times 12) - (\%C \times Mw)]} = \text{organic groups nm}^{-2} \quad (4)$$

where $\%C$, n , Mw and S are as in Equation (3).

Assuming³⁶ there are 4.8 surface hydroxyl groups per 100 \AA^2 (or 1nm^2) available for reaction, the determined number of organic groups N_G present indicates the degree of coverage.

After establishing the number of aminopropylsilane groups N_G present due to modification (i.e. aminopropylation) of the silica surface, the extent of the reaction of the amino function of the

spacer chain ($\text{Si}(\text{CH}_2)_3\text{NH}_2$) with a substrate can be monitored by elemental analysis. This determination is expressed as either the percentage of initial aminopropyl groups reacted (Equation 5), or the number of initial aminopropyl groups reacted g^{-1} (Equation 6), by the following Equations:

$$\% \text{ APS groups reacted} = \left\{ \frac{\%C \left(\frac{602300 + \text{Mw}_1}{N_G \times S} \right) - 100C_1}{\left(C_2 - C_1 \right) - \left(\frac{\text{Mw}_2 - \text{Mw}_1}{100} \right) \%C} \right\} \quad (5)$$

where %C is the per cent carbon from elemental analysis after the reaction of the modified silica with the substrate; N_G is the initial number of APS groups present on the silica before reaction; Mw_1 , the molecular weight of bonded organic moiety on the silica surface due to modification (for APS $\text{Mw}_1=58$); Mw_2 , the molecular weight of bonded phase after the modified silica has reacted with the substrate; C_1 , amount (mass per mole) of carbon in the bonded organic moiety on the support surface before reaction (for APS $C_1=36$); C_2 , amount (mass per mole) of carbon in the bonded phase after the modified silica has reacted with the substrate, and S the surface area of silica m^2/g .

The number of groups per gram that have reacted is given by:-

$$= N_G \times S \times \% \text{ APS reacted} \quad (6)$$

where N_G and S and %APS reacted are defined in Equation 5.

1.2.4 The Liquid Chromatography Column

The column is usually a stainless steel tube several centimetres long and a few millimetres wide, packed with particles of stationary phase a few microns in diameter.

During the development of a chromatographic separation, two processes proceed progressively and simultaneously in the column. Firstly, the bands of the individual solutes (in the case of a racemic solution these are the enantiomers) in the sample are moved apart as a result of their different interactions with the stationary phase. Secondly, as the bands are moved apart, they spread or disperse, which may blur the separation that has been obtained. The column, by appropriate design, must minimise this dispersion, so that having been moved apart and separated, the individual components enter the detector as separate bands.

1.2.4.1 Characteristic Parameters in HPLC

On reaching the end of the column, the various compounds are carried to the detector, where their concentrations are recorded as a function of separation time as shown in Figure 5.

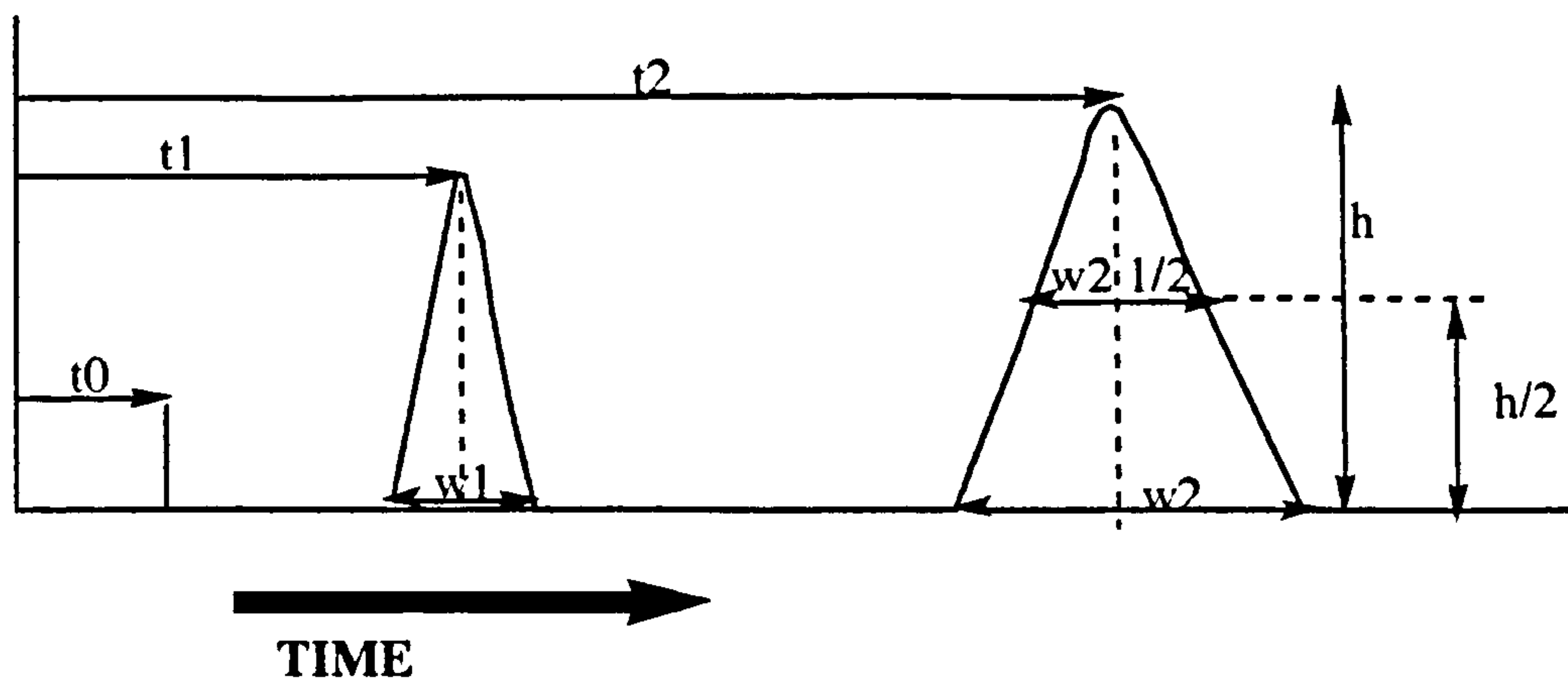


Figure 5 Characteristics of a chromatogram

The retention of a sample component can be expressed in terms of time (or volume), with respect to a non-retained component. If the elution time of the non-retained component is t_0 and that of the sample component (solute) is t_1 , then the capacity factor k' may be expressed as ;

$$k'_1 = \frac{t_1 - t_0}{t_0} \quad (7)$$

This value, k' , represents the ratio of the amount of constituent in the stationary phase to the amount of the constituent in the mobile phase, thereby quantifying retention. The capacity factor for a given substance is a complex function of the relative affinities of that substance for the stationary and mobile phases in the column. The capacity factor may depend upon a number of characteristics of the column and of the stationary phase, including the fraction of the column volume occupied by the mobile phase and the surface area of the stationary phase.

The column's selectivity for two different solutes (or enantiomers) is given by α . Selectivity, α , is a chemical factor and reflects the composition of both the mobile phase and the stationary phase.

$$\alpha = \frac{k'_2}{k'_1} \quad (8)$$

Two components must have a differing capacity factor or retention time in order to be separated.

The separation or resolution, R_s , of two adjacent bands is defined as equal to the distance between the two band centres, divided by the average band width (see Figure 5), and is given in Equation 9.

$$R_s = \frac{(t_2 - t_1)}{0.5(w_1 + w_2)} \quad (9)$$

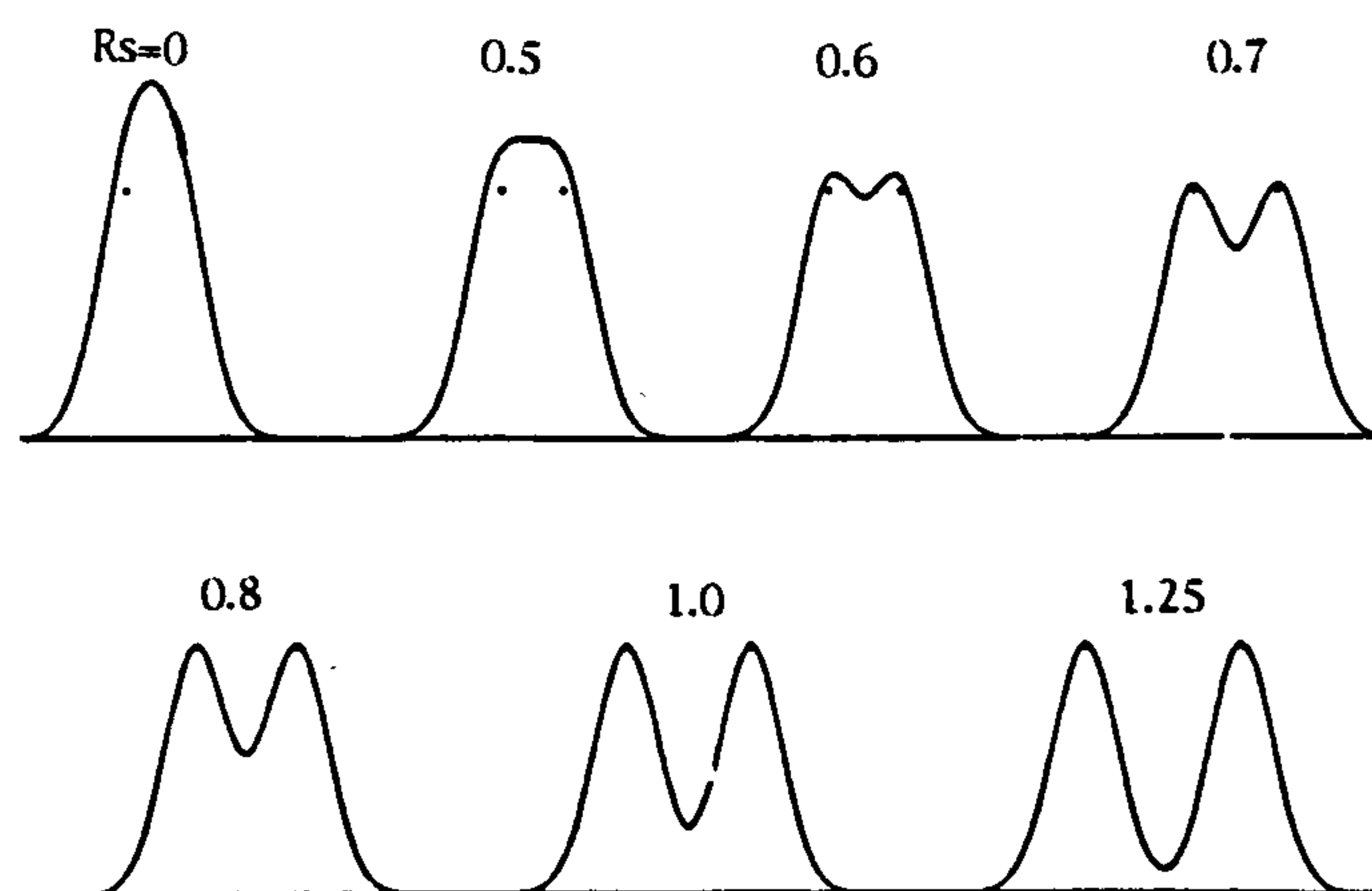


Figure 6 Standard resolution curves for a band size ratio of 1/1 and R_s values of 0.4-1.25

When $R_s = 1$ the two bands are reasonably well separated (see Figure 6), and smaller values of R_s give poorer separation. To control separation or resolution, the variation of R_s with experimental conditions must be known, ie k' , N and α (where N is the number of theoretical plates) and this can be expressed¹³ by Equation 10.

$$R_s = \underbrace{\left(\frac{1}{4}\right)}_a \underbrace{\left[\frac{k'}{1+k'}\right]}_b \underbrace{\left[\frac{(\alpha-1)}{\alpha}\right]}_c \sqrt{N} \quad (10)$$

where k' is the mean of the two, k'_1 and k'_2 values.

As each term is roughly independent, optimisation of each one in turn can occur. Separation selectivity measured by α is varied by changing the composition of mobile phase. Separation efficiency measured by N (term c) is varied by changing column length L or solvent velocity u . Term (a), involving the capacity factor k' , is varied by changing the solvent strength of the mobile phase.

The ability of an efficient chromatographic system to produce sharp peaks results from the minimal dilution of the sample bands as they pass through the column.

Assuming that retention of a substance on a column occurs by a single mechanism and that band broadening occurs randomly, statistical theory predicts that constituent peaks emerging from the column will have a symmetrical gaussian shape. For such peaks, the number of theoretical plates can be calculated using the Expression 11.

$$N = 5.54 \left(\frac{t^2}{w_{1/2}^2} \right) \tag{11}$$

Where, N is number of theoretical plates for the column and $W^{1/2}$ the width of peaks at half height (in the same units as t).

In the testing of kinetic performance of a column, the measured theoretical plate number is higher for peaks with larger k' values. This is due to extra column effects which cause widening of solute bands as retention time increases. The quantity N is proportional to the column length L as expressed in Equation 12.

$$N = L/H \tag{12}$$

Where H is the height equivalent of a theoretical plate (HETP).

According to chromatographic theory^{36,37,12} four processes contribute to band dispersion, so the plate height can accordingly be expressed as a sum of three terms. Using the dimensionless notation³⁸ the dependence of plate height upon velocity can be adequately expressed for all practical purposes by:

$H =$	$Au^{0.33}$	+	B/u	+	$Cu_{mobile} + Cu_{stat}$	(13)
	contribution		contribution		contribution from	
	from flow in		from axial		slow equilibration	
	inter-particle		diffusion		between mobile and	
	space				stationary phases	

1.3 CHIRAL SEPARATIONS BY HPLC

1.3.1 Introduction

Ever since Pasteur reported³⁹ that the resolution of racemic sodium ammonium tartrate yielded two enantiomorphic crystals, scientists have been interested in optically active compounds. Although nature is able to routinely achieve asymmetric synthesis, modern organic chemistry is now preoccupied with this problem, especially in the areas of drugs, crop protectants and pesticides. Only recently in pharmacology and medicine have the implications of asymmetry in the human biosystem been appreciated. The stereochemical composition of biologically active molecules is important, especially in the development, regulation and clinical application of new drugs. Interest in the stereoisomer composition, particularly the enantiomeric composition, is based on recognition of the existence of pharmacodynamic and pharmacokinetic differences⁴⁰ between drug enantiomers. Enantiomers of a biologically active molecule may differ in potency, pharmacological action, metabolism and toxicity. The situation facing pharmacologists and clinicians has been summarised by Ariens⁴¹.

The magnitude of the problem is illustrated by the fact that a significant portion (approximately 25%) of widely prescribed drugs contain racemic mixtures. In the late 1950's racemic *n*-phthaloylglutaric acid imide was marketed as the sedative thalidomide, the therapeutic activity of which resided in the R(+)-isomer (see Figure 7).

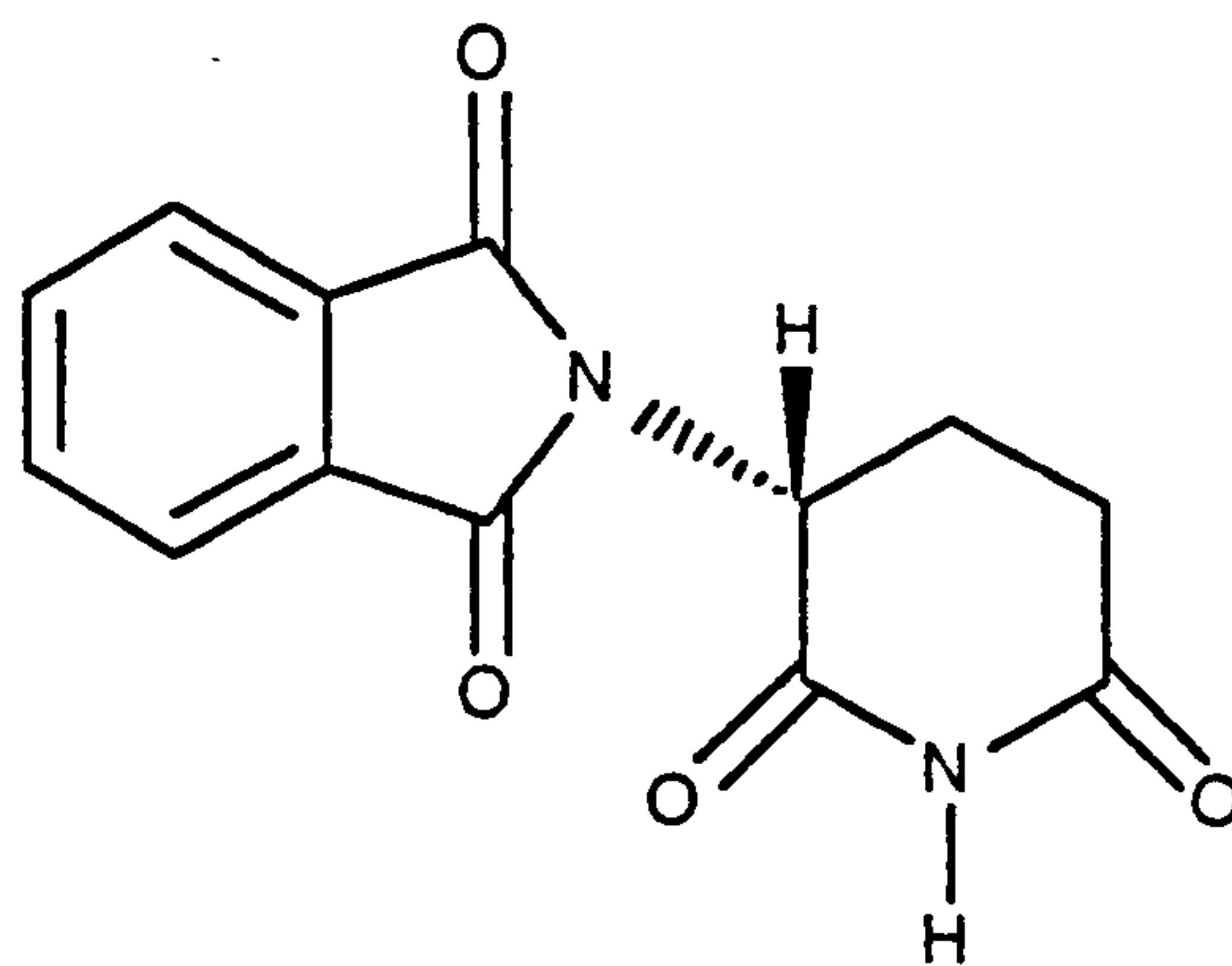
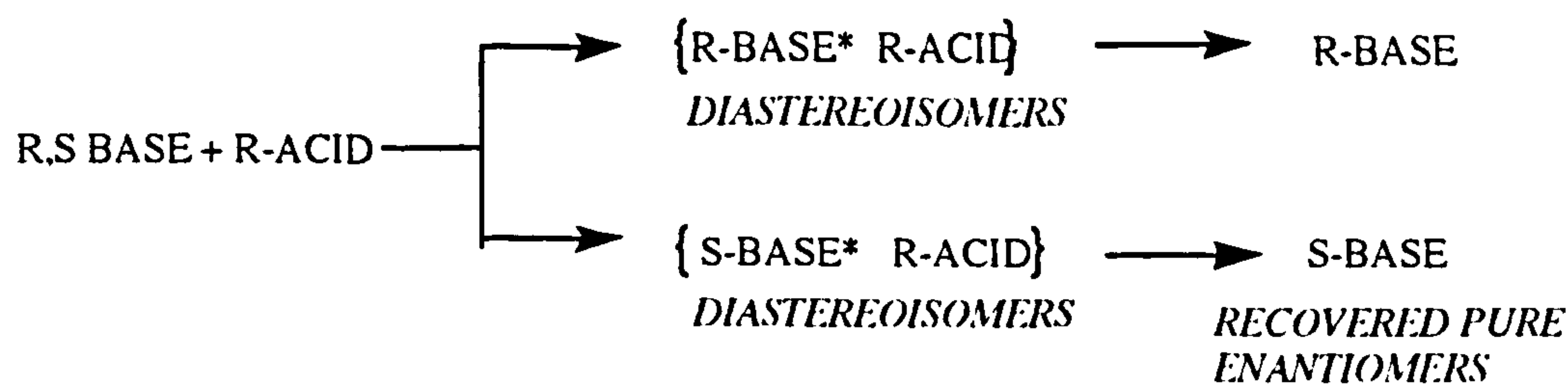


Figure 7 Structure of thalidomide

Unfortunately, the S(-)isomer had different properties, and its presence in the commercial racemate caused serious fetal abnormalities⁴².

Regulatory authorities now demand more stringent investigations to evaluate the safety and effectiveness of therapeutic drugs if they are asymmetric. They require for example, analytical measurements of enantiomeric composition during process development and manufacture and insist upon separate pharmacological evaluation of each enantiomer. The demand for quantitative analytical methods to resolve enantiomer mixtures has lead to an intense study of stereoselective analytical techniques, particularly chromatographic separations.

Traditional approaches to resolving enantiomers has previously used indirect methods⁴³. These are dependant upon the reaction of a racemic mixture with an optically pure chiral reagent to form a pair of diastereoisomers.



Scheme 3 Resolution of a racemic mixture into enantiomers via formation of diastereoisomers

For example a mixture of organic base enantiomers reacts with an optically pure organic acid to give two diastereoisomers. The physiochemical properties of the diastereoisomers are different and they can be separated by fractional distillation, chromatography⁴⁴ or crystallisation.

The diastereomeric method has been successfully used and is still widely used at the process scale. However, it has a number of serious disadvantages⁴⁵; for example, stereochemical impurities in the derivatising agents, and different reaction rates or equilibrium constants when they react with another chiral molecule.

A direct method of analysis overcomes these inherent problems and can be achieved using chromatographic techniques. The important criterion for chromatographic resolution is that the chiral recognition is achieved by some optically active moiety which is selective. The selectand must associate preferentially with one of the enantiomers and can be present as the stationary phase or as a mobile phase additive. Gas chromatographic and high performance liquid chromatographic chiral stationary phases have been developed and are now commercially available.

1.3.2 History of Cellulose In Chromatography

Long before HPLC had emerged as a powerful tool for separation, Easson et al,⁴⁶ whilst studying the relationship between chemical composition and molecular dissymmetry, observed enantiomeric separations. The first indication of chiral recognition by cellulose was in the 1950's when racemic amino acids were found to give two spots in paper chromatography^{47,48,49,50}. It was during these studies that Dalgleish correctly attributed the separations to enantioselective adsorption on the optically active cellulose molecules of paper, and proposed tentative requirements for such a process; (a) for stereochemical specificity in adsorption, three points of attachment are required; (b) resolution of the amino acid involves the carboxylic acid group, the amino group and a structural component of the side chain, all participating in molecular interactions envisaged to be due to H-bonding or steric repulsion.

Although Dalgleish's studies were not unique, they are referred to because of the acknowledgement of the structural requirements for asymmetric recognition, a feature which Pirkle⁵¹ has recently restated as the "Three Point Rule".

The optical resolution of amino acids and their derivatives was used extensively to show the chiral recognition properties of cellulose. It was performed on paper, on thin layer, and on a powdered cellulose column. Other than amino acids, some synthetic alkaloids, a chiral nickel complex and α,α' -diaminodicarboxylic acids have been resolved on cellulose.

Extensive study by Yuasa *et al*⁵² showed that protection of the hydroxyl groups of cellulose with BrCN resulted in the loss of chiral recognition and deprotection in the recovery of it. They also showed that upon treatment with aqueous sodium hydroxide, which caused rearrangement of the naturally occurring cellulose polymorph to an unnatural one, cellulose lost its chiral recognition ability. No efficient optical resolution has been performed on regenerated cellulose.

1.3.2.1 Derivatives of Cellulose

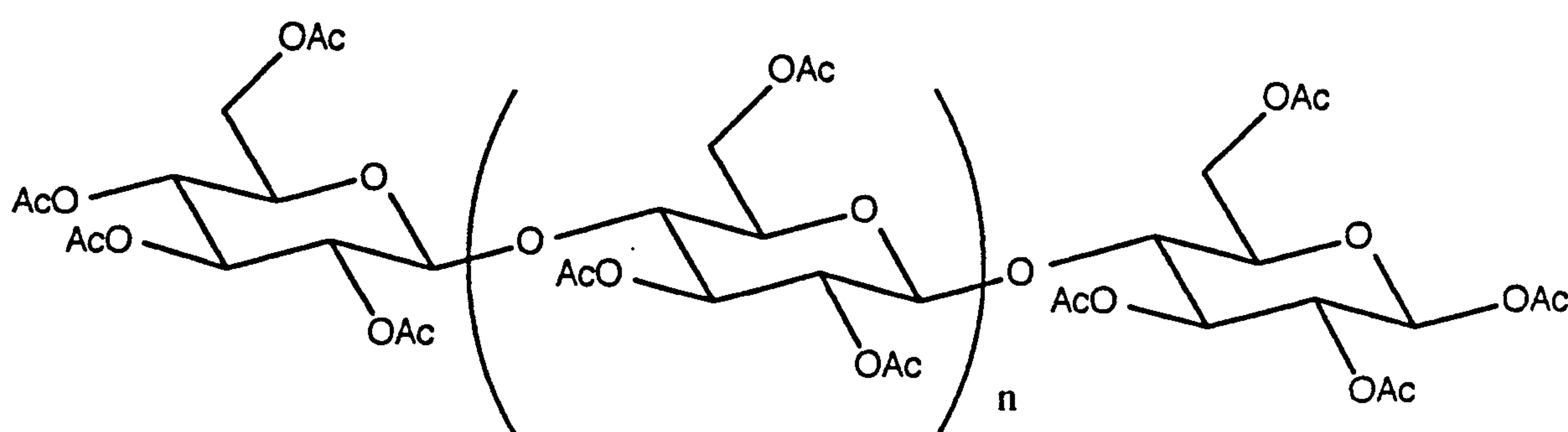


Figure 8 Structure of cellulose acetate

Cellulose acetate (Figure 8) was first employed to separate enantiomers of a biphenyl derivative by column chromatography. However, poor efficiency was obtained⁵⁰. The nature of the cellulose acetate was not known, but it was believed to be something similar to microcrystalline cellulose triacetate, (MCCTA). MCCTA is the product of the heterogeneous acetylation of microcrystalline cellulose⁵³ and was successfully utilised by Hesse and Hagel⁵⁴. Their results strongly emphasised the importance of a particular morphology of MCCTA that was responsible for chiral recognition. It was from their study of the

polymorphic states of MCCTA, that they advocated the concept of inclusion chromatography.⁵⁵ MCCTA can exist as the metastable CTA I which gives the more stable polymorph CTA II upon dissolution and precipitation. CTA I showed chiral recognition towards trogers base, whilst CTA II possessed no enantiomeric selectivity, which led to the conclusion that "sorption was not achieved by simply adhering to one glucose ester moiety, but by insertion between two such moieties."

Other research groups investigated the use of MCCTA. In Germany Mannschreck et al, resolved racemic compounds possessing aromatic groups^{56,57,58} on MCCTA. In Japan, Shibata et al ^{59,60} postulated that CTA II should have an excellent ability for chiral recognition in its crystalline state. 25 cm columns packed with CTA I and the CTA II powder showed⁶¹ striking differences in both enantioselectivity and magnitudes of relative retention, k' .

Later, it was suggested that the crystallinity of CTA II is not directly related to the capacity for chiral recognition.⁶² The powdered, crystalline and amorphous forms of CTA II were compared for their enantiomeric selectivity and it was found that the amorphous form gave the best resolution, showing that the chiral recognition ability was not dependant upon crystallinity. Microcrystalline triacetate CTA II has been used as a bulk packing, especially when cross-linked, but its pressure resistance is limited to around 80 bar. A recent report claims that its usefulness can be improved significantly by coupling a swollen

microcrystalline cellulose triacetate column with an achiral alkyl silica column⁶³.

The first successful commercial packing of this type consisted of silica-supported cellulose triacetate. Its versatility lead to the development of a range of such phases by changing the derivatisation of cellulose⁶⁴. A variety of cellulose derivatives supported on a carrier were examined extensively by Shibata et al^{65,66} and Okamoto^{67,68,69}.

Cellulose triesters eg benzoate (CTB)^{70,71}, nitrate, cinnamate, propionate and tris(carbamates) eg phenyl^{72,73} and methyl⁷³, are known to exhibit chiral recognition. In contrast, cellulose ethers showed much poorer ability and no enantiomer separation was observed except on tribenzyl and substituted tribenzyl ethers⁷⁴. The investigation showed⁷⁵ that each derivative had its own selectivity for substrates: in other words, there was no generally useful "best one" that could be chosen.

Study of other polysaccharide derivatives apart from celluloses was expected to give information regarding the mechanisms of chiral recognition on carbohydrate derivatives. Those investigated included amylose, chitosan, inulin and dextran^{69,73,76,77}, but no general principle governing chiral recognition could be derived and it was concluded that the chiral adsorption behaviour of polysaccharide derivatives needed further careful examination.

1.3.2.2 Cellulose and Amylose Tris(phenylcarbamates)

Previous studies⁷⁸ by Okamoto showed that cellulose tris(phenylcarbamate) when coated on aminopropylated silica, separated the widest range of racemic compounds, and gave a practically useful HPLC column. He then synthesised a large number of cellulose tris(phenylcarbamate) derivatives⁷⁸ in order to correlate their optical resolution abilities with the characteristics of the substituents on the phenyl rings (see Figure 9).

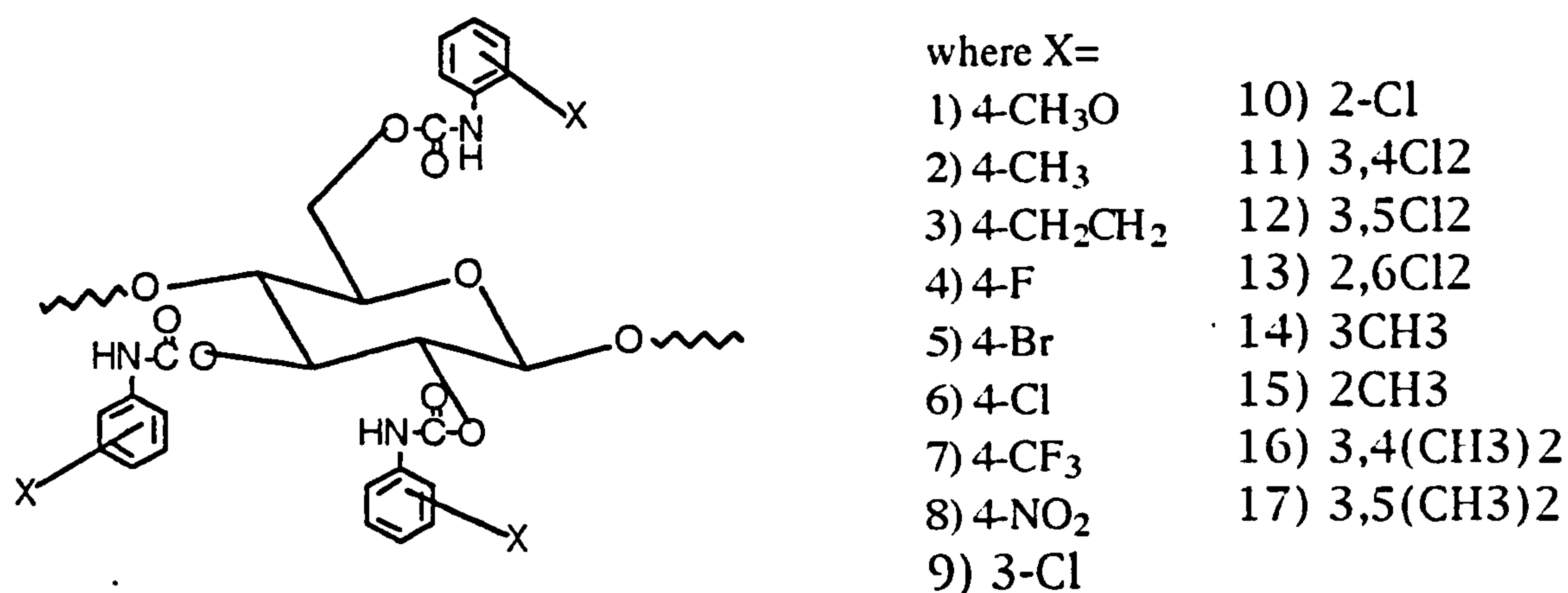


Figure 9 Range of different ring substituents investigated for chiral recognition⁷⁸

This investigation showed that the inductive effect of the substituents greatly influenced the optical resolution ability when they were at the 3 or 4 position. 2 substituted derivatives showed a low degree of resolution. Among nine 4-substituted phenylcarbamates the 4-methyl, 4-ethyl, 4-chloro or 4-trifluoromethyl derivatives showed the most efficient chiral recognition for racemic compounds. Dimethylphenyl and

dichlorophenylcarbamates substituted at the 3,4 or 3,5 positions showed higher chiral recognition ability than the mono substituted derivatives. These two CSP have been used to resolve a variety of racemic compounds.^{64,78,79} Cellulose tris(3,5-dimethylphenylcarbamate) possesses a high durability when hexane containing 0-30%^{v/v} of propan-2-ol is employed as an eluent, whereas cellulose tris(3,5-dichlorophenylcarbamate) phase does not remain stable when used with hexane containing greater than 10% propan-2-ol because of its high solubility. Thus, the latter CSP is not suitable for the separation of compounds which are well retained on the CSP.

This defect of the tris(3,5-dichlorophenylcarbamate) phase prompted Okamoto et al⁸⁰ to prepare more durable CSP's which could be applied regardless of eluents. They chemically bonded cellulose tris(3,5- dichlorophenylcarbamate) and cellulose tris(3,5-dimethylphenylcarbamate) to 3-aminopropyl silica gel with diisocyanates⁸⁰. This was performed by coating 3-aminopropyl silica with 6-O-triphenylmethyl cellulose. The trityl group was removed by acid hydrolysis and the cellulose reacted with 4,4-diphenylmethane diisocyanate, then an excess of 3,5-dichloro or 3,5-dimethylphenyl isocyanate.

On comparing the optical resolving power of these CSP's with that of cellulose tris(3,5-dichlorophenylcarbamate) and cellulose tris(3,5-dimethylphenylcarbamate) physically coated on

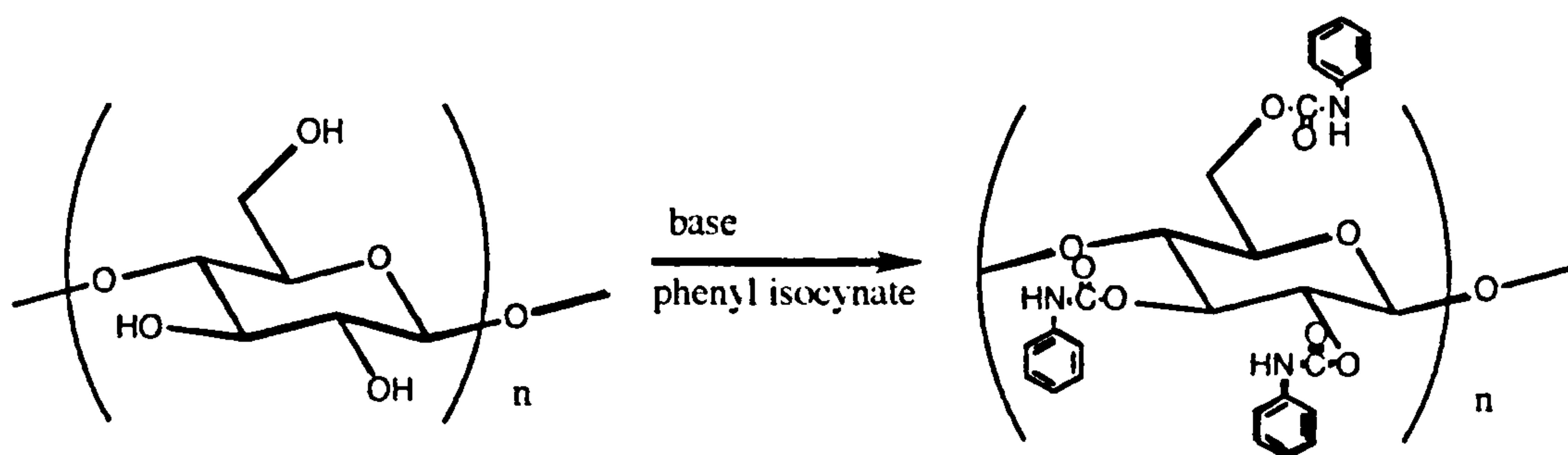
aminopropylated silica gel, Okamoto et al⁸⁰ found that the chemically bonded phases gave poorer chiral recognition.

Many derivatives of cellulose and amylose have been examined. In most cases, the tris(3,5-dimethylphenylcarbamate) derivative gave the highest optical resolving power for both polysaccharides. Although chemical bonding of the polysaccharide derivative to a silica gel matrix is possible, no such bond is introduced on any of the commercially available phases. Therefore, any solvent that dissolves or leads to swelling of the derivative should be avoided. Hexane modified with a certain amount of alcohol (typically propan-2-ol) is the recommended mobile phase for coated derivatives. As the adsorbent-analyte interaction is essentially polar in nature, the greater the amount or the polarity of the alcoholic modifier the shorter the analysis time. There are several examples of the addition of a modifier to the mobile phase: for example, when the analyte bears an amino group, the presence of a small amount of amine (eg diethylamine) suppresses the tailing of the elution peak⁷⁸. Okamoto et al⁸⁰ resolved a variety of racemic carboxylic acids using a hexane/propan-2-ol eluting system containing a small amount (1%) of a strong carboxylic acid like, formic acid and trifluoroacetic acid. Cellulose tris(3,5-dimethylphenylcarbamate) has been employed in the reverse phase mode. Ikeda⁸¹ reported efficient optical resolution of verapamil and propanolol using a mobile phase consisting of 2 volumes of 0.05 molar sodium perchlorate at pH 3.0, mixed with one volume of acetonitrile. Racemic propanolol was also resolved with a water/acetonitrile and acetic acid mobile phase in the

ratios of 75 : 25 : 0.05. In both cases, the CDMPC column was quite stable during the analysis.

1.3.2.2 1 Preparation of Carbohydrate Derivatives

The first preparation of a carbohydrate derivative was accomplished by Tessmer⁸² in 1885. Since then many other such derivatives have been reported. The reaction of cellulose and partly hydrolysed cellulose acetates with alkyl and aryl isocyanates has been studied by Hearon, Hiatt and Fordyce⁸³. Schriebebeli⁸⁴, later studied the reaction of cellulose with phenyl isocyanate as a function of time and temperature. X-ray studies have indicated that the reaction is helped by "wetting" the polysaccharide, swelling its structure, and that reaction does not occur within the crystalline portion until one quarter to one third of the hydroxyl groups have reacted. For this reason, the carbohydrate is refluxed in dry solvent for 16 hours before the reaction. Isocyanates hydrolyse easily to the corresponding amine (and CO₂) which in turn reacts readily with the isocyanate to form a symmetrical urea. This side reaction with water is very undesirable since it removes reagent and produces an impurity which is bothersome to remove. Therefore, extreme care should be taken to dry thoroughly all starting material, solvents and equipment to exclude all moisture from the reaction mixture.



Scheme 4 Reaction process for the preparation of cellulose tris(phenylcarbamate)

The phenylcarbamate derivatives are prepared by the reaction of microcrystalline cellulose (Avicel, Merck or Sigma) or amylose (from potato starch low in amylopectan, type 3, Sigma) with 3.5 equivalents of isocyanate in pyridine for 62 hours at 116°C and isolated as methanol insoluble fractions.

1.3.2.2.2 Mechanisms for the Reaction of Phenyl Isocyanate with Cellulose

Phenyl carbamates of cellulose may be prepared by a reaction of phenyl isocyanate upon cellulose (previously dried) in the presence of a tertiary amine.

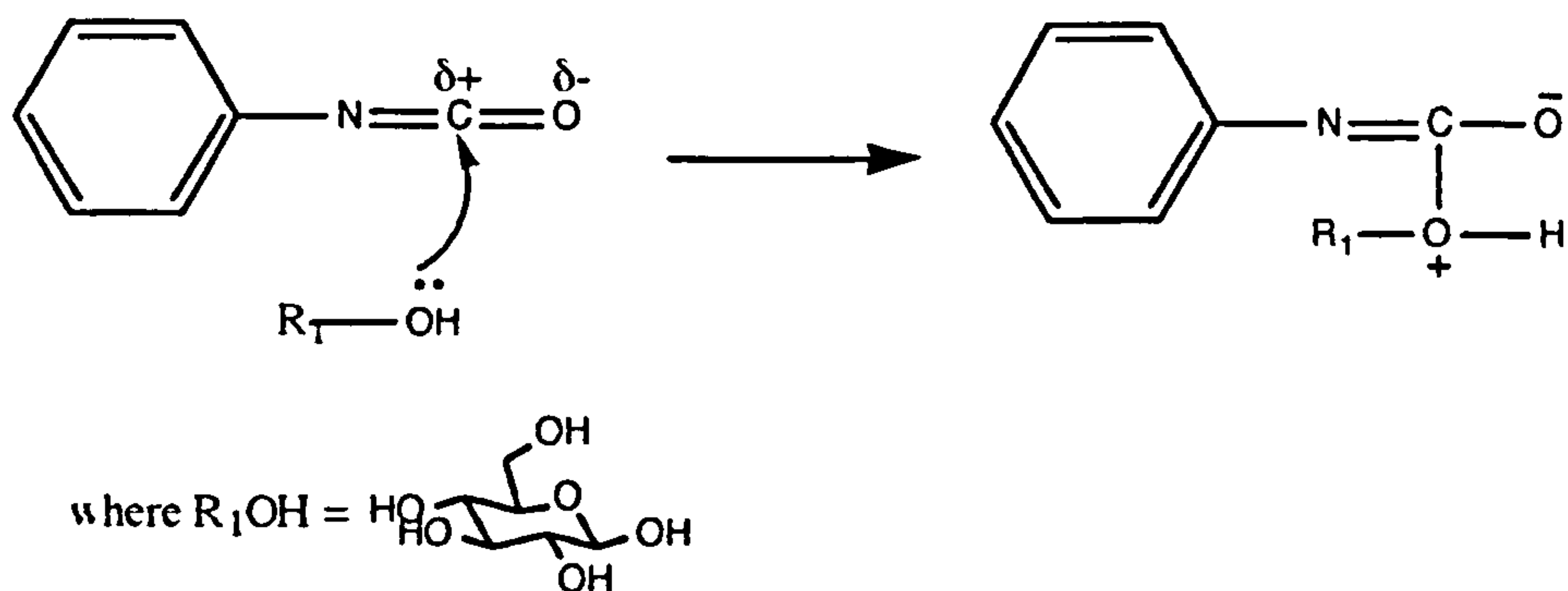


Figure 10 Nucleophilic attack on phenyl isocyanate by an hydroxyl group on cellulose

Pyridine is employed as a solvent for the reaction as it does not react with the isocyanate and is a catalyst. The reaction involves nucleophilic attack by the cellulose hydroxyl group, on the carbonyl carbon atom of phenyl isocyanate. The transition state of the isocyanate addition is cyclic with the proton expected to transfer directly to the nitrogen atom. Baker⁸⁵ found that normally the strongest bases were the best catalysts and suggested the following intermediate:-

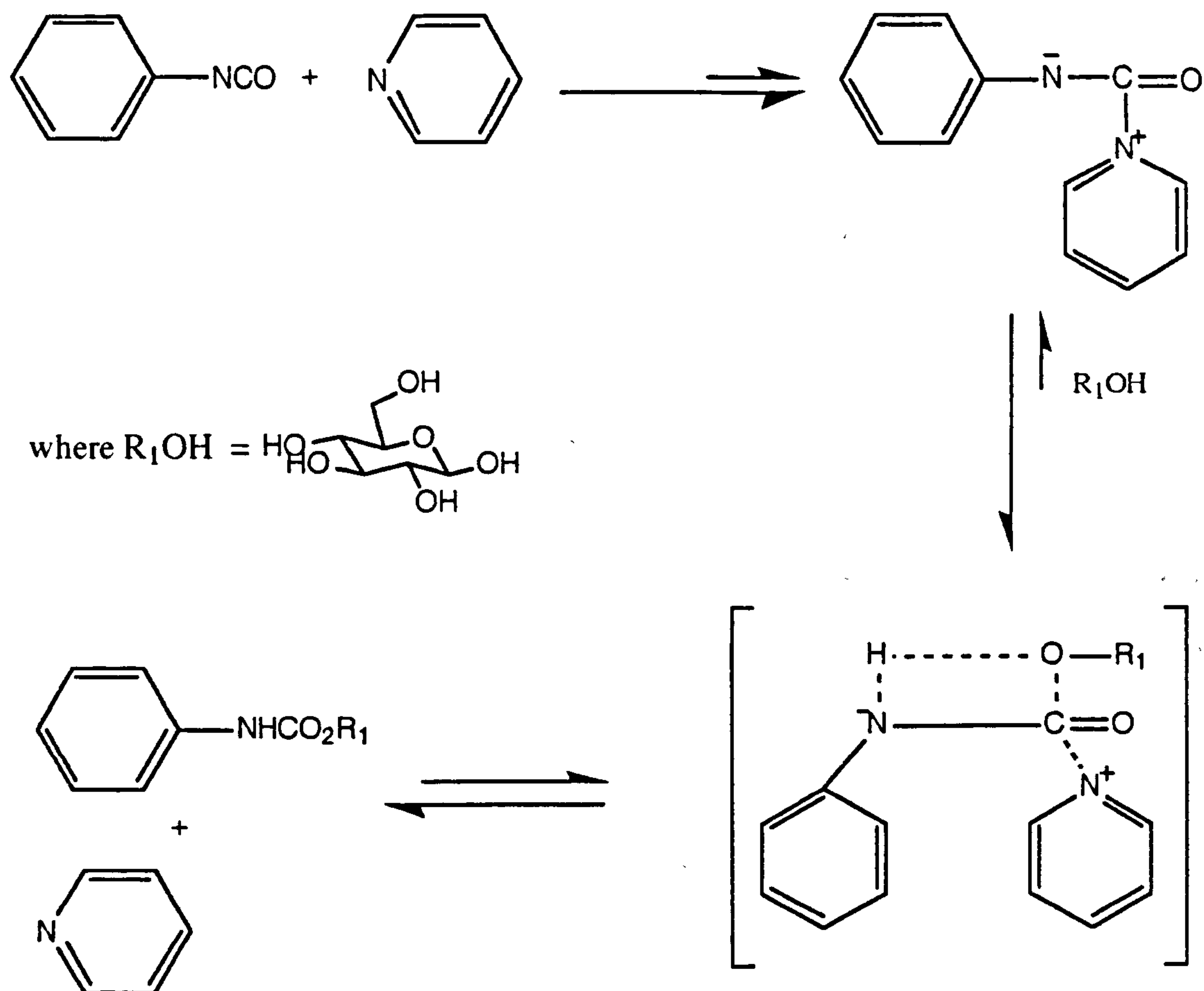


Figure 11 Intermediate proposed by Baker⁸⁵

1.3.2.2.3 Preparation of a Liquid Coated Chiral Phase on a Solid Support

In order to permit a large number of distribution stages in the HPLC column, the support surface should be homogeneously coated with a liquid layer of defined thickness, producing a maximised liquid/liquid interface. There are different techniques for the preparation of columns that contain a liquid coated packing¹³. The method employed to coat aminopropylated silica

with cellulose tris(phenylcarbamate) is the "solvent evaporation" technique, in which the derivative is dissolved in a solvent and absorbed onto aminopropylated silica gel by slowly removing the solvent. The coated silica is then packed into a stainless steel column by the slurry method¹³.

1.3.3 Mechanisms in Chiral Recognition

Enantioselective complexation between two molecules arises from intermolecular forces such as hydrogen bonding, dipole stacking and steric interactions.

Recent calculations⁸⁶ which treat the binding between two chiral species in terms of "multiple interactions", have shown that the energy differences between diastereomeric complexes result from six-centre forces occurring simultaneously between triplets of atoms or functionality in two species. This validates a long-standing precept of chiral recognition known as the "three point rule":

Chiral recognition requires a minimum of three simultaneous interactions between the CSP with at least one of these interactions being stereochemically dependant.

That is, at least one of the interactions will be absent or significantly altered by replacing one enantiomer with the other, without conformational change in any component. The requirement for a minimum of three simultaneous interactions

can be justified by using simple tetrahedral structures (see Figure 12)

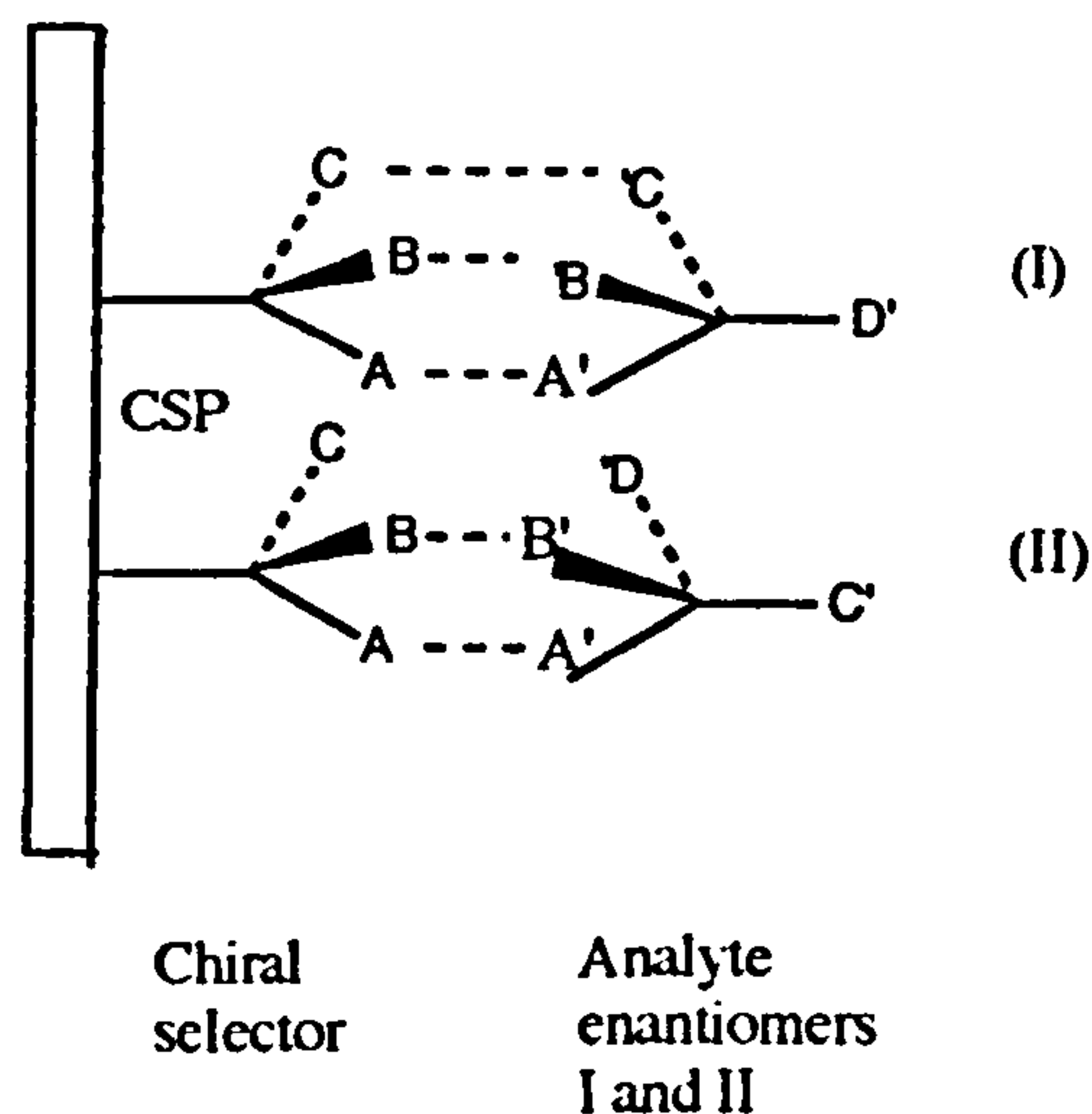


Figure 12 Three point interaction model of chiral recognition

Reproduced from D.R Taylor and K.Maher, J. Chromatographic Science 1992, 30, 67-85, by permission.

As the species approach one another, there are three possible points of interaction between the CSP (A,B and C) and the chiral solute (sites A', B' and C'). Enantiomer I is shown to be capable of three simultaneous interaction A-A', B-B', and C-C' whereas enantiomer II is capable of only two simultaneous interactions. If all three interactions are free energy lowering, stabilising the transient complex between CSP and enantiomer I, then enantiomer II will be less retained by the CSP. Alternatively, a destabilising of the transient complex will reverse the order of elution.

The Three Point Model suggests that at least one interaction must depend on the stereochemistry at both the chiral centres, and the interactions should be different in nature, otherwise the formation of unfavourable associations may occur, ie if both A-A' and B-B' are both similar to hydrogen bonding interactions, then A-B' and B-A' associations could take place causing both enantiomers to be retained to the same extent, with loss of resolution (See Figure 13).

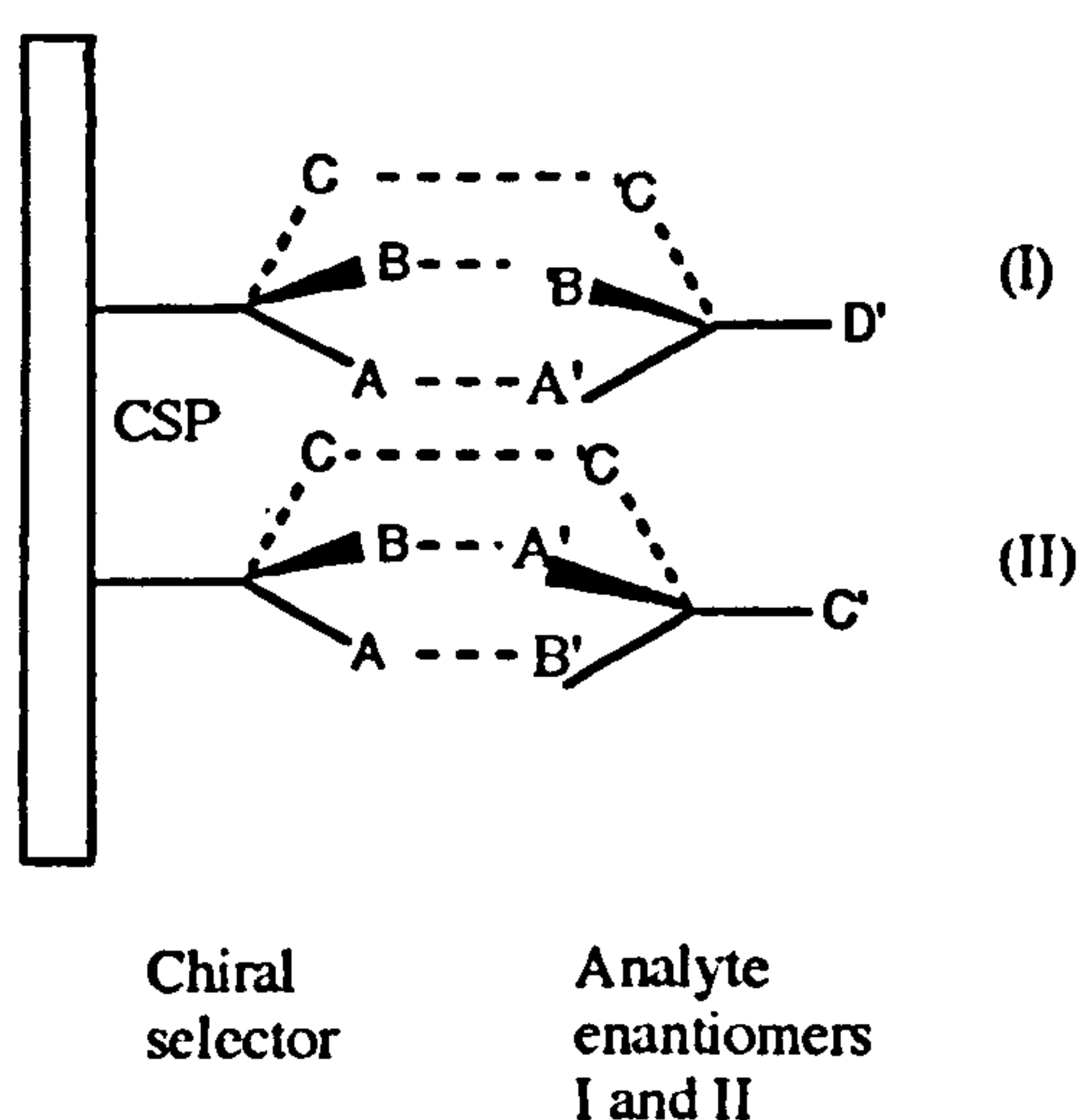


Figure 13 Two similar interactions resulting in non-discrimination

Reproduced from D.R Taylor and K.Maher, J. Chromatographic Science 1992, 30, 67-85, by permission.

Chiral recognition also occurs if two bonding and one repulsive interactions are involved. Repulsive interactions occur when a bulky group is bonded to the chiral centre and are often referred to as steric. The stereoselectivity obtained with two attractive interactions at π - π and hydrogen bonding sites, together with a steric interaction (see Figure 14) has been explained by Pirkle⁸⁷.

The enantiomer II is least likely to be retained due to a large bulky group being in an unfavourable position, resulting in a stronger net repulsion.

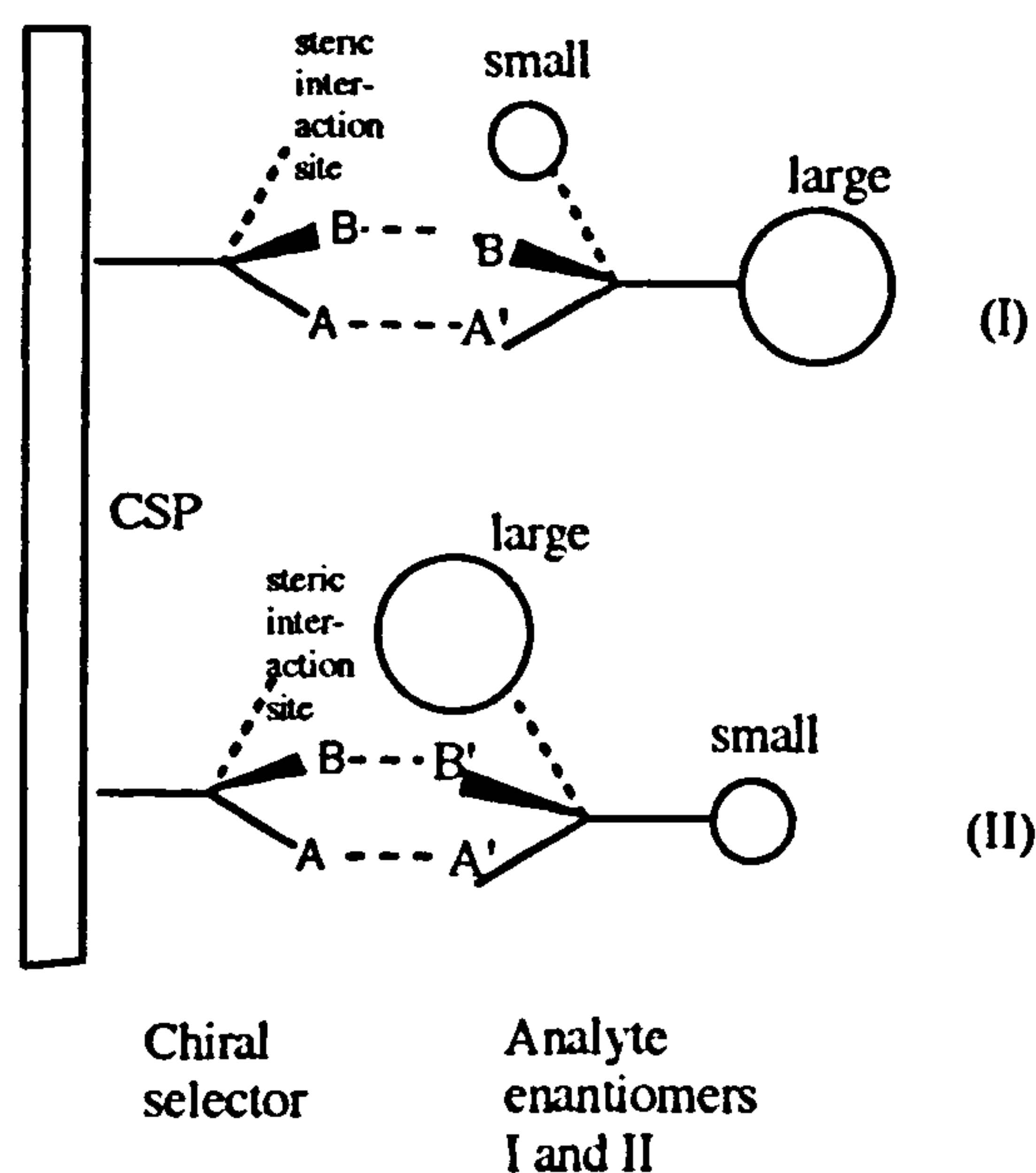


Figure 14 Discrimination from one repulsive and two attractive interactions

Reproduced from D.R Taylor and K.Maher, J. Chromatographic Science 1992, 30, 67-85, by permission.

Confusion regarding interpretation of the Three Point Rule arises when it is sometimes assumed that the rule implies that interactive functionality must be similarly arranged with respect to the stereogenic centres of the selector and analyte. Consider the case in which dipoles lie along the AB and A'B' vectors in Figure 15. "Stacking" of these dipoles is functionally equivalent to two point to point interactions, with chiral recognition resulting from the discriminating C-C' interaction. Similar arguments can be used for π - π interactions between aromatic rings.

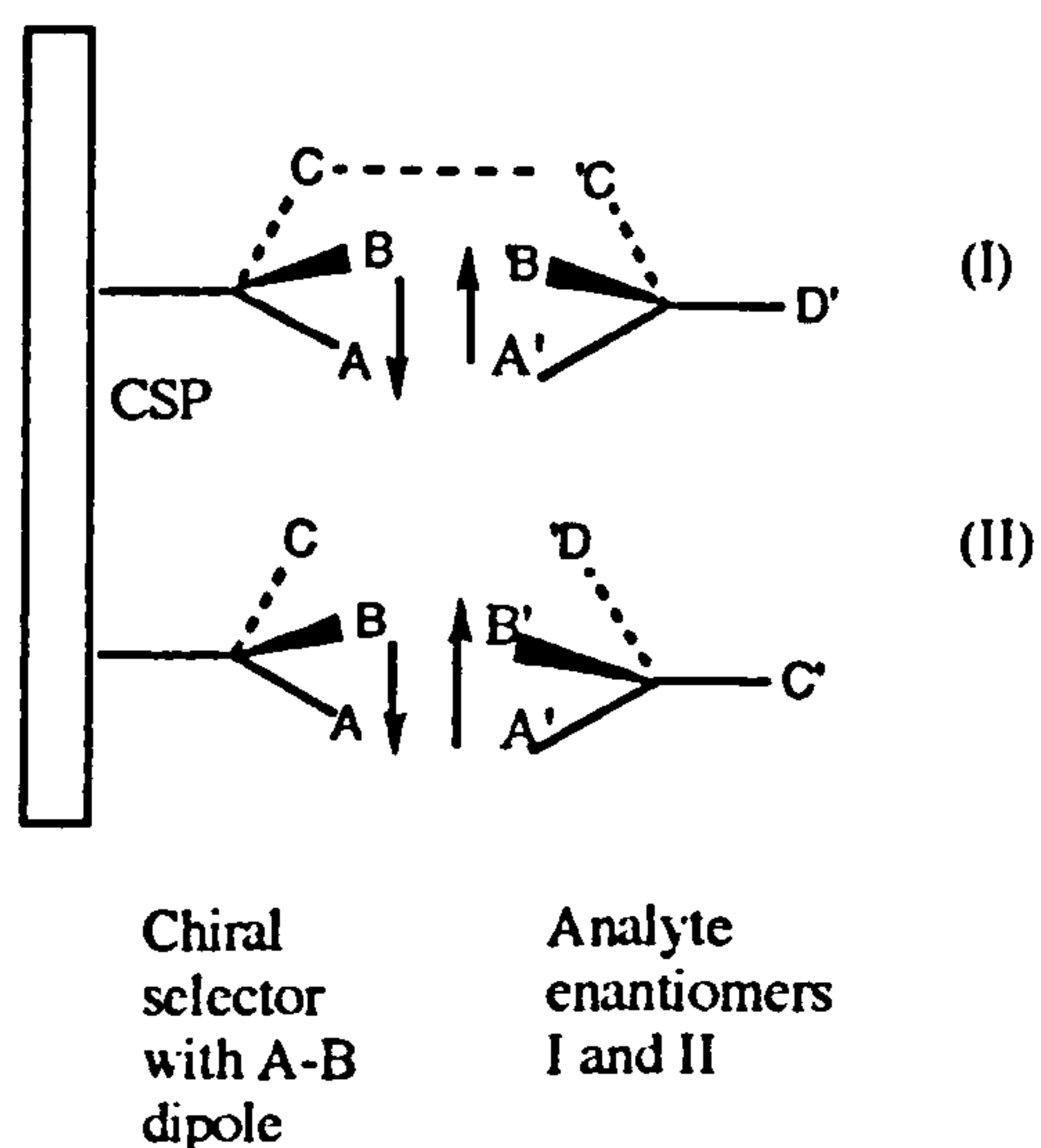


Figure 15 Discrimination via dipole stacking interactions

Reproduced from D.R Taylor and K.Maher, J. Chromatographic Science 1992, 30, 67-85, by permission.

Thus, in order for enantiomers to be chromatographically separated on a CSP, two conditions must be fulfilled. The first we have just observed, that the complex must be formed between the CSP and at least one of the analyte enantiomers; the second is that the complexes must differ in their free energy of formation.

The chromatographic parameters, retention and selectivity are thermodynamically controlled, whereas band shapes are influenced by the kinetics of mass transfer. Describing the chromatographic separation of enantiomers, $\alpha_{II,I}$ is the ratio of the capacity factors for the I and II enantiomers of the analyte on a given CSP.

$$\alpha_{II,I} = \frac{k'_{II}}{k'_I} \quad (14)$$

Because capacity factors are equilibrium constants, Equation 14 may be written as⁸⁸

$$\Delta(\Delta G) = -RT \ln \alpha_{II,I} \quad (15)$$

Owing to the nature of chromatographic processes, relatively small values of $\Delta(\Delta G)$ suffice to afford observable chromatographic separations. A value of 50 calories affords a separation α of 1.09. ii the chromatographic system is of high efficiency, so that narrow peaks are afforded, relatively small $\Delta(\Delta G)$'s will suffice for the analytical scale separation of enantiomers.

1.3.3.1 Structural Factors Affecting Chiral Recognition on Polysaccharide Derivatised CSP's

Attractive interactions play an important part in the retention on this type of CSP. Okamoto et al reported⁷⁸ that the main adsorbing sites are considered to be the polar carbamate groups whose adsorbing powers may be strongly influenced by the nature of the substituents on the phenyl ring. These groups can interact with a solute via hydrogen bonding with N-H and C=O groups and the dipole-dipole interaction on C=O (see Figure 16).

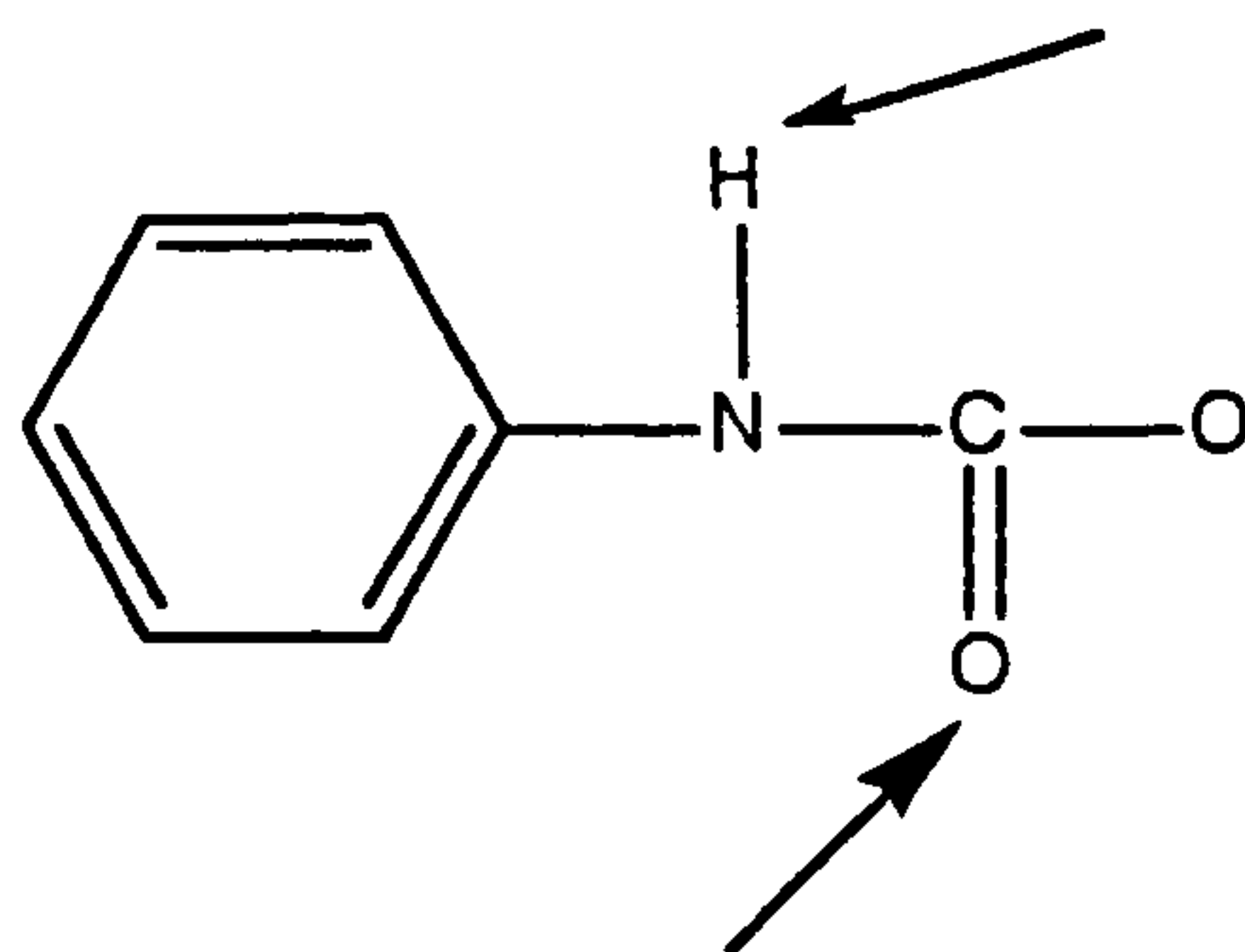


Figure 16 Main absorbing sites on the carbamate group

Nmr studies of cellulose tris(phenylcarbamate)s having electron withdrawing groups on the ring (e.g. Cl, Br, CF₃) showed the N-H proton resonance shift downfield as the power of the electron withdrawing substituents on the phenyl ring increased. This observation may be ascribed to the fact that the acidity of the N-H proton increases with an increase of electron withdrawing power of the substituents. However, an electron withdrawing group in the phenyl ring would make the lone pair of electrons from the oxygen atom in the C=O function less readily available for hydrogen bonding. Stronger hydrogen bonds with the carbonyl oxygen would occur with electron donating substituents than with electron withdrawing substituents. The phenyl groups may also have important roles for the cellulose and amylose tris(phenylcarbamate)s in providing a sterically regular structure and as sites for possible π - π interactions.

The structure of cellulose tris(phenylcarbamate) (CTPC) in solution and in the solid state has been studied in detail^{89,90}. The experimental data show that it is a stiff rod-like molecule. This has been ascribed to hydrogen bonding between adjacent

carbamate groups. CTPC also forms a liquid crystal phase⁹¹ when cast from THF solution, which shows very high crystallinity under a polarising microscope. This means that the carbamate coated on aminopropylated silica gel from solution in the preparation of the CSP also has an ordered structure in which phenyl carbamate groups are arranged regularly.

Cellulose and amylose differ only in configuration on the 1-position of each glucose unit. Therefore, if chiral recognition could be obtained on only a single glucose unit, then both polysaccharide derivatives should exhibit similar chiral recognition. However, this is not the case, as the different extents of chiral recognition's observed in previous work⁹² on these two stationary phases suggests that two or more carbamate groups of adjacent glucose units may be involved in chiral recognition. The arrangement of glucose units along the polysaccharide chains differs between tris(phenylcarbamate)s of cellulose and amylose, giving rise to different chiral cavities or spaces built between carbamate groups on adjacent units. In CDMPC, the carbamate at the 6 position can be close to both the carbamates at the 2 and 3 positions on the neighbouring glucose units. ADMPC, a carbamate group at the 6 position can be close to the carbamate group at the 6 position on two neighbouring glucose units.

The complex process of enantiomeric separation on polysaccharide carbamate phases cannot be explained by relatively simple models. Chiral recognition stems from a weighted time-average of the contributions of all the possible complexes; different directions

of approach, different conformers and different combinations of 3 simultaneous interactions are all involved. One may reasonably question whether any model of the chiral mechanism yet postulated bears much resemblance to reality.

1.3.4 Categories of HPLC Chiral Phases

The large number of HPLC-CSP's available to the analyst present a broad range of possibilities and the problem of which to select. Although the mechanisms for each division or type of CSP phases are unclear, the following simple classification can be used:-

1.3.4.1 Type A - Chiral Cavity Packings

Cram and co-workers⁹³ first demonstrated chiral resolutions by inclusion of an analyte into a chiral cavity. This was performed using chiral crown ethers⁹⁴ bound to silica gel and today these are commercially available. However, due to the structure and physical properties, attention has focused more on the use of bound cyclodextrins (CDS) for this type of chiral stationary phase.

Cyclodextrins are cyclic oligosaccharides containing 6-12 D (+) glucopyranose units which are α -(1,4) linked. There are 3 naturally occurring CDS's, which have the shape of a torrid or hollow truncated cone with a depth of 7Å and differing internal diameters, making each type unique. α -Cyclodextrins (6 glucose

units) have an internal diameter from 4.5 to 6.5Å ; β -cyclodextrins (7 linked glucose units) has an internal diameter of 6-8.0Å and the internal diameter of γ -cyclodextrin (8 linked glucose units) is approximately 8-10.0Å (see Figure 17)

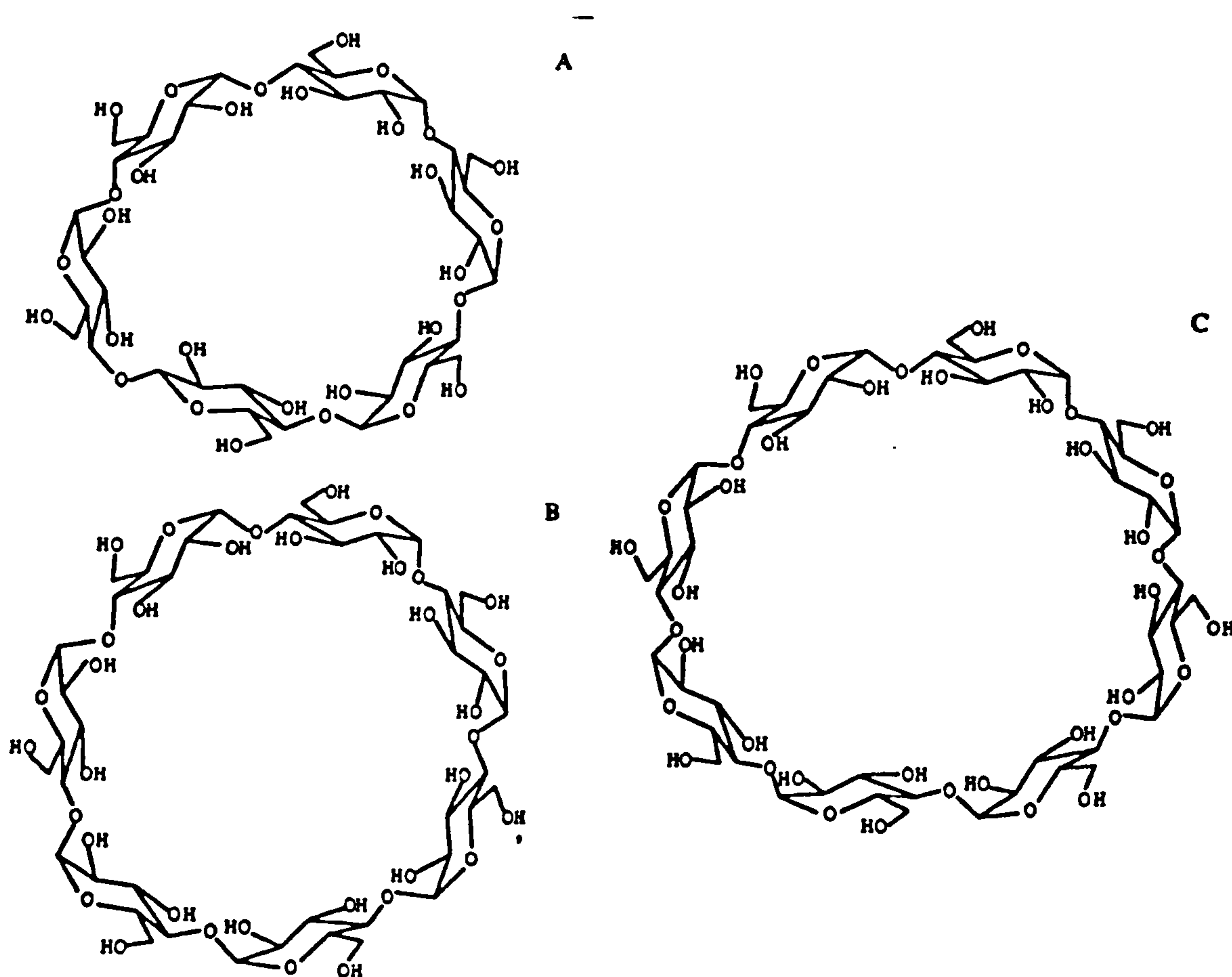


Figure 17 The three commonest cyclodextrins A) α -cyclodextrin B) β -cyclodextrin and C) γ -cyclodextrin

The secondary 2-and 3-hydroxyl groups on the glucose ring sit at the mouth of the cyclodextrin cavity, the primary OH groups point outwards and are on the reverse side of the molecule. This results

in a hydroxyl-free interior of the torroid which is relatively hydrophobic, thus allowing CD's to form inclusion complexes with non-polar compounds.

There are several factors⁹⁵ that determine the inclusion complex formation and the size of a solute binding constant to cyclodextrin. The "hydrophilic effect", in which the water-insoluble portion of the molecule resides in the non polar cyclodextrin cavity, ensures that the molecule is strongly included, setting up polar groups for chiral interactions between polar segments of the guest molecule and the secondary hydroxyl groups at the mouth of the cyclodextrin cavity.

It is apparent that the relationship in size and geometry of the guest molecules and the cavity is important. For separation of two enantiomers, there must be a difference in the energetics of the inclusion processes. Small molecules which fit loosely into the cavity are generally not separable because the binding constant and binding selectivity is often less than for tighter fitting molecules.

The unique size of the cavity for each cyclodextrin (α , β and γ) offers excellent selectivity's for a variety of structures. For example, α - cyclodextrin is suitable only for smaller molecules such as tryptophan, tyrosine and their analogs⁹⁶. β - Cyclodextrin has been used to resolve dansylamino acids, β -naphthyl ester derivatives of amino acids and barbiturates⁹⁷. The use of γ -

cyclodextrin has been reported for the separation of di and tri peptides⁹⁸.

Derivatising cyclodextrins has further developed them as chiral selectors, as this significantly changes their physicochemical properties as well as complexation behaviour. Treatment of the hydroxyl groups on the lip of the cavity on each glucose residue affects inclusion by partially blocking the mouth and reducing the hydrogen bonding interactions. As a result, the retention of hydrophobic molecules is greater and elution requires more organic modifier

1.3.4.2 Type B Pirkle type.

This type of CSP contains a relatively simple structure, consisting of one or two centres of asymmetry, chemically bonded to a silica support. The enantiomeric recognition involves H-bonding, dipolar and charge transfer interactions and steric hindrance. (See Figure 18)

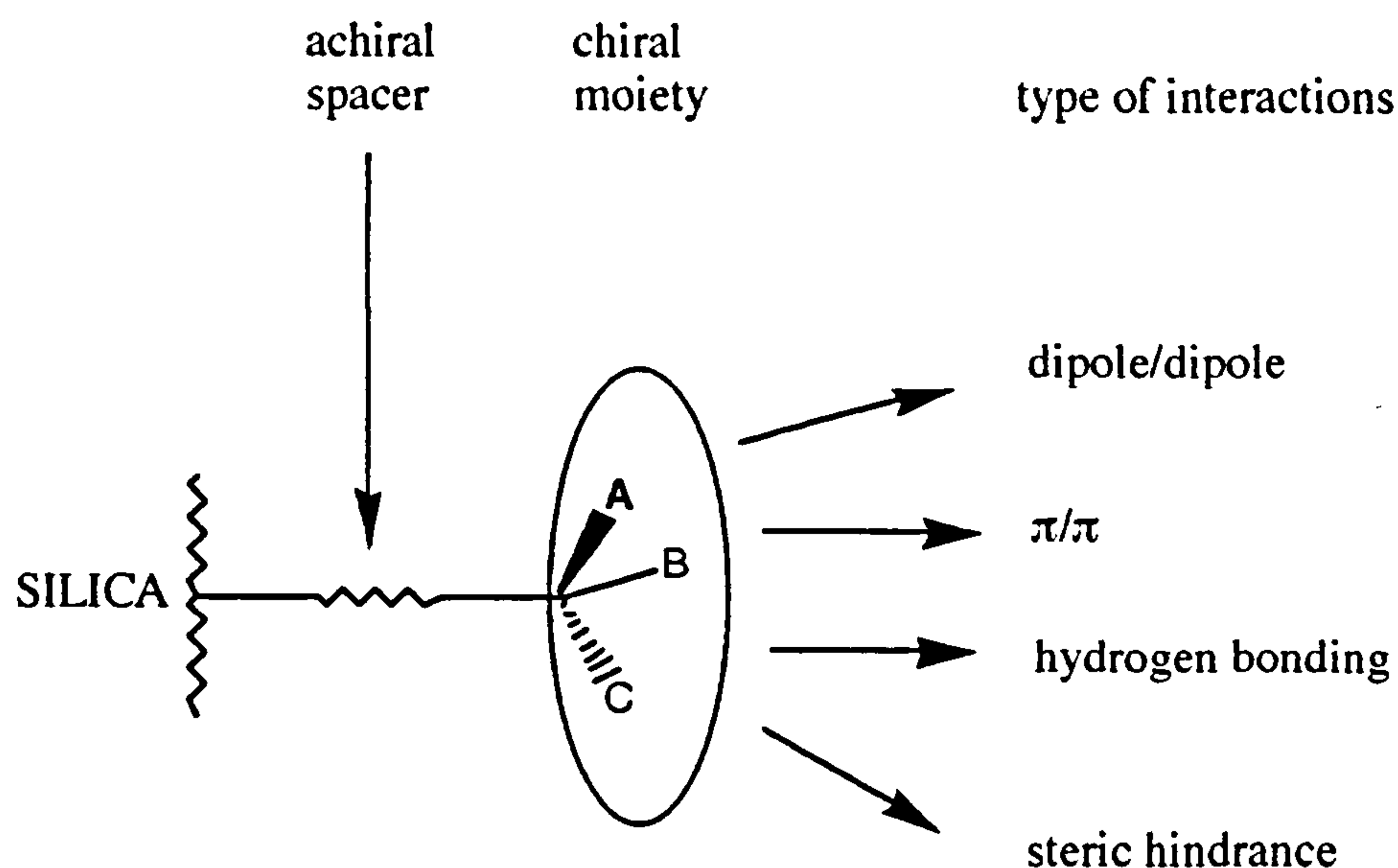


Figure 18 Class B CSP and type of interactions that can be involved during the chiral recognition process

The invention of this type of phase is credited to W H Pirkle⁵¹ who proposed a rational approach to CSP design starting from nmr studies of diastereomeric solvates¹⁰⁰. The nmr studies showed that chemical shift non equivalence could be induced between the enantiomers of a variety of racemates by complexation with a single enantiomer of a series of trifluoromethyl aryl carbinols. The reason for the non equivalence was attributed to diastereomeric complex formation between the enantiomers of the racemate and the carbinol.

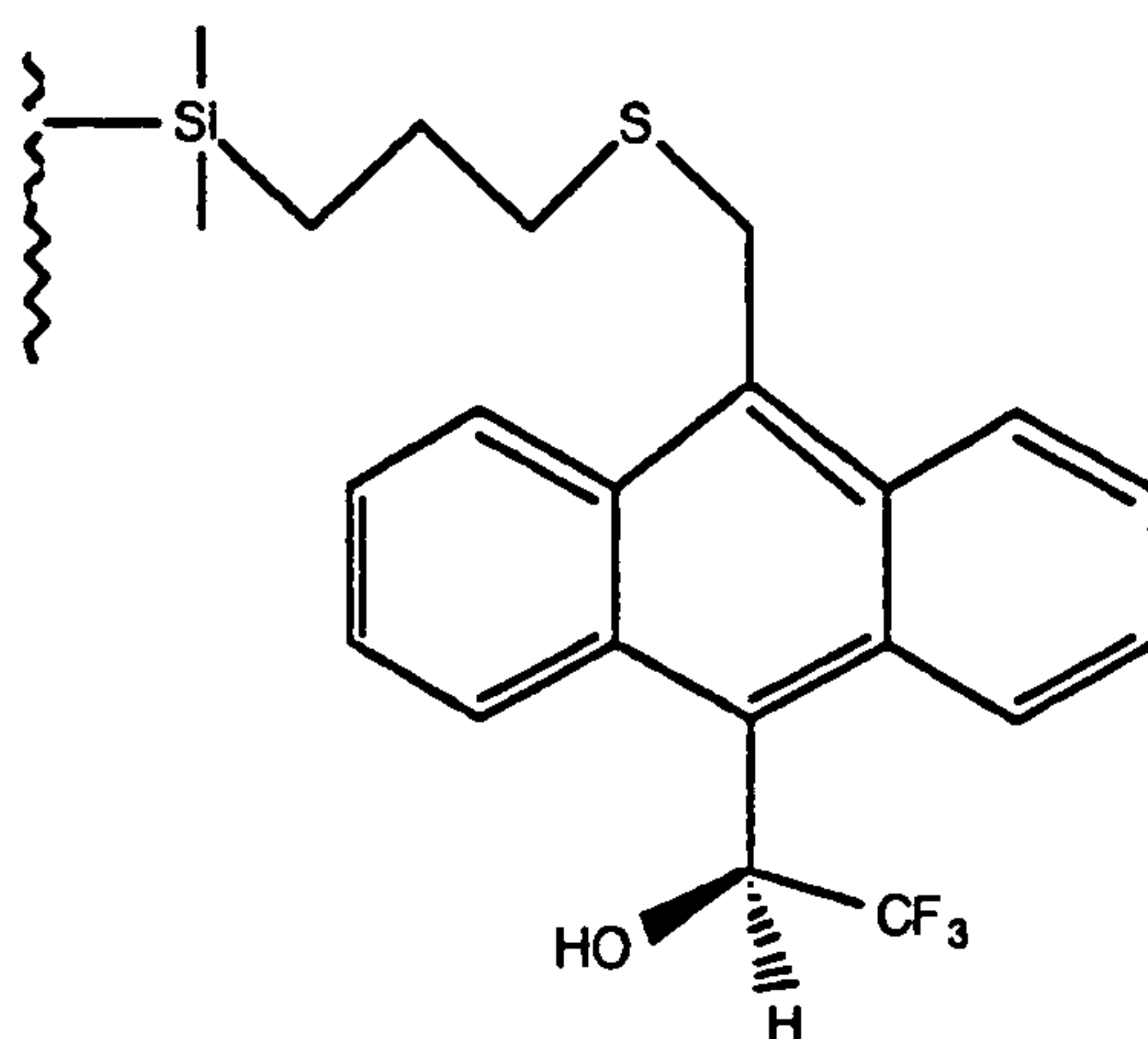


Figure 19 CSP derived from R-2,2,2-trifluoro-1-(9-anthryl) ethanol.

Pirkle predicted that "fixing" the chiral solvating agent to silica gel could provide a CSP for chromatographic resolution. This gave rise to the CSP shown in Figure 19, which separated the enantiomers of a large number of π acceptor substituted amines, amino acids and sulphoxides¹⁰¹. This phase also displayed a broader scope of application, including resolution of 3,5-dinitrobenzoyl (DNB) derivatives of amino acids, amines and alcohol's.

At this point, Pirkle introduced the "reciprocity concept"¹⁰² as follows:- "the diastereomeric interactions that allow a column derived from chiral A to resolve racemic B also allows a column derived from chiral B to resolve racemic A". This concept has proved useful in the design of CSP's and by this process Pirkle designed the "2nd generation" CSP containing the 3,5-dinitrobenzoyl (DNB) moiety. These CSP's possess a π electron acceptor group in the vicinity of the asymmetric centre. For the

formation of a charge transfer complex the solute should have a π -donor group such as an aromatic ring with an alkyl, ether or amino substituent. Moreover, the solute needs to be able to act as a donor or acceptor for H-bonds or enter into a dipole stacking process (see Figure 20).

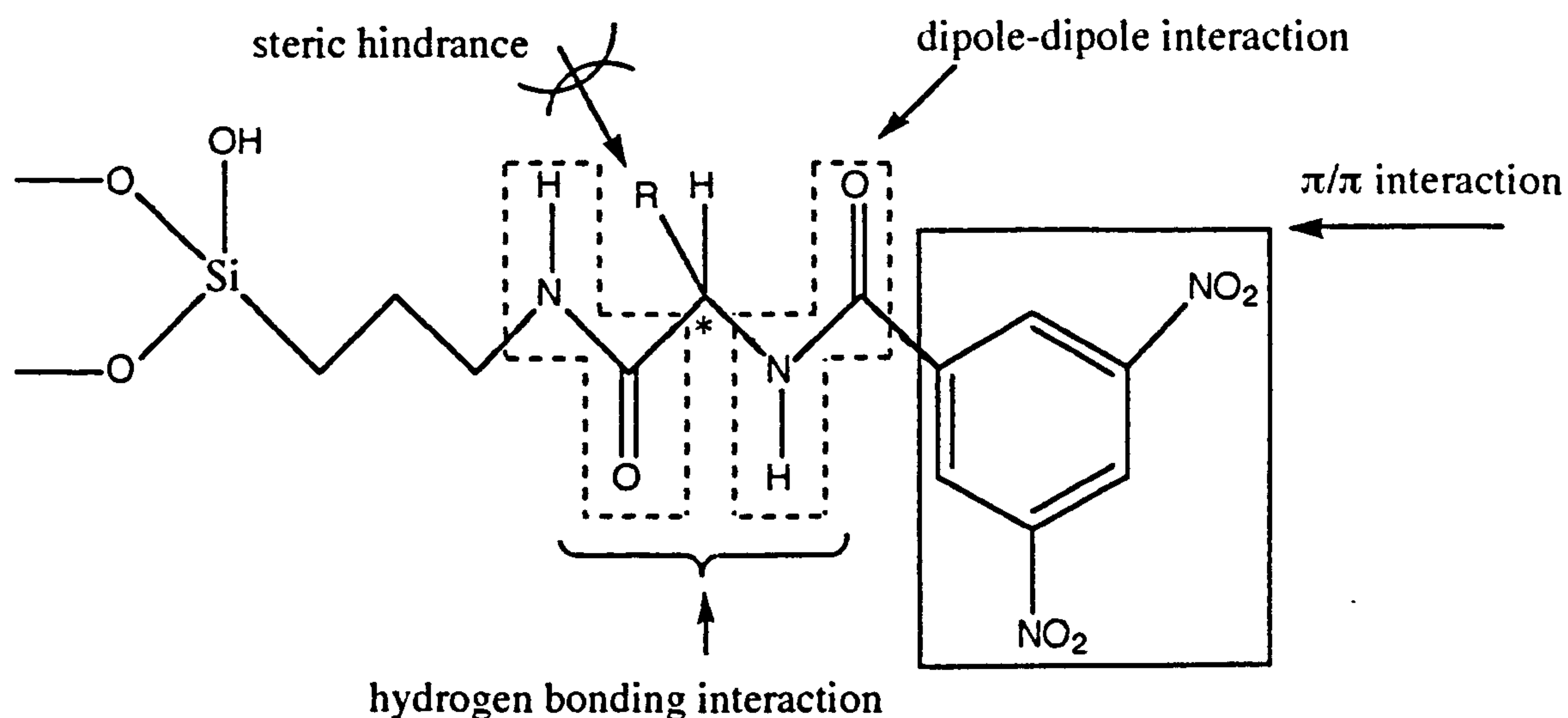


Figure 20 Possible stereoselective sites of interaction on a Pirkle type CSP.

There are several commercially successful CSP's developed by Pirkle, two being the N-(3,5-dinitrobenzoyl)phenylglycine ionically or covalently linked to aminopropyl silica as illustrated in Figure 21.

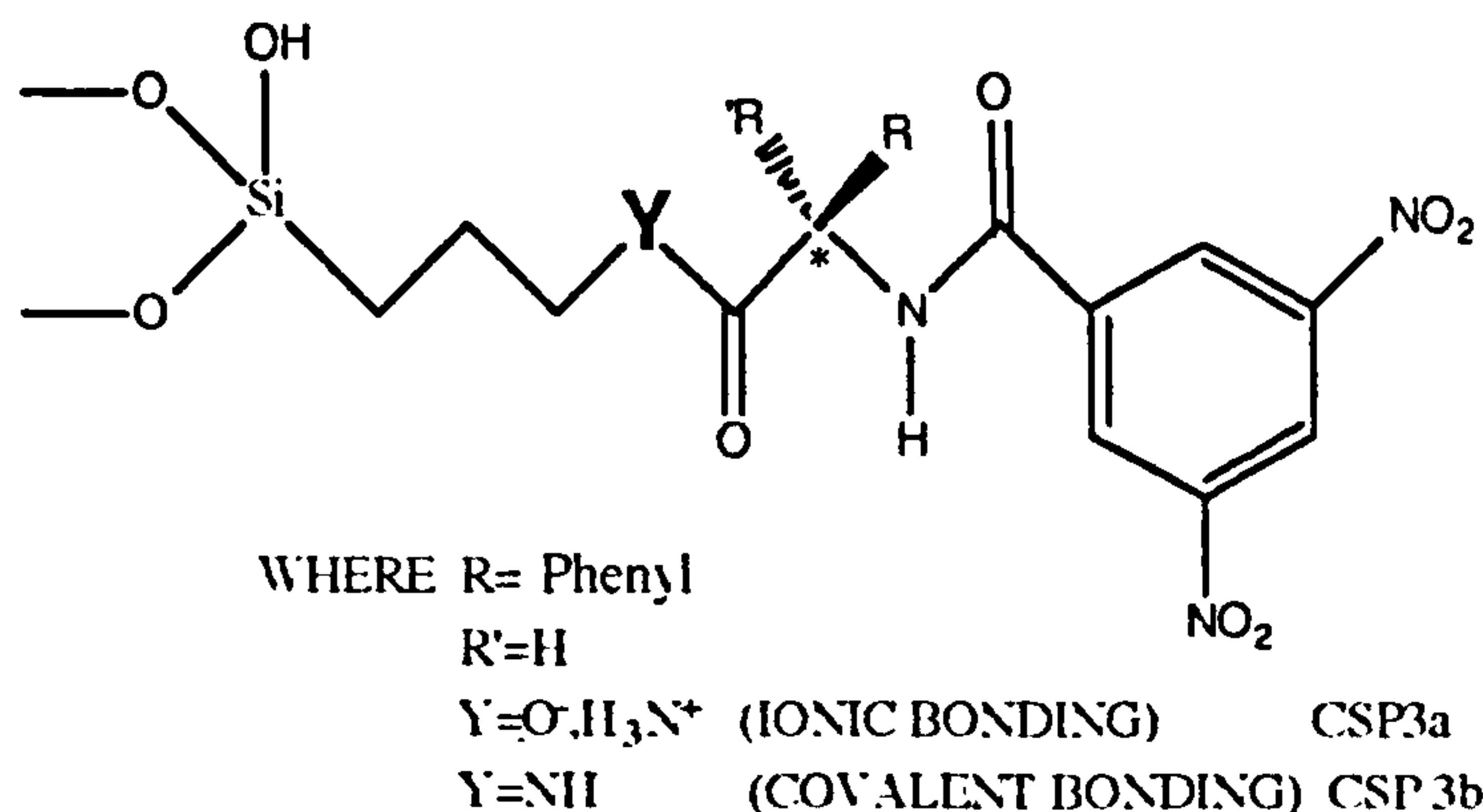


Figure 21 CSP derived from (R) N-(3,5-dinitrobenzoyl) phenylglycine.(CSP 3a and 3b; ionic and covalent bondings respectively.

Other DNB phases followed eg derivatives of leucine have been used to separate a large number of compounds ¹⁰³.

The early commercial availability of Pirkle phases resulted in numerous reports of chiral separations. However, few authors made systematic attempts to propose patterns of chiral recognition consistent with chromatographic data^{104,105,106,107,108}.

Pirkle et al⁵¹ investigated the principles believed to be important in chiral discriminations. They advocated two recognition mechanisms involving either hydrogen bond formation or dipole stacking. The dominance of one of the two competing mechanisms depends mainly on the analyte and the CSP structures. These mechanisms work in opposite stereochemical senses and act via intercalative or non-intercalative processes. The intercalative process involves penetration of the matrix-bound chiral unit when

the CSP chiral strand "recognises" the analyte. This mechanism is favoured by the CSP which has a long anchor chain preventing interference from the surface of the silica support. This is associated by Pirkle with dipole stacking between planar analyte functions and planar amide units in the CSP (see Figure 22). Spectroscopic studies of interactive complexes¹⁰⁸ have led to a greater understanding of the dipole stacking mechanism. The mechanism is disrupted when a long alkyl chain is situated at the innermost end of the analyte preventing resolution.

Side by side hydrogen bonding was first discovered by the reversal of the elution order for enantiomers with certain analyte or spacer chain lengths. Reversal in the elution order occurs when the non-intercalative process selectively retains the opposite enantiomer to that which is most strongly retained by dipole stacking.

Investigations into the resolution of enantiomers on Pirkle type phases^{51,99,109,104}, have provided evidence for chiral recognition mechanisms. To assist in the understanding of these mechanisms, computer assisted modelling has also been applied to the study of these interactions^{110,111,112}. Such studies have provided confirmation that the CSP strand and the analyte may contribute to separation processes, but to compute every significant energy difference is difficult. Whilst the mechanism differs for each analyte, there are some features consistently present in resolved samples, eg π donor functionality or dipolar π groups conformationally influenced by stereogenic centres.

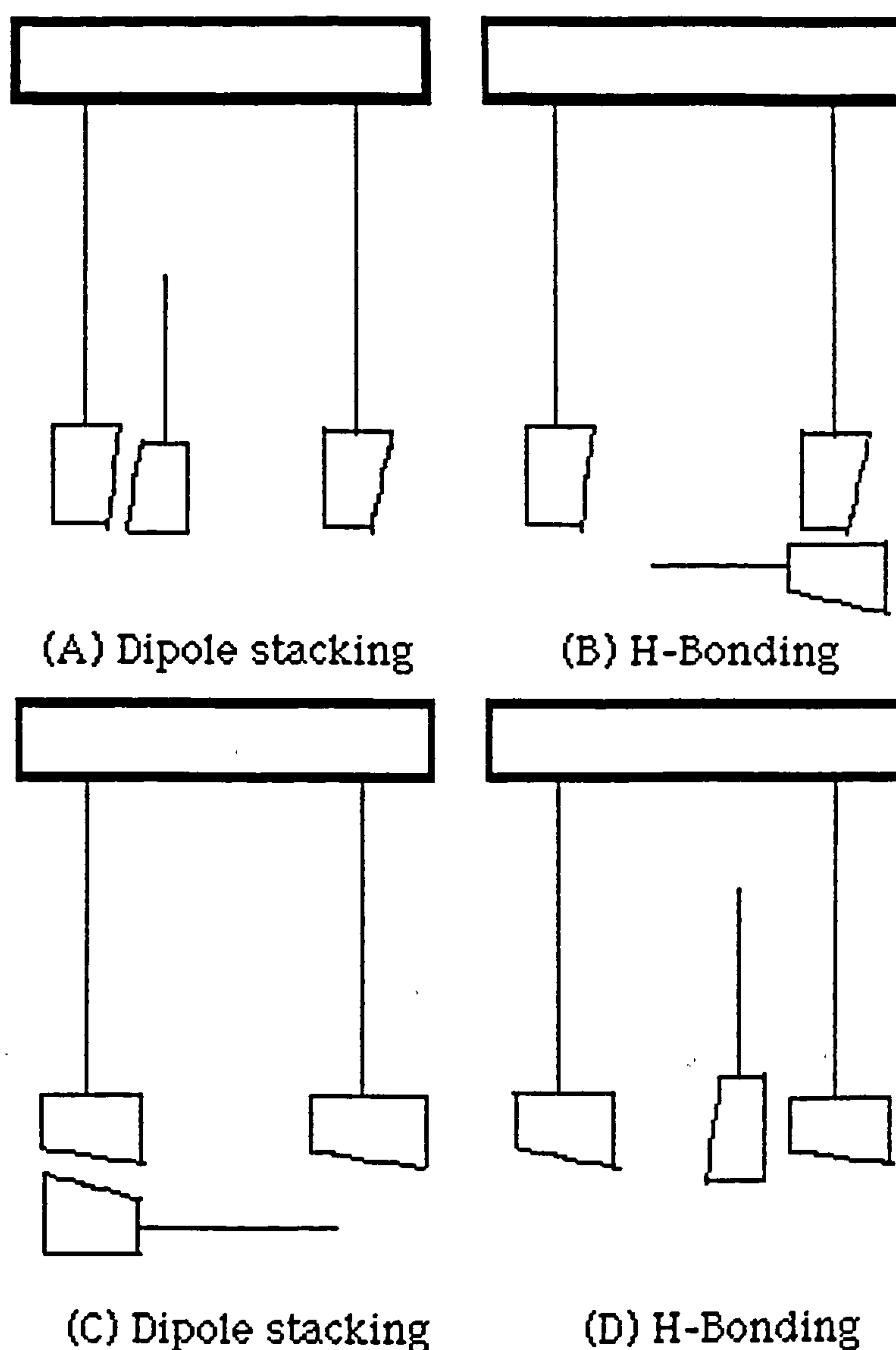


Figure 22 Orientation of attached chiral selector on intercalative([A],[D]) and non-intercalative([B],[C])

There are many examples of "Pirkle type" phases which have been developed by other groups^{113,114,115,116,117}, including those who have applied the ideas of reciprocity^{118,119}, to design second generation CSP's. Oi^{120,121} separated the enantiomers of N- and O-dinitrobenzoyl and dinitrophenyl derivatised amines, alcohol's and related compounds. However, it was observed that great care must be taken when designing a new reciprocal CSP^{122,123}, as the

models do not take into account the influence of silica. Alterations in behaviour of the chiral entity when linked to silica as well as the intrinsic role of silica may explain the observed deviations from the reciprocity concept.

Although many examples of CSP's derived from N-(3,5-dinitrobenzoyl)- α -amino acids are known, there is but one report of such a phase derived from an β -amino acid. Typically β -amino acid derived CSP are conformationally too flexible to afford appreciable levels of enantioselectivity. β -Lactams may be viewed as conformationally constrained β -amino acids and this is the most recent CSP phase to emerge from Pirkle et al¹²⁴. Several CSP's such as (see Figure 23), have been prepared and evaluated. The added conformational rigidity enhances enantioselectivity for some analytes but diminishes it for others owing to enhanced or diminished spacial complementarity of the mutual interaction sites of the CSP and the analytes. One member of the β -lactam family is especially useful for separation of underivatized β -blockers¹²⁴.

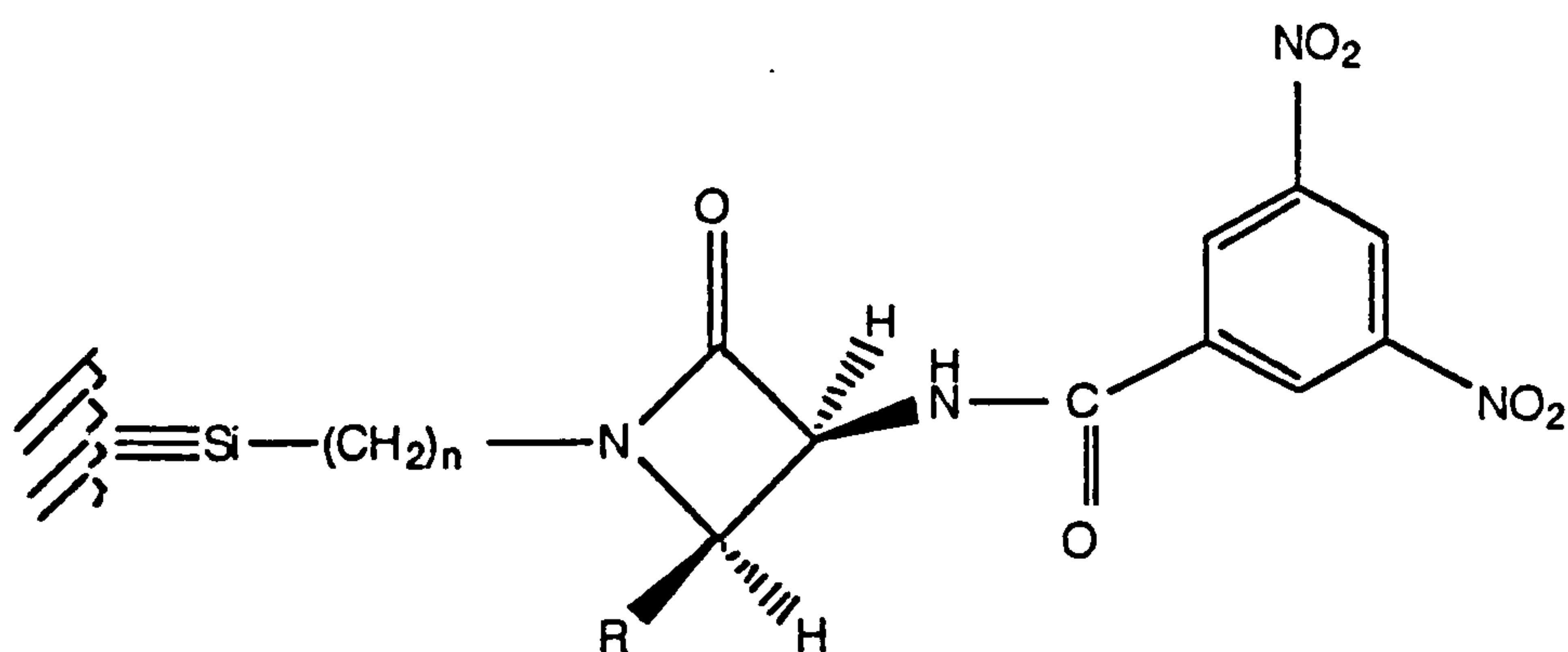


Figure 23 CSP derived from the β lactam family

To design the Pirkle type phase a combination of dipole-dipole (dipole stacking), hydrogen bonding, charge transfer (π - π) and steric interactions should all be considered. As so many of these types of CSP's are becoming commercially available, for application to analytical situations, some form of expert system or chiral database may become essential to simplify the selection.

1.3.4.3 Type C - Charge Transfer Packings

This involves materials designed exclusively for charge transfer complexation. Gil-Av¹²⁵ resolved helicene enantiomers which adopt a helical structure and do not possess any acidic or basic function on the asymmetric molecule to assist chiral recognition. The resolution was achieved by bonding a chiral charge transfer acceptor, tetranitro-9-fluorenylidene-amino-oxypropionic acid (TAPA) to amino propylated silica gel. (see Figure 24).

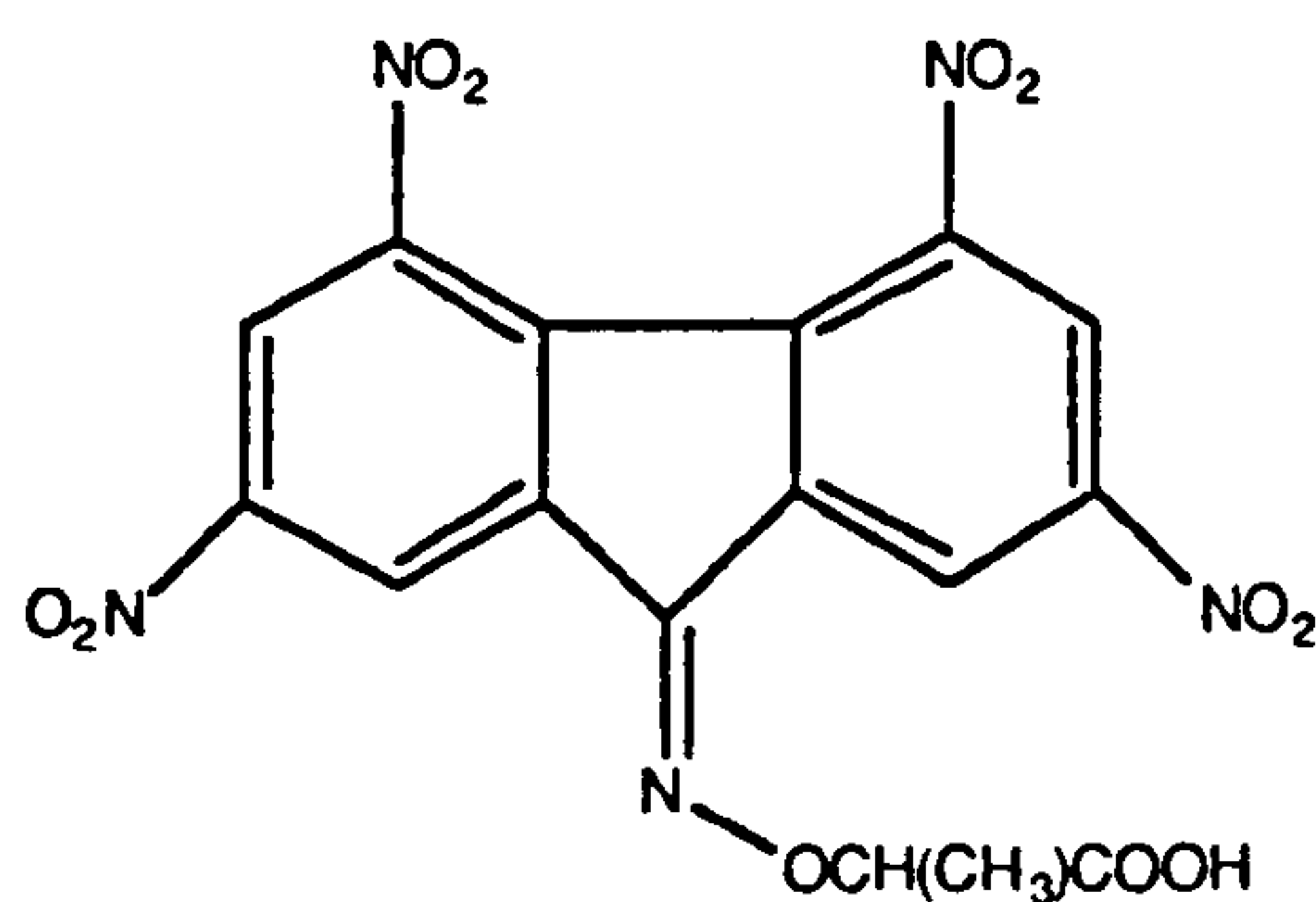


Figure 24 Structure of TAPA

A variety of helicenes have been resolved with high separation factors by HPLC phases containing species such as TAPA^{125,126,127},

an atropisomer of a binaphthyl-2-2-diyl hydrogen phosphate^{128,129}, N-2,4-dinitrophenyl- α -aminoamides^{130,131}, and riboflavin¹³². The resolution of helicene enantiomers by phases which contained a wide range of structural classes of enantiomers, usually including an electron deficient centre such as a nitroaryl ring, led Matlin et al¹³³ to adopt the principal of reciprocity. They prepared a reciprocal phase, bonding hexahelicene-7-yl acetic acid (Figure 25) to APS. The phase proved suitable for the resolution of nitroarylated enantiomers of many racemates.

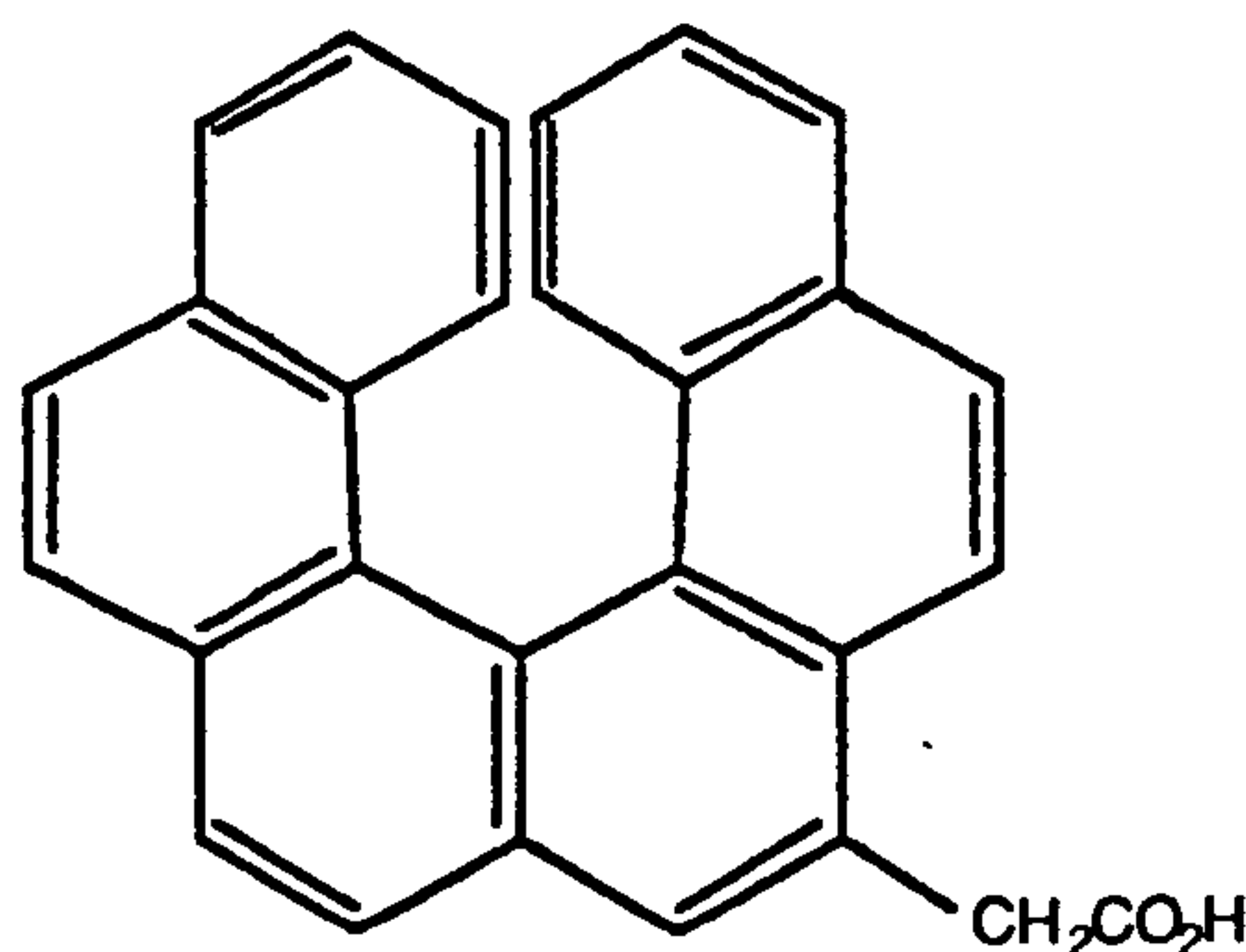


Figure 25 Structure of hexahelicene-7-yl acetic acid

1.3.4.4 Type D- Ligand Exchange Phases

Ligand exchange chromatography (LEC) is a chromatographic process in which formation and breaking of labile coordinate bonds to a transition metal cation is responsible for the separation of complex-forming compounds.

The formation of coordination complexes arises when suitable ligands (those that contain electron donating heteroatoms eg N,O,S

or π electron donating double bonds) donate electrons into the unfilled d-shells of the transition metals. Amongst suitable metals are the bivalent cations of Cu, Zn, Ni and Co. However, Cu^{2+} gives the more stable complexes and is preferred for LEC applications.

The separation of two analytes in LEC is based upon the difference in thermodynamic stabilities of adsorbates that are formed between the ligand, metal cation and the analyte enantiomers. Factors affecting the selectivity and efficiency of separation include pH, mobile phase ionic strength and temperature.

Davankov was the first to report chiral resolutions by LEC¹³⁴ using resin packings of styrene-divinylbenzene to which amino acid residues (eg S-proline) were bonded. The resin was saturated with Cu^{2+} ions giving a reversibly formed bis-proline copper complex. When other amino acids were passed through they exchanged coordination sites with the proline residues at pH 10-11. Although good selectivity's were obtained, efficiencies were very low and complex mobile phases containing buffers and Cu^{2+} ions were necessary. Gubitz et al¹³⁵ greatly improved the efficiency by chemically bonding the amino acid via an alkyl chain to the silica gel support, and the Cu^{2+} ions reversibly attached as previously. It has also been shown by Karger et al^{136,137}, that the efficiency of these packings can be further improved by surrounding the ligand bearing chain with inert spacers such as n-butyl or n-decyl groups. This modification has lead to the resolution of important amino alcohol's including β -hydroxyphenylethylamines, propanolamines and catecholamines.

1.3.4.5 Type E - CSP's Based on Polymers

These CSP's are high molecular mass polymers. Some are essentially natural in origin (such as those derived from cellulose) and others now discussed are synthetic, based upon polyacrylates and polyacrylamides.

In an attempt to mimic and improve upon natural polymers such as cellulose, chiral synthetic polymers have been developed. Many isotactic vinyl polymers $-(CH_2-CXY)_n-$ adopt the helical shape, (a characteristic structure for many natural macromolecules) and are known to exist in equal amounts of right and left handed helices, corresponding to enantiomeric forms. The helical structure is maintained by introducing very bulky X or Y groups. Such polymers can be prepared enantioselectively by conducting the polymerisation process in a chiral environment: for example, by using a chiral catalyst. The first example of this type of optically active polymer was developed by Okamoto¹³⁸, poly(triphenylmethyl methacrylate) PTrMA, being synthesised by asymmetric polymerisation of triphenylmethyl methacrylate (TrMA)¹³⁹. When TrMA was polymerised by a chiral anionic initiator, such as - sparteine-fluorenyllithium or $\pm(2S,3S)$ -dimethoxy-1,4-bis(dimethylamino)butane (DDB)-lithium amide¹⁴⁰, an optically active polymer was obtained (see Figure 26).

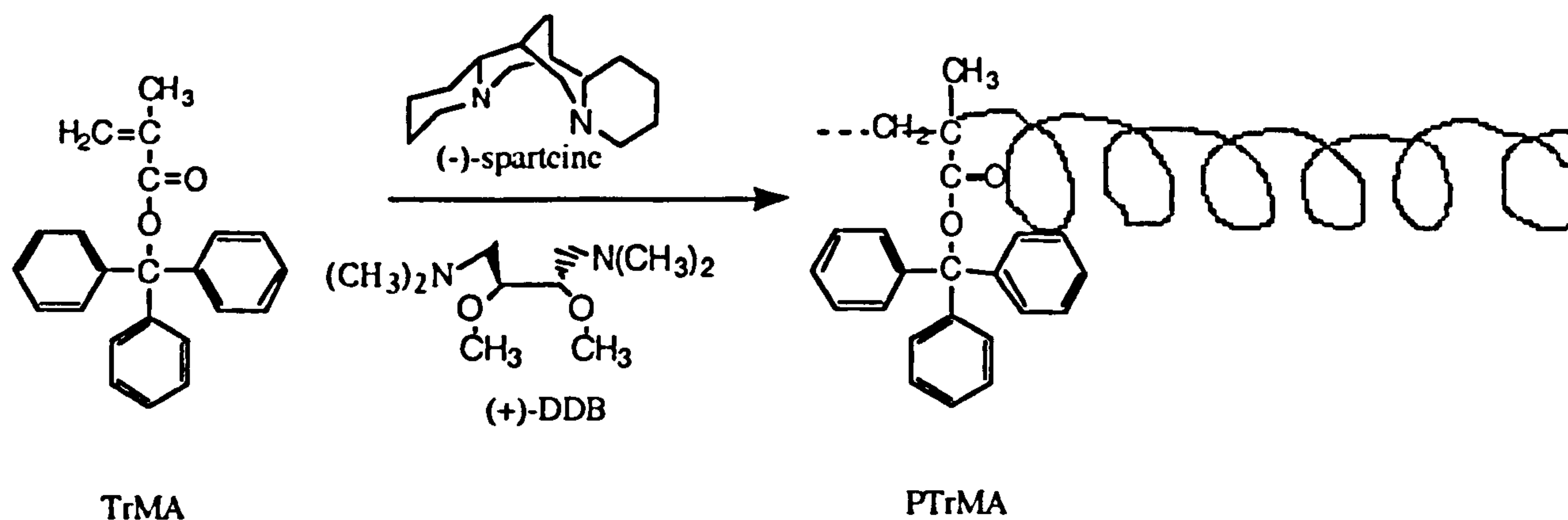


Figure 26 Helical polymer PTrMA

The chirality arises from the helical structure¹⁴¹ fixed by the 3 phenyl groups of PTrMA taking either the left or right handed propeller structure. When coated on silanised silica, the resulting CSP was suitable for the separation of racemic alcohols, esters, amines and hydrocarbons¹⁴². It has been generally found that separable analytes possess a rigid non-planar structure, eg trans disubstituted cyclic molecules with 3-6 membered rings¹⁴³.

There is an almost infinite number of possibilities for preparing synthetic polymer CSP's from chiral monomeric units and the recent advances in coating silica with polymers¹⁴⁴ should facilitate progress in this area in the future.

1.3.4.6 Type F - Protein Bonded Phases

From a chromatographic point of view, the complexity of the molecular structure of proteins makes them very interesting, especially as highly selective interactions between certain

molecules and proteins in biological systems have been documented.

The early examples of this type of CSP based upon bovine serum albumin (BSA)^{145,146}, or acid glycoprotein¹⁴⁷, were of limited value in that the columns suffered from a lack of reproducibility and a tendency to deteriorate in use. The more recent commercial phases, however, appear to be more reliable.

BSA is an extensively investigated protein^{148,149}. Its amino acid sequence has been completely determined and the secondary structure is known. However, no complete X-ray crystallographic data is available. It is a globular transport protein¹⁵⁰ known to have a number of different types of binding sites for ionic substances. There are several ways to immobilise BSA. Stuart and Doherty¹⁵¹ bound BSA to agarose and resolved D,L-tryptophan. Allemark¹⁴⁶ used HPLC grade silica to support the protein and found this CSP suitable for the separation of enantiomers of amino acids and their derivatives¹⁵². Other silica based BSA columns have been reported^{153,154,155}, and have shown resolution of a wide variety of anionic and neutral compounds, but they are unsuitable for cationic solutes. Successful analysis of racemates^{156,157,159} in biological fluids have been performed when the CSP phase is coupled to an achiral column. The presence of aromatic and polar groups in the solute appears to be important for enantioselectivity¹⁵¹. The efficiency and selectivity of the BSA phase is extremely sensitive to variations in pH and phosphate buffer concentration in the mobile phase¹⁵².

α -1-Acid glycoprotein (AGP) is a globular protein found in human plasma, of high molecular mass (about 41000) containing 181 amino acid units and 5 carbohydrate units. The resolution of a series of basic drugs was reported by Hermansson in 1983¹⁵⁹ by using silica bonded AGP¹⁶⁰. This CSP was also useful for the resolution of acidic racemates¹⁵⁰. The AGP CSP is a good analytical column to use in clinical and pharmacological studies^{161,162} because it works excellently in aqueous buffers. The effect of the main operational parameters (ie temperature, pH, ionic strength, flow rates of mobile phase) has been studied in detail by Schill et al¹⁶³. Due to the complex structural features of AGP, the mechanism of the interactions cannot be easily determined. Nevertheless, AGP is one of the most widely used CSP's.

1.4.CARBOHYDRATES

1.4.1 Classification of Carbohydrates

Carbohydrates are classified according to their degree of polymerisation as monosaccharides, oligosaccharides and polysaccharides. Monosaccharides are simple sugars which cannot be hydrolysed into smaller molecules and are the building blocks from which the two other classes are assembled, by the formation of glycosidic linkages. The simple polymers of monosaccharides are defined as oligosaccharides which contain between two and ten monosaccharide units. Polysaccharides are higher molecular weight sugar polymers containing in excess of ten monosaccharide unit. However, in nature, there are very few carbohydrates which

contain between five and fifteen sugar residues. The majority of naturally occurring polysaccharides contain about 85-100 sugar residues with cellulose having a mean molecular weight distribution equivalent to 1000 residues.

1.4.2 Oligosaccharides

1.4.2.1 Glycosidic Bond Formation

When two or more monosaccharides are joined together, the bond that holds them together is known as the glycosidic bond. This is formed between the hydroxyl group on the anomeric carbon atom of one of the monosaccharides and any hydroxyl group on the other monosaccharide through the formation of an acetal (see Figure 27)

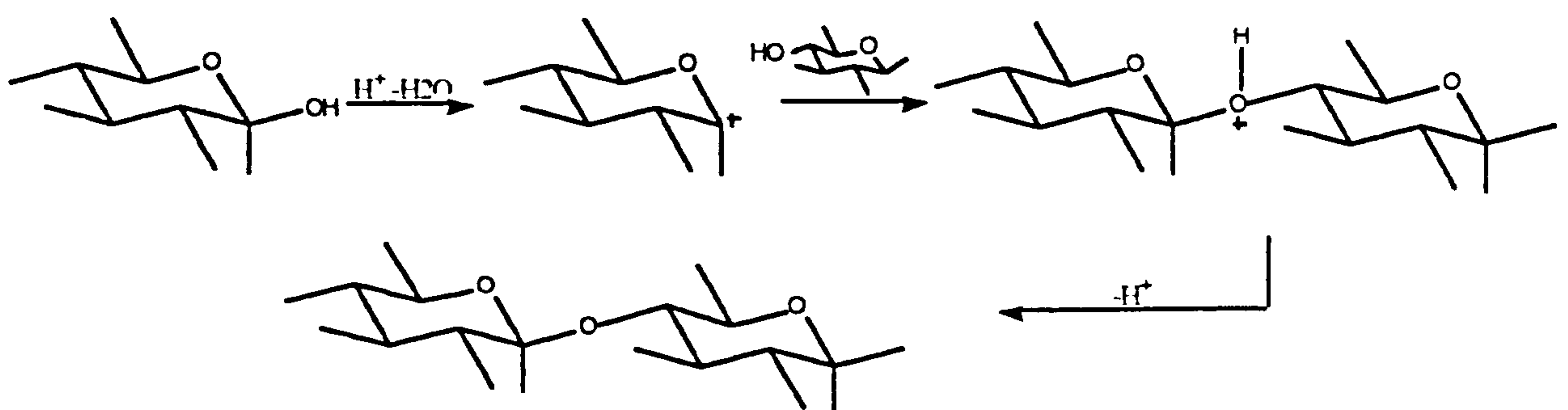


Figure 27 Formation of a glycosidic bond.

Formation of a disaccharide by the condensation reaction between two identical hexopyranose ring structures can result in many different isomers due to glycosidic linkages between C-1 of one residue, in either anomeric configuration, and C-2, C-3, C-4 or C-6 of the other pyranose residues. These are termed (1,2) α -D-

(1,3) β -D-linkages etc. where α and β refer to the anomeric configuration at C1.

1.4.2.2 Occurrence of Oligosaccharides

Many oligosaccharides can be obtained by the partial hydrolysis of polysaccharides in which the oligosaccharide frequently represents the repeating sequence of the polymeric carbohydrate.

1.4.2.2.1 Cellobiose

When cellulose (cotton fibres) is treated for several days with sulphuric acid and acetic anhydride, a combination of acetylation and hydrolysis takes place¹⁶⁴ and the octaacetate of (+) cellobiose is obtained. Alkaline hydrolysis of the octaacetate yields (+) cellobiose itself (see Figure 28).

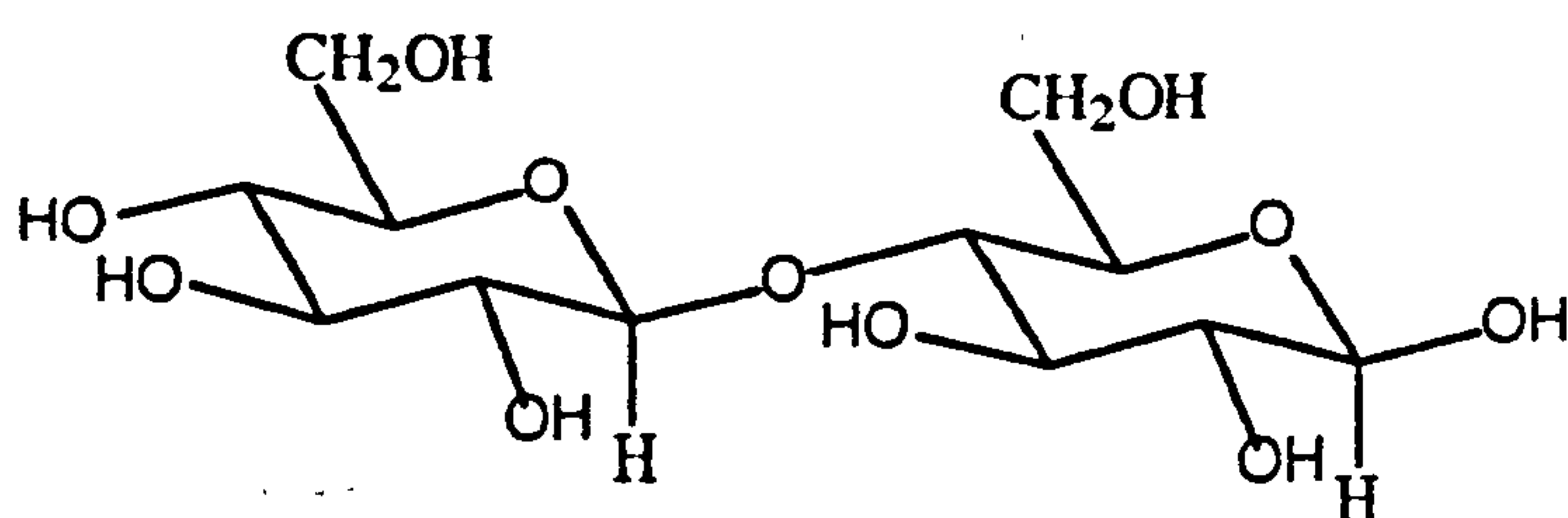
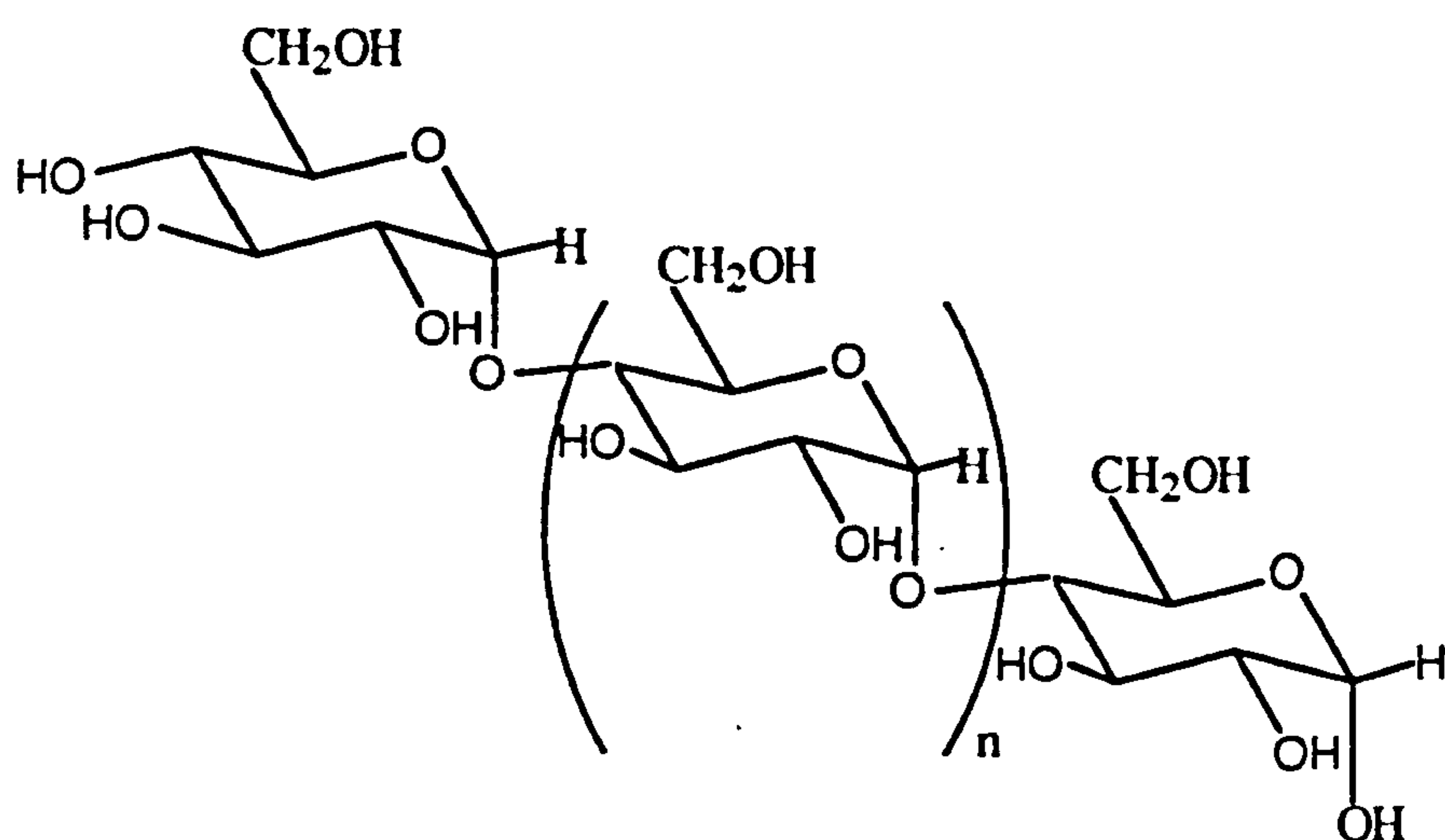


Figure 28 Structure of Cellobiose (4-O- β -D-Glucopyranosyl- β -D-glucopyranose)

1.4.2.2.2 Maltose and Oligosaccharides of the Malto Series

Due to the low abundance in nature of the lower molecular weight polymers in the maltose series, preparation of these compounds is dependent on the breakdown of larger polymers. Published methods for this preparation are based upon the enzymatic hydrolysis of starch¹⁶⁵ acid hydrolysis of starch¹⁶⁶, amylopectin¹⁶⁷ or amylose¹⁶⁸, and salivary amylase digestion of amylose¹⁶⁹. Since amylose is a cheap, readily available α -D-(1,4) polymer of D-glucose, it makes an ideal starting material. Under controlled conditions, the products from the enzyme or acid catalysed hydrolysis of amylose are a mixture of several lower molecular weight oligomers eg maltotriose, maltotetraose, maltopentaose etc. (see Figure 29).



Where :-

- n=0 Maltose
- n=1 Maltotriose
- n=2 Maltotetraose
- n=3 Maltopentaose
- n=4 Maltohexaose
- n=5 Maltoheptaose
- n=6 Maltooctaose
- n=7 Maltonanaose

Figure 29 Structure of the α -malto-oligosaccharide series

The separation of the components previously performed by thin layer chromatography^{170,171,172,173} or by column chromatography on cellulose¹⁷⁴, charcoal¹⁷⁵ and exclusion gel^{176,177}, has often been time consuming and difficult. Considerable progress has been made in the analytical separation and quantitation of starch-derived oligosaccharides by HPLC using columns packed with amine-modified silica gel^{178,179,180}, reverse phase silica^{181,182} and ion exchangers^{183,184,185}. A few attempts^{186,187} have been made to apply these techniques to preparative carbohydrate isolations, but most researchers have been reluctant to adopt these methods because of their great expense and their requirements for special instrumentation. Hicks *et al*¹⁸⁸ described several new methods for preparative HPLC of malto-oligosaccharides. They concluded that aminopropyl silica (APS) columns had the greatest capacity and highest resolving capability. However, the APS phase was also the least durable, requiring careful pre-treatment of samples to avoid rapid loss of capacity.

1.4.3 Polysacharrides

Polysaccharides are natural macromolecules of many hundreds or even thousands of monosaccharide units per molecule. As in oligosaccharides, these units are held together by glycosidic linkages which can be broken by hydrolysis. All macromolecular carbohydrate materials have definite, 3 dimensional structures.

1.4.3.1. Structure

The geometry of the individual sugar rings in a polysaccharide is essentially rigid but the relative orientations of component residues (i.e. rotation) about the glycosidic linkage determines the overall conformation of the polysaccharide. Two torsion (rotational) angles are required in order to define the glycosidic bond between two carbohydrate residues a) and b) (see Figure 30).

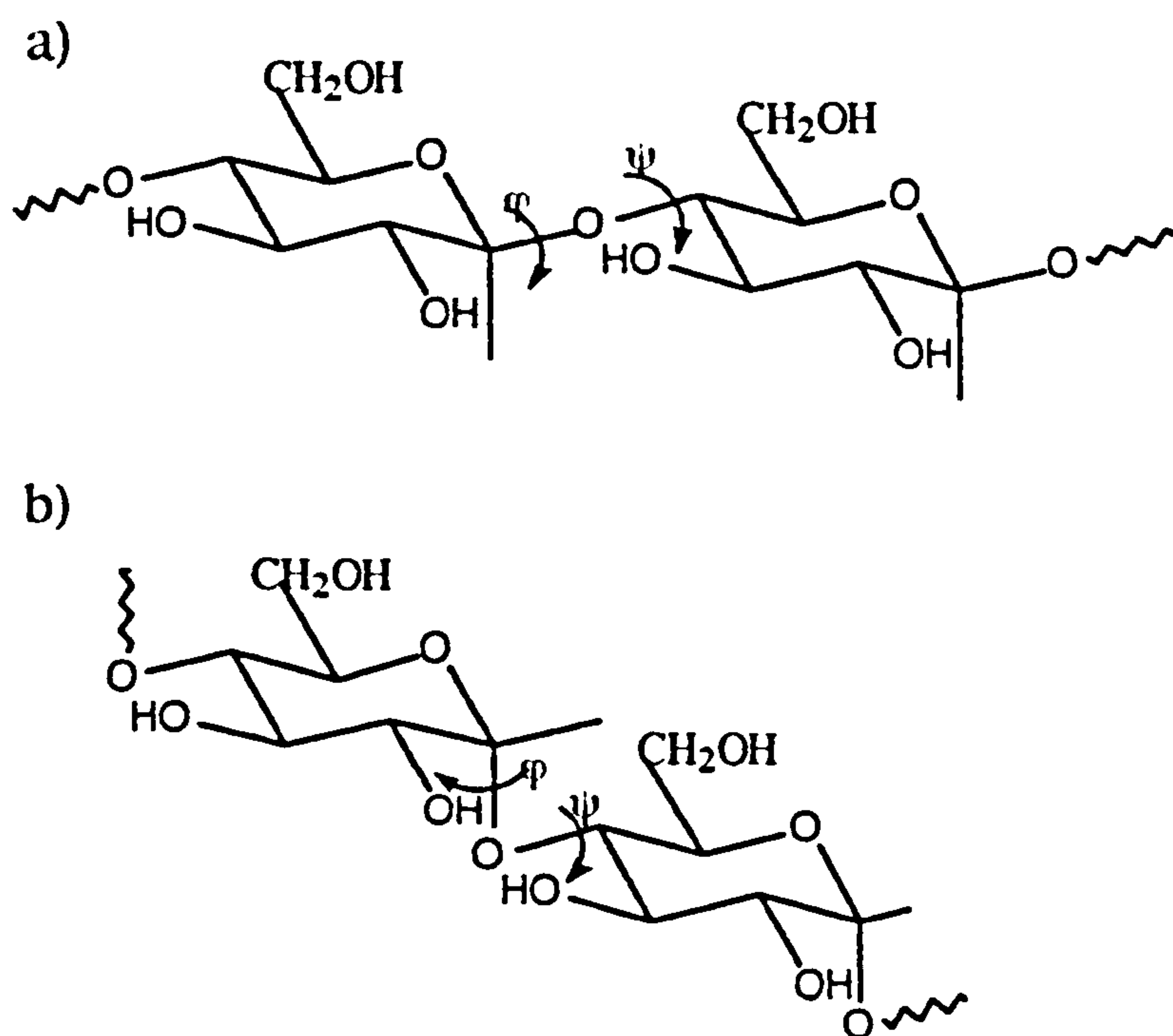


Figure 30 Rotation of individual residues about the glycosidic bond in a) cellulose b) amylose

The angle ϕ is the rotation around the bond between the anomeric carbon atom and the oxygen atom that join the two residues, the angle ψ is around the bond between the glycosylated oxygen atom of residue a) and the carbon atom of residue b). The range of values obtained for rotational values ϕ and ψ is restricted by

steric hindrance between the two adjacent ring residues. The restriction is greatest for glycosidic linkages involving axial groups (i.e. amylose), and for residues containing such bulky substituents in equatorial positions adjacent to the glycosidic linkage. This has the net result of stiff chains with, for example, coil shapes predominating in solution.

Repetition of the monomeric sequence in the structure of polysaccharides leads to sterically regular gross conformations which are held rigid by interactions between hydroxyls. A useful concept which has been used to describe the overall chair conformation is to regard the structure as a helix and specify two parameters, namely the number n of monomer residues per helix turn and the projected length h of each monomer residue on the helix axis. These parameters can be calculated from the values of φ and ψ ¹⁸⁹. The allowed conformations of homopolysaccharides have values of n and h which fall into ranges which permit distinct types to be identified. Type A is the extended ribbon structure with values for n from 2 to + or - 4 and h is close to the absolute length of the residue. Where values of n cover a wider range ($n = 2 +$ or -10) and h approaches zero, the B type conformation is obtained (see Figure 31)

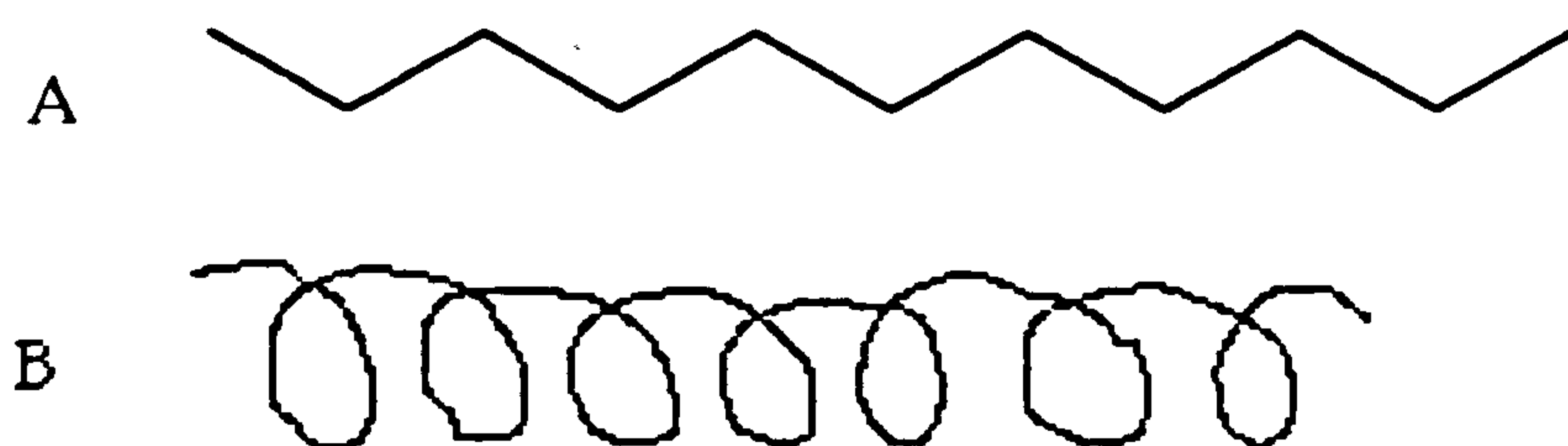


Figure 32 Type A extended ribbon, type B flexible helix

Of these two types, (1,4) β -D-glucans adopt the type A structure and type B is obtained with (1,4) α -D-glucans.

The characteristic properties of cellulose are due to the tendency of the individual chains to form microfibrils through inter and intra-molecular hydrogen bonding to give a highly ordered structure. This regular arrangement of molecules is sufficient to allow X-ray diffraction patterns to be obtained and these patterns indicate that cellulose from almost every natural source has the same pattern.

Two crystalline forms of amylose exist depending upon its origin. Type 1, from cereal starches occurs as a right-handed double helix in which the chains are parallel within the helix and are packed in an anti-parallel fashion. Type 2 from tuber starches is a double stranded helix which has a right-handed helical conformation. The helices are anti-parallel and have an open channel in a hexagonal array which is filled with water molecules (up to 4 times more water content than in type 1). Many properties of amylose can be explained by its molecular conformation in solution. Its normal conformation in aqueous solution is that of a random coil and this will complex with agents to form a helical structure consisting of about 6-D-glucose residues per helical turn. This is the conformation that gives rise to the characteristic blue colour of amylose-iodine complexes, with the iodine occupying a position at the centre of the helix.

1.4.4 Reaction of Sugars

1.4.4.1 Derivatisation

The hydroxyl groups of a carbohydrate material react readily as nucleophiles with corresponding reagents in the presence of an acidic catalyst or a basic catalyst to give a derivative. This reactivity is used extensively in carbohydrate chemistry for protection and activation.

One example of derivatisation is the reaction between the hydroxyl groups of glucose and acetic anhydride in the presence of an acid catalyst or basic catalyst such as sodium acetate or pyridine. The peracetylated product is a water insoluble derivative that crystallises readily and can be used as an intermediate for the Koenigs-Knorr glycosidation reaction.

1.4.4.2 Koenigs-Knorr Procedure

The Koenigs-Knorr method of glycosidation consists of a two-step reaction (see Figure 32): introduction of a leaving group at the anomeric centre and catalytic nucleophilic substitution of this leaving group.

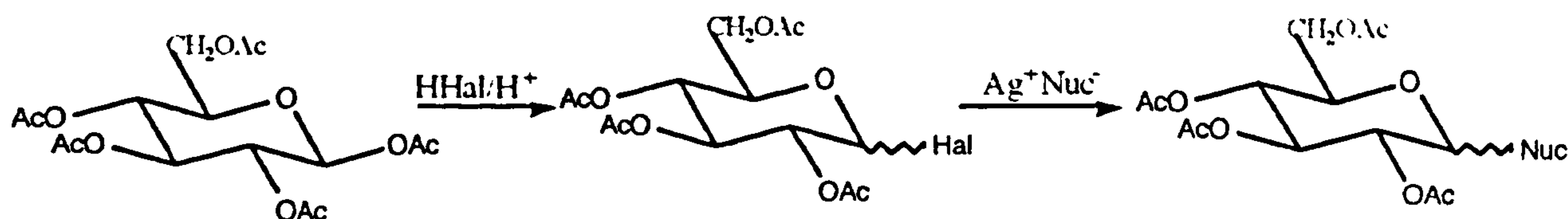
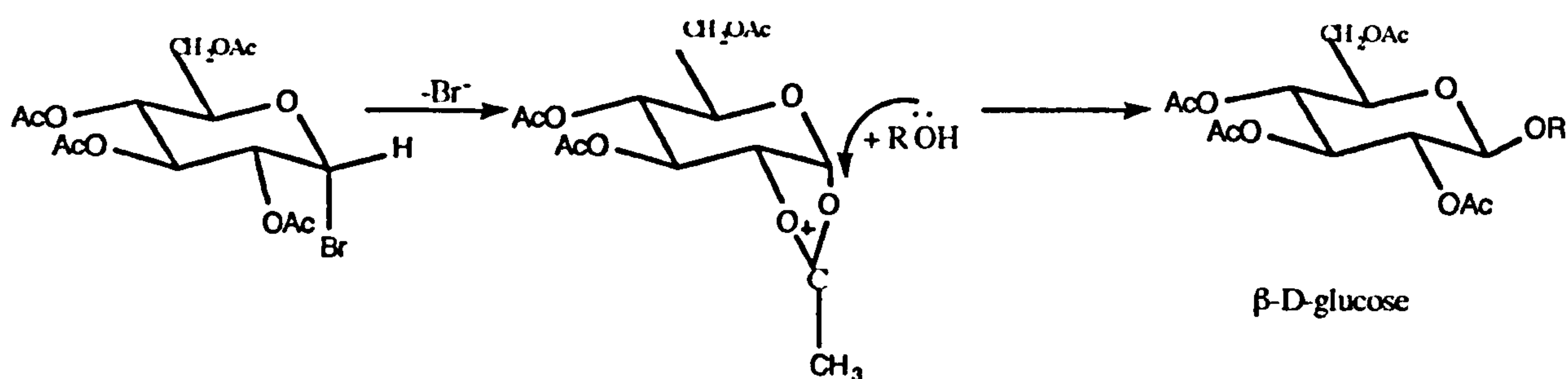


Figure 32 Koenigs-Knorr process

In general, for a sterically uniform α or β coupling, both steps must proceed under steric control. This is achieved mainly by exploitation of stereo-electronic effects (anomeric effects) and neighbouring group participation. The reactivity of the glycosyl halides can be varied over relatively wide ranges by the choice of halogen and the protecting group. For the displacement of the glycosyl halide, recent reviews^{190,191}, have indicated that the following procedures have been particularly suitable.

a) The neighbouring group assisted procedure (Scheme 5)



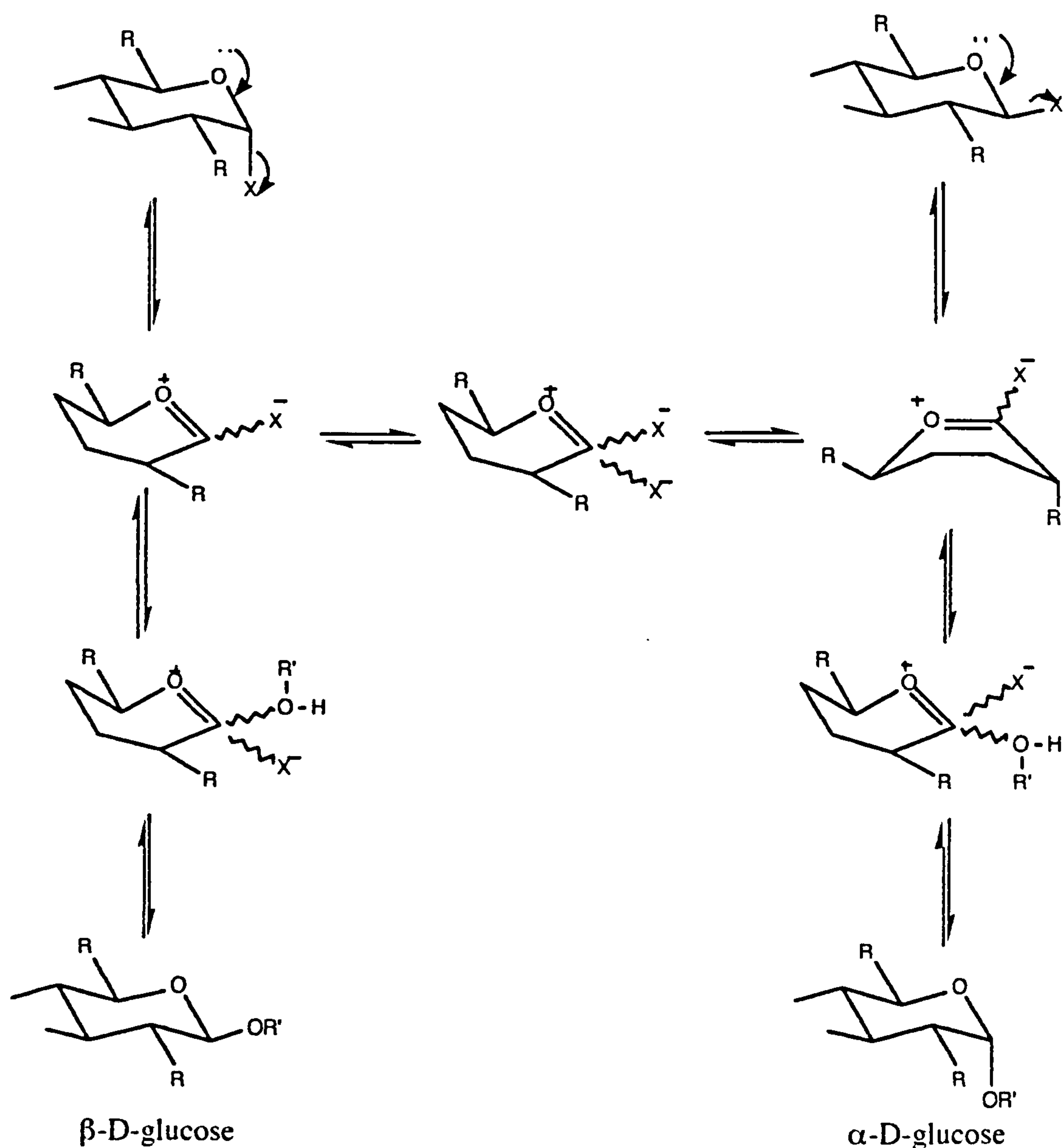
catalyst : $\text{Hg}(\text{CN})_2$, HgCl_2 , AgClO_4 , Ag triflate

Scheme 5 Neighbouring group assisted procedure

In this procedure the more stable α -D-halide (with a neighbouring group active substituent at C2 e.g. an O-acetyl group) is substituted. A stabilised cyclic acyloxonium intermediate is formed via a carbonium ion and can be opened at the anomeric centre by a nucleophile only in a direction trans to the substituent at C-2. As can be seen in Scheme 5, in the D-gluco series, this opening results in the β -D-glucopyranoside.

b) The non-neighbouring group assisted procedure (Scheme 6)

In the in situ anomerisation procedure, a non-active substituent must be present at C2. Use is made here of the possibility of producing, via suitable catalysts, an equilibrium between the α halide and the β halide that establishes itself quickly via ion pairs (Scheme 6)¹⁹². As the β -D-halide (top right) is de-stabilised by an anomeric effect, which is particularly powerful for halide substituents, there is a higher portion of the α -D-halide (top left) .



Scheme 6 In Situ Anomerisation procedure (with non-neighbouring group participation)

If the kinetics of the glycosidation reaction are considered, it is found that the reaction of the unstable β -D-halide to give the α -D-glycoside (right path Scheme 6) is fast in comparison to the conversion of the more stable α -D-halide into the β -D-glycoside (left path Scheme 6). Under certain reaction conditions, this difference in reaction rates can be used so that the reaction

proceeds almost exclusively along a fast path from the β -D-halide to the desired α -D-glycoside¹⁹³.

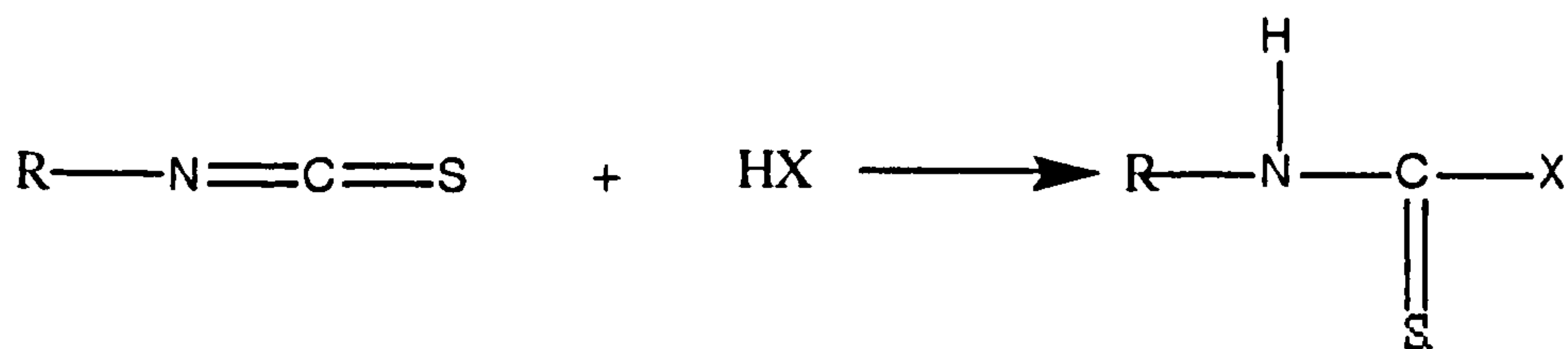
Apart from trialkylammonium halides, the most suitable catalysts for starting from α -D-halides in the in situ anomerisation procedure are mercury salts and silver perchlorate and triflate. The application of these general procedures has lead to excellent results^{190,191}. In spite of the development of efficient variants severe inherent disadvantages of the Koenigs-Knorr procedure cannot be overcome. These disadvantages include the following:-

- (i) Relatively harsh conditions are needed for the generation of the glycosyl halide, so there are solvent limitations.
- (ii) The glycosyl halides exhibit low thermal stability and must often be generated in situ and at low temperatures.
- (iii) The glycosyl halides are highly sensitive to hydrolysis.
- (iv) Heavy metal salts are expensive and toxic.

1.4.4.4 Monosaccharide Isothiocyanates:- Synthesis, Chemistry and Preparative Applications

Sugar isothiocyanates have been used extensively for the synthesis of heterocyclic derivatives of sugars¹⁹⁴. They are important reagents as the NCS group has strong electrophilic character and undergoes many reactions, such as nucleophilic additions (Scheme 7) and cycloadditions¹⁹⁵. Nucleophiles attached

to a labile hydrogen atom that is able to protonate a nitrogen atom can react with isothiocyanates, whereas the electronegative residue bonds to the carbon atom of the -NCS group.



Scheme 7

1.4.4.4.1 Methods of Synthesis of Sugar Isothiocyanates

Sugar isothiocyanates are readily synthesised by a variety of methods from the corresponding halides¹⁹⁵. The most general and widely used method for the preparation of sugar isothiocyanates is the classical Fischer¹⁹⁶ synthesis. This involves treatment of an acylated glycosyl halide with an inorganic thiocyanate in a polar solvent, directly forming either a thiocyanate or an isothiocyanate.

Kinetically controlled reactions of the thiocyanate anion with organic compounds (among them halides) may lead to the thiocyanates by nucleophilic attack of the sulphur atom, to the isothiocyanates by nucleophilic attack of the nitrogen atom, or a mixture of the two. The thermodynamically more stable isothiocyanate may also be formed by a secondary isomerisation reaction. In common with other ambident species¹⁹⁷, the relative nucleophilicity¹⁹⁸ $k_{\text{S}}/k_{\text{N}}$ of the sulphur and nitrogen atoms of the thiocyanate anion may depend on the interplay of different

factors, including the solvent, the catalyst, counter ions, the temperature, the nature of the leaving group and the concentration and the structure of the organic compound (particularly the geometry of the molecule). Such physicochemical methods as infra-red¹⁹⁹ and proton nmr²⁰⁰ spectroscopy permit rapid detection of isocyanate products.

Sugar thiocyanates rearrange readily to corresponding isothiocyanates ^{201,202,203,204,205}. The first comprehensive article by Renson²⁰⁶ concerned with the isomerisation of organic thiocyanates into isothiocyanates suggested that the halides may react by an S_N1 or S_N2 mechanism. The thiocyanate is formed by the S_N1 mechanism and, on isomerisation, produces the isothiocyanate. Isomerisation of organic thiocyanates to isothiocyanates is also discussed in other articles ^{207,208,209,210,211}.

Emil Fischer¹⁹⁶ obtained the first sugar isothiocyanate, 2,3,4,6 tetra-O-acetyl-β-D-glucopyranosyl isothiocyanate (2) by treatment of 2,3,4,6-tetra-O-acetyl-α-D-glucopyranosyl bromide (1) with silver thiocyanate in anhydrous xylene. Smith and Emerson²¹² showed that the isothiocyanate (2) could also be prepared by the thermal isomerisation of the corresponding thiocyanate (3), obtained by treatment of (1) with potassium thiocyanate in acetone.

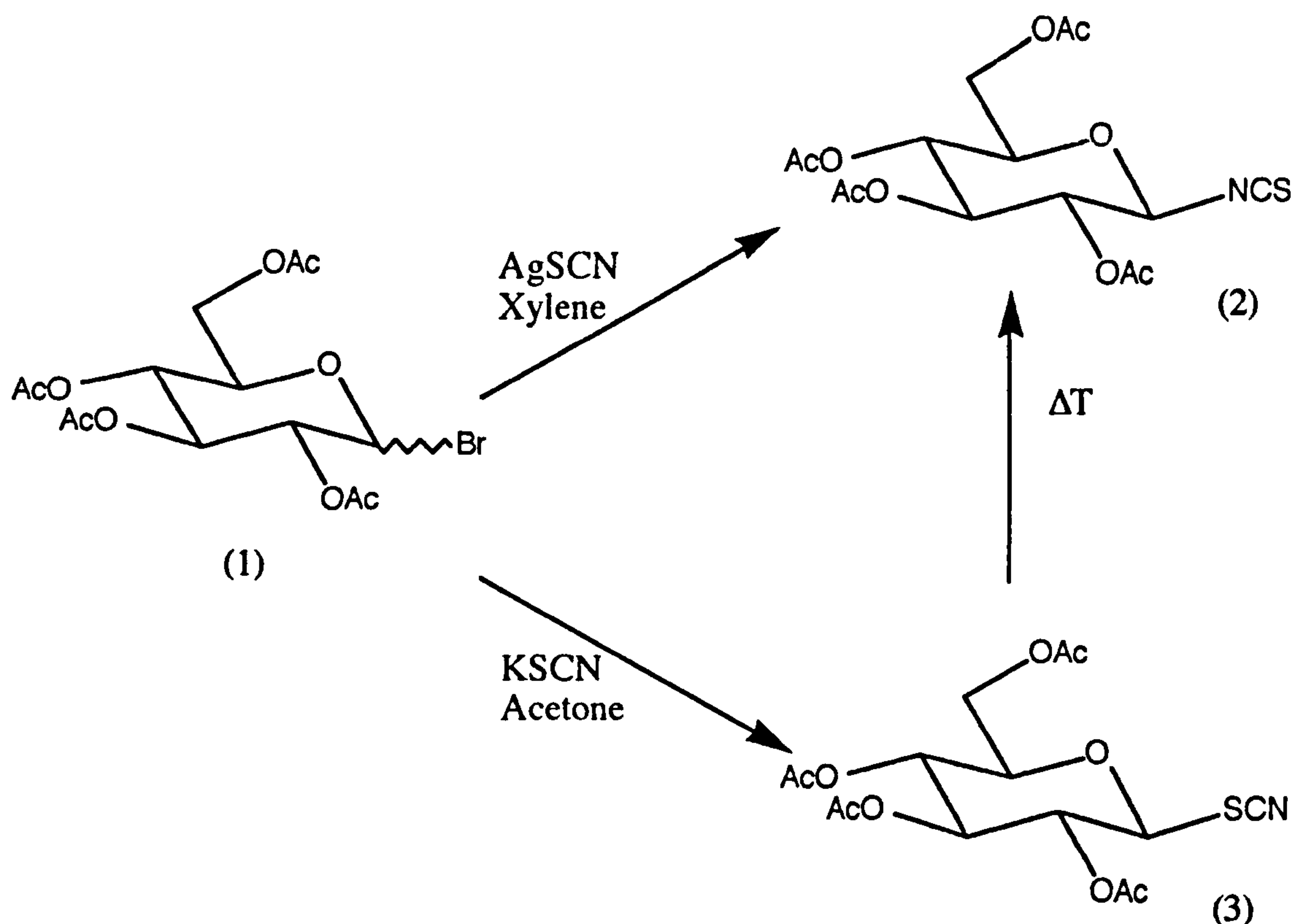


Figure 33 Fischer synthesis of sugar isothiocyanates from the reaction of the sugar halide and an inorganic thiocyanate salt.

Many modifications of the Fisher method for the preparation of sugar isothiocyanates have been made including, for example, use of nonpolar solvents and silver thiocyanates^{213,214,215,216,217}. Johnson²¹⁸ prepared per-O-acetyl- β -D-glucopyranosyl isothiocyanate with silver thiocyanate in dried xylene and Michael et al^{213,215,216} showed that the introduction of the isothiocyanate group in the anomeric position of the sugar can be performed using silver thiocyanate in acetonitrile. Ogura²¹⁷ has synthesised disaccharide isothiocyanates in yields of 75% using a procedure in which lead thiocyanate or silver thiocyanate was added to

peracetylated D-glycosyl bromide in dry benzene or a benzene-toluene (1:1) mixture.

Other thiocyanates have been employed in this reaction. Khorlin *et al*²¹⁹ reported that the treatment of peracetylated lactosyl bromide with ammonium thiocyanate at 60°C gave the lactosyl isothiocyanate in a 49% yield. However, from the results of the infra-red spectrum ($\text{N}=\text{C}=\text{S}$ 2120cm^{-1}), their experiments suggested the possibility that lactosyl thiocyanate might have been formed in this reaction. De las Heras²²⁰ described a new, cheap procedure for the synthesis of sugar isothiocyanates by the reaction of acetylated sugar halides with potassium thiocyanate in a polar aprotic solvent (acetonitrile) in the presence of a tetraalkylammonium salt as catalyst. Traces of isomeric thiocyanate were detected in the products, suggesting that the reaction may occur via the preliminary formation of the glycosyl thiocyanate, which in presence of the catalyst isomerises to give the corresponding isothiocyanate²²¹.

1.4.4.4.2 Reaction of Isothiocyanates with Ammonia and Amines

The earliest chemistry of sugar isothiocyanates can be traced back to Emil Fischer's paper in 1914, in which he described the conversion of isothiocyanates into thioureido derivatives by the action of ammonia.¹⁹⁶ Since then, the thioureido derivatives have become important intermediates in synthetic approaches to nucleoside analogues. Ogura and Takahashi^{222,223} detailed the reaction of sugar isothiocyanates with amines. They found that

treatment of 2,3,6-tetra-O-acetyl- β -D-glucopyranosyl isothiocyanate with ammonia in methanol gave the corresponding thioureide (see Figure 34) in 74% yield.

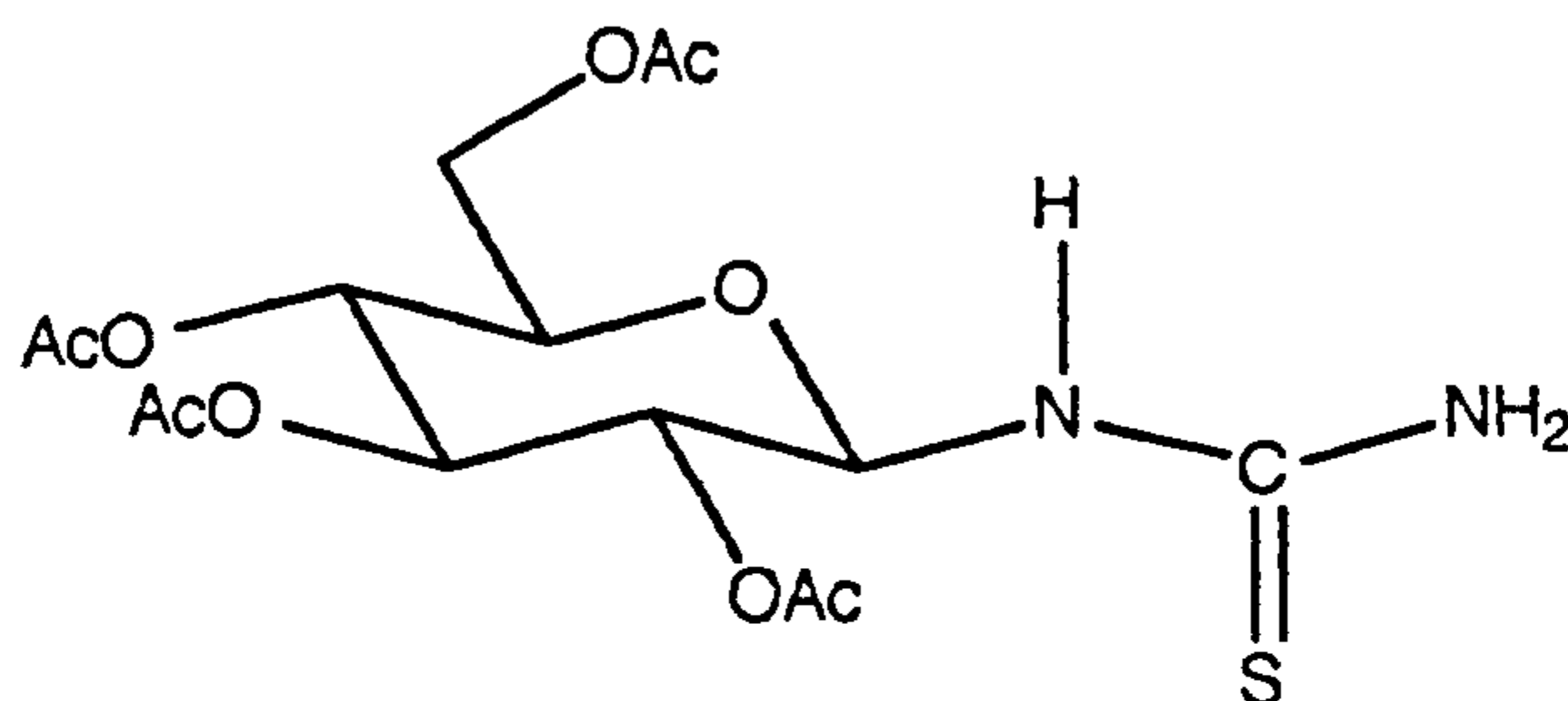


Figure 34 Structure of a thioureide

Similar reactions of the same isothiocyanate with amino compounds (benzylamine, N-propylamine) gave N-glycosyl-N'-substituted thioureides in excellent yields²²⁴.

1.4.4.4.3 Spectroscopic Properties of Sugar Isothiocyanates

The infra-red spectra of isothiocyanates and thiocyanates are more informative than proton nmr and uv data, especially for larger oligosaccharides. In contrast to thiocyanates, which have a sharp band at $2175\text{-}2100\text{cm}^{-1}$, the isothiocyanates are distinguished by a strong, wide band in the range of $2020\text{-}1990\text{cm}^{-1}$.

CHAPTER 2

OPTIMISATION OF THE SUPPORT FOR COATED CHIRAL STATIONARY PHASES IN HPLC

In previously published work⁶⁸⁻⁸⁰, polysaccharide derivatives as chiral stationary phases have been supported on a silanised silica of pore size 4000Å and at a loading of 20 per cent. However, no justifications for the selection of this pore size or loading have been presented. Therefore, at the outset of the present work it was decided to investigate the effect of the amount of CSP loaded onto the silica support and the influence of the silica pore size on the performance of the chiral phase.

2.1 INFLUENCE OF CHIRAL STATIONARY PHASE (CSP) LOADING

The porous packing material used to support the chiral stationary phase should be coated with a homogenous layer of uniform thickness. In this way a maximum liquid-liquid interface is produced, permitting a large number of distribution stages in the column. In this study, the silica used was Hypersil APS (Table 1) which was coated using the evaporation technique¹³ with three different loadings of cellulose tri(phenylcarbamate) (CPC). The prepared phases were packed into 15cm x 0.46cm (i.d.) stainless steel columns using hexane; 2-propanol.

Pore size Å	Particle size dp μm	Pore volume Vp cm ³ /g	Surface area SBETm ² /g
120	5	0.65	180

TABLE 1 Physical properties of Hypersil APS

The performance of each column was measured, the dead volume t_0 was determined by eluting with a non-retained solute, (1,3,5-tri-*tert*-butyl benzene), and the capacity factor, the selectivity coefficient and resolving power determined by eluting with five racemic mixtures: stilbene oxide, 2,2,2-trifluoro-1-(9-anthryl) ethanol (2,2,2-TFAE), benzoin, trogers base and 1-phenylethanol.

It has been established²²⁵ that the total porosity of a column packed with a porous support is about 0.84, whereas the porosity of the column packed with non-porous glass beads is about 0.42. These values indicate that the porosity due the pore system is also 0.42. If the pores are completely filled with a CSP, the porosity ϵ_t of such a column is practically identical with ϵ_t value of a column packed with non-porous glass beads.

The porosity of a column is the fraction of the bed volume which is occupied by the mobile phase and is defined²²⁶ as:-

$$\epsilon_t = \frac{4F}{\pi d_u^2} = \frac{4F(t_0)}{\pi d^2 L} \quad (16)$$

where F is the flow rate ($\text{cm}^3 \text{ min}^{-1}$); u is the mean linear velocity L/t_0 ; t_0 is the elution time (seconds), L the length of the column (mm) and d the column diameter (mm).

As can be seen in Equation (16), the accuracy of the porosity measurement is limited by any error in the determination of the volume $\pi d^2 L$ of the unpacked column, or in the measurement of t_0 and the flow rate F .

%LOADING	t_0 /sec	$F/\text{cm}^3\text{min}^{-1}$	L /mm	ϵt	HETP
5	189.0	0.54	125	0.78	0.133
10	189.0	0.52	125	0.75	0.114
20	186.6	0.49	125	0.70	0.107

Table 2 Effect of loading on column porosity (ϵt) and HETP for a non-retained solute

For a non-retained solute there is a decrease in the height equivalent to a theoretical plate as the CSP loading increases. This is due to an overall increase in the volume occupied by the coated phase reducing the space available for band broadening. The filling of the space within the porous silica structure is supported by the decrease in porosity with each increment of loading.

Taking the value of 0.42 as the porosity of the pore system for aminopropylsilica and utilising the determined porosity data it is

possible to evaluate the filling of the porous structure with loading using Equation (17).

$$\frac{(0.84 - \epsilon_t)}{0.42} \times 100 = \% \text{ pores filled} \tag{17}$$

where ϵ_t is the determined porosity.

LOADING	%filled pores
5	14
10	20
20	33

Table 3 Filling of the pores with loading increase

One would expect a linear increment of the filling of the pores with loading. However, Table (3) shows that this did not occur, which may be due to not all of the measured pore volume being accessible to the coated phase. The result is a "sticky support" due to the CSP coated on the outside of the silica rather than within the pores.

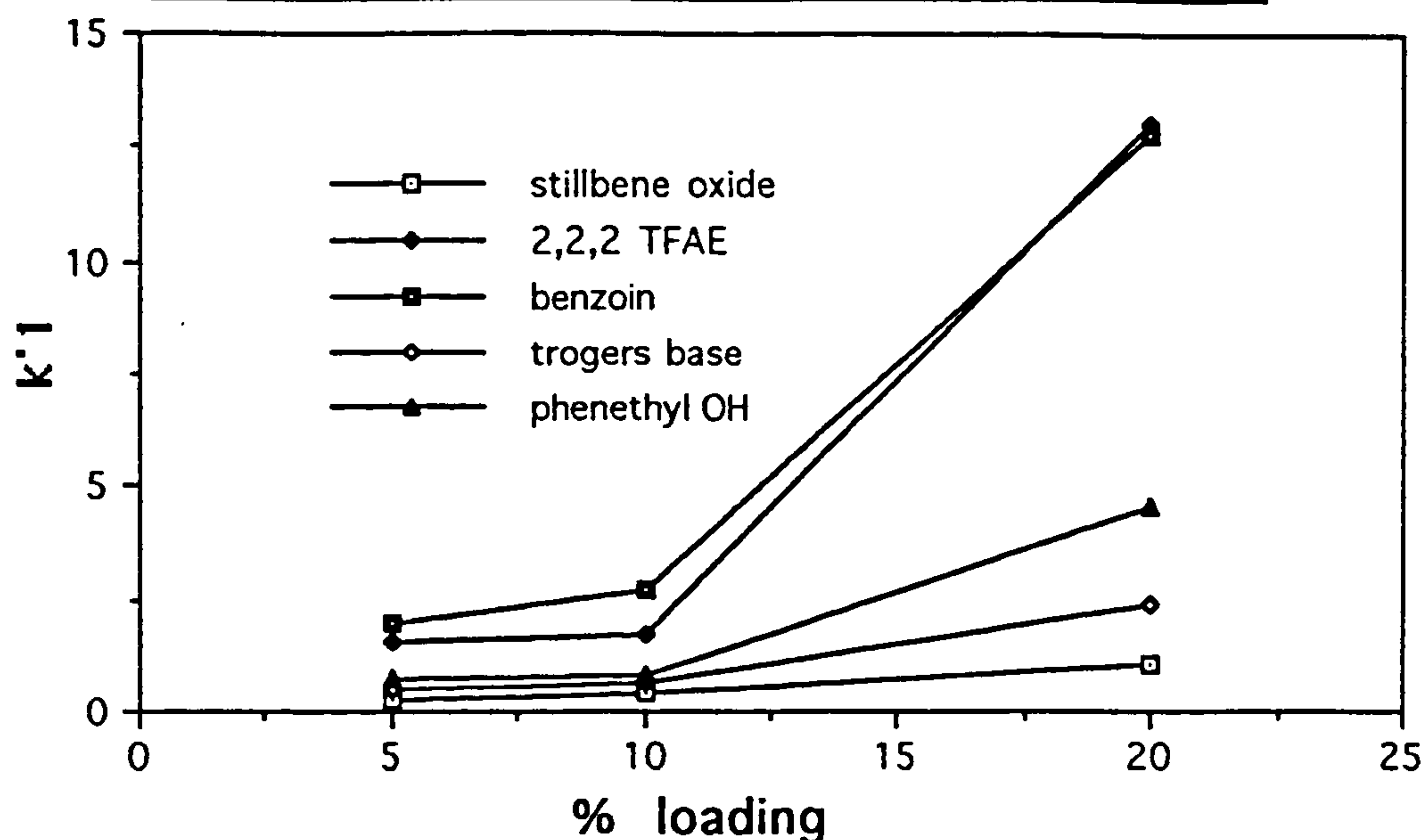
Assuming that the retention of a solute is due to the intermolecular forces (e.g. dipole-dipole, hydrogen bonding and π - π interactions), a linear relation between the capacity factor k' and the percentage loading should be observed. The capacity factor relates to the equilibrium distribution of the sample within the column. k' is defined as the ratio of the total amount of solute in the stationary phase to the amount in the mobile phase at equilibrium.

$$k' = \frac{C_s V_s}{C_m V_m} = K \frac{V_s}{V_m} \quad (18)$$

Here, V_s and V_m are the volume of stationary and mobile phases and $K = C_s/C_m$ is the well known distribution constant, which measures the equilibrium distribution of x between the stationary and mobile phase. From equation (18), k' is proportional to V_s , and therefore the k' values of the sample bands will change with the relative loading of support by the stationary phase. Graph 1 shows a non-linear relationship from which it is difficult to draw conclusions as only three loadings were investigated. For example, at 10% loading a threshold effect may be reached and a linear relationship may be in operation beyond this point. At low loading the non-linearity may be attributed to uneven coating of the high surface area silica support, in which additional adsorption interactions contribute to retention. For example, interactions with the silica support may be due to insufficient or thin film thickness arising from low CSP concentrations or poor coating procedure.

As expected, each solute is retained longer on the column when the percentage loading of CSP is increased as shown in Graph 1.

GRAPH 1 Effect of the %loading of CPC on the Capacity factor k' for each solute

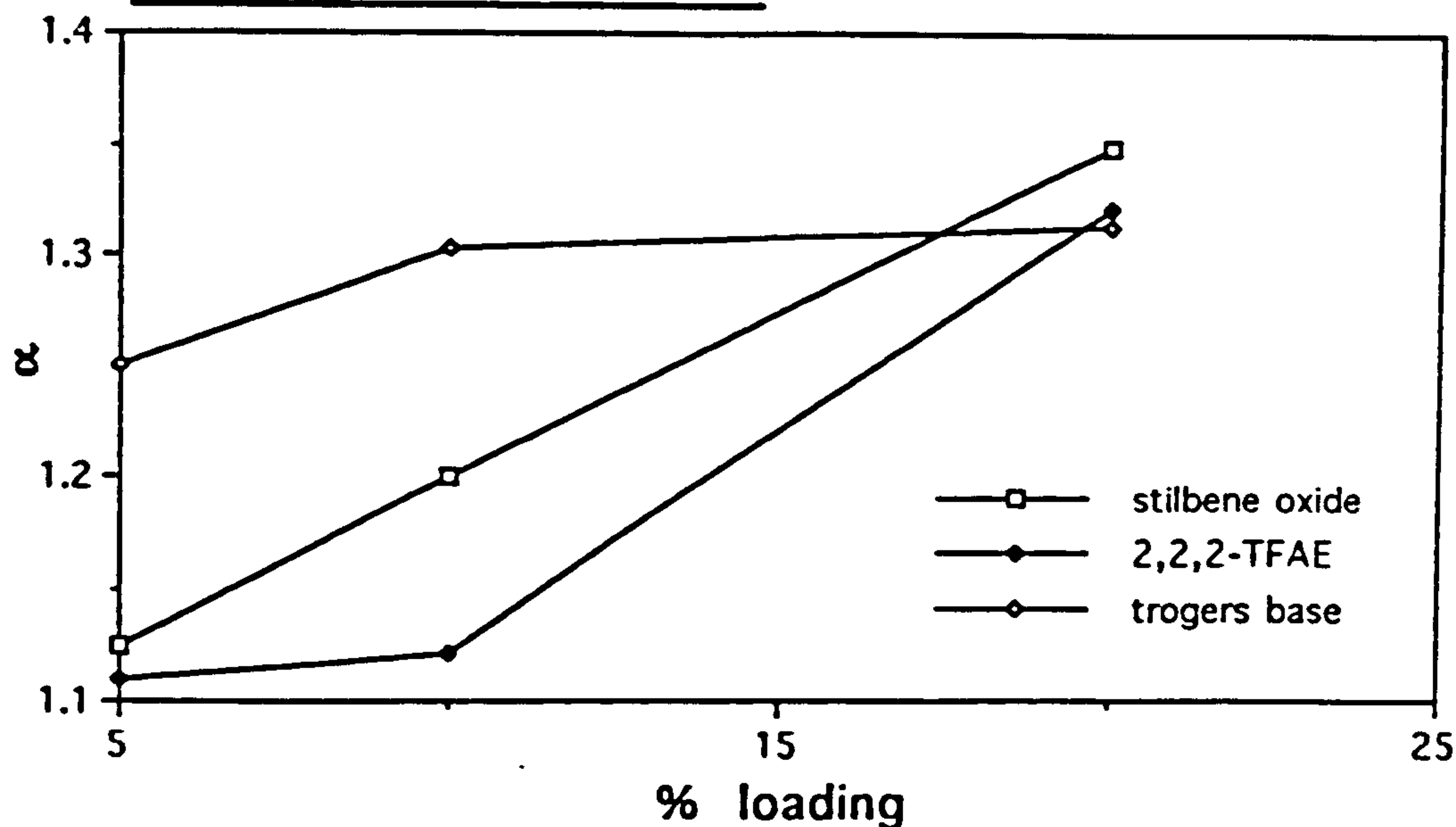


HPLC conditions; flow rate $0.6 \text{ cm}^3/\text{min}$; mobile phase 97.5% hexane 2.5% IPA

For the range of solutes tested the CPC phase showed chiral recognition towards three racemic compounds: stilbene oxide; 2,2,2-trifluoro-1-(9-anthryl) ethanol, (2,2,2-TFAE) and trogers base, at all levels of loading.

The selectivity coefficient α is associated with the molecular forces between the solute and the two phases. For good separation of the two components, the relative retention should range from 1.05 to 2.0 and for all three solutes this criterion is reached (see Graph 2). The degree of selectivity for each solute is different. The selectivity for 2,2,2-TFAE is improved at higher loadings; the improvement in selectivity for trogers base is more noticeable from 5 to 10 per cent CPC loading and stilbene oxide shows a linear relation between selectivity and per cent loading. The best selectivity for each solute is obtained at a higher per cent loading.

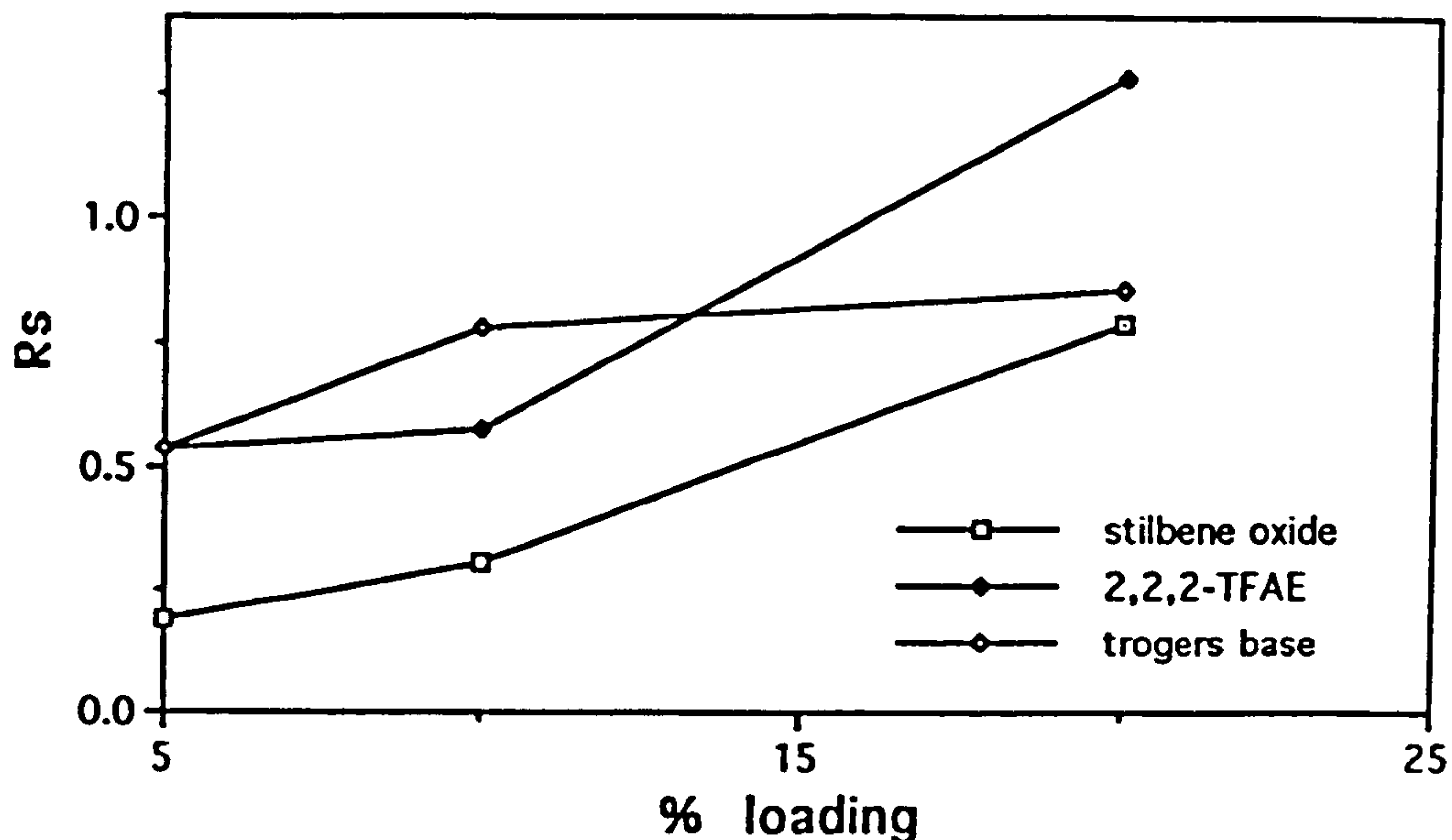
GRAPH 2 Effect of loading on selectivity for the resolved solutes



HPLC conditions; flow rate $0.6 \text{ cm}^3/\text{min}$; mobile phase 97.5% hexane 2.5% IPA

The resolution R_s for each pair of enantiomers is also increased as the loading is increased (see Graph 3). However, the experimental values of R_s indicate that baseline resolution (when $R_s > 1.25$) was only achieved for one compound, 2,2,2-TFAE, on 20 percent loading.

GRAPH 3 Effect of loading on resolution



HPLC conditions; flow rate 0.6 cm³/min; mobile phase 97.5% hexane 2.5% IPA

The resolution of adjacent peaks, if inadequate, can be improved in two independent ways; either by increasing the peak separation and/or by decreasing peak width. These two approaches to improving resolution are achieved by altering the relative retention α , the capacity factor k' and the number of theoretical plates²²⁷ N . This is represented by:-

$$R_s = \underbrace{\left(\frac{1}{4}\right)}_i \underbrace{\left[\frac{k'}{1+k'}\right]}_{ii} \underbrace{\left[\frac{(\alpha-1)}{\alpha}\right]}_{iii} \sqrt{L/H} \quad (19)$$

where $k' = \frac{k'_1 + k'_2}{2}$

Considering the first two terms k' and α : k' , as we have seen, is dependent upon column loading of the stationary phase and the partition coefficient should be chosen such that k' of a given pair has a value ranging from 1-5. The selectivity term (α), depends solely on the molecular forces between the solute and the two phases. As the stationary phase is chosen and fixed, then the relative retention can only be varied by changing the mobile phase composition. The optimum range for α is 1.05 to 2 and an increase in α from 1.05 to 1.1, for example improves resolution by a factor of 2 for the same L/H . As the experimental values fit these two criteria of k' and α , then poor resolution may result from the efficiency of the column which is characterised by N . On substituting the experimental values of R_s , k' and α into equation (19) we find that H (see Table 4) the plate height increases as the loading is increased.

SOLUTE	%loading	α	k'_1	R_s	H mm
STILBENE OXIDE	5	1.125	0.276	0.188	0.140
	10	1.200	0.405	0.308	0.216
	20	1.349	1.075	0.709	0.323
2,2,2TFAE	5	1.110	1.600	0.533	0.106
	10	1.121	1.737	0.571	0.117
	20	1.322	13.00	1.278	0.249
TROGERS BASE	5	1.250	0.476	0.538	0.131
	10	1.304	0.622	0.778	0.122
	20	1.313	2.350	0.860	0.308

Table 4 The determined efficiency of the columns (H) for each solute HPLC conditions; flow rate $0.6 \text{ cm}^3/\text{min}$; mobile phase 97.5% hexane 2.5% IPA

The HETP has increased for the columns as the loading increases for a retained solute (Table 4), from the values obtained for a non-retained solute (see Table 1). This is a sign of hindered mass transfer and this will reduce the overall efficiencies of the columns, resulting in a decrease in resolving power. The processes that take place in the column giving rise to non-ideal behaviour and the consequent increase in plate height H are described by the abbreviated Equation (20).

$$H = Av^{0.33} + B/v + Cv_{\text{mobile}} + Cv_{\text{stat}} \quad (20)$$

Where A , B and C are constants, Cv_{mobile} and Cv_{stat} are contributions from slow equilibration between mobile and stationary phases. Cv_{stat} is related to the thickness of the coated layer by:-

$$Cv_{\text{stat}} = \frac{Csdf^2\mu}{Ds} \quad (21)$$

Where df is film thickness, Cs = plate height coefficient μ = mobile phase velocity and Ds = solute diffusion coefficient in stationary phase.

The Cv_{stat} term results from the resistance to mass transfer at the solute/stationary phase interface. It is proportional to df^2/Ds where df is the effective thickness of the stationary phase and Ds is the diffusion coefficient of the solute in the stationary phase. Slow mass transfer in the stationary phase means a longer time spent in the phase for a solute molecule. The faster the mobile phase moves through the column and the slower the rate of mass

transfer, the broader the solute band will be. The rate of mass transfer can be improved by reducing the film thickness (i.e. H decreases as per cent loading decreases) of the stationary phase, and so reducing the distance that a solute molecule must diffuse within a stationary phase, albeit with consequent loss of retention and selectivity for the solute.

To summarise, the best retention, selectivity and resolution occurred at the higher 20 percent loading for all three solutes. However, at the higher loading the overall efficiency of the column was reduced due to slow mass transfer or non-uniform film thickness.

It was considered possible that the efficiency of the more heavily loaded columns might be improved by choosing a larger pore size to accommodate the coated chiral stationary phase.

2.2 EFFECT OF PORE SIZE ON THE CHROMATOGRAPHIC BEHAVIOUR OF CHIRAL PHASES

In chromatography, silica is the most widely used support. It is commonly accepted^{36,228,229} that its chromatographic properties depend on its specific surface area, its pore volume, its average pore diameter and the concentration of silanol groups per unit surface area.

In this investigation into the effect of silica pore size on chromatographic behaviour, four different pore sizes 120Å, 500Å,

1000Å and 4000Å (see Table 5) were selected and it can be seen that large pores have low surface area.

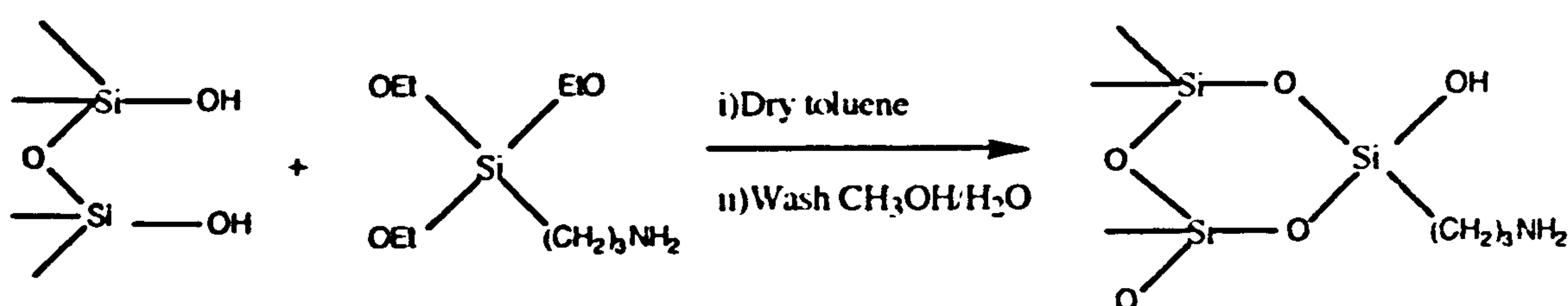
SILICA TYPE	PORE DIA D Å	PARTICLE SIZE dp μm	PORE VOL Vp cm ³ /g	SURFACE AREA SBETM ² /g
Hypersil	120	5	0.65	180
Nucleosil	500	7	0.80	35
Nucleosil	1000	7	0.75	25
Nucleosil	4000	7	0.75	10

TABLE 5 Comparison of the different silica's physical properties

There is a limiting maximum value of the mean pore diameter D in relation to the mean particle diameter dp of the support. If the mean pore diameter, D, is of the same order of magnitude as the mean particle diameter, dp, then the eluent flow may partially penetrate these large pores, which have nearly the same dimensions as the interstitial voids between the particles. Under these conditions, a physically coated stationary phase held in the large pores can be stripped out by erosion. As a consequence, in order to ensure a stable system, a significant difference in the silica pore size and the particle size should be established. In practice, the pore diameter of the packing should not exceed one tenth of the particle diameter²³⁴. The 4000Å, 7μm Nucleosil approaches this limit (D/dp=0.06).

2.2.1 Aminopropylation of Silica

An important feature in the use of silica supports in chromatography is the chemical nature of the surface. To provide reasonable attraction of the chiral stationary phase, the surface is modified. Before surface modification, the silica has to be prepared to give a consistent and reproducible coverage of surface hydroxyl groups for reaction. The polar hydrated silica surface is then modified by silanisation with 3-aminopropyltriethoxysilane to give an aminopropyl silica surface (see Scheme 8).



Scheme 8 Aminopropylation of silica

2.2.1.1 Number of Aminopropyl Silane Groups per nm²

The silica surface concentration of APS groups was calculated using Equation 4 (see page 23) as the number of groups nm⁻² (NG). To permit comparisons of data from the different silica surface areas the number of moles of organic modifier N_M μmolesm^{-2} was calculated using Equations 3 (see page 23).

SILICA APS	PARTICLE SIZE D nm	PORE SIZE Å	S.A SBETm ² g ⁻¹	%C	NM μmolesm ⁻²	NG nm ⁻²
Hypersil	5	120	180	1.90	3.03	1.82
Nucleosil	7	500	35	0.79	6.35	3.83
Nucleosil	7	1000	25	0.57	6.39	3.85
Nucleosil	7	4000	10	0.26	7.25	4.37

Table 6 The number of aminopropyl silane groups and number moles of organic modifier calculated from the %C data

NM is often used to define the extent of reaction and depends, amongst other things on the surface area of the silica gel before bonding. There are different kinds of sites on the surface of a silica particle^{230,231}.

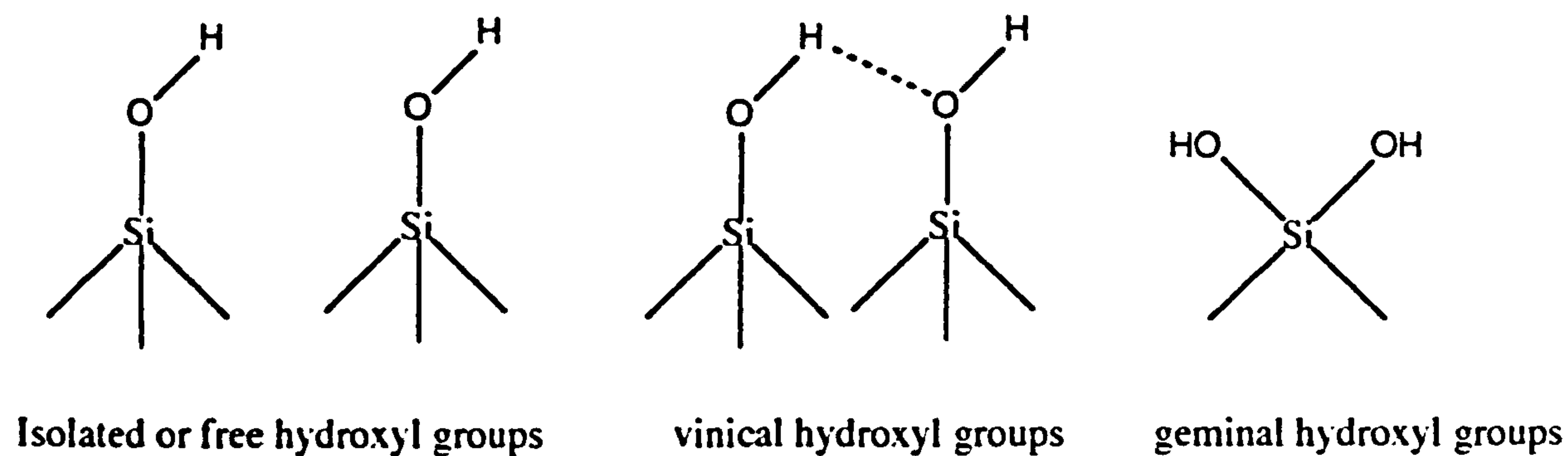


Figure 35 Arrangement of hydroxyl groups on a silica surface

The structure adopted on the surface is dependent upon the method of preparation and subsequent treatment of the silica gel. It is generally accepted that the surface of a silica particle is covered with a monolayer of silanol groups with an irregular distribution. Maximum coverage density is obtained when the maximum number of free hydroxyls (Figure 35) are available on the surface; this is why pre treatment of the silica is necessary. For example, heating silica to above 130⁰c in a vacuum removes residual water (see Figure 36) which is hydrogen bonded to the silica surface, and exposure of dry silica to an atmosphere of controlled humidity (storage over saturated LiCl solution which produces 12% relative humidity) for 24 hours rehydrates any siloxane groups to free hydroxyl groups.

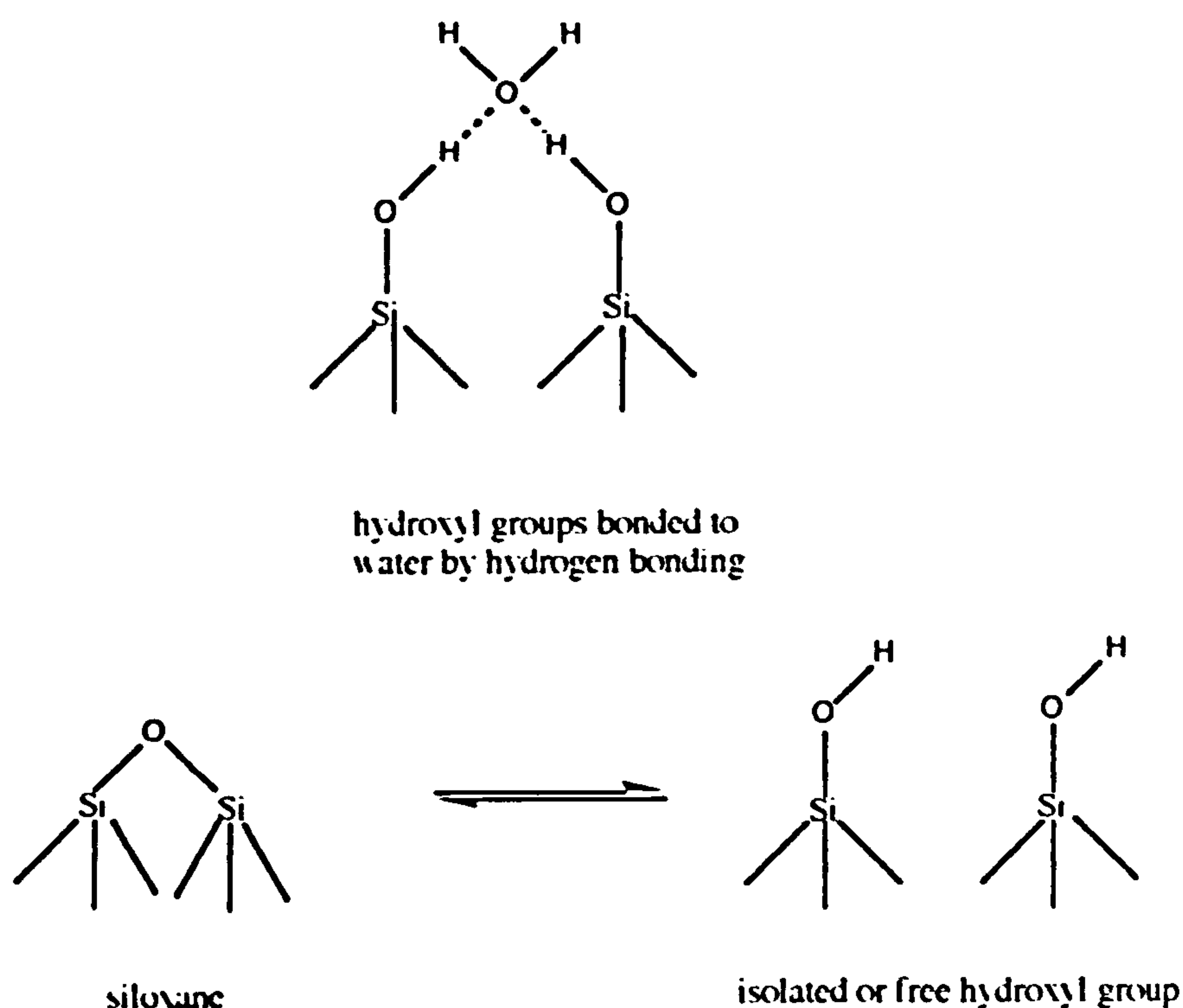


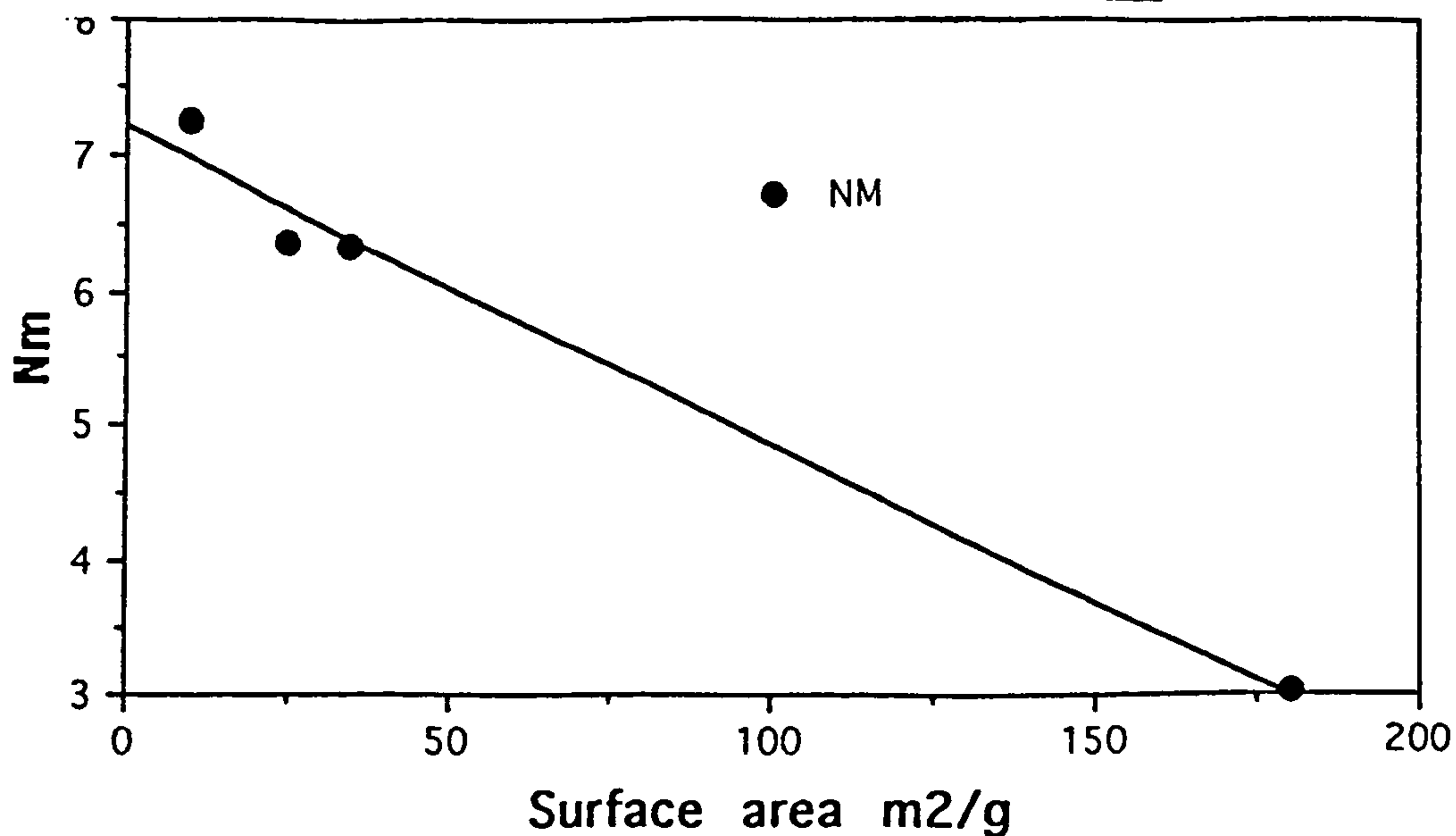
Figure 36 Possible forms of the silica surface

Zhurarlev and Kiselev²³² investigated a series of silica samples that differed widely in origin. From the results, they claimed that the mean surface hydroxyl concentration appears to be independent of the specific surface area of the silica. Unger²³³ has shown that $8\mu\text{molesm}^{-2}$ is the maximum value of surface hydroxyl groups, which correlates to a maximum value of 4.8 silanol groups per nm^2 .

Considering the carbon per cent data obtained from the APS modification of silica, it is apparent that less than the maximum possible number of surface hydroxyls have reacted. This may be due to incomplete hydration of siloxane bonds or due to steric hindrance. In previous studies²³⁴ employing a small modifier, trimethylchlorosilane, the surface concentration obtained was about $4.2\mu\text{mole/m}^2$, this meaning that only 50% of the total hydroxyl groups had reacted with the monofunctional modifier. From our data, (0.79% C for $7\mu\text{m}$ Nucleosil APS 500\AA), a surface coverage of 3.83 silane molecules per nm^2 is calculated. This value is less than the number of available silanol groups (4.8nm^{-2}) so a monofunctional stoichiometric reaction is feasible. However, if the modifier reacts difunctionally then 7.6 silanol groups would be required to complete the stoichiometry. As this is not possible it can be considered that the reaction proceeds via a mixed mono / di-functional process. The remaining ethoxy groups are hydrolysed to a hydroxyl group through washing with methanol/water.

The variation of N_M with surface area/pore size is shown in Graph 4. Expressing this data by use of this parameter serves two purposes. Firstly, it conforms to current practice and facilitates comparison and secondly, it calls attention to the fact that N_M is dependent on surface area and that a roughly linear relationship between surface area and carbon per cent exists²³⁵.

GRAPH 4 Relationship between surface area and the number of organosilane groups/nm²



To assess the error involved in these calculations one must question the accuracy of the measurements of surface area and carbon content. In regard to carbon content measurements, the critical cases involved the low surface area materials. Since their loadings are very low, a small amount of organic contamination can result in a large error.

2.2.1.2 Effect of Surface Modification on the Pore Structure of Silica

Modification of the silica surface not only changes its chemical nature but also affects its pore structure. The attachment of a monolayer is expected to cause a decrease in the mean pore diameter by the thickness (t) of the layer. Correspondingly, the specific surface area and specific pore volume also decrease. In this empirical investigation, we prefer to treat this subject exclusively on monolayer types of chemically bonded silica packing.

The most striking feature that determines the extent of pore structure is the ratio of the size of the modifier molecule to be bonded to the pore size of the silica. Unger's treatment²³⁴ of this theory gave the change in the surface area of the modified pore as:-

$$\frac{S_{\text{mod}}}{S} = \frac{2\pi l(r-t)}{2\pi r l} = \frac{r-t}{r} \quad (22)$$

where S is the surface area S_{BET} m^2/g , r is pore radius of untreated silica \AA , t is thickness of the layer and its volume (V) changes as

$$\frac{V_{\text{mod}}}{V} = \frac{\pi l(r-t)^2}{\pi r^2 l} = \left(\frac{r-t}{r}\right)^2 \quad (23)$$

Equations (22) and (23) treat the pore as an open cylinder and ignore the area occupied by the modifier when it attaches itself to

the bottom of the pore. Suprisingly, this approach has been shown to give a good agreement between the experimentally determined surface areas and pore volumes, and the calculated data²³⁶.

Silica	r Å	S(S _{BET}) m ² /g	PORE VOL cm ³ /g	(r-t)/r	[(r-t)/r] ²	%S(S _{BET}) CHANGE	%PORE VOL CHANGE
Hypersil	60	180	0.65	0.870	0.760	13.0	24.0
Nucleosil	250	35	0.80	0.970	0.940	3.0	6.0
Nucleosil	500	25	0.75	0.980	0.970	2.0	3.0
Nucleosil	2000	10	0.75	0.996	0.992	0.4	0.8

Table 7 Effect on the silica surface area and pore volume after conversion to aminopropyl silica

For our own study the thickness of an aminopropylsilane layer was estimated from molecular models of the modifier using Van der Waals radii obtained from the Sirius molecular graphics computer package, where -Si-(CH₂)₃NH₂ = 6.63Å

On the basis of these calculations one can draw the following conclusions about the change in surface structure and pore size with aminopropylation (see Table 7). Firstly, there is a considerable reduction in the specific surface area on silanisation of the smallest pore size (120Å); secondly, as the pore size increases then the overall effect on the surface area decreases, and thirdly, the modification of the silica surface has a greater significance for the pore volume, with a filling of almost 25% occurring for the smallest pores. It must be remembered that the

model of the cylindrical pore is a rather poor description of the real pore system. The real pore structure provides intersecting voids and channels of varying cross-section.

To conclude, the experimental data for the preparation of an APS support has shown that a good coverage with APS is obtained ($5.8 \mu\text{moles/m}^2 \pm 1.8$), which is equivalent to 70% of the available hydroxyl groups. On modification, a large change in the surface area is observed with the smallest pore diameter (120Å, ca. 13.0%), whereas a negligible decrease in pore volume is noticed with the large pore sizes (4000Å, ca. 0.4%).

2.2.2 Variation of the Chromatographic Properties with Pore Size

2.2.2.1 Retention k'

Retention of a solute by a CSP coated onto a silica support can arise from interactions with the CSP itself or with the polar sites on the support.

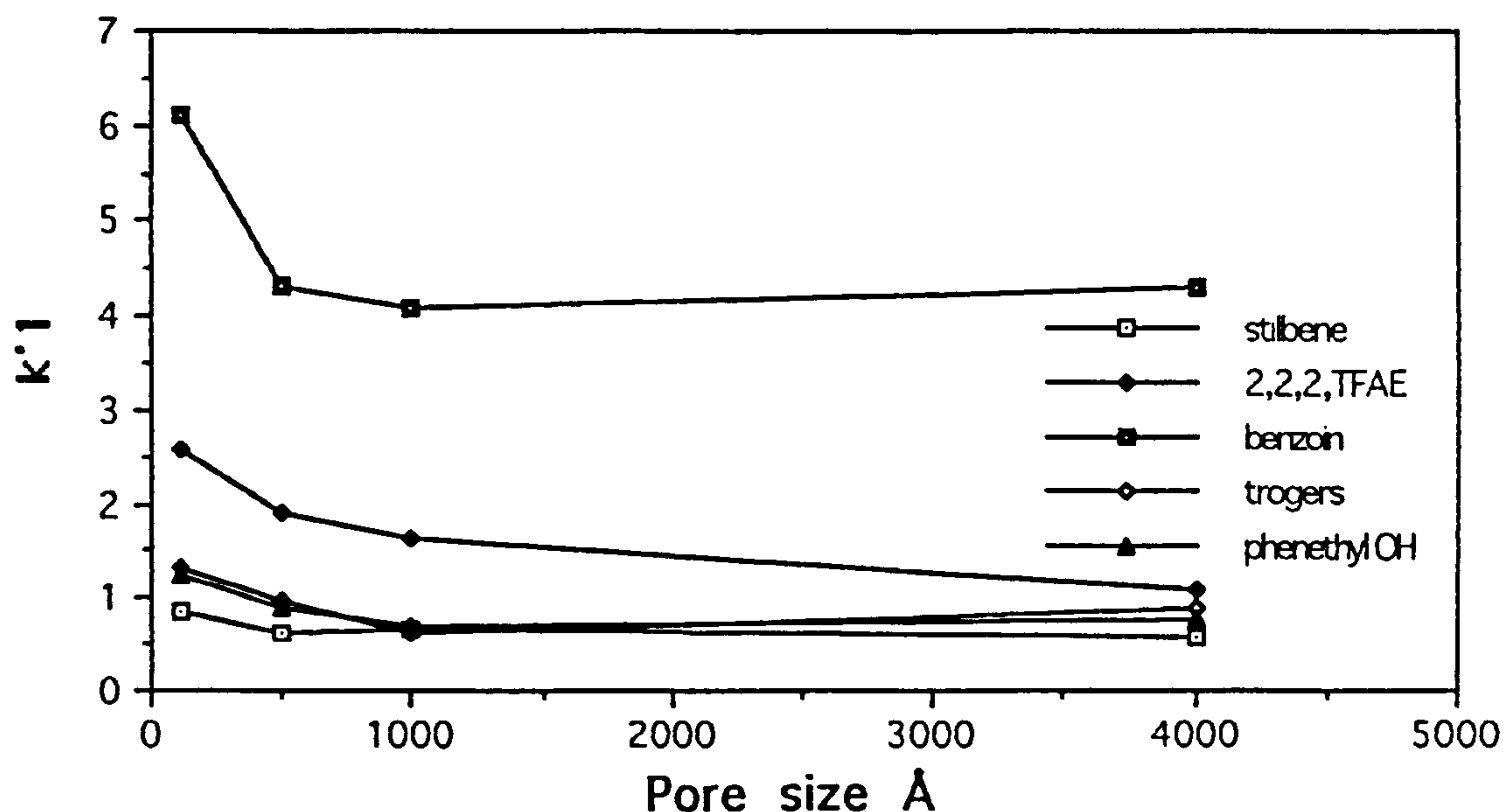
On comparing the total surface area available for coating onto each of the four silica's (see Table 7), it can be observed that Hypersil 120Å has the largest surface area by a factor of 18 and yet the smallest pore volume. It is possible that these two properties will affect the uniformity of CSP layer: at a fixed CSP loading, the larger surface area will be coated with a smaller thickness of CSP and produce a much smaller pore volume, preventing access to parts of the porous structure. In practice, we observe that the

preparation of a CSP using Hypersil APS 120Å coated with 20% w/w CPC produced a "sticky" phase, indicating that more of the CPC was immobilised on the surface of the silica due to the inaccessibility of the porous structure. This did not occur with the larger pored silica's (i.e. 500Å, 1000Å and 4000Å).

Retention processes resulting from polar hydroxyl sites on the support are non-stereoselective and arise from the non-uniform coating of the CSP. This type of adsorption produces peak tailing which should be noticeable at very low concentrations of polar modifier in the mobile phase (less than 0.1%v/v) and should diminish when the polar modifier increases. This phenomena was not observed as the chromatograms obtained gave symmetrical peaks.

Retention of a solute will be greater when there is an increase in the number of opportunities for retentive interactions with the CSP. A larger surface area should increase the number of interactions between the solute and stationary phase, as would increasing the length of the column. Graph 5 shows a trend towards longer retention (k'_1) on the smallest pore size (larger surface area) support (120Å).

GRAPH 5 Effect of pore size on capacity factor k'



Mobile phase composition; hexane/propan-2-ol, 90:10

2.2.2.2 Selectivity α .

The selectivity of a CSP is a chromatographic property in which the separation is due to the differences in the free energy of formation of a diastereomeric complex between the solute and the stationary phase.

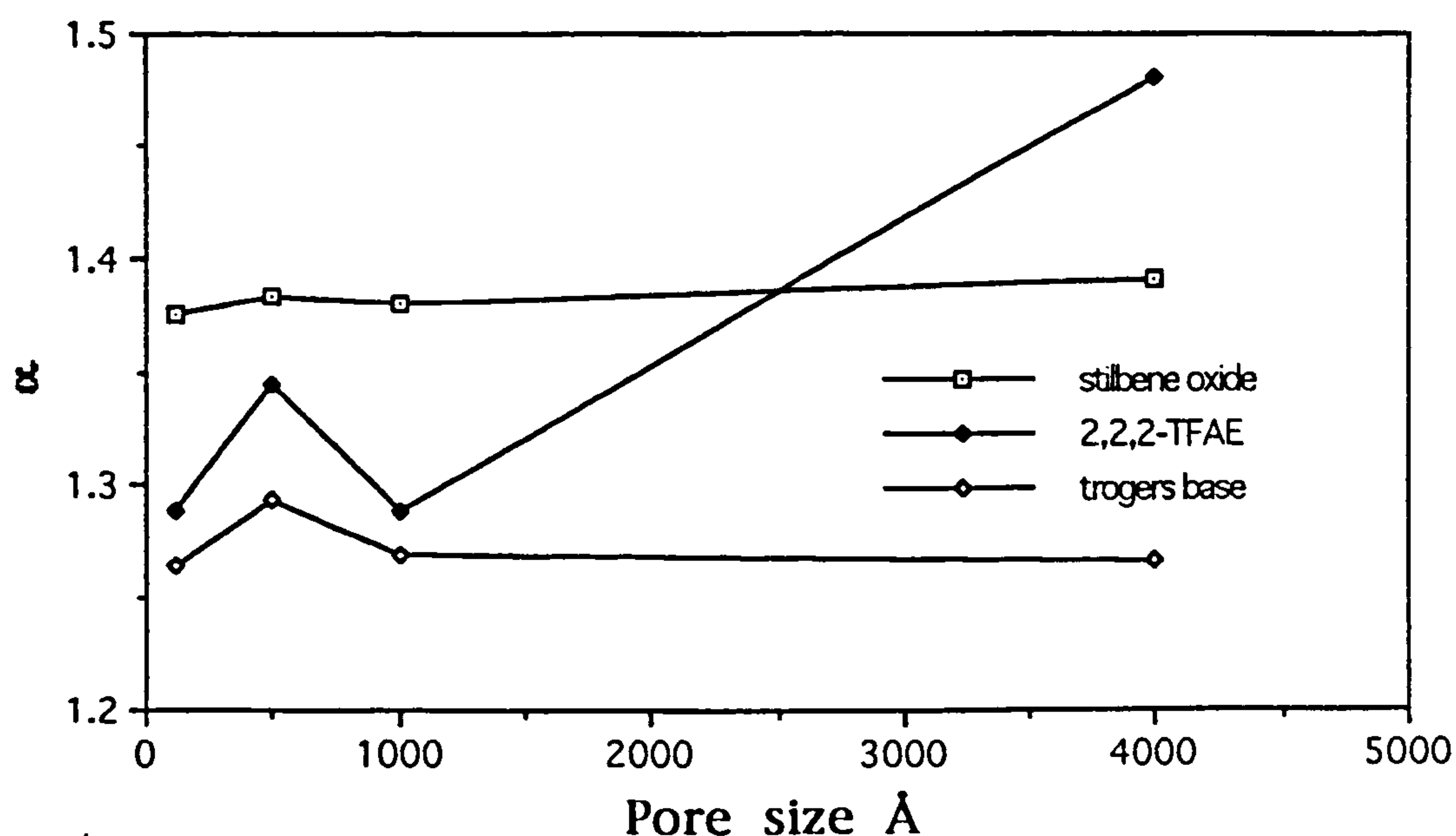
$$\Delta(\Delta G) = -RT \ln \alpha \quad (24)$$

The cellulose tris(phenylcarbamate) phase showed chiral recognition for only 3 of the 5 racemic solute mixtures, these being stilbene oxide, 2,2,2-TFAE, and trogers base.

As we have just seen, retention of the solutes is longest on the cellulose phenyl carbamate column which has the smallest pore

size. On examining the selectivity coefficient α for the 3 resolved solutes, we find that an increase in the retention of a solute does not necessarily cause an increase in enantiomer selectivity. Comparisons of the relative retention for each support on the varying surface areas (Graph 6) shows that no uniform trend can be established.

GRAPH 6 Effect of pore size on selectivity



Mobile phase composition; hexane/propan-2-ol, 90:10

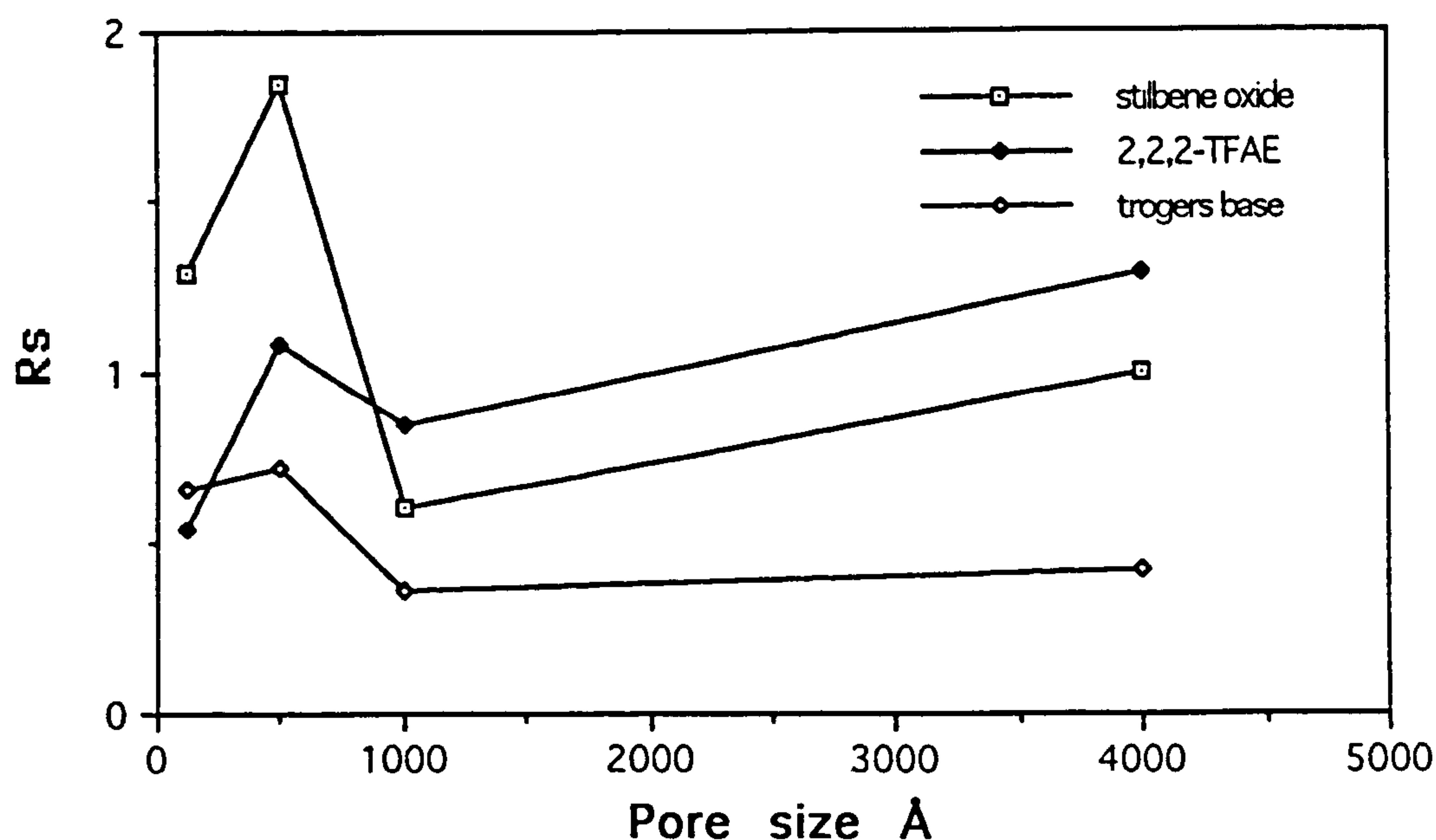
The two enantiomers of stilbene oxide show an almost equal relative retention with the range of pore sizes. The selectivity for the enantiomers of trogers base follows a very similar trend on silica pore sizes 120Å, 1000Å, 4000Å and is improved on 500Å. When considering the relative retention of 2,2,2-TFAE enantiomers, an anomalous result on the 4000Å pore size is observed. Apart from this latter result, the best values were

generally obtained on the 500Å support for each racemate resolved.

2.2.2.3 Resolution Rs.

The resolving power of each column follows a similar trend to that observed for the selectivity coefficient α , in that there is no clear advantage in the selection of large pore sizes. In fact, the resolving power for two of the solutes, stilbene oxide and trogers base, was best on the smaller pore size supports (120Å, 500Å). One interesting feature is that the anomalous position for 2,2,2-TFAE on the 4000Å observed in Graph 6 is less marked in Graph 7. As α and R_s are related by Equation (10), this observation may be attributed to a less efficient column reflected in a decrease in N .

GRAPH 7 Relationship between Resolution and pore size



Mobile phase composition; hexane/propan-2-ol, 90:10

2.2.2.4 Conclusion

The study of pore size on the chromatographic properties showed:-

- i) Retention was longest on the smallest pore size (120Å)
- ii) Longer retention did not necessarily give improved selectivity and resolution.
- iii) Comparisons of selectivity and resolution showed in most cases that the 120Å pore size behaved similarly to the 1000Å and 4000Å pore sizes.
- iv) The best results for selectivity and resolution were obtained on the 500Å pore size.
- v) Coating the 120Å silica with 20%w/w CPC produced a phase that was "sticky" causing aggregation and, as a consequence, difficulty in packing into an HPLC column.

In the light of these observations, aminopropylated 500Å Nucleosil 7µm silica was selected as a support for all further investigations of carbohydrate carbamate CSP's in the present project.

CHAPTER 3

PREPARATION OF CSP'S AND INVESTIGATION OF THEIR CHIRAL RECOGNITION PROPERTIES

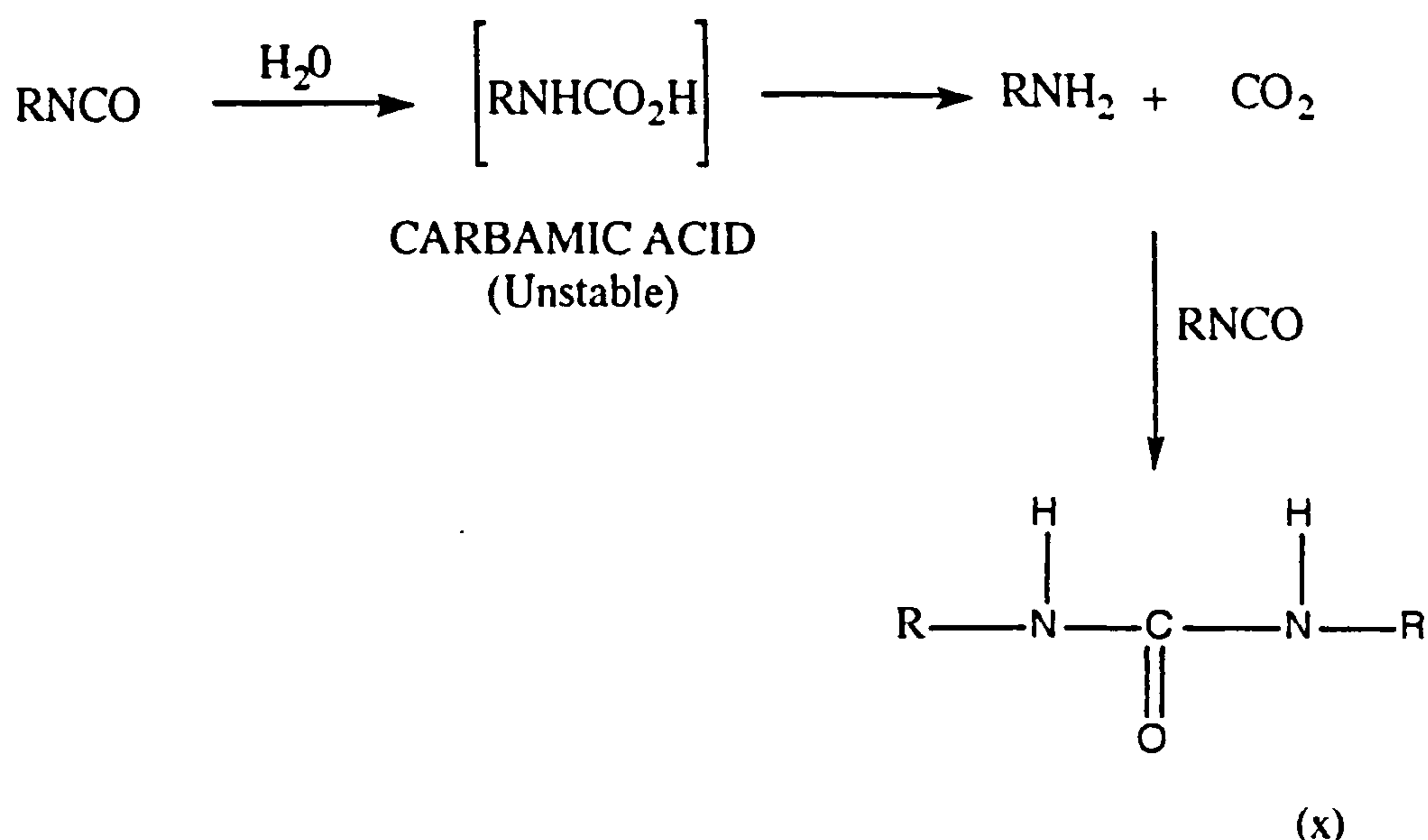
Early attempts at chromatographic separation of enantiomers were almost exclusively focused on the use of natural chiral absorbents such as cellulose. The drawbacks to such a material are numerous as it possesses poor mechanical properties and its high polarity and porous structure give rise to unfavourable kinetic behaviour. Attempts to improve the chromatographic and enantioselective properties of cellulose have concentrated on the derivatisation of the cellulose hydroxyl groups to decrease polarity of the material and to provide additional sites for interaction between the CSP and analyte. The first commercial packings of this type consisted of microcrystalline or silica-supported cellulose triacetate. Their versatility has lead to other innovations in cellulose derived CSP's by treatment of cellulose and other polysaccharides with aryl isocyanates. In published procedures, these CSP's have been physically coated on wide pore 4000Å aminopropylated silica gel.

In the present investigation, 5 chiral stationary phases were prepared and coated onto 500Å, 7µm aminopropylated Nucleosil. The phases were, 3 cellulose derivatives, *the tris(phenylcarbamate)*, *tris(3,5,-dimethylphenylcarbamate)* and *tris(naphthylcarbamate)*; and 2 amylose derivatives: *tris(phenylcarbamate)*, and *tris(3,5-dimethylphenylcarbamate)*.

3.1.Preparation of CSP's

Reactions of cellulose with isocyanates have been described in the patent literature. According to a US Patent ²³⁷, cellulose or its derivatives containing free hydroxyls react with aliphatic or aromatic isocyanates in the presence of a tertiary organic base. The result is a carbohydrate polymer with up to three derivatised hydroxyl groups per in-chain monosaccharide unit (see structures 1 and 2 Table 8). Several factors must be considered in the preparation of carbamates from polysaccharides. Among these are the nature of the cellulose material, the reaction solvent, concentration of the reagent, and the time and temperature of the reaction.

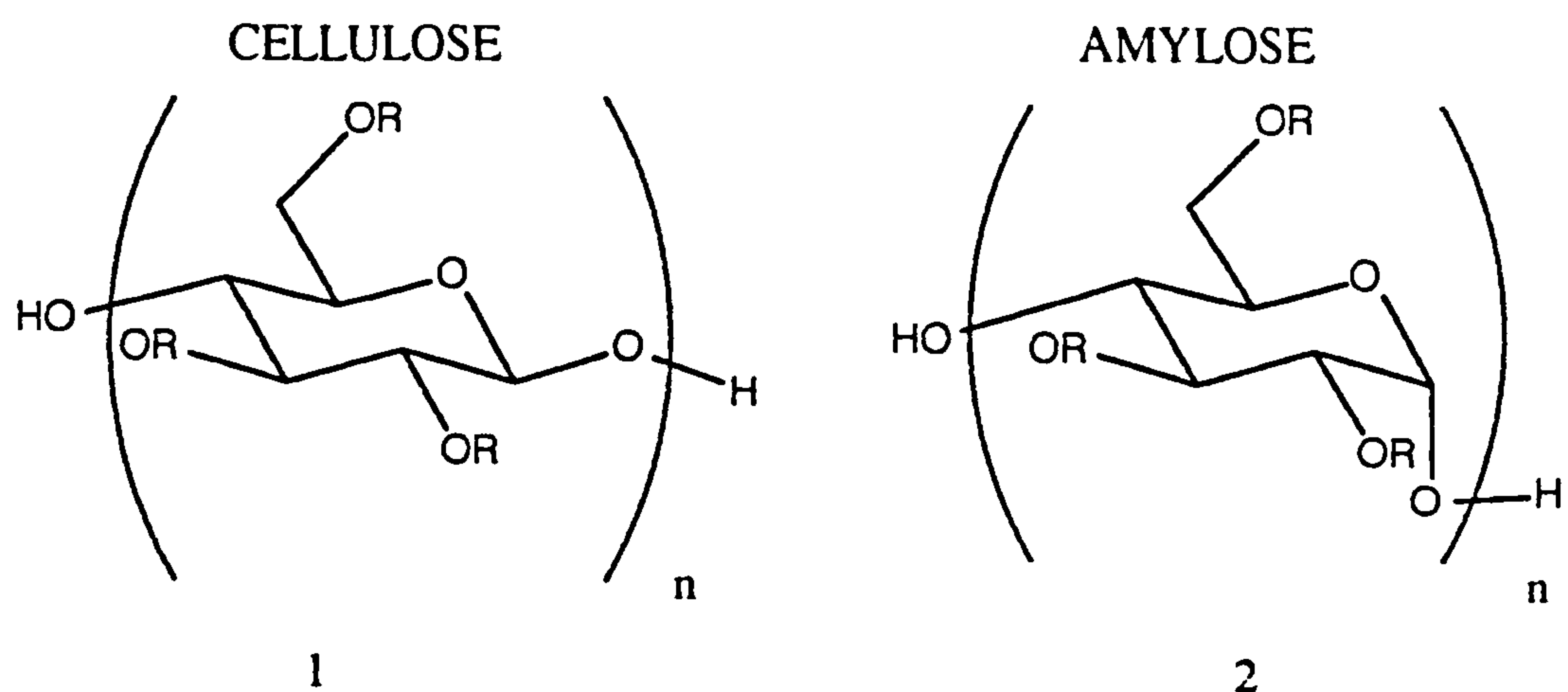
In the present work, the cellulose tris(arylcarbamate) derivatives were prepared from microcrystalline cellulose (Avicel, Merck) and the corresponding amylose derivatives from amylose (Type III, m.w.16000, Sigma, "essentially free from amylopectin".) All components in the reaction were kept extremely dry as organic isocyanates react readily with water to give the primary amine, which in turn will react with more isocyanate to yield a symmetrical urea (x) (see Scheme 9) as the final product, which is bothersome to separate from the carbohydrate carbamate.



Scheme 9

The carbamoylation of cellulose presents the difficulty that the reaction is usually started with cellulose in suspension, so the reagents must penetrate the fibre and "wet" the surface. Pyridine was selected as a suitable solvent for its wetting power, catalytic activity²³⁸, solubility of the product and boiling temperature. Hearon et al²³⁸ indicated that no appreciable reaction occurred at 50°C but at 100°C complete esterification was accomplished within 48 hours.

The experimental procedure we adopted for esterification involved drying the polysaccharides over P₂O₅ for 24 hours, refluxing in dry pyridine for 16 hours, then reacting with a 3.8-fold excess of isocyanate (3.8 isocyanate equivalents per glucose in-chain residue) and precipitation of the product in methanol to produce the derivatised polysaccharide (1 and 2) (Figure 37) in good yield.



where R is the derivative as shown in Table 8.

Figure 37

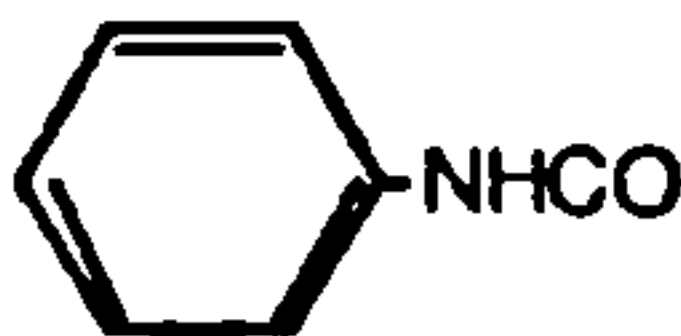
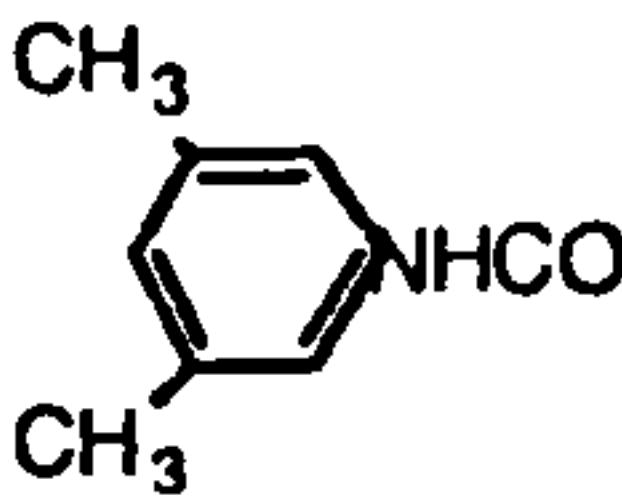
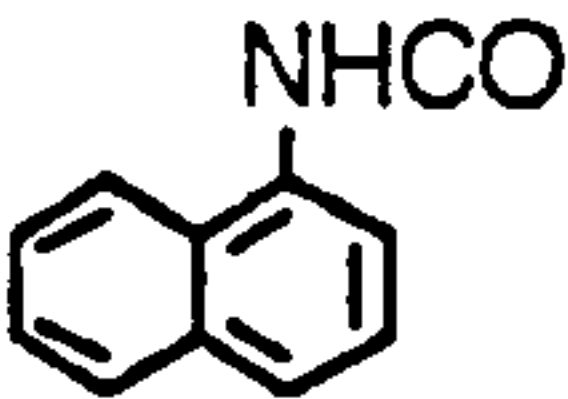
POLYSACCHARIDE	DERIVATIVE		
			
CELLULOSE	CPC	CDMPC	CNC
AMYLOSE	APC	ADMPC	/

Table 8 Acronyms of the 5 CSP's studied

Elemental analysis, ¹H nmr and ir spectra indicated that almost all the hydroxyl groups of the polysaccharide were converted to carbamate groups. The presence of impurities from the formation of the symmetrical urea was detected by ir (carbonyl stretch at 1635cm⁻¹), ¹H nmr (N-H urea at 8.6ppm) and by an excessive nitrogen content in the elemental analysis.

The extent of derivatisation of the polysaccharide can be deduced by analysing the results from the 3 techniques. The ir data, although not quantitative, showed a strong peak at 1717cm^{-1} due to the carbonyl stretch and would indicate the presence of unreacted hydroxyl groups by the appearance of a broad peak at 3600cm^{-1} due to free hydroxyl. The nmr spectra can reveal useful information, but care has to taken when considering the quantitative accuracy of the technique. An estimate of the extent of derivatisation was obtained by comparing the ratios of the signals from the protons on the sugar ring with those from the N-H protons. For complete derivatisation the ratio should be 7:3 (i.e 2.33:1) and, as shown in Table(9), the ratios of the signals are close to the values calculated for tri-substitution. It may also be possible to use the integrals from the aromatic protons, but incorrect conclusions may result from the presence of solvent or catalyst trapped in the polysaccharide matrix and from the presence of other impurities such as the symmetrical urea (x).

CSP	N-H INTEGRAL	^1H INTEGRAL	RATIO	%tri- substitution
CPC	2.30	5.09	2.21	94.8
CDMPC	2.60	5.48	2.10	90.2
CNC	2.84	7.04	2.45	105.1
APC	2.43	5.40	2.22	95.6
ADMPC	2.70	6.23	2.31	99.2

Table 9 Evaluation of the extent of derivatisation of the polysaccharides using ^1H nmr data

To monitor the degree of derivatisation by elemental analysis, the theoretical %C, H and N was calculated for an in chain model glucosyl unit, mono, di or tri-substituted at the 6, 2 and 3 positions respectively. Table (10) illustrates the variation in the elemental analysis for each degree of derivatisation with phenylcarbamate.

DEGREE OF SUBSTITUTION	ELEMENTAL %C	ANALYSIS %H	%N
MONO	55.52	5.34	4.98
DI	60.00	5.00	7.00
TRI	62.43	4.82	8.09
EXPERIMENTAL	62.36	4.40	7.91

TABLE 10 Theoretical and experimental composition data elemental for a glucosyl unit mono, di, or tri- substituted with phenylcarbamate.

The same approach was used to assess derivatisation of the other polysaccharides and it can be concluded that from the elemental analysis, the hydroxyl groups were almost completely converted to carbamate moieties in all cases (see Table 11).

CSP	EXPERIMENTAL			THEORETICAL		
	%C	%H	%N	%C	%H	%N
CPC	62.36	4.40	7.91	62.43	4.82	8.09
CDMPC	65.60	6.06	6.93	65.67	6.14	6.97
CNC	69.40	4.53	6.26	69.95	4.60	6.27
APC	61.48	4.80	8.08	62.43	4.82	8.09
ADMPC	65.10	6.13	6.09	65.67	6.14	6.97

Table 11 Elemental analysis results for the derivatisation of polysaccharides

3.1.1 Aminopropyl Silica Coating Procedure

There are several different techniques for the preparation of coated packings for HPLC, each having advantages in certain applications. To produce a uniformly coated support, it is important to consider the physical properties of the phase (such as volatility, stability and viscosity) and also the structural properties of the silica (i.e. pore size and particle size). Taking these properties into account, the solvent evaporation technique was selected, as employed by Okamoto for his CSP column preparation⁷⁸.

In this coating procedure, the non-volatile CSP (cellulose aryl carbamate, 0.75g) was dissolved in a volatile organic solvent (THF,

10cm³). To remove air pockets from the porous silica structure, the silanised macroporous silica gel (3g) was gently refluxed in THF (10cm³) for 30 minutes and cooled. To the wetted silica gel, half the CSP solution was added and the solvent removed under vacuum, employing a rotary evaporator. The remainder of the CSP solution was added and the solvent removed as previously. The coated CSP was then sieved to remove aggregated particles and the packing material obtained was packed into a stainless steel column (15cm x 0.46cm id).

3.1.2 Packing Procedure

The optimum procedure for packing columns which possess a uniform bed with no cracks or channels is by the slurry packing technique¹³. This requires that the coated silica is initially suspended in a solvent, the one selected in this case being a mixture of hexane/IPA (50:50) which was chosen to maintain an adequate particle dispersion without aggregation or stripping of the coated phase and at the same time thoroughly wet the packing. The solvent mixture also held the particles in suspension long enough to be packed into the column before sedimentation-sizing occurred.

After pouring the suspension of coated silica in hexane/IPA into the "bomb", the slurrying mixture was rapidly forced downward into the wetted column. With a constant pressure pump, the slurry flow rate is dependant on the pressure used, and as the packed bed is formed the flow rate decreases. Once the volume of slurrying solvent (hexane/IPA) had passed through the column

leaving the coated silica, a less viscous and less dense solvent (hexane) was forced through the column at the same pressure but at a much higher flow rate to allow a uniform and densely compacted bed to develop.

Silica's with large pore sizes (i.e. 500Å to 4000Å) are inherently weaker than those with a smaller pore size and care had to be taken not to fracture the weaker particles, producing fines that tend to plug the column outlet and cause packing structure irregularities. In order for the particles to withstand the mechanical stress of the packing procedure, the packing pressure was limited to 4500 psi and maintained until 250cm³ of eluent was collected.

3.2 Chiral Recognition by Polysaccharide Carbamate Phases

The chiral recognition properties of each of the five polysaccharide carbamate phases was tested with a range of 5 test solutes: stilbene oxide, 2,2,2-trifluoro-1-(9-anthryl) ethanol (2,2,2TFAE), benzoin, trogers base and 1-phenylethanol with a range of IPA concentrations in hexane as the mobile phase at ambient temperature.

The resolution of racemic 2,2,2-trifluoro-1-(9-anthryl) ethanol on cellulose tris(3,5-dimethylphenyl) carbamate is shown in Figure 38. The enantiomers were completely separated. The capacity factors (k'_1 and k'_2) were 0.94 and 2.14 respectively. The

separation factor α and the resolution factor R_s were found to be 2.26 and 4.53 respectively.

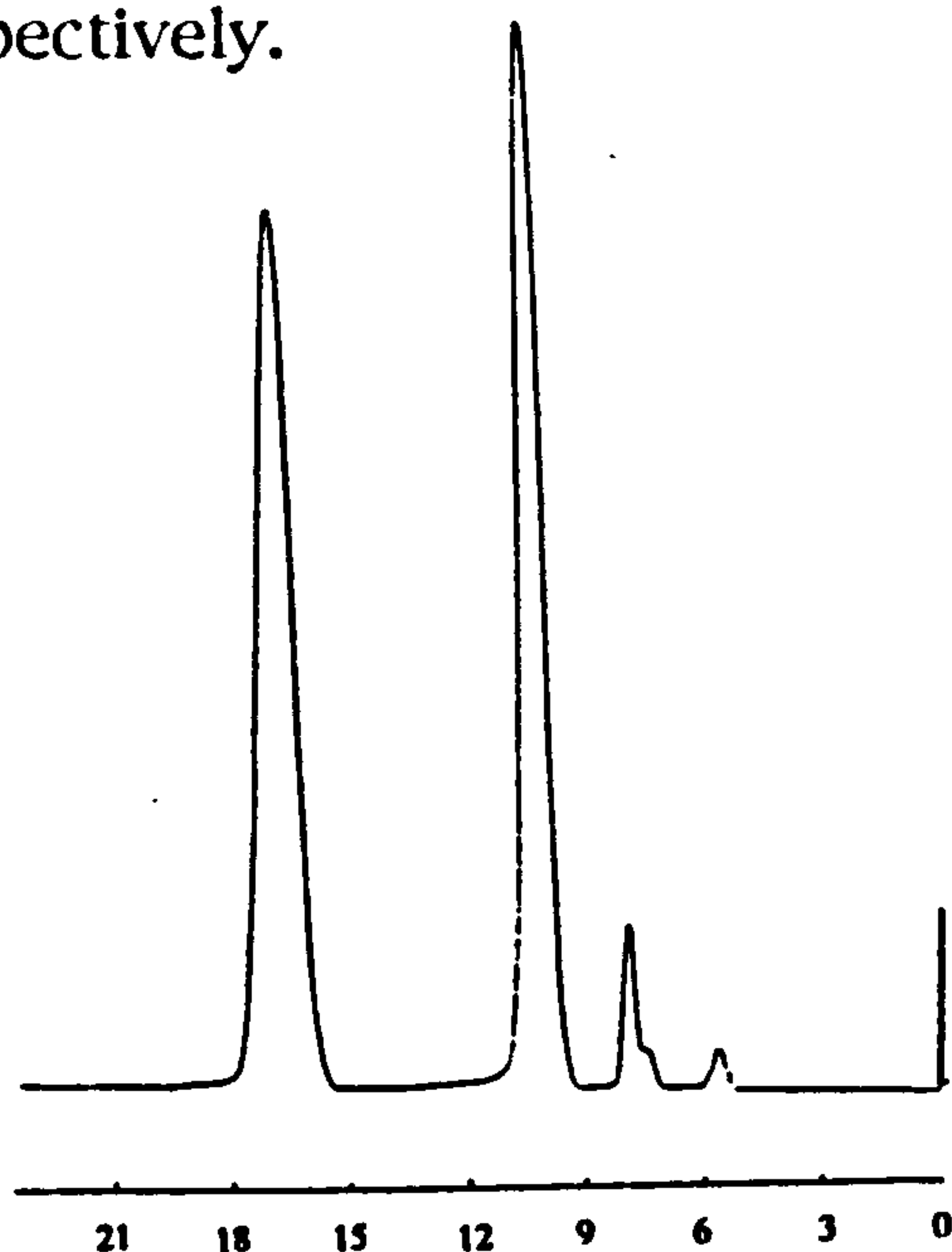


Figure 38 Enantiomeric separation of 2,2,2-trifluoro-1-(9-anthryl) ethanol on CDMPC. HPLC conditions: mobile phase hexane/ 2-propanol 90:10v/v, flow rate $0.6\text{cm}^3\text{min}^{-1}$.

Chiral recognition was exhibited by 4 phases: CPC, CDMPC, APC and ADMPC, in which each polysaccharide ester had its own analyte specificity. The CNC phase produced broad peaks and exhibited very poor enantiomeric selectivity.

Previous studies⁷⁸ of the CPC and CDMPC phases have shown that they adopt a sterically regular structure which is held together by the aryl groups. They exist as stiff rod-like molecules due to hydrogen bonding between adjacent carbamate groups which fix the glucosyl units. When cast from tetrahydrofuran, they adopt an ordered structure, in which the aryl groups are arranged regularly. The introduction of a naphthyl group caused a loss of the enantiomeric selectivity ($\alpha=1$). This may be because the

naphthyl groups disrupt the regularly arranged structure of the phase.

Loss of chiral recognition was observed by Okamoto⁷⁸ for 2,6-disubstituted carbamates. He attributed their low efficiency to the disordered structure of the carbamate. These carbamates did not give a liquid crystal phase in tetrahydrofuran, showed no crystallinity when cast from solution and showed relatively strong NH peaks at 3400cm^{-1} (as well as at 3300cm^{-1} for H-bonded NH) in the ir which is assigned to free NH.

The ir spectra of the three cellulose carbamates CPC, CDMPC and CNC are shown in Figure 39. The presence of an extra NH peak at 3400cm^{-1} was noted for the CNC phase. Disruption of the hydrogen bonding between adjacent CNC unit residues, due to the sterically bulky naphthyl group causing twisting of naphthyl groups about the C-N bond, may affect the environment of the chiral cavity and thus lead to the observed loss of enantioselectivity for this phase.

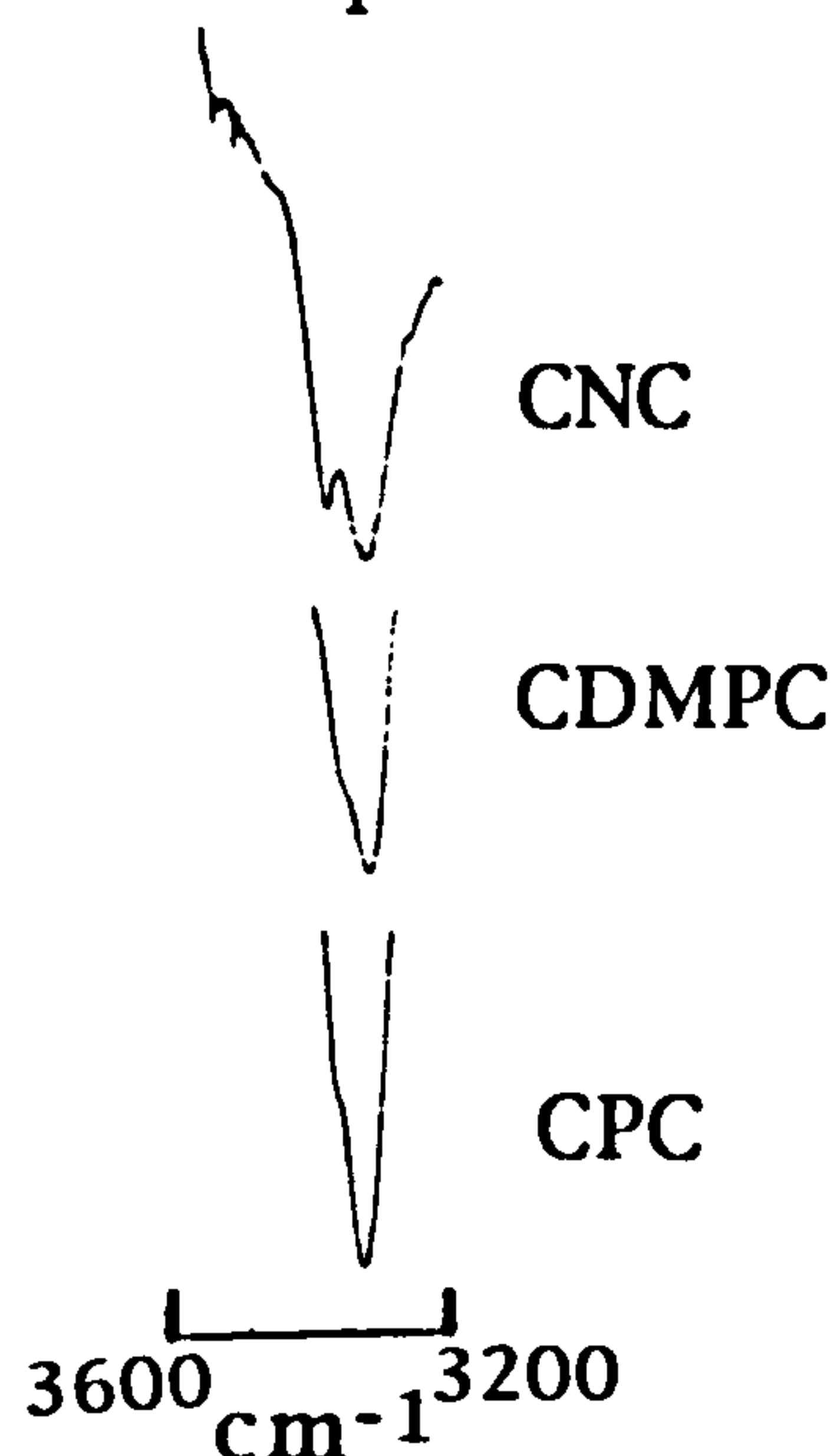


Figure 39 Comparison of ir spectrum for CNC; CPC and CDMPC.

As expected, the retention of the solutes on each phase decreased with an increase in the polarity of the mobile phase. This reduction in retention may reflect the disturbance of intermolecular forces between the solute and the absorbing site of the carbamate derivative (see Figure 40).

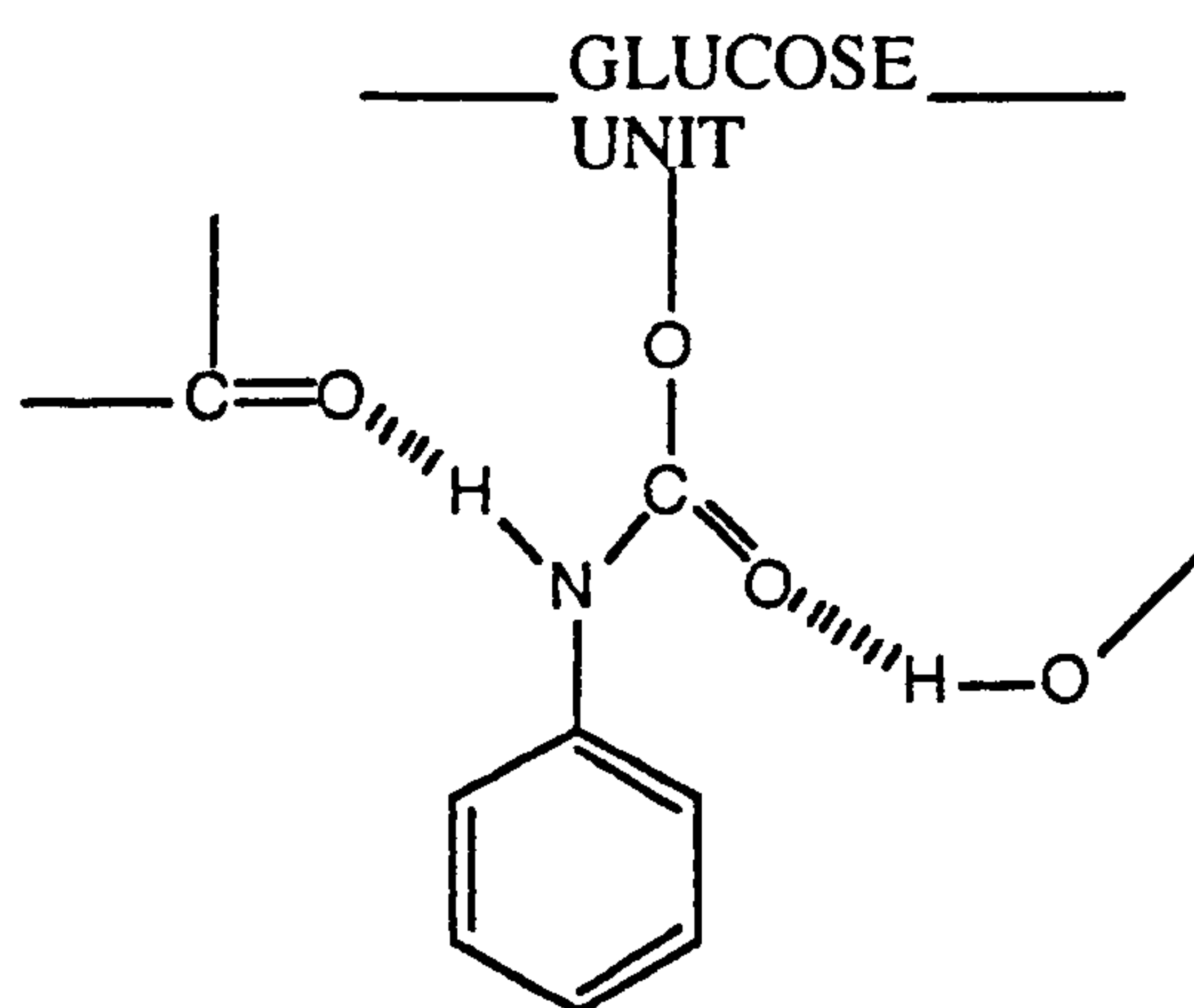


Figure 40 Absorbing site of phenyl carbamate derivative

For comparison, the capacity factors on all 4 CSP's (CPC;CDMPC;APC and ADMPC) are shown in Table (12). The racemic compounds 2,2,2-TFAE and 1-phenylethanol carrying a hydroxyl group were retained longest on the cellulose tris(3,5-dimethylphenylcarbamate) phase. In contrast, benzoin, which possesses a carbonyl (as well as hydroxyl) group was retained longest on cellulose tris(phenylcarbamate).

SOLUTE	CHIRAL STATIONARY PHASE			
	CPC	CDMPC	APC	ADMPC
STILBENE OXIDE	0.609	0.618	0.682	0.556
2,2,2-TFAE	1.522	1.812	0.909	1.333
BENZOIN	4.304	1.750	0.556	0.556
TROGERS BASE	0.978	0.800	1.091	0.889
1-PHENYL ETHANOL	0.891	1.533	0.682	1.111

Table 12 Capacity factor k' for all the test solutes on 4 different CSP's (mobile phase 90/10, hexane/IPA)

This result may be ascribed to the interaction shown in Figure (40) and the influence of the substitution on the phenyl ring in the carbamate moiety. When the aryl substituent is electron donating (i.e. methyl), the hydrogen bonding between C=O and the hydroxyl group of the solute may be enhanced. Therefore, a change in the capacity factor may be associated with a change in the polarity of the urethane moiety induced by substitution. This is supported by nmr spectroscopy. ^1H nmr spectra of the N-H protons of the cellulose carbamate derivatives CPC, and CDMPC in d_6 acetone are shown in Table 13. The spectra clearly reveal 3 carbamate N-H protons which shift upfield as the electron donating power of the substituents on the phenyl ring increases i.e. $\delta\text{CPC} > \delta\text{CDMPC}$.

CSP	1H ppm	2H ppm	3H ppm
CPC	8.42	8.69	8.88
CDMPC	8.22	8.46	8.67

Table 13 ^1H nmr chemical shifts of N-H protons in CPC and CDMPC (conditions 50mg sample in d_6 acetone)

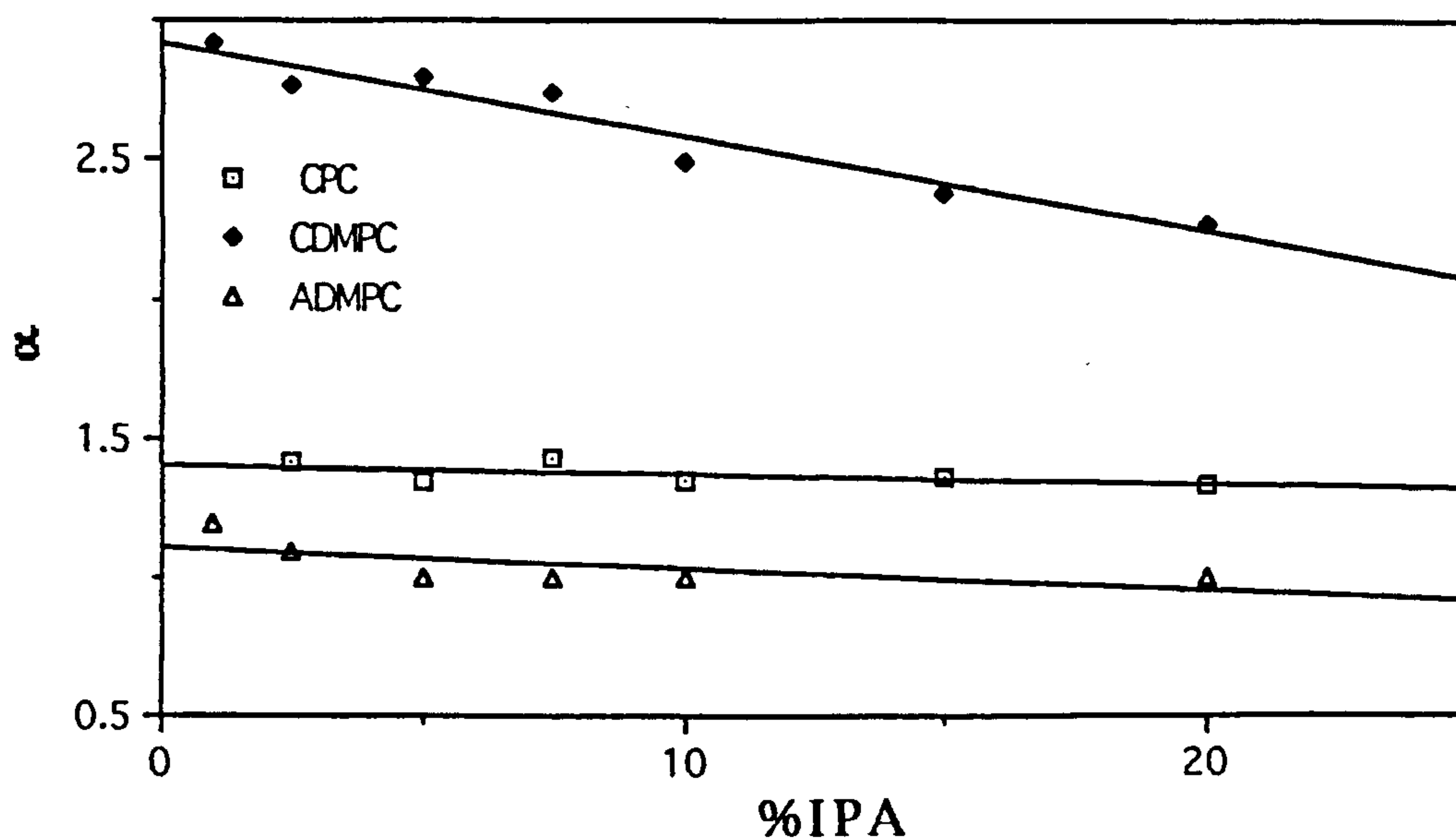
As we have seen (Table 12), the retention of a solute depends on the substituent on the phenyl ring. This also applies to stereoselectivity, as the relative retention for each solute is different on each of the cellulose and amylose CSP's (Graphs 8-12).

Apart from the peculiar changes in selectivity for 1-phenylethanol displayed by APC, the relative retention of the racemic solutes on 4 CSP's show linear trends with increasing polar modifier in the mobile phase (only the results for the CSP phases which exhibited enantiomeric selectivity towards each racemic solutes , $\alpha > 1$, were plotted).

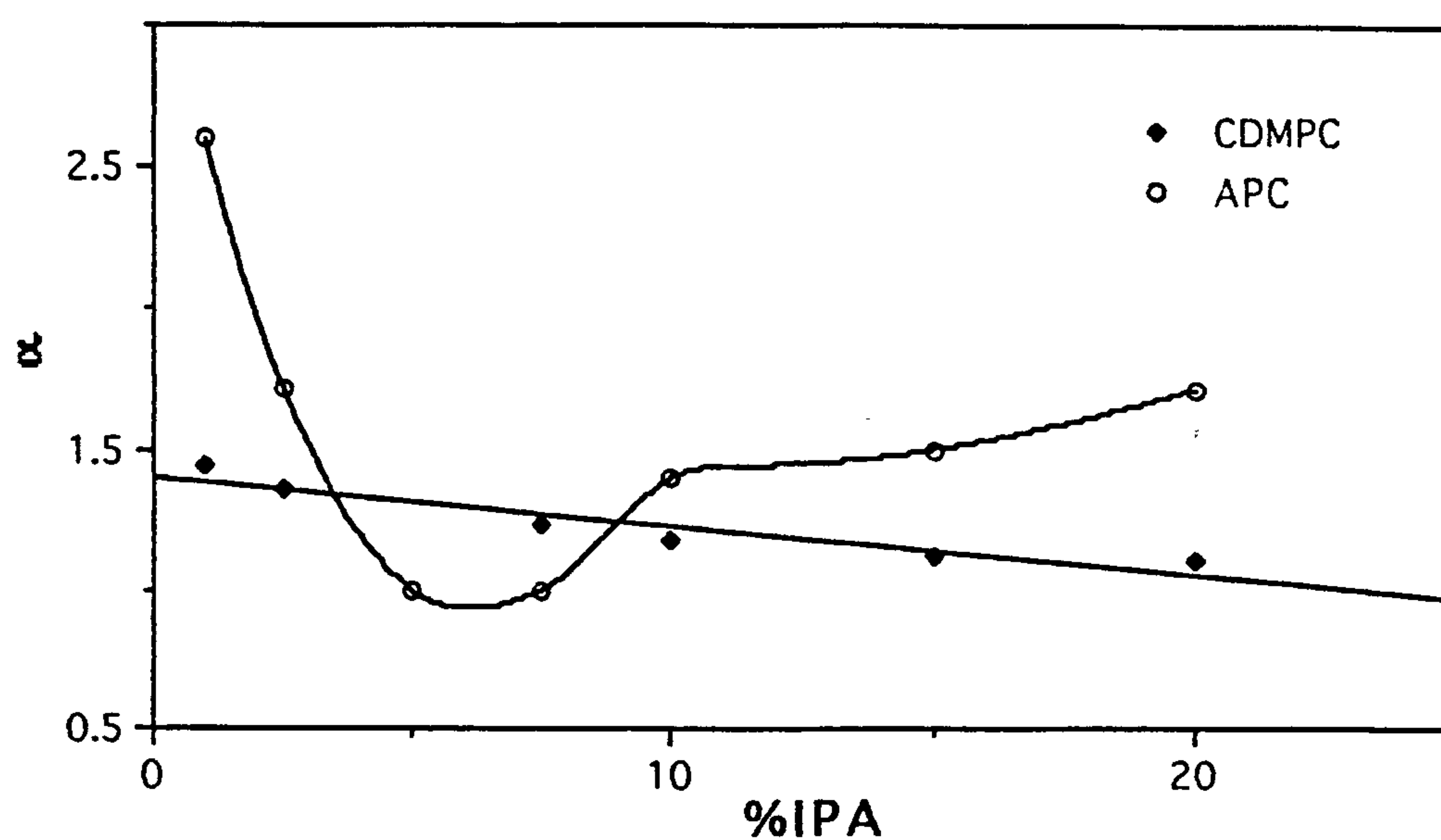
CDMPC produced the best overall enantiomeric selectivity as chiral recognition was exhibited towards all 5 racemic solutes. The extent of relative retention by CDMPC was generally the most strongly dependent upon the concentration of polar modifier in the mobile phase, as illustrated by the steepness of the gradients for the relationship between α and %IPA for the solutes in Graphs 8,9,10 and 11. This may indicate the disturbance of hydrogen-bonding and dipole-dipole interactions between the CSP and solute. The effect of increasing the polar modifier in the mobile

phase was shown to have very little influence upon the selectivity exhibited by APC, CPC and ADMPC phases (see Graphs 8,9, 10 and 12). The relative lack of effect of propan-2-ol in the mobile phase on α suggests that the selectivity of these phases is not only due to N-H or C=O functions, but also π - π interactions from the aromatic groups.

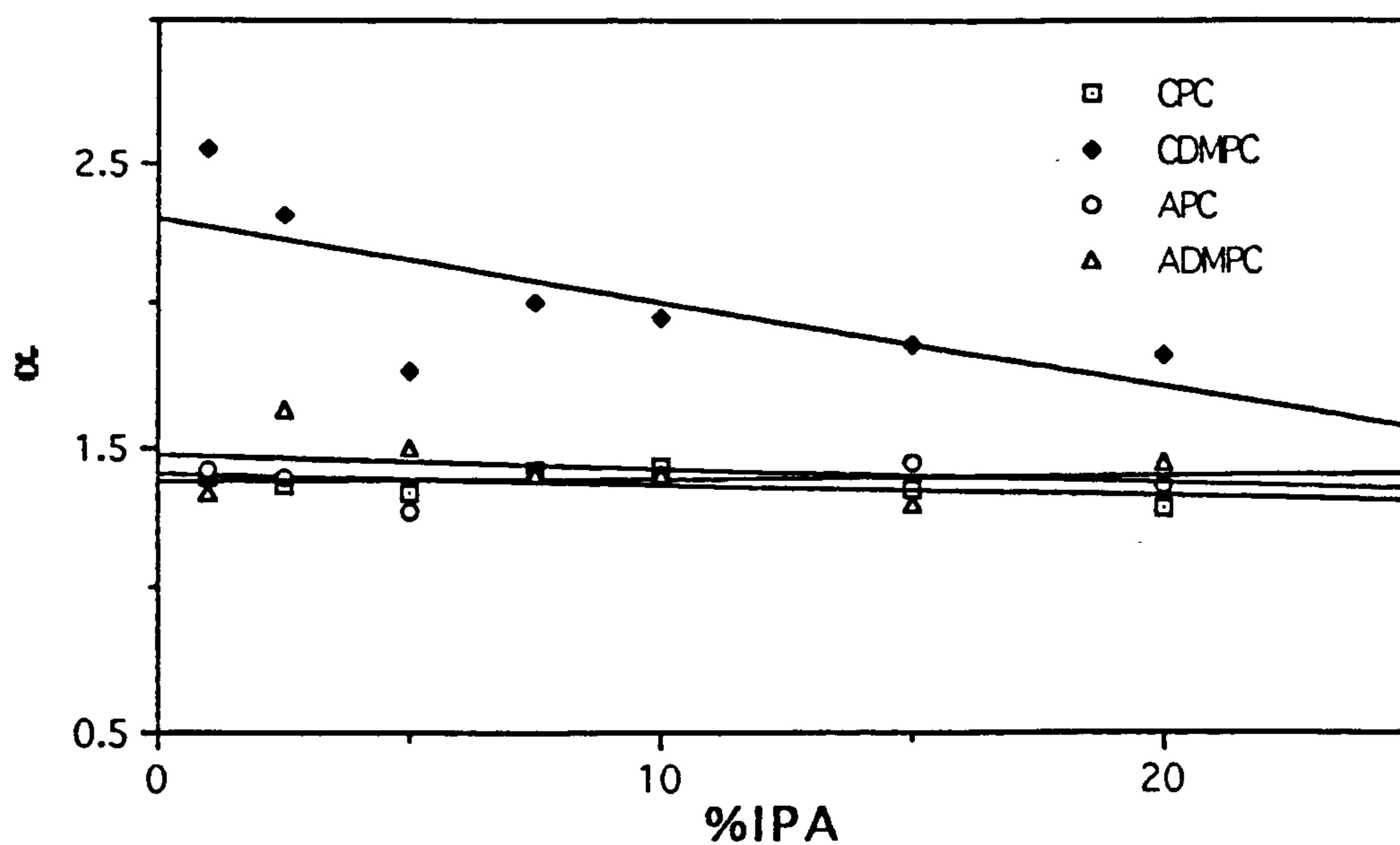
GRAPH 8 Relative retention of 2,2,2-TFAE by CPC, CDMPC, and ADMPC



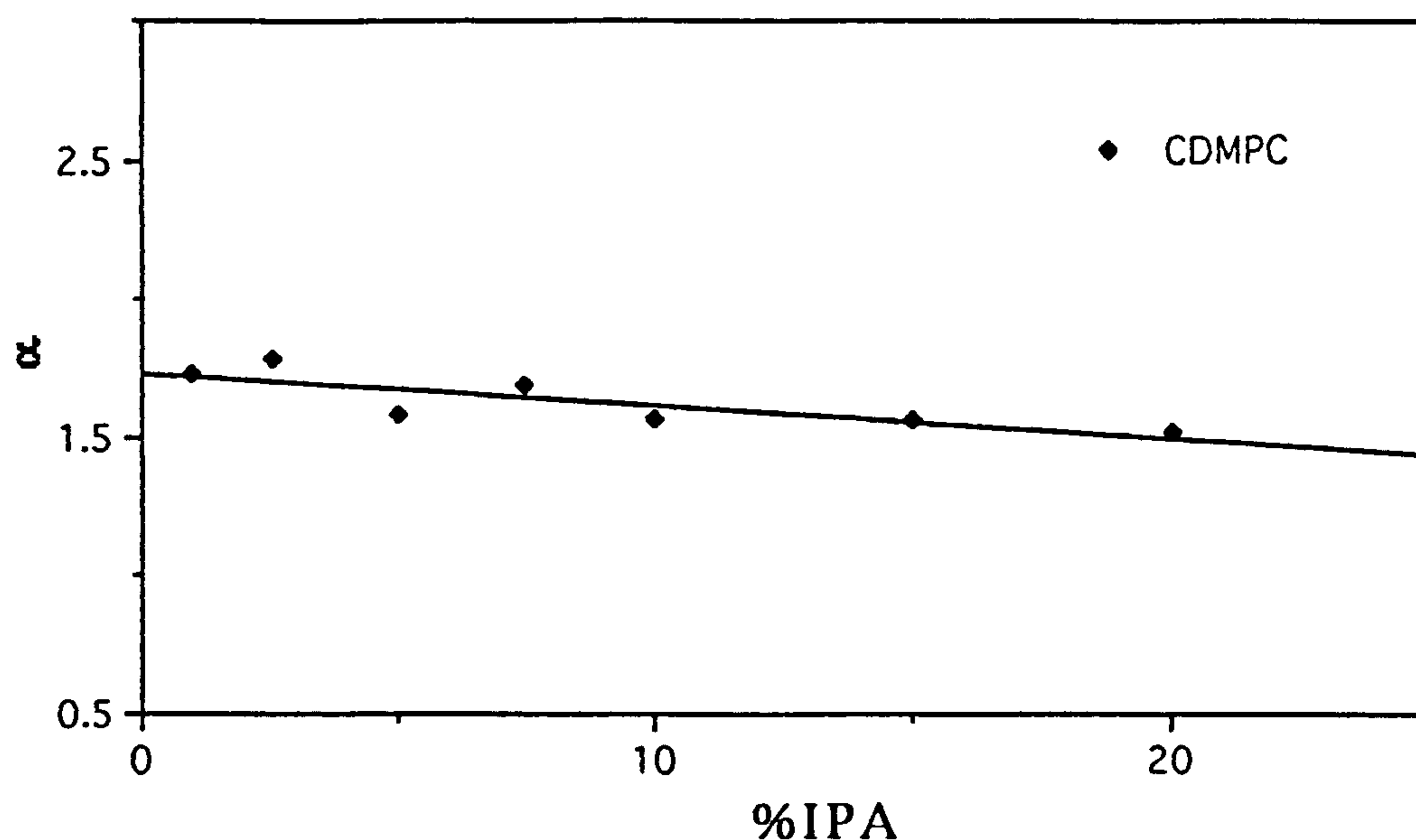
GRAPH 9 Relative retention of 1-phenylethanol
on CDMPC and APC



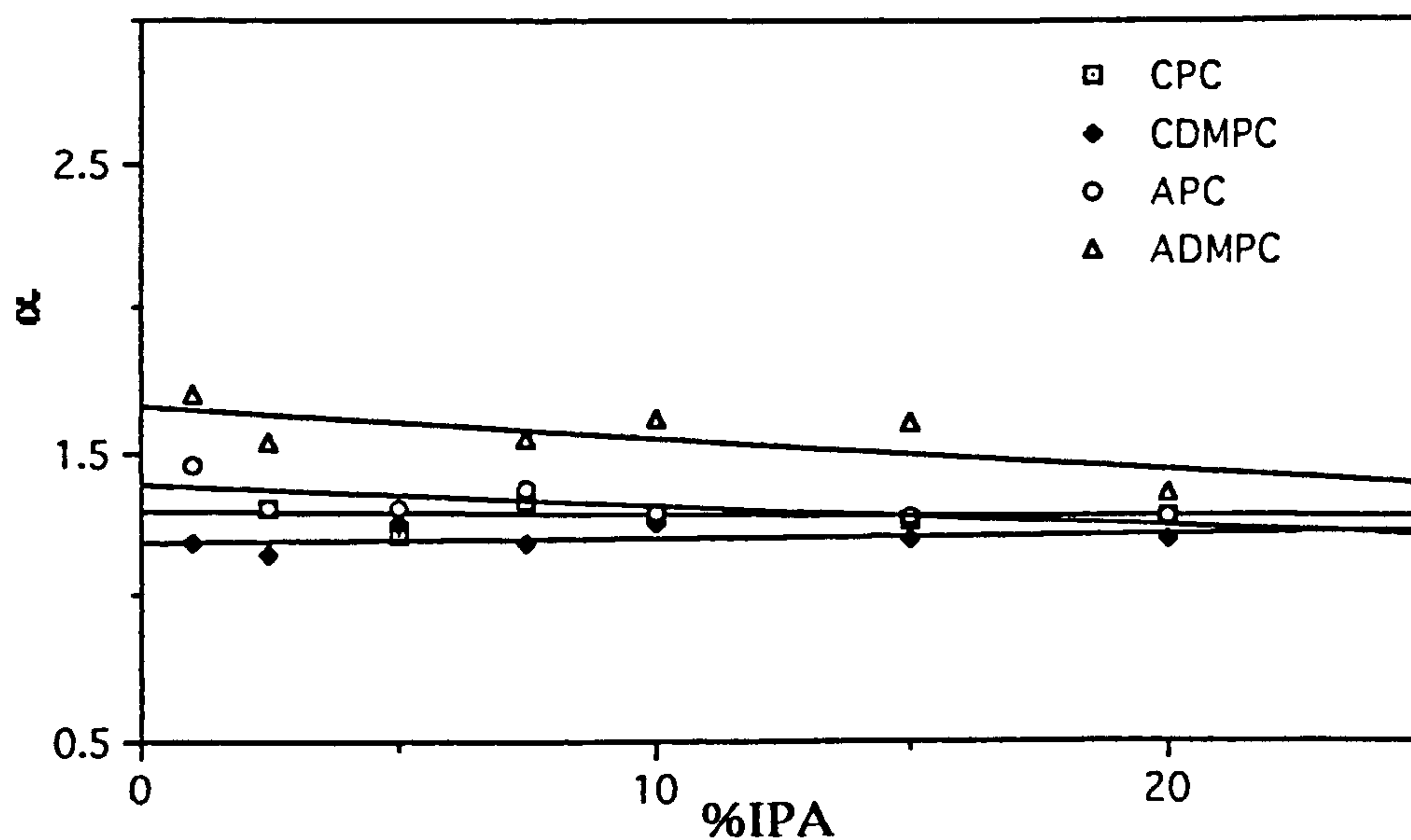
GRAPH 10 Relative retention of stilbene oxide
by CPC, CDMPC, APC and ADMPC.



GRAPH 11 Relative retention Of benzoin on CDMPC



GRAPH 12 Relative retention of trogers base on CPC,CDMPC, APC and ADMPC

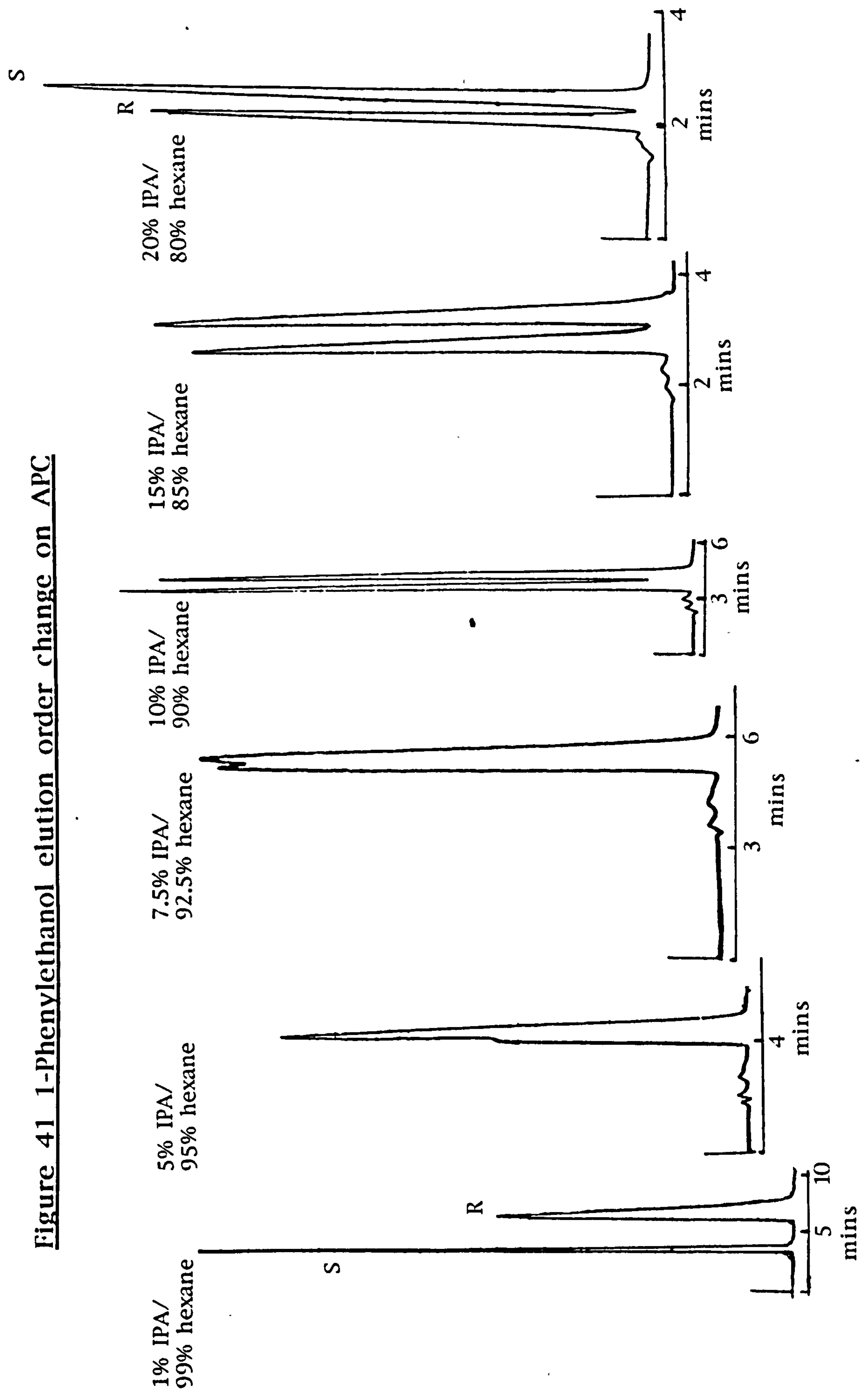


The effect of the alcoholic mobile phase modifier on retention and chiral selectivity suggests that, for the system studied, i) the mobile phase modifier competes with the solutes for hydrogen bonding sites on the CSP; ii) this competition takes place at both chiral and achiral sites on the CSP. This mechanism is consistent

with previous studies on the effect of alcoholic modifiers on k' and α on CSP's²³⁹. The results of investigations using Pirkle type CSP's by Wainer²³⁹ indicate that the primary effect of an alcoholic modifier occurs through interactions with the CSP. This does not preclude interactions between the modifier and the solute, but these interactions appear to play a lesser role in the variation of chromatographic parameters. Wainer also suggests that the effect of the modifier on α may be due in part to its binding to achiral sites near, or at, the chiral cavities of the CSP, altering the steric environments of these cavities.

The complex process of enantiomeric separation cannot, however, be explained by relatively simple models. This is illustrated when we consider the elution of 1-phenylethanol on the APC phase (see Graph 9). Selectivity decreases initially with an increasing propan-2-ol concentration, until it is lost (i.e. $\alpha=1$), then as more polar modifier is added selectivity returns. We observe that the elution order at low propan-2-ol concentration is $S < R$ and that on increasing the propan-2-ol concentration above 10% in the mobile phase, the elution order is reversed. This is illustrated in Figure 41.

Figure 41 1-Phenylethanol elution order change on APC



Cellulose and amylose differ in configuration only at the 1-position of each glucosyl unit. If chiral recognition is solely due to interactions between the solute and the derivatised glucose unit, then the corresponding carbamate derivative of the polysaccharide would exhibit similar chiral recognition. The results in Table 14 clearly show that this is not the case. The arrangement of glucosyl units along the polysaccharide chain differs between the tris(phenylcarbamate) of cellulose and amylose. It is this difference which leads to the different arrangements of carbamate groups that are responsible for chiral recognition. For CPC and APC, the difference in chiral recognition properties may be attributable to the different chiral cavities or spaces built by two or more carbamate groups on adjacent units. In CDMPC, the carbamate at the 6 position can be close to both the carbamates at the 2 and 3 positions on the neighbouring glucose unit. In ADMPC, a carbamate group at the 6 position is in close proximity to the carbamate groups at the 6 position on two neighbouring glucose units.

The selection of smaller pore size (500Å) silica as the support for polysaccharide carbamates produced CSP columns which showed similar chiral selectivity to those CSP columns onto a wider pore size (4000Å) silica. Selectivity's for the 5 solutes are in good agreement with those obtained by Okamoto on the wider pore size (see Table 14).

		CHIRAL STATIONARY PHASE									
RACEMATE		CPC ^a		CDMPC b		CNC ^b		APC ^b		ADMPC b	
		k' ₁	α	k' ₁	α	k' ₁	α	k' ₁	α	k, l	α
STILBENE	this work	0.61(+)	1.43	0.62(-)	2.00	0.86	1.3	0.54	1.40	0.55	1.40
OXIDE	Okamoto	0.67(+)	1.46	0.74(-)	1.68			0.39	1.46	0.42(+)	3.04
2,2,2-	this work	1.52(-)	1.34	1.81(-)	2.43	2.15	1.0	0.90	1.00	1.33	1.00
TFAE	Okamoto	1.56(-)	1.45	2.13(-)	2.59			0.61	1.00	1.30(+)	1.15
BENZOIN	this work	4.30(+)	1.00	1.75(+)	1.57	5.95	1.0	4.72	1.00	4.02	1.00
	Okamoto	5.28(+)	1.00	2.43(+)	1.58			3.72	1.00	3.14(-)	1.21
TROGERS	this work	0.98(+)	1.29	0.80(+)	1.25	0.82	1.0	1.09	1.29	0.88	1.62
BASE	Okamoto	1.12(+)	1.37	0.97(+)	1.32			0.77	1.28	0.53(+)	1.58
I-PHENYL	this work	0.89	1.00	1.53	1.17	0.68	0.9	0.68	1.01	0.54	1.00
ETHANOL	Okamoto										

Table 14 comparison of capacity factors and selectivity coefficients with literature values obtained on 4000Å APS (mobile phase hexane/IPA 90:10 :a j.chrom 363 ,173-186, 1986 ;b Bull. Chem Soc. Jpn.955-957,1990

The optical resolution ability of the derivatives carrying various substituents on the phenyl rings is greatly dependant on the kinds of substitution. The inductive effect of the substituents affects the polarity of the urethane bond, which is the most important adsorbing site for a solute. The chiral recognition ability also depends on the high order structure of the polymers. Therefore, the mechanism of optical resolution on these CSP's cannot be

simply understood since the structures, including the high order structure of the polysaccharide derivatives, delicately vary according to the substituents. The CDMPC phase showed high chiral recognition and can separate a broad range of racemic compounds.

CHAPTER 4

The nature of the chiral recognition processes in chiral stationary phases based on carbamates of cellulose and amylose remain largely unknown at the present time. On the one hand, Okamoto's studies of the electronic effects of aryl substituents on retention and resolution, supported by our own studies (Chapter 3), suggest that direct docking (H-bonding) of the analyte to individual carbamate residues is of considerable importance. In some cases, this may be accompanied by π - π interactions with adjacent aryl π systems. On the other hand, the steric effects associated with ortho-substitution; bulky aryl groups, changes in solvent structure and changes in the α/β orientation of the glycosyl linkages all support the idea that inclusion complexation of the analyte within the "chiral ravines" defined by the 3-dimensional structure of an ordered network of adjacent polymer strands is of major significance for the chiral recognition process.

A major objective of the present project has been to attempt to prepare carbohydrate phases based on short oligosaccharides, both as physically coated and as chemically bonded phases, which would allow assessment to be made of the relative importance of local versus long range effects in contributing to chiral recognition.

Due to the low abundance in nature of the lower molecular weight oligosaccharides, the preparation of these compounds is dependent upon the breakdown of the polysaccharides.

4.1 INTRODUCTION TO THE SEPARATION AND MASS SPECTRAL ANALYSIS OF SUGARS

4.1.1 Separation of Sugars by HPLC

In the last 17 years, considerable progress has been made in the analytical separation and quantitation of oligosaccharides by HPLC¹⁷⁸⁻¹⁸⁸. In the method adopted, the oligosaccharides were separated on aminopropyl silica gel, and were eluted in increasing molecular weight with a binary mobile phase mixture of acetonitrile-water. The eluted compounds were detected at 190nm.

The separation of sugars using a chemically bonded aminoalkyl phase depends upon the partition of the solutes between a stagnant aqueous liquid phase and a moving acetonitrile-water mixture^{240,241}. The bonded hydrophilic amino groups cause demixing of the aqueous acetonitrile mixture, but do not otherwise participate in the separation process. The amount of water enrichment is expected to be dependant on the nature and the amount of bonded amine. Chemically modified silica can lose amine by hydrolysis, resulting in decreased sugar retention. Using unchanged retention times are obtained after deterioration in k' by the addition of amine to the eluent. Wheals²⁵² and his co-workers investigated the influence of different amines on sugar retention. Both retention and separation efficiency appeared to be influenced by the type of amine added.

4.1.2 Studies of Free Sugars and Derivatised Sugars by Mass Spectrometry

A diverse range of mass spectrometric methods has been used to characterise oligosaccharides by identifying molecular weight, sequence and isomeric structures. The electron impact and chemical ionisation techniques both require the sample to be volatile and in the gas phase for ionisation. Since volatility is reduced by the number of polar functional groups, permethylation, acetylation and trimethylsilyl derivatisation have been employed to increase sample volatility. Extension of mass spectrometry to large, involatile and often thermally fragile bio molecules has required methods capable of ionising molecules directly from the solid or liquid state. This has led to the development of new techniques including field desorption²⁴³, fast atom bombardment (FAB)^{244,245}, liquid secondary ion mass spectrometry (LSIMS)²⁴⁶ and electrospray²⁴⁷.

These techniques have made possible the analysis of intact oligosaccharides without prior derivatisation to replace all labile hydrogen atoms. Whilst field desorption played an important role²⁴⁶, it has been overshadowed by the ease of maintaining a stable molecular ion beam with FAB and LSIMS for use with sector instruments. LSIMS is carried out using an energetic primary beam composed of focused cesium ions²⁴⁶ and FAB uses xenon atoms²⁴⁵ to eject/ionise the polar, labile analyte from the surface of a polar liquid matrix. Oligosaccharides can be sputtered from such viscous liquid matrices in the form of protonated or

deprotonated molecular ions, despite their extreme hydrophilicity. Significant increases in sputtering efficiency may be accomplished through chemical derivatisation of the hydrophilic sugar to a more surface-active hydrophobic sugar derivative and selection of an appropriate matrix²⁴⁸.

An important new technique for the analysis of large biomolecules is electrospray²⁴⁷. This technique produces a distribution of highly charged ions with a maximum mass to charge a ratio within the range of a quadrupole analyser.

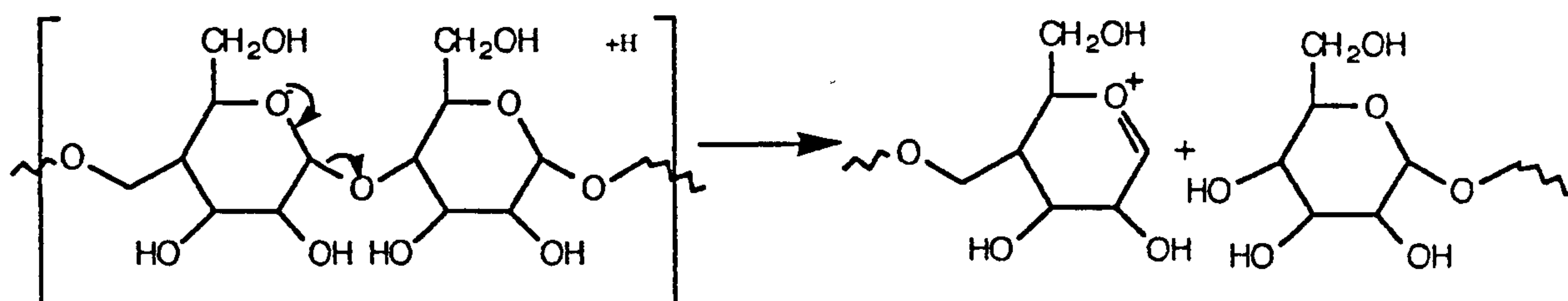
4.1.2.1 Mass Spectral Analysis of the Free Sugars

When free sugars are analysed by FAB MS, the pseudomolecular ion region can be assigned without difficulty in the positive mode as $[M+H]^+$ and $[M+(\text{glycerol})+H]^+$ and $[M+(\text{glycerol})_2+H]^+$, which are assigned to the formation of an adduct ion with the matrix.

Although it is useful for determining molecular weights, the mass spectra obtained for free oligosaccharides often give ambiguous sequence data. The reason for this may be deduced from a consideration of the fragmentation pathways²⁴⁸.

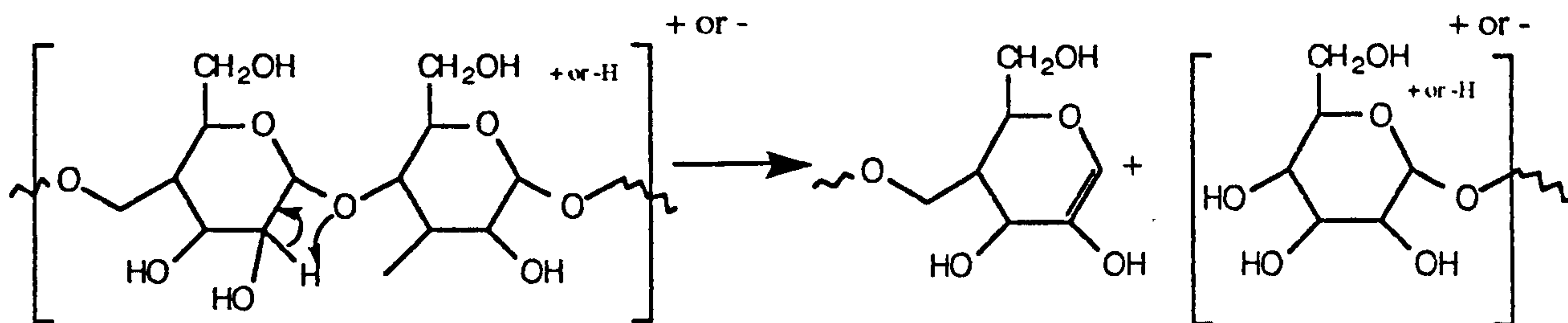
Pathway A

Description:- Glycosidic cleavage to form an oxonium ion; charge retained on non-reducing end; positive ion mode of FAB only; often referred to an A₁ type cleavage. This is similar to the cleavage seen in EI mass spectrometry.



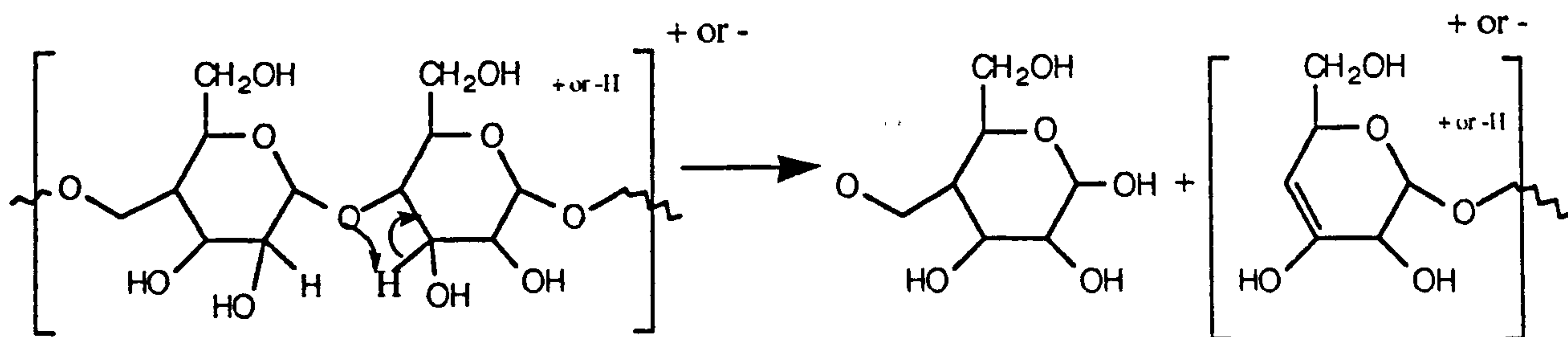
Pathway B

Description:- Glycosidic cleavage with a hydrogen transfer; charge retained on a reducing end; positive and negative modes; often referred to as β cleavage.



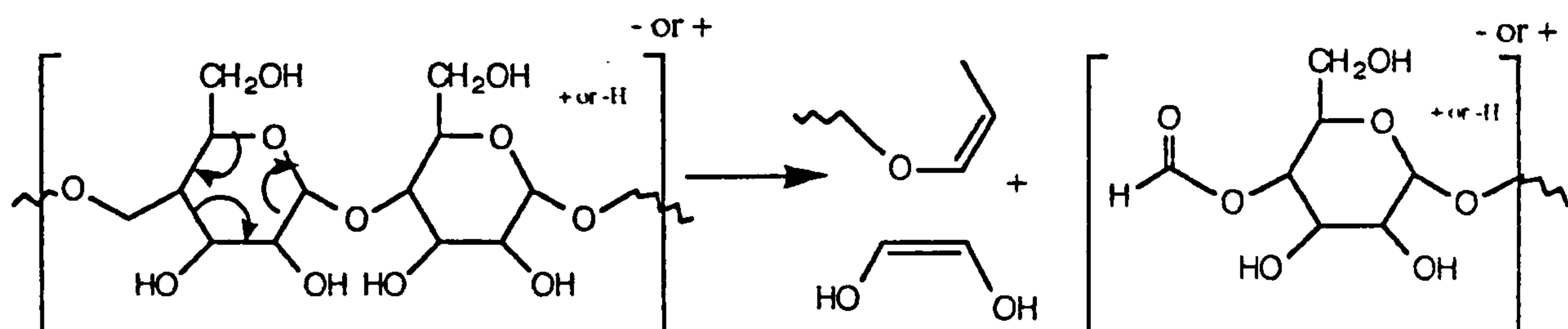
Pathway C

Description:- glycosidic cleavage with a hydrogen transfer; charge retained on the non-reducing end; positive and negative modes.



Pathway D

Description:- Ring cleavage; charge retained on reducing end; ions are 28 mass units heavier than those formed on pathway B. Positive and negative modes of FAB.



In an underivatised, unreduced oligosaccharide, pathways B and C are not distinguishable, and it is not possible to establish whether the resulting fragment ions are derived from the non-reducing or the reducing end of the molecule. A further complication is the presence of ions resulting from "double cleavages", for example, a combination of pathways A and B operating at different glycosidic linkages, which give apparent non-reducing and sequence ions that are not, in fact, derived from the non-reducing terminus.

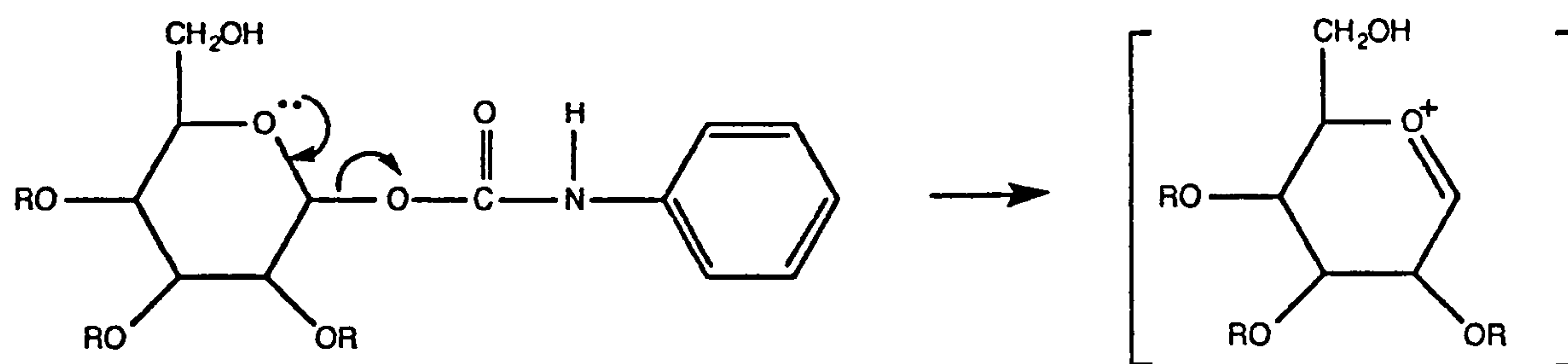
The number of fragment ions afforded by underivatised carbohydrates vary considerably, depending upon the structure of the molecule, its purity, amount loaded and nature of the matrix used. In summary, the fragmentation data obtained from underivatised samples need to be interpreted with caution, and the primary objective should be molecular weight assignment. Sequencing should be carried out using derivatives.

4.1.2.2 Mass Spectral Analysis of Derivatised Samples.

The per-O-acetyl and per-O-methyl derivatives have been used extensively for sequence analysis and for providing molecular weight information²⁴⁸. The per-O-carbamoyl derivatives also resolve the problems of ambiguity (as opposed to the free sugars), because a true, non-reducing residue will be fully substituted, whereas a non-reducing residue resulting from mass spectrometric cleavage will carry a free hydroxyl group. Pseudomolecular ions are detected in the positive ion mass spectra enabling deduction of the molecular weight as $[M+Na]^+$.

Fragment ions

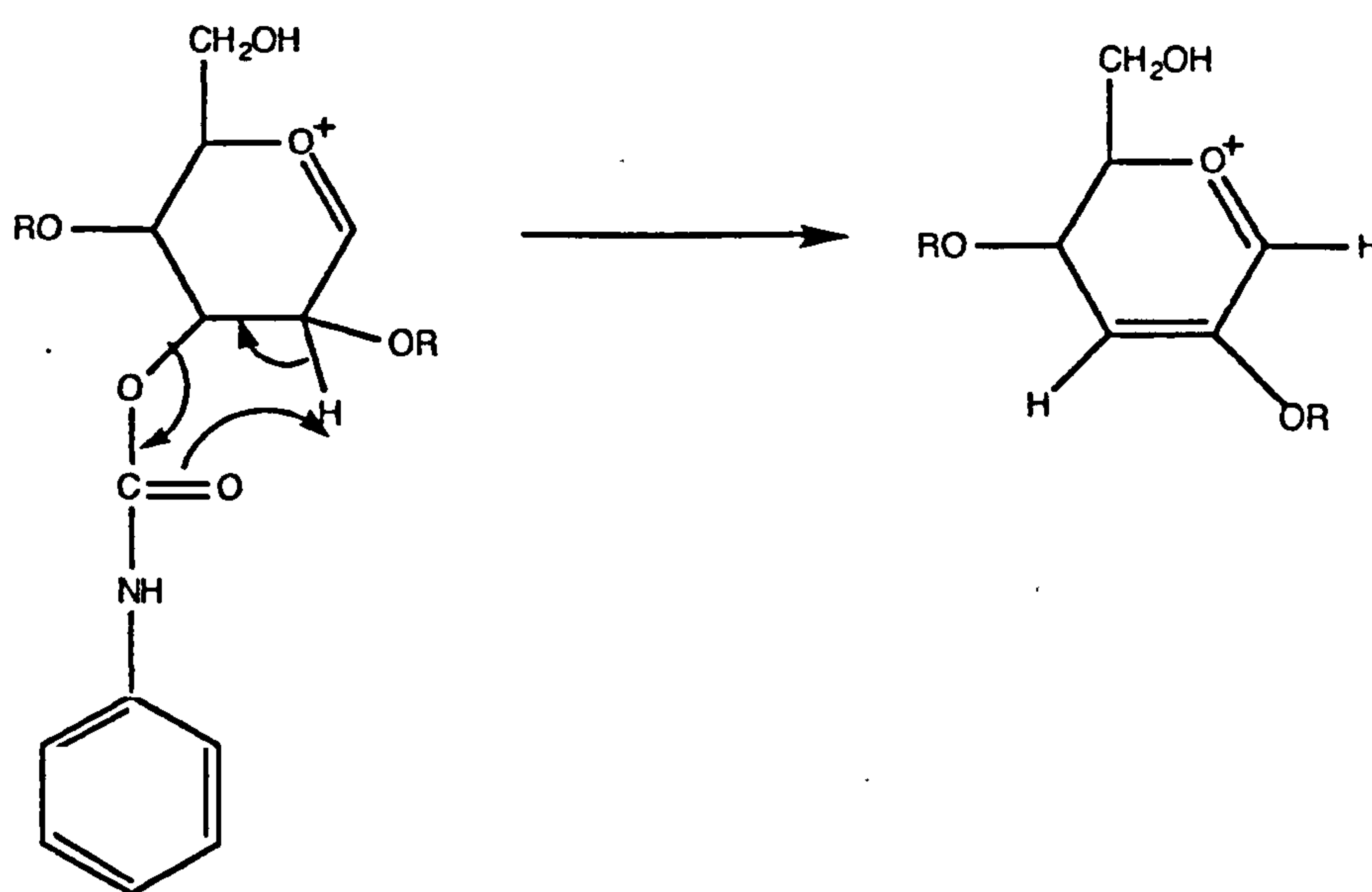
Fragment ions resulting from cleavage of the pseudomolecular ion $[M+Na]^+$ are observed. These ions originate from the loss of an R group (where $R = \text{C}_6\text{H}_5\text{NCO}$) initially at the anomeric carbon to producing the following fragment (Scheme 10).



Scheme 10 Fragment pattern for an anomeric carbamate group

This sequence is then repeated removing another carbamate group from the monosaccharide ring via elimination producing a

combination of a fragment of ions at m/z $[M-2R+Na]^+$; m/z $[M-2R]^+$, m/z $[M-OR-R+H]^+$ and at m/z $[M-2OR]^+$ (Scheme 11). The elimination of a third carbamate group proceeds via a similar sequence, i.e. m/z $[M-3R+Na]^+$; m/z $[M-3R]^+$; m/z $[M-OR-2R]^+$, m/z $[M-OR-2R-H_2O]^+$, then at m/z $[M-OR-2R-2H_2O]^+$. Loss of the fourth and fifth group also occurs with a similar sequence.



Scheme 11 Elimination of a carbamate group

To aid the interpretation of the mass spectra of carbamate di and of tri-saccharides, the labelling sequence L-N-P (where letters refer to fully carbamated sugar residues see Figure 42) was used where the non-reducing end is referred to as L and the reduced end as P 247,248.

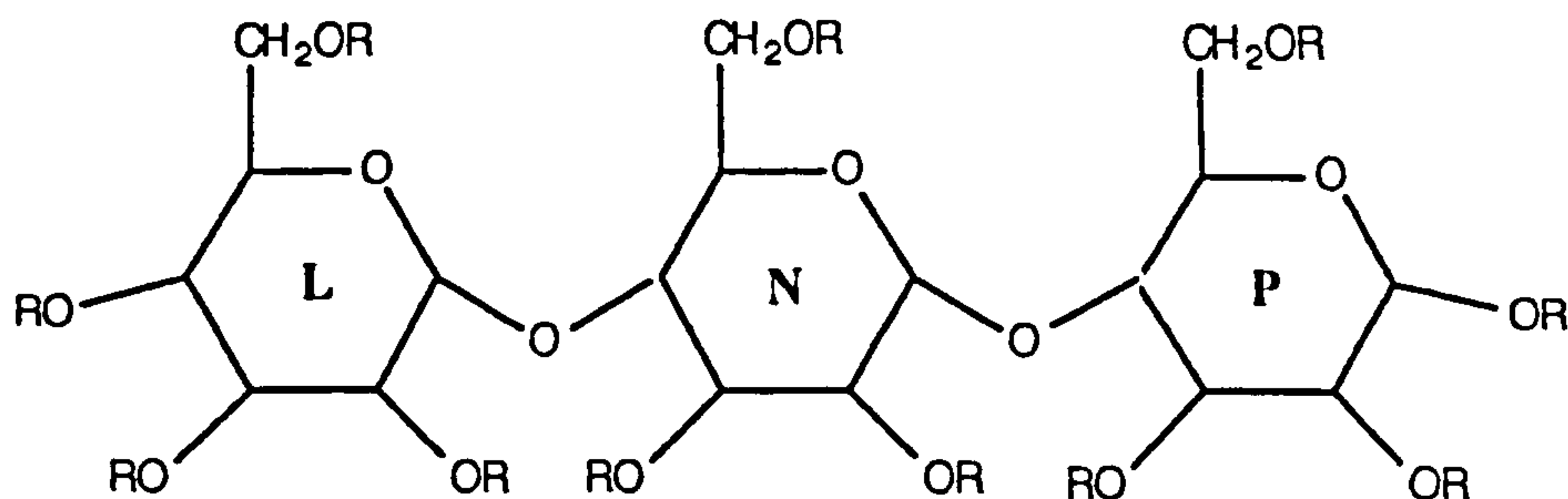


Figure 42 Ring labelling sequence for oligosaccharides

Thus for a disaccharide the loss of the aryl carbamate group (where $R = \text{C}_6\text{H}_5\text{NCO}$) at the anomeric carbon produces an ion at m/z $[M-R]^+$

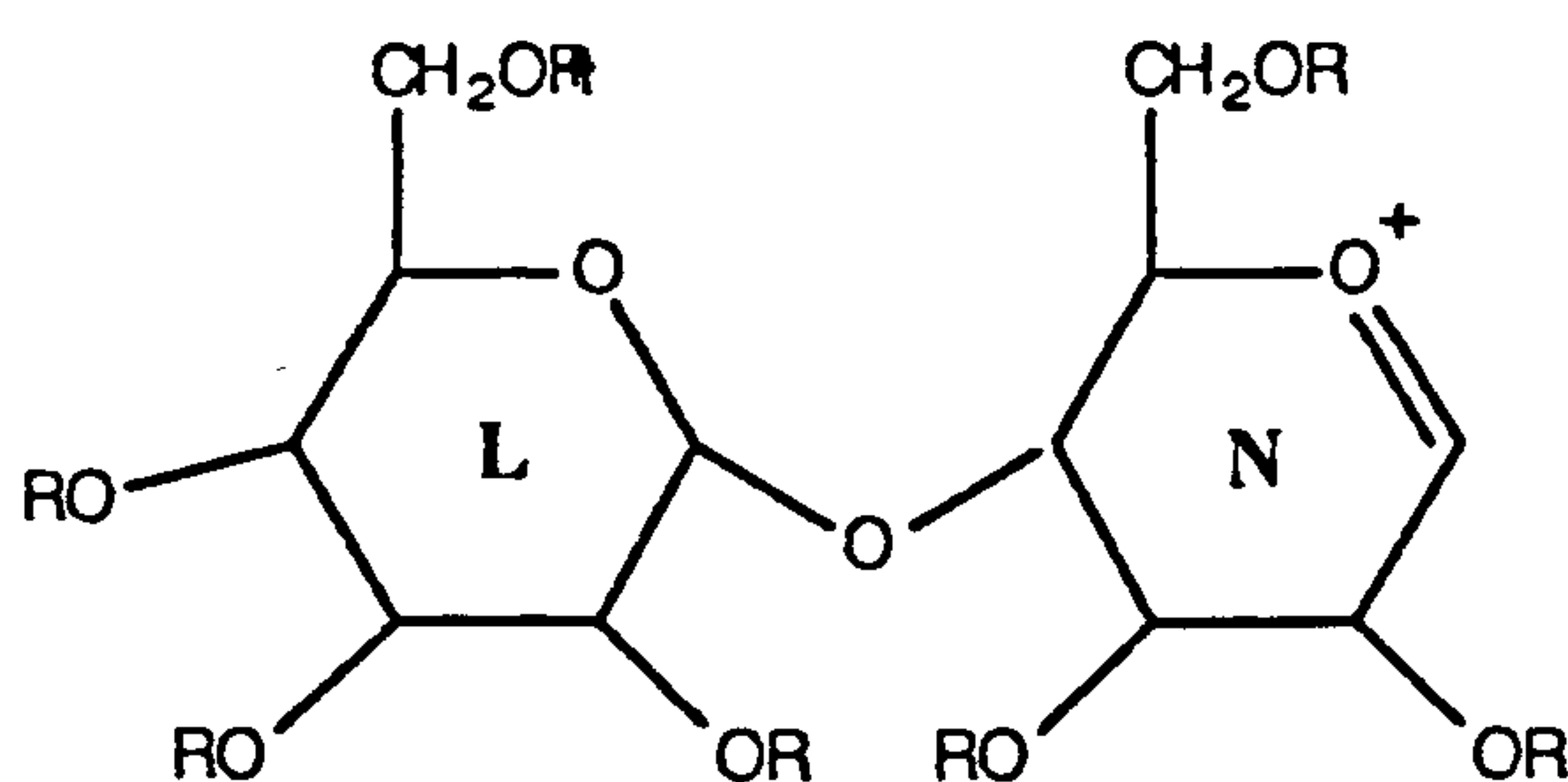


Figure 43 Oxonium ion formation from the removal of an R group from ring N

The sequence is then repeated (as for a monosaccharide) at the reducing end of the molecule with the elimination of a second group m/z $[M-OR-R]^+$; m/z $[M-2OR]^+$; a third group m/z $[M-2OR-R]^+$; m/z $[M-3OR]^+$; a fourth group m/z $[M-3OR-R]^+$. The elimination of the fourth group may not come from the same ring system: it is possible that it fragments from a position from the unreduced end of the molecule, ring L. A fifth group is eliminated producing an ion at m/z $[M-5R-3H]^+$ which must be from the non-reducing end of the sugar molecule, ring L.

The appearance of a characteristic ion at m/z 751 in the spectrum of maltose octa(phenylcarbamate) is a result of the glycosidic cleavage to form an oxonium ion with the charge retained on the non-reducing end, L. This is an A₁-type cleavage (see page 138).

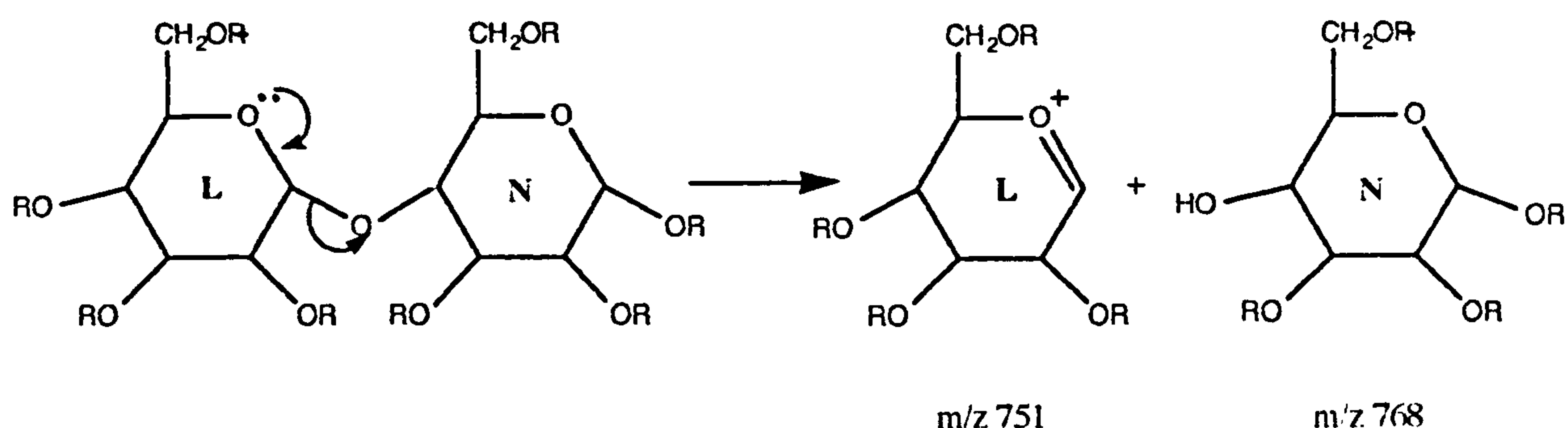


Figure 45 A₁ type cleavage

The absence of an ion in the spectrum at m/z 768 may suggest that the cleavage occurs after fragmentation and loss of the carbamate group from the reducing end of the sugar. The sequence for the loss of R groups from the non-reducing end of the sugar, L, is repeated as for a monosaccharide.

A₁ type cleavage of the trisaccharide at the α -1,4-glycosidic bond which joins rings N and P, forms an oxonium ion on the N ring m/z [M-O]⁺, then the same sequence begins as for the disaccharide, with another A₁ type cleavage of the glycosidic bond joining rings L and N producing an ion at m/z [M-N-P]⁺. The remaining monosaccharide unit fragments as previously.

4.2 Generation and Purification of Oligosaccharides

4.2.1 Oligosaccharides of Cellulose

Partial hydrolysis of cellulose with the aid of concentrated hydrochloric acid produces mixtures of the oligosaccharides from which components having degrees of polymerisation of 2-6 may be isolated. Oligosaccharides having higher degrees of polymerisation are not readily obtained, due to their low solubility¹⁶⁴.

When samples of cellulose, Whatman paper and cellulose powder, were hydrolysed according to the literature¹⁶⁸ analysis of the hydrolysis product by thin layer chromatography (TLC) showed that the solution contained a very high proportion of cellobiose (80%) and decreasing amounts of the di-,tri- and tetra-saccharides. Due to the poor yields of the higher oligosaccharides and the difficulty in their separation and purification, studies of the β -linked oligosaccharides were deferred in favour of the α -linked oligosaccharides, the malto- series.

4.2.2 Oligosaccharides of Amylose

The investigation employing the malto series was facilitated by the commercial availability of maltose, maltotriose and a mixture of the higher molecular weight malto-oligosaccharides with α -1,4-linkages. Analysis by TLC showed the mixture to be rich in oligomers with 3-6 glucose units and to contain smaller amounts

of those with 7-9 glucose units. A method of separation was then developed by using HPLC.

4.2.2.1 Analytical Separation of the Malto-oligosaccharide Series on Aminopropyl Silica Gel

Nucleosil APS (7µm, pore size 100Å) was slurry packed into a stainless steel column (25cm x 0.46cm id), producing a column which was evaluated to have approximately 4000 theoretical plates. The conditions for the separation of the malto-series were optimised with known standards. A solution of the malto-oligosaccharide mixture of concentration 5000 ppm was separated and the capacity factor k' for each standard was used to identify the resolved peaks. See Table 15.

PEAK NUMBER	k'1	IDENTITY
1	0.50	Glucose
2	0.70	Maltose
3	0.94	Maltotriose
4	1.29	Maltotetraose
5	1.73	Maltopentaose
6	2.08	Maltohexaose
7	2.41	Maltoheptaose
8	2.94	Maltooctaose
9	3.46	Maltononaose

Table 15 Capacity factors of malto-oligosaccharides on Nucleosil-APS eluted with Acetonitrile/water (55:45)

4.2.2.2 Separation by Preparative HPLC

Nucleosil (7 μ m, pore size 100Å:100g) was reacted with γ -aminopropyltriethoxysilane, to give a modified APS surface with 2.59 APS groups/nm². The modified silica was slurry packed into 31.0cm x 2.54cm column at 6000psi producing a preparative column whose performance was evaluated to have 3500 theoretical plates. The malto-oligosaccharide mixture (350mg injected via a 2cm³ loop) was eluted with acetonitrile-water (55:45) at 15cm³ min⁻¹ at room temperature and detected at 190nm.

The preparative separation was similar to that observed on an analytical scale. The individual peaks were collected, the solvent partially removed under vacuum with a rotary evaporator and the residue freeze dried. Analysis of each fraction using the analytical column showed the purity to be about 90%, based on peak areas for each component.

4.3 Results of the Mass Spectral Analysis of Oligosaccharides

4.3.1 Mass Spectral Analysis of Free sugars Separated by Preparative HPLC

As we observed in Section 4.1.2 the number of fragment ions afforded by underivatised oligosaccharides varies considerably and the FAB MS should be treated with caution and used mainly for the determination of molecular weight. The collected fractions

obtained from the preparative HPLC separation of the malto-series mixture were shown to have the following masses:-

MALTO- OLIGOSACCHARIDE HPLC Peak No	Compound	m/z PSEUDO-MOLECULAR ION	
		[M+H] ⁺	[M+(glycerol)] ⁺
4	Maltotetraose	698	760
5	Maltopentaose	829	924
6	Maltohexaose	992	/
7	Maltoheptaose	1153	/
8	Maltooctaose	1316	/
9	Maltonanaose	1477	/
	Maltoheptaose <i>standard</i>	1153	/

Table 16 Pseudo-molecular ion obtained from FAB-MS analysis of the separated oligosaccharides.

Analysis of the glucose, maltose and maltotriose was performed by negative ion electrospray. The solvent used was a 50:50 mixture of acetonitrile and water. The spectrum for glucose showed extensive polymerisation with the ion at m/z 179 [M-H]⁻; accompanied by the dimer m/z 359 [2M-H]⁻ as the most abundant ion,, the trimer at m/z 540 and smaller ions attributed to the tetramer m/z 720 and the pentamer at m/z 900. Maltose gave m/z 341 and a major peak due to the dimer m/z 684. For maltotriose, no monomer was observed and the ion at m/z 522 may be due to the M+H₂O species and other peaks due to varying degrees of hydration.

4.3.2 Analysis of Derivatised Oligosaccharides

4.3.2.1 Preparation of Derivatives

Initially, derivatisation was performed on the lower malto-oligosaccharides (maltose and maltotriose), as they are readily available commercially at moderate expense. As both maltose and maltotriose were available only in the monohydrate form, great care had to be taken to ensure that no water was present when the sugars were reacted with the aryl isocyanate. This was achieved by dissolving the sugar in pyridine and drying the solution with type 3A molecular sieves for 62 hours. The sugar solutions were then reacted at 80°C for 16 hours with the aryl isocyanate to form the aryl carbamate. Elemental analysis and ¹H nmr showed that the hydroxyl groups were completely derivatised to carbamate moieties.

4.3.2.2 Analysis by FAB-MS

The 3,5-(dimethylphenylcarbamate) derivatives (see Figure 45 a b and c)

A sequence of fragment ions from the pseudomolecular ion $[M+Na]^+$ for glucose 3,5-(dimethylphenylcarbamate) is observed. These ions originate from the loss of an R group (where $R = (CH_3)_2C_6H_3NHCO$) initially at the anomeric carbon producing fragments at m/z 791 $[M-R+Na+H]^+$; m/z 768 $[M-R+H]^+$ and m/z 751 $[M-OR]^+$. This sequence is then repeated removing another carbamate group from the monosaccharide ring via elimination producing ions at m/z 644 $[M-2R+Na+2H]^+$; m/z 621 $[M-2R+2H]^+$

and m/z 604 $[M-OR-R+H]^+$ and at m/z 584 $[M-2OR]^+$. The elimination of a third carbamate group proceeds via the same sequence, i.e. m/z 497 $[M-3R+Na]^+$; m/z 471 $[M-3R]^+$; m/z 457 $[M-OR-2R]^+$ and m/z 439 $[M-OR-2R-H_2O]^+$, then at m/z 421 $[M-OR-2R-2H_2O]^+$. The fourth group also shows the same sequence:- m/z 327 $[M-4R+4H]^+$; m/z 310 $[M-4R+2H-H_2O]^+$; m/z 292 $[M-4R-2H_2O+2H]^+$; m/z 274 $[M-4R-3H_2O+H]^+$; and m/z 256 $[M-4R-4H_2O]^+$.

The FAB spectrum for maltose octa(3,5-dimethylphenyl carbamate) produces a pseudomolecular ion at m/z 1541 $[M+Na]^+$ and a similar fragmentation pattern is observed as for the glucose derivative (see Figure 45b). The loss of the aryl carbamate group (where $R=(CH_3)_2C_6H_3NHCO$) at the anomeric carbon produces an ion at m/z 1373 $[M-R+3H]^+$ which fragments to yield an ion at m/z 1354 $[M-OR]^+$. The sequence is then repeated at the reducing end of the molecule when a second group is lost m/z 1208 $[M-OR-R+2H]^+$; m/z 1189 $[M-2OR]^+$; a third group m/z 1042 $[M-2OR-R]^+$; m/z 1026 $[M-3OR]^+$; a fourth group m/z 879 $[M-3OR-R+H]^+$. The elimination of the fourth group may not come from the same ring system, it is possible that it fragments from a position from the unreduced end of the molecule, ring L. A fifth group is eliminated producing an ion at m/z 712 $[M-5R-3H]^+$ which must be from the non-reducing end of the sugar molecule, ring L. The ion at m/z 751 is a result of the glycosidic cleavage to form an oxonium ion with the charge retained on the non-reducing end, L (A₁-type cleavage). The absence of an ion in the spectrum at m/z 768 may suggest that the cleavage occurs after fragmentation and loss of the carbamate group from the reducing end of the sugar. The sequence for the loss of R groups from the non-reducing end of

SAC115217 x1 Bgd=3 24-APR-92 16 04.0 03 18 ZAB-E FB.
 BpM=8 I=10v Hw=8 TIC=951968000 Acnt: CRAWFORD Sys: LOWESTAB
 GLU 3-5 SPH NO8A PT= 0° Cal: IN

HMR: 27192800
 MASS: 274
 x10.0°

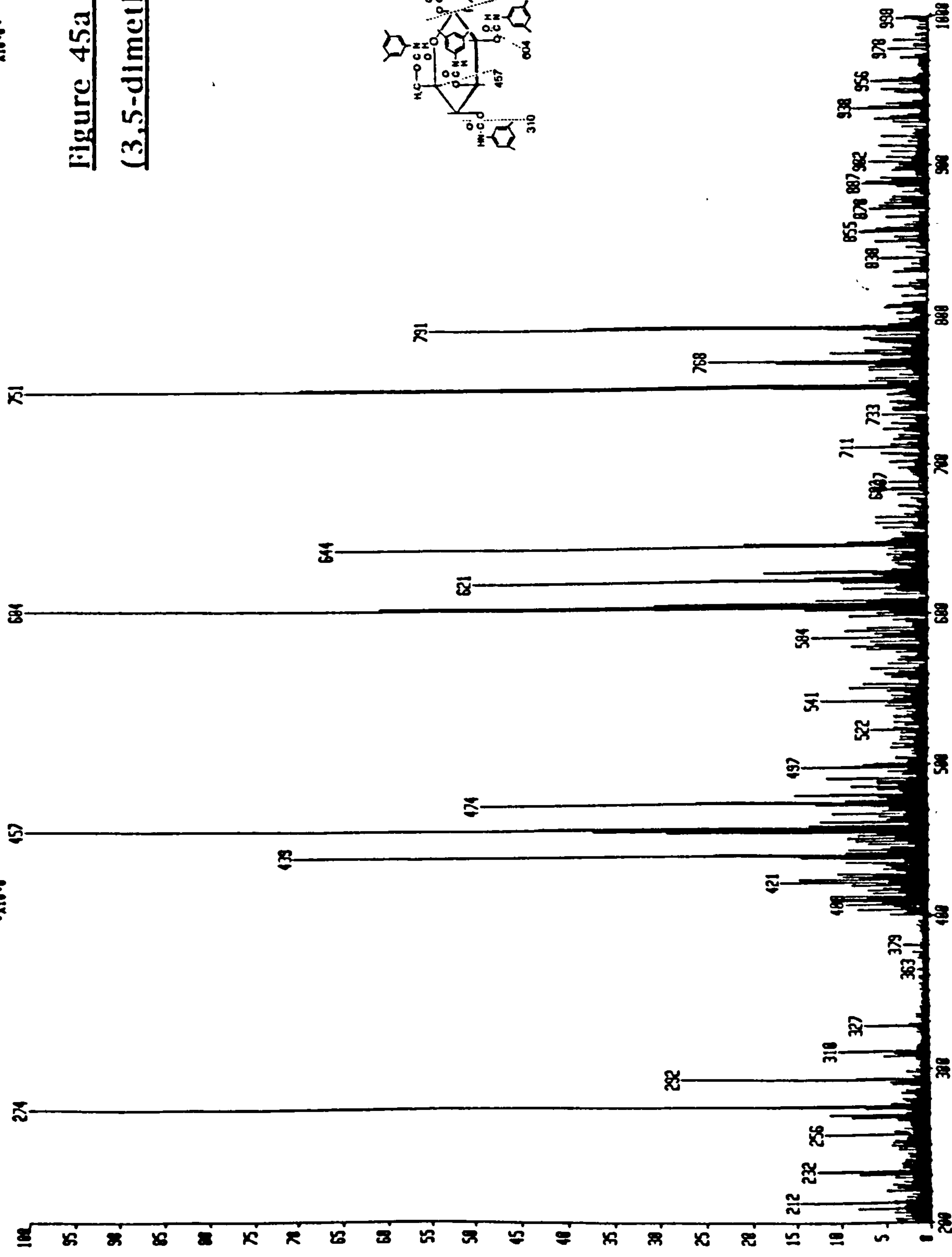


**Figure 45a FAB MS of Glucose penta
 (3,5-dimethylphenylcarbamate)**

17-MHR-92 13 48-0 01:31 ZAB-E FB
Acnt: CRAWFORD Sys: LOMASFAB
PT= 8° Cat: IM

HMR: 12784888
MASS: 457

100.000000
100.000000
100.000000

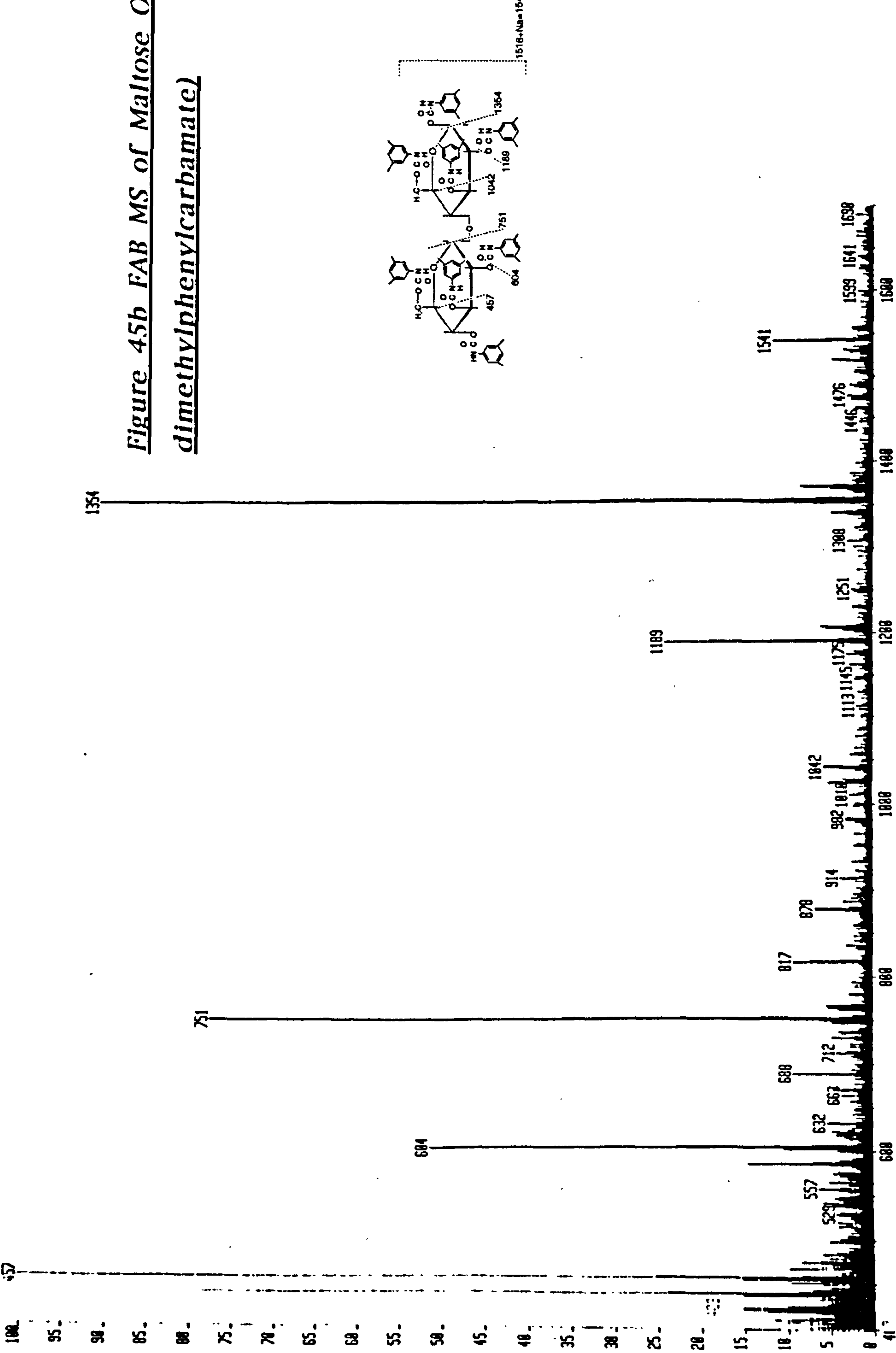
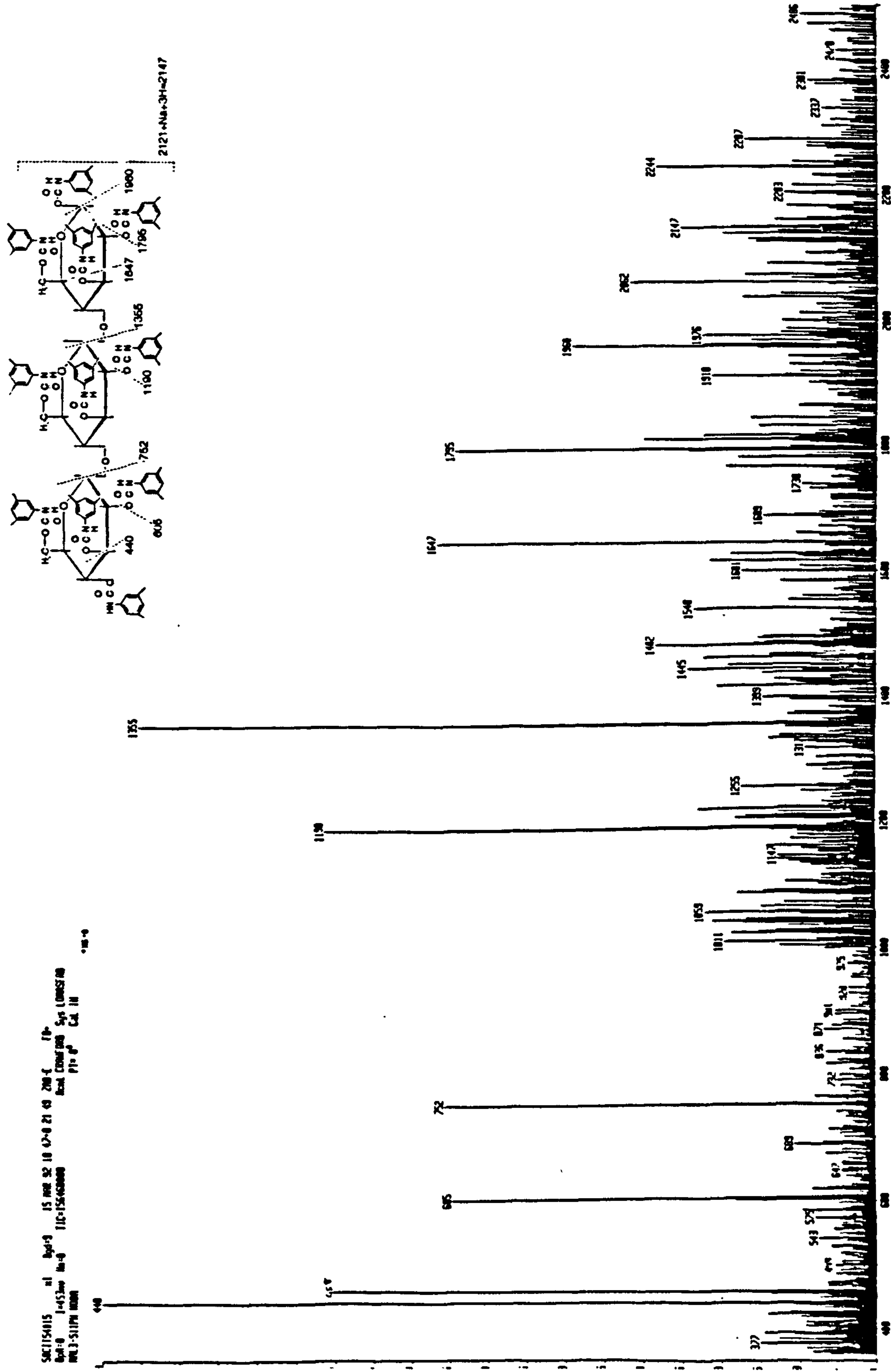


Figure 45b FAB MS of Maltose Octa(3,5-
dimethylphenylcarbamate)



the sugar, L, is repeated as for glucose penta(3,5-dimethylphenylcarbamate).

The pseudomolecular ion m/z 2147 $[M+Na+3H]^+$ is present for the trisaccharide, maltotriose undeca(3,5-dimethylphenylcarbamate). The sequence of fragment ions (see Figure 45c) for this compound is very similar to that obtained with the corresponding maltose and glucose derivatives. Elimination at the anomeric carbon in the P ring of and R group produces an ion at m/z 1976 $[M-R+2H]^+$; at m/z 1960 $[M-OR+1H]^+$. The familiar sequence for the elimination of R groups is then observed with the loss of 4 OR groups from the P ring and then the loss of a fifth group from the N ring m/z 1317 $[M-4OR-R]^+$. The loss of this fifth R group is from one of the other monosaccharide rings (i.e. L or N) and occurs with the trisaccharide intact. The presence of the 3 monosaccharide rings α -1,4 linked is confirmed with the presence of ions at m/z 975 $[M-7OR]^+$ and at m/z 646 $[M-9OR]^+$. A_1 type cleavage of the trisaccharide at the α 1,4-glycosidic bond which joins rings N and P, forms an oxonium ion on the N ring m/z 1355 $[M-P]^+$, then the same sequence begins as for the maltose octa(3,5-dimethylphenylcarbamate) derivative, with another A_1 type cleavage of the glycosidic bond joining rings L and N producing an oxonium ion at m/z 752 $[M-P-N]^+$. The remaining monosaccharide unit fragments as for the glucose penta(3,5-dimethylphenylcarbamate).

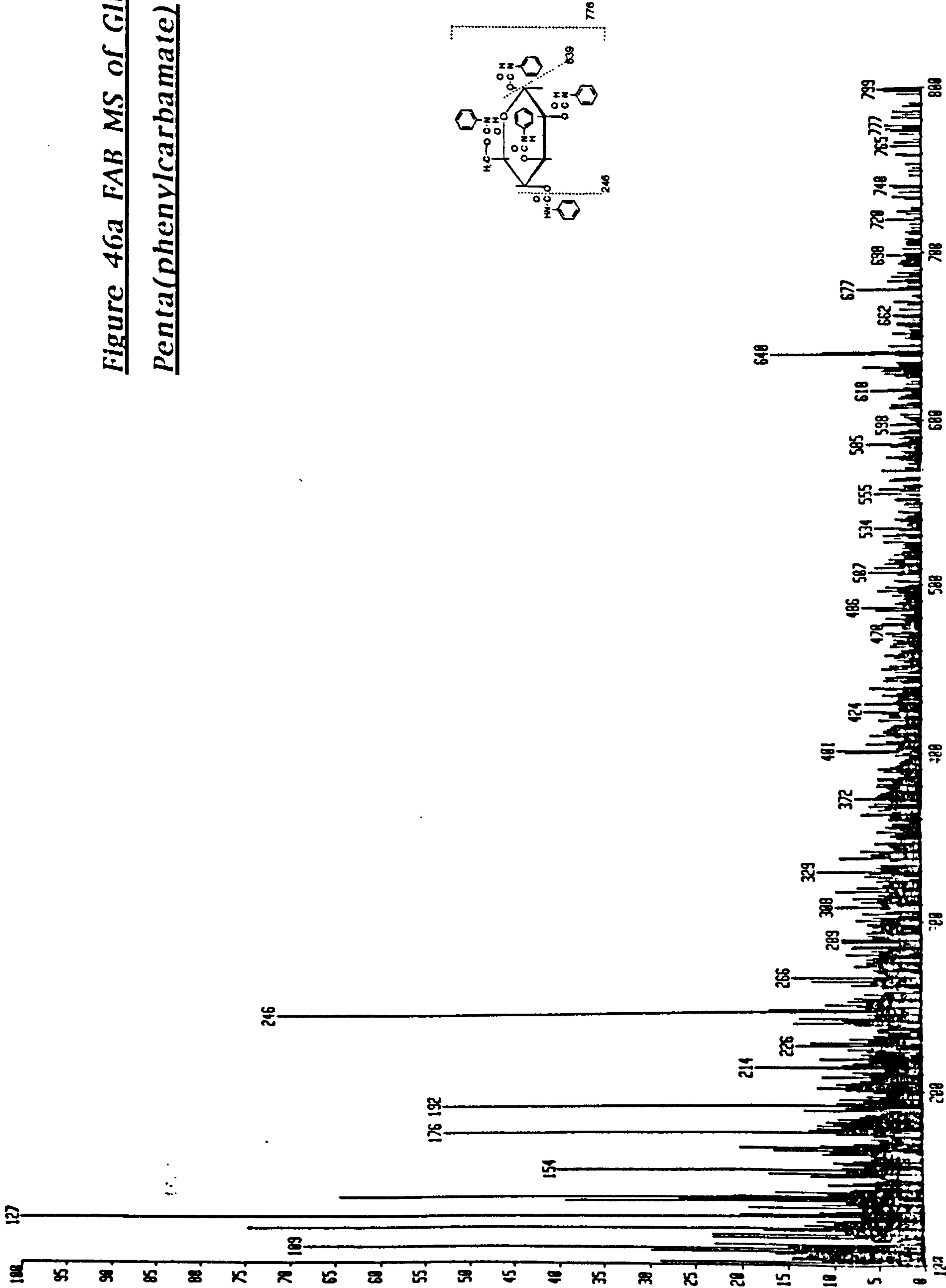
The Phenylcarbamate Derivatives (see Figure 46 a ,b and c)

The phenyl carbamate derivatised oligosaccharides produced very similar FAB spectra to those observed for the (3,5-dimethylphenylcarbamate)s, with the pseudomolecular ions and fragmentation ions displaced by multiples of 14 mass units according to the number of extra methyl groups present. Thus the molecular ions were associated with sodium to give $[M+Na]^+$ ions. The sequence of fragmentation's showed the elimination of R groups from the ring, which gave the regular pattern of $[M-R+Na]^+$ and $[M-OR]^+$ ions. The α -1,4-linkages were broken by type A1 cleavages to produce the corresponding oxonium ions.

39C115813 x1 Bqd=1 7-MAR-91 18 48-0 01 23 2AB-E FB+
Bp#-0 1=244mv Hn=0 TIC=83233880 Acnt CRAWFORD Sys LOWMSFAB
PCBG LOW RES FAB SCAN MODR PT= 80 Cal. IN

HMR: 1682888
MASS: 127

Figure 46a FAB MS of Glucose
Penta(phenylcarbamate)



S0C174386 x1 89d=1 8-FEB-92 10 54.0 04.52 ZAB-E FB
Bolt=0 I=10v Hn=0 Acnt CRAWFORD Sys LOMASFAB
MPLT-2-8PM08 MOD001 PT=0 Cal:1W

HR: 2331000
HRSS: 1158

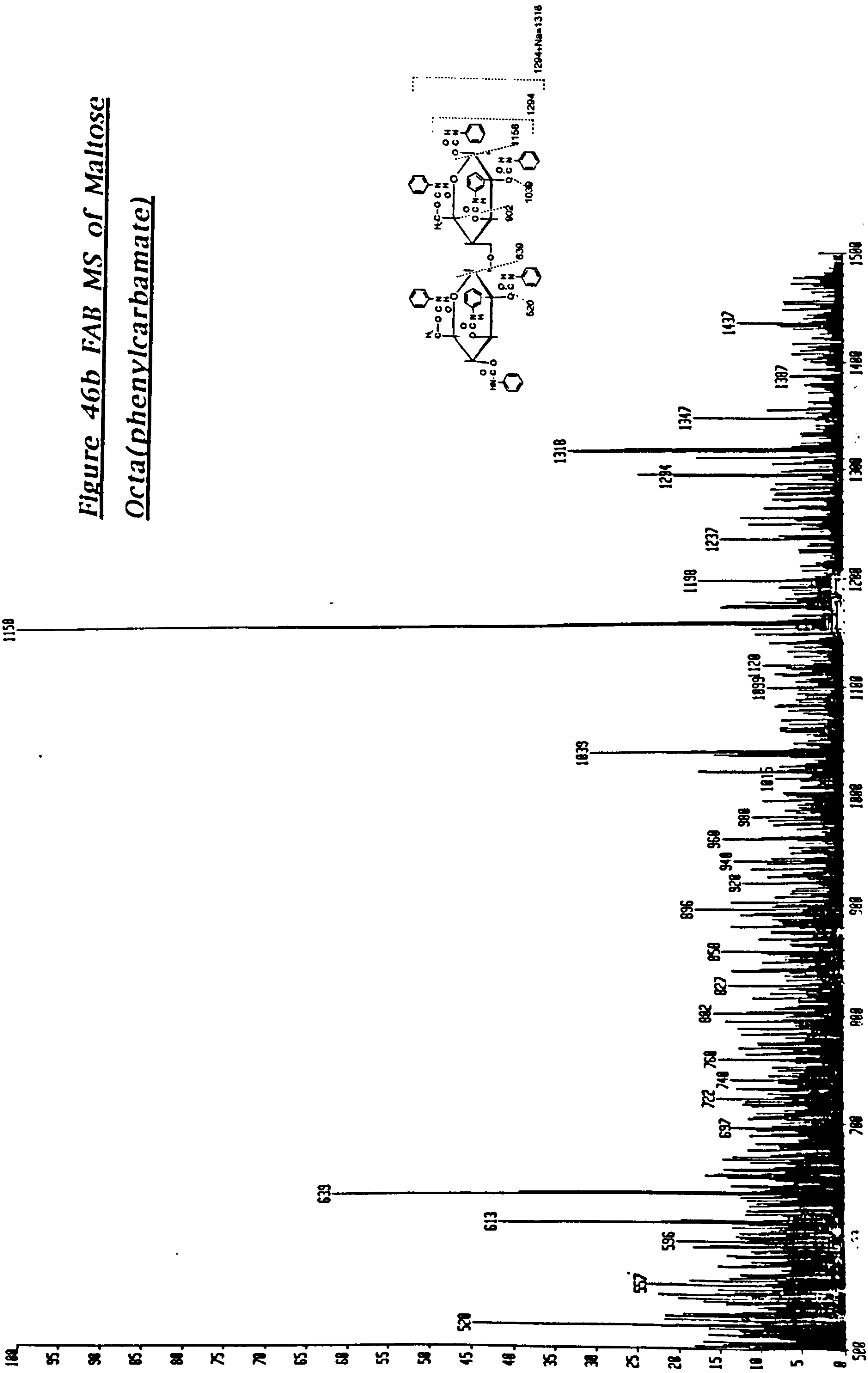
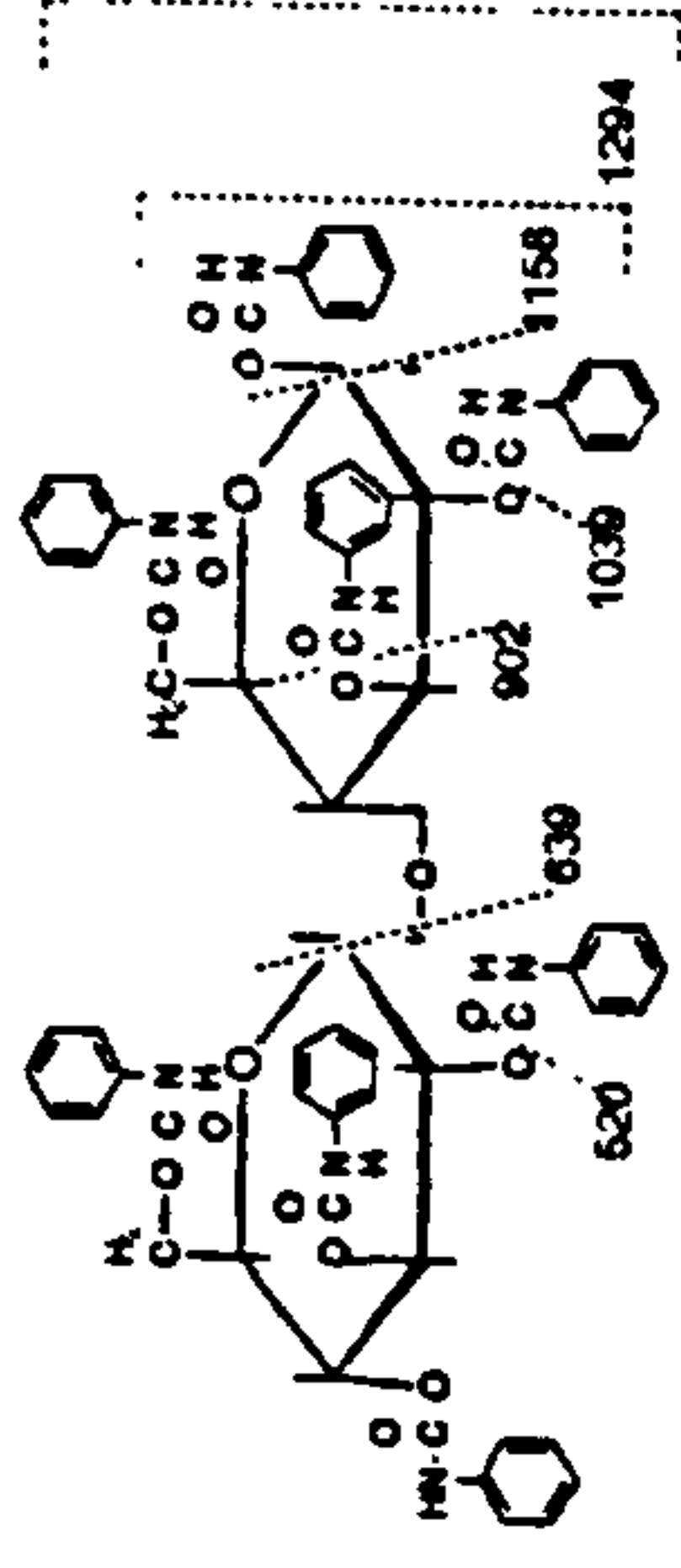


Figure 46b FAB MS of Maltose
Ota(phenylcarbamate)



58C114515 x1 89d=1 0-FEB-92 11 19:08 02.47 ZAB-E 18-
BpM=0 I=5.8v Ha=0 TIC=584916932 Acnt CRAWFORD Sys LOMSTRAB
MLT-3-12-PH1 NUBAR PT= 0° Cal: 1M

HMR: 37990000
MASS: 246
XS=0♦

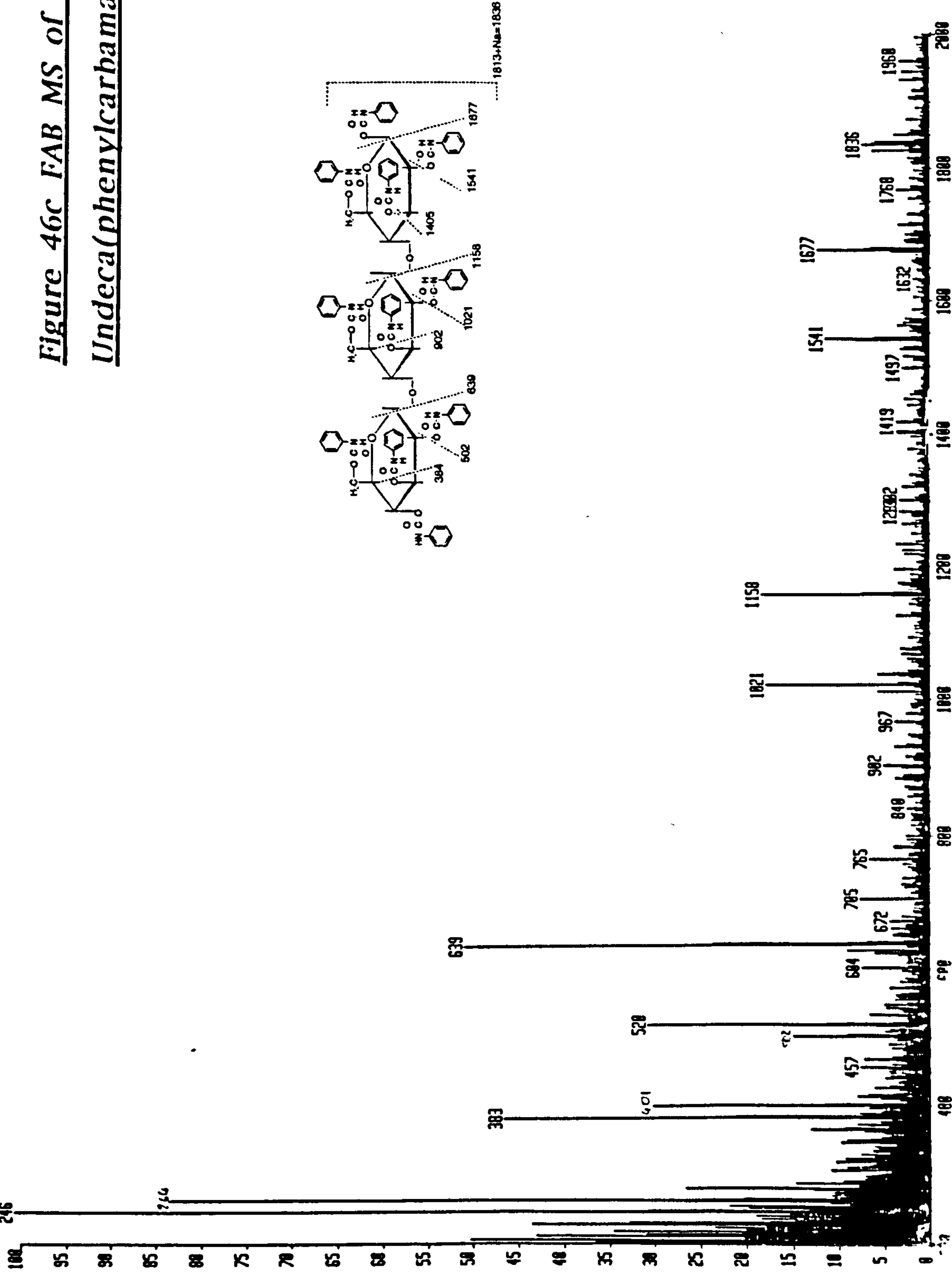


Figure 46c FAB MS of Maltotriose
Undeca(phenylcarbamate)

4.3.2.3 Liquid Secondary Ion Mass Spectrometry (LSIMS)

The samples of derivatised oligosaccharides were applied to a matrix of m-NBA (meta-nitrobenzyl alcohol). Trifluoroacetic acid (1%) was added to the matrix to aid protonation as positive ion spectra were required.

Analysis of the (3,5-dimethylphenylcarbamate) derivatives (see Figures 47 a,b and c)

The LSIMS spectrum of glucose penta(3,5-dimethylphenylcarbamate) produced a pseudomolecular ion $[M+H]^+$ at m/z 916. The sequence of fragmentation included (see Figure 47a) the loss of an R group at the anomeric carbon yielding the oxonium ion at m/z 790 $[M-R+Na]^+$; m/z 767 $[M-R]^+$; m/z 750 $[M-R-H_2O+H]^+$; the elimination of a second group m/z 644 $[M-2R+Na+2H]^+$; m/z 621 $[M-2R+2H]^+$; m/z 604 $[M-2R-H_2O+H]^+$ and m/z 586 $[M-2R-2H_2O]^+$. The presence of ions at m/z 474 $[M-3R+3H]^+$; m/z 457 $[M-3R-H_2O+2H]^+$; m/z 439 $[M-3R-2H_2O+H]^+$ and m/z 421 $[M-3R-3H_2O]^+$ signified the elimination of the third carbamate group from the monosaccharide.

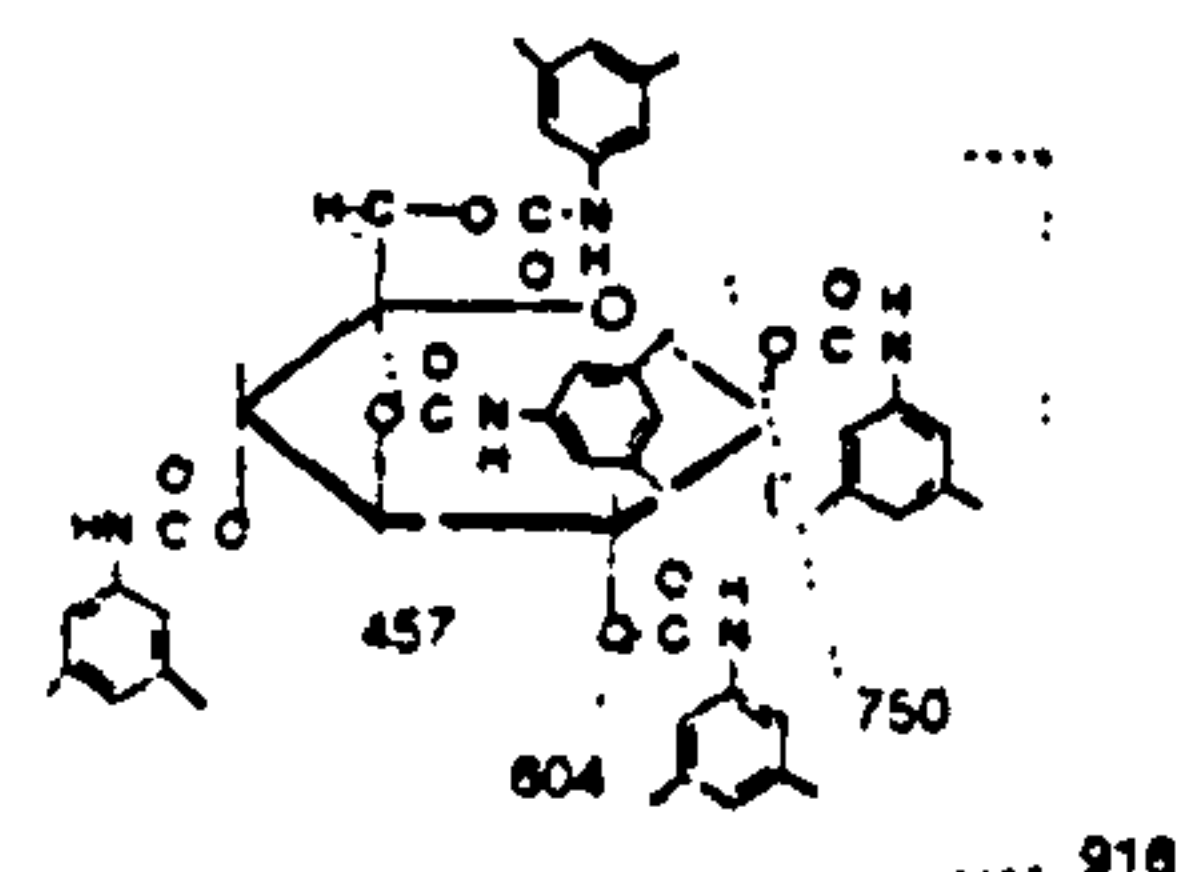
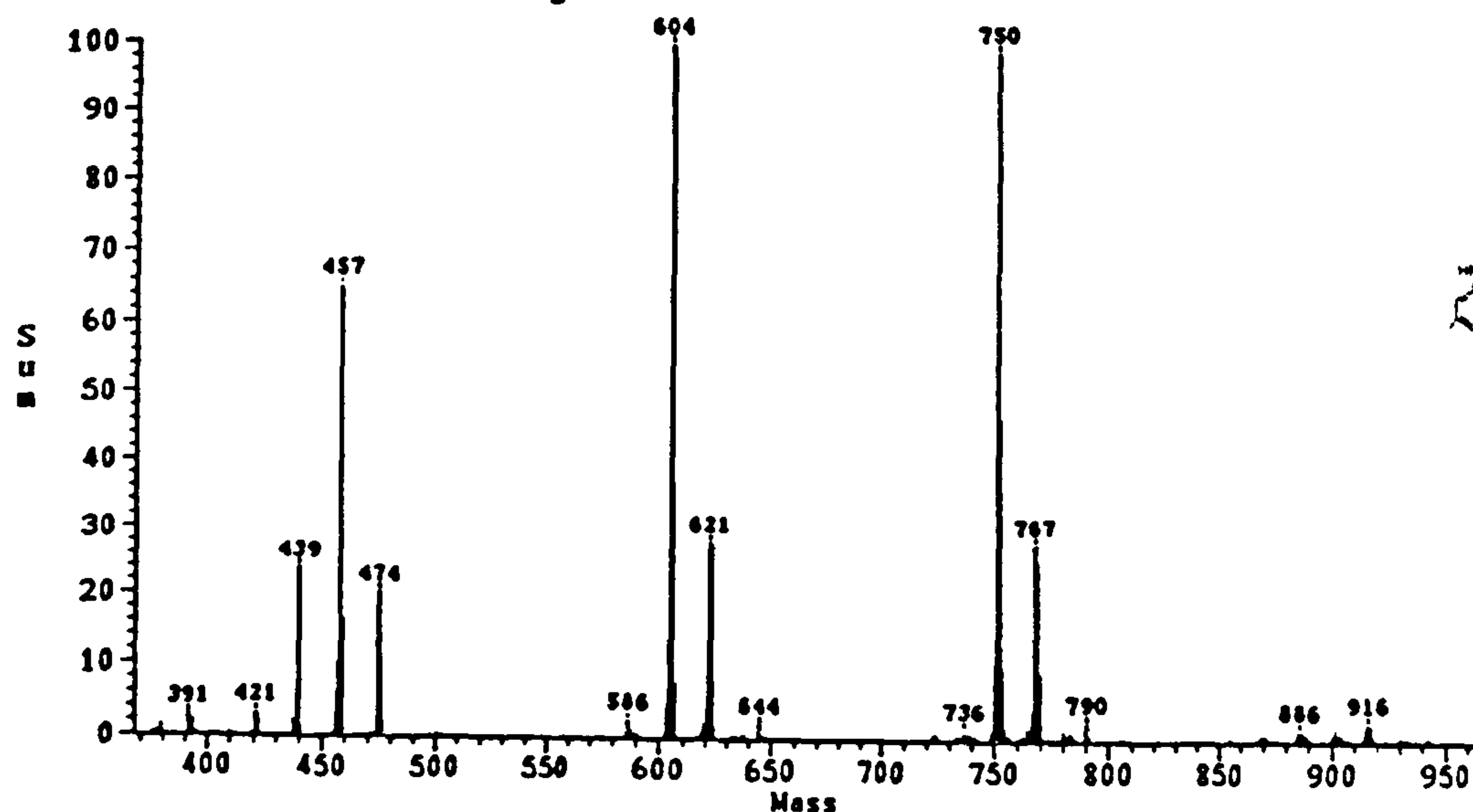
LSIMS of maltose octa(3,5-dimethylphenylcarbamate) revealed a similar picture to that for the corresponding glucose derivative (see Figure 47b): a pseudomolecular ion at m/z 1519 $[M+H]^+$; then

a similar fragmentation pattern m/z 370 $[M-R]^+$; m/z 1354 $[M-OR]^+$ to form the oxonium ion on the N ring; elimination of a second group gave ions at m/z 1206 $[M-OR-R]^+$; m/z 1189 $[M-2OR]^+$; a third group m/z 1041 $[M-2OR-R+H]^+$; m/z 1023 $[M-3OR]^+$. A1 type cleavage of the glycosidic bond yielded another oxonium ion on the L ring m/z 751 $[M-N]^+$ then the elimination sequence of R was repeated.

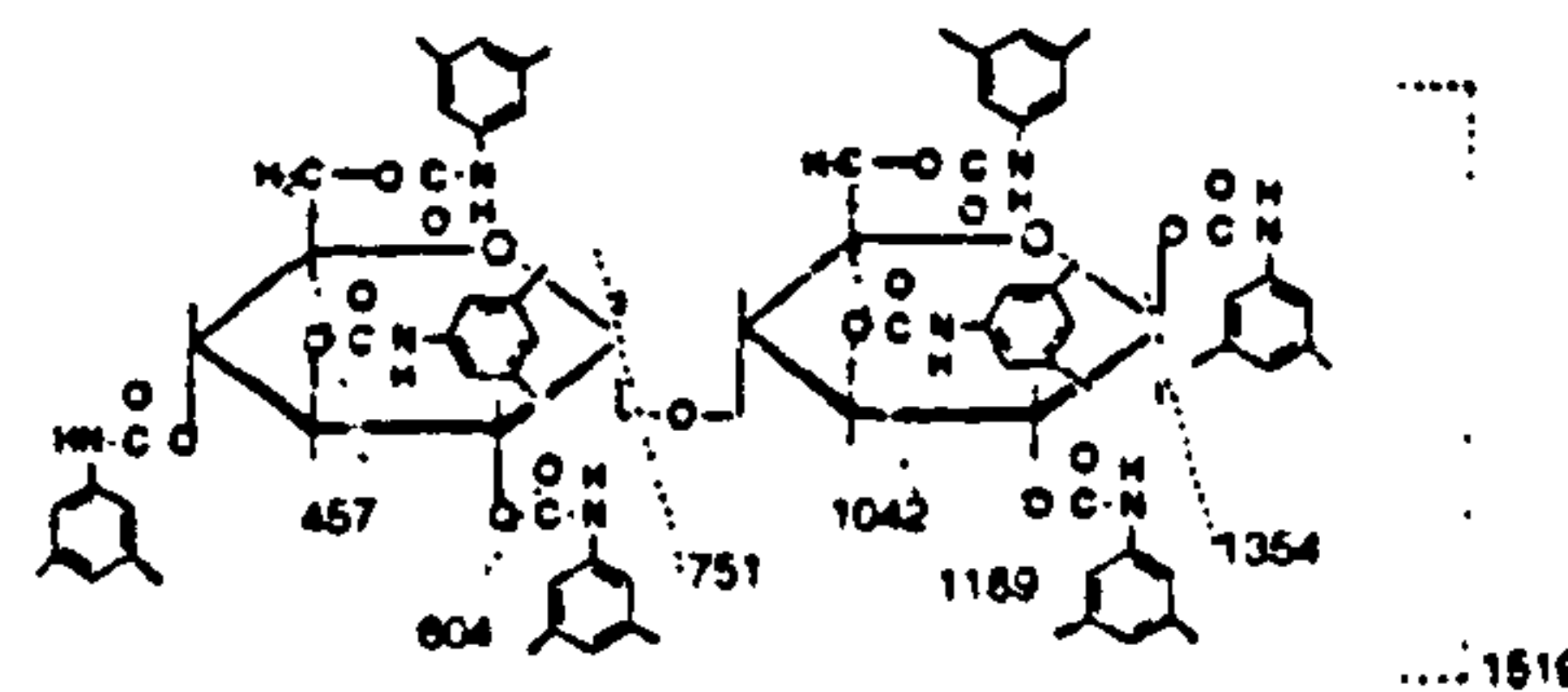
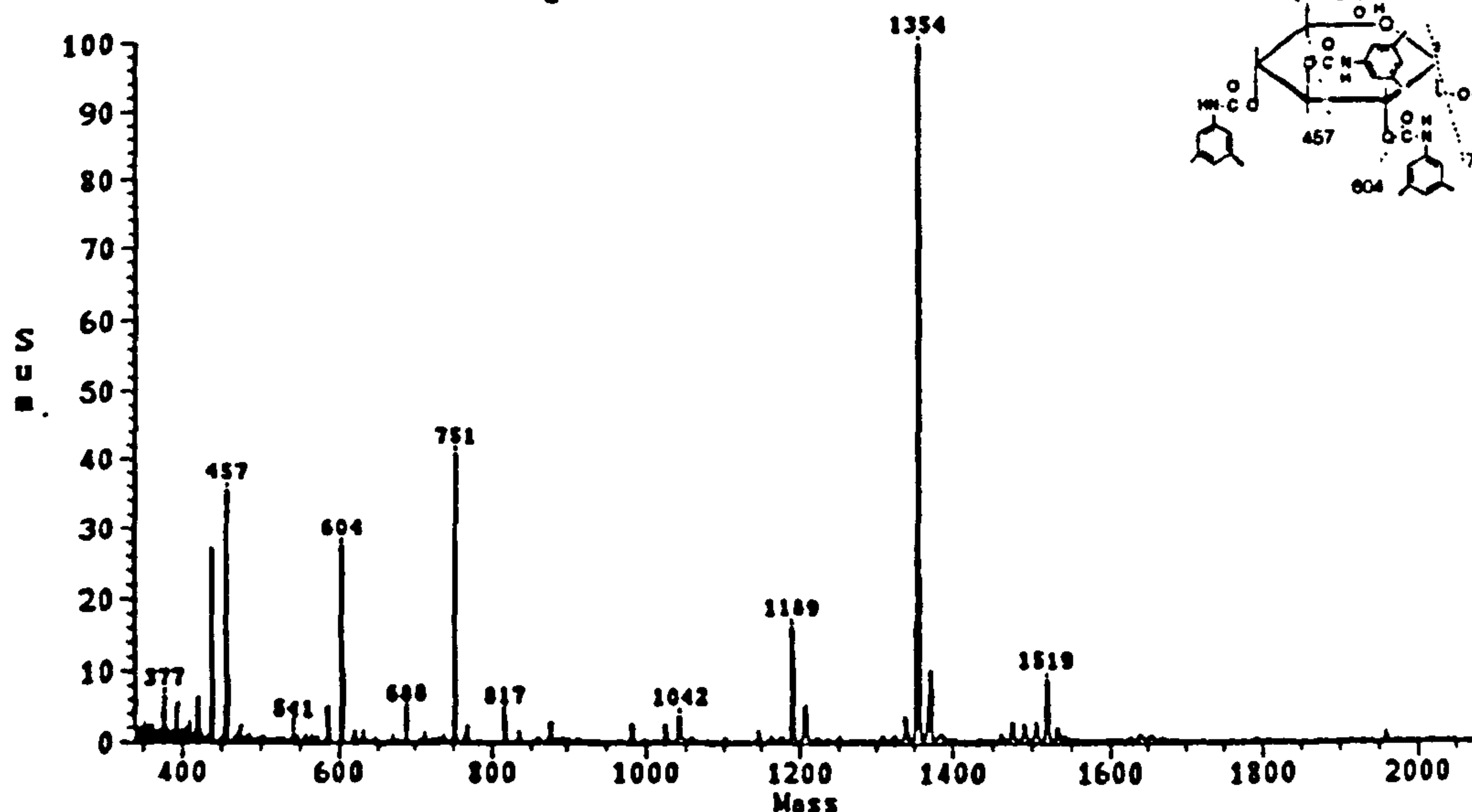
LSIMS of maltotriose undeca(3,5-dimethoxyphenylcarbamate), produced a pseudomolecular ion at m/z 2122 $[M+H]^+$; then the fragmentation sequence involving the loss of the carbamate groups and A1 type cleavages was repeated (see Figure 47c).

Figures 47 LSIMS-MS of a) Glucose penta(3,5-dimethylphenylcarbamate): b) maltose octa(3,5-dimethylphenylcarbamate) c) Maltotriose undeca(3,5-dimethylphenylcarbamate)

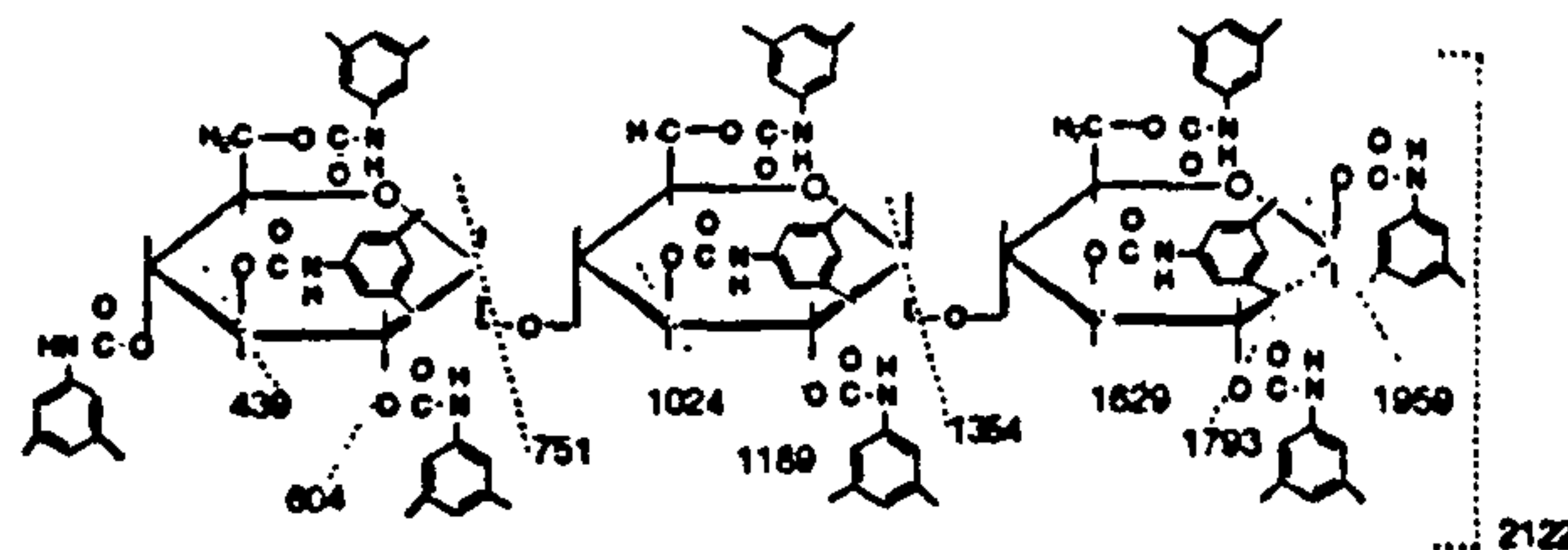
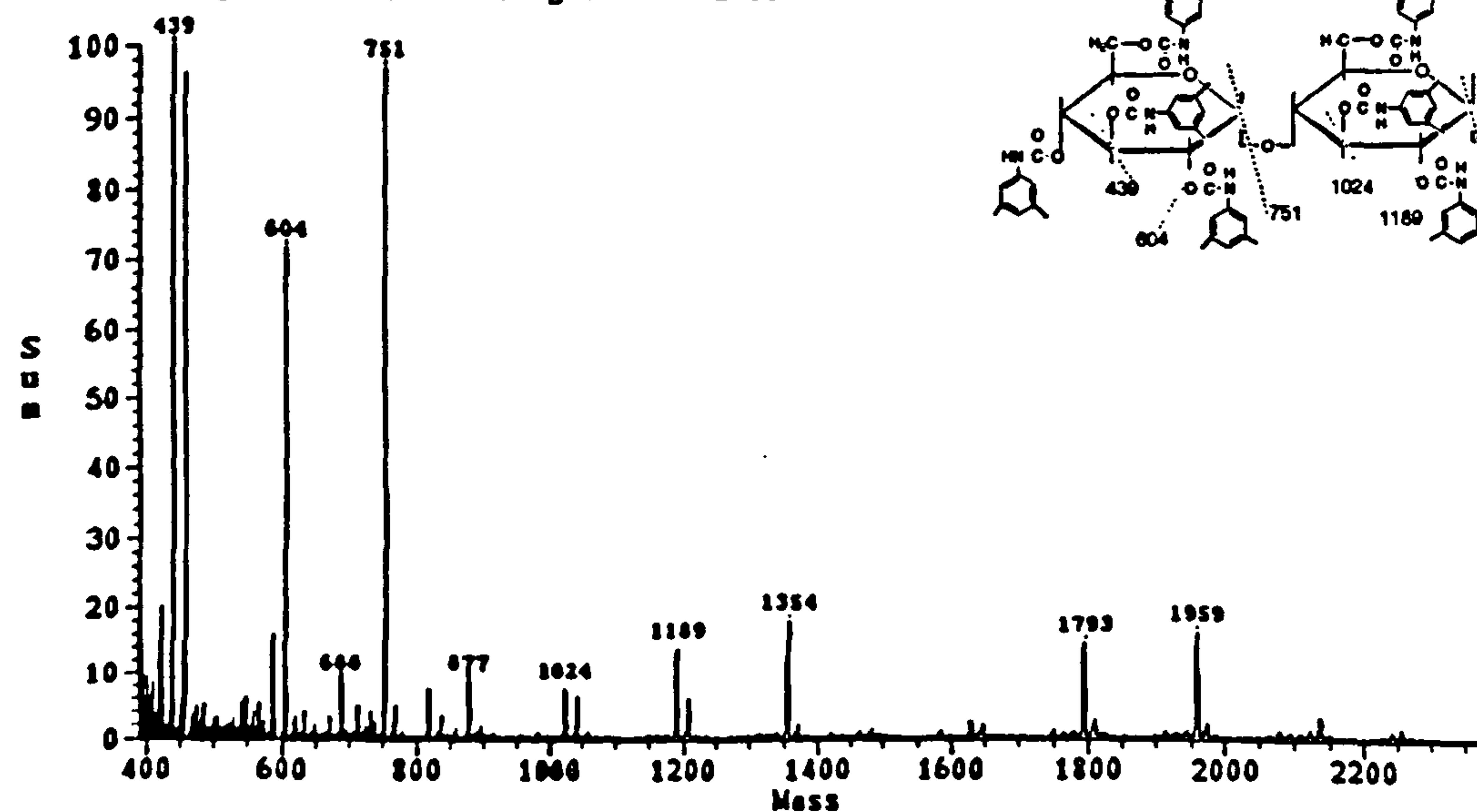
WU3 in acid/m-NBA. 9 Sep 92 4:14 pm LRP +LSIMS
WU0003 sum of 5 scan ranges 100% 34768mV



WU7 in acid/m-NBA. 9 Sep 92 5:40 pm LRP +LSIMS
WU0015 sum of 2 scan ranges 100% 9301mV



WU10 in acid/m-NBA. 9 Sep 92 5:54 pm LRP +LSIMS
WU0017 sum of 3 scan ranges 100% 24153mV



The Phenyl Carbamate Derivatives (see Figures 48 a, b and c)

LSIMS of glucose penta(phenylcarbamate) showed a molecular ion m/z 775 $[M]^+$ and very little fragmentation (See Figure 48a). The ions that were recorded were, due to elimination of the carbamate group at the anomeric carbon m/z 639 $[M-OR]^+$ and an ion at m/z 246 $[M-3OR-R+H]^+$.

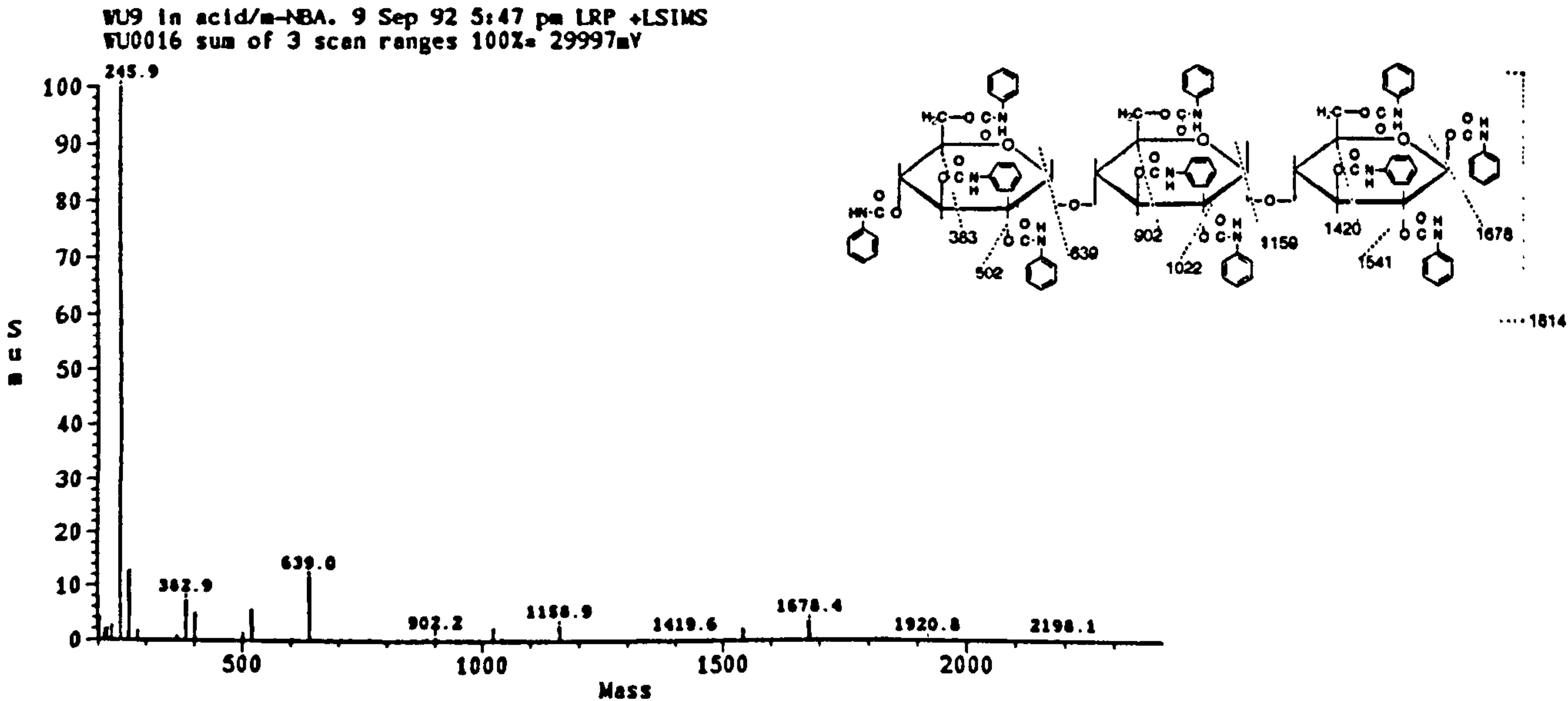
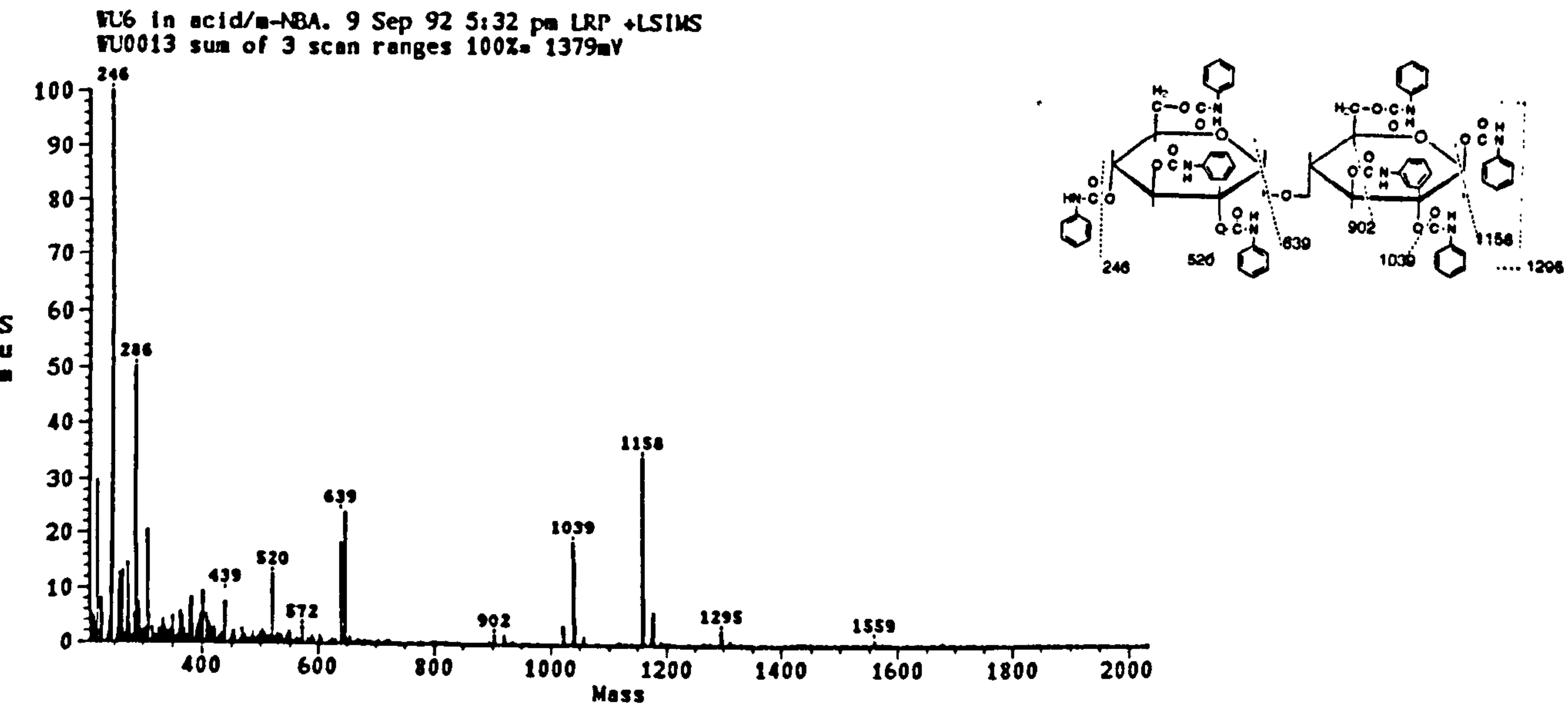
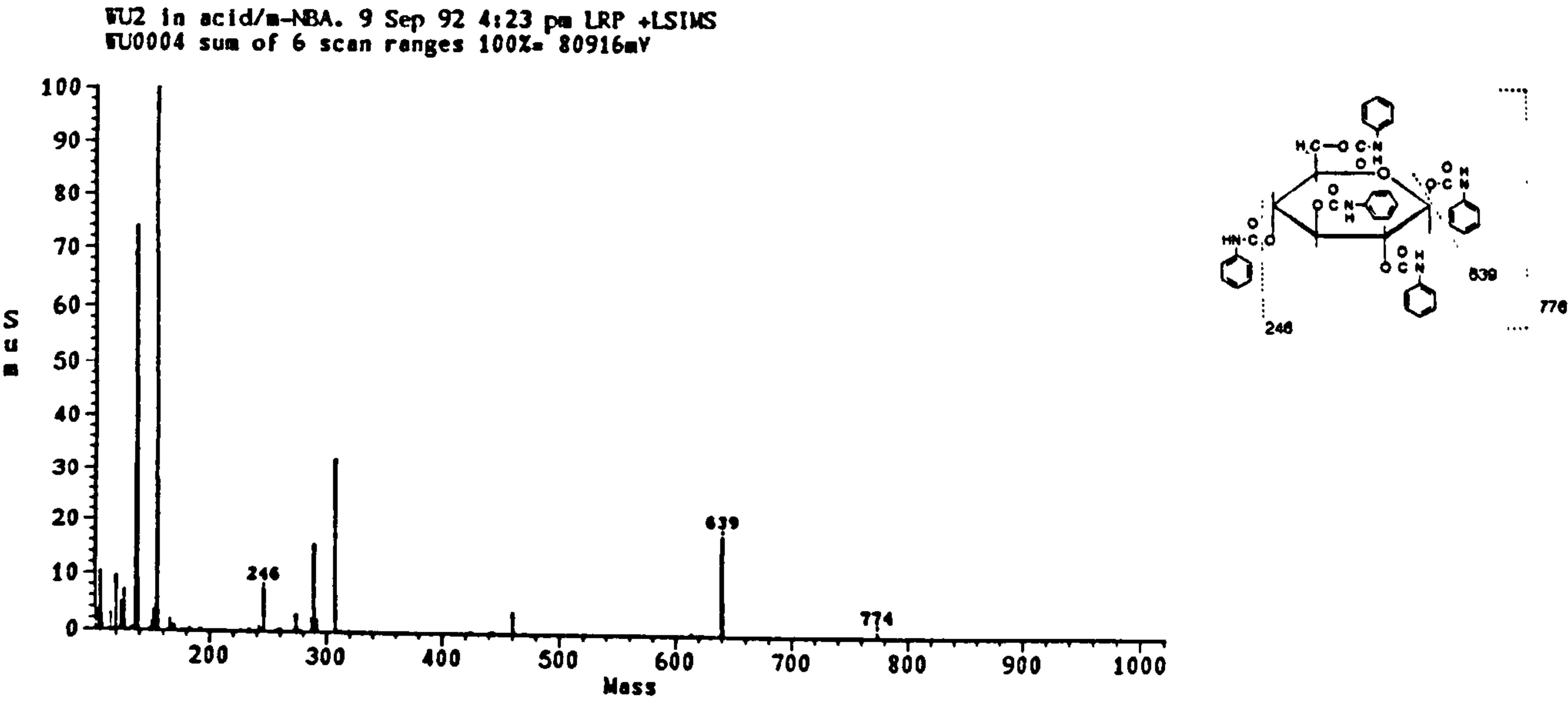
LSIMS of Maltose octa(phenylcarbamate) gave a more fragmented spectra (see Figure 48b). The pseudomolecular ion at m/z 1295 $[M+H]^+$. Then the fragmented sequence of ions at m/z 1174 $[M-R]^+$; m/z 1158 $[M-OR]^+$; m/z 1056 $[M-2R+2H]^+$; m/z 1039 $[M-OR-R+H]^+$; m/z 1021 $[M-2OR]^+$; m/z 902 $[M-2OR-R]^+$. A₁ type glycosidic cleavage yields an ion at m/z 639 $[M-N]^+$ and elimination of the R groups occurs as previously on ring L.

To investigate the effect of β -1,4 linkage and α -1,4 linkage with LSIMS, cellobiose octa(phenylcarbamate) was analysed by this technique. A pseudomolecular ion was observed at m/z 1295 $[M+H]^+$ then a very similar sequence pattern was obtained for the maltose derivative with corresponding ions at m/z 1175 $[M-R+H]^+$; m/z 1158 $[M-OR]^+$; m/z 1056 $[M-2R+2H]^+$; m/z 1039 $[M-OR-R+H]^+$; m/z 1021 $[M-2OR]^+$; m/z 938 $[M-3R+3H]^+$; m/z 920 $[M-OR-2R+2H]^+$; m/z 902 $[M-2OR-R+H]^+$ then the elimination of R groups from the L ring with the β -1,4 linkage in tact, m/z 614 $[M-5OR]^+$; m/z 494 $[M-6OR]^+$. Presence of an ion at m/z 639 $[M-N]^+$ from A₁

type cleavage of the β -1,4 linkage forms the expected oxonium ion. The highest intensity peaks are produced from the ions of the disaccharide as opposed to the cleaved rings.

LSIMS of maltotriose undeca(phenylcarbamate) produced a pseudomolecular ion at m/z 1814 $[M+H]^+$ and a similar sequence of fragmentation's to those observed previously with the glucose and maltose derivatives (see Figure 48c).

Figures 48 LSIMS-MS of a) Glucose penta(phenylcarbamate);
b) maltose octa(phenylcarbamate) c) Maltotriose
undeca(phenylcarbamate)



CHAPTER 5

PREPARATION OF MONOSACCHARIDE AND DISACCHARIDE CSP's

The contribution which macromolecular structure and inter-strand ordering makes to chiral recognition by carbohydrate carbamate phases is not fully understood (Chapter 3). In the present project, we have carried out an investigation in which the phenyl carbamate of the simple linear oligomer, cellobiose, was compared with the phenyl carbamate of the corresponding polymer, cellulose.

5.1 Cellobiose Octa(phenylcarbamate) Coated on to APS Silica (500Å).

Cellobiose octa(phenylcarbamate) was prepared by reacting cellobiose with phenyl isocyanate in pyridine under anhydrous conditions for 10 hours at 80°C. Elemental analysis (see Table 17) and nmr showed that the hydroxyl groups were almost completely converted to carbamate moieties.

	%C	%H	%N
Experimental	62.75	4.88	8.74
Theoretical octa-substitution	63.06	4.79	8.66
Theoretical hepta-substitution	62.30	4.85	8.34

Table 17 Theoretical and observed analytical data for the derivatisation of cellobiose with phenyl isocyanate

The cellobiose octa(phenylcarbamate) was coated onto 500Å aminopropylated silica at a concentration of 20%w/w. The results for the optical resolution of 5 racemic compounds are summarised in Table 18.

RACEMATE	Cellobiose ^a		CPC ^b	
	k' ₁	α	k' ₁	α
stilbene oxide	0.30	1.00	2.84	1.39
2,2,2-TFAE	2.58	1.00	2.21	1.15
benzoin	0.36	1.00	5.28	1.00
trogers base	0.36	1.22	1.12	1.00
1-phenethanol	0.53	1.00		2.61

TABLE 18 Comparison of the optical resolution obtained on columns of the phenyl carbamates cellobiose and cellulose (a-eluent;hexane-propan-2-ol (97.5:2.5) 0.5 cm³min⁻¹ b-eluent; hexane : propan-2-ol (90:10) 0.5cm³min⁻¹

A lower concentration of polar modifier was added to the mobile phase for the cellobiose octa(phenylcarbamate) column, since the disaccharide derivative was soluble in polar solvents. Although the disaccharide derivative showed chiral recognition towards

trogers base, ($\alpha=1.22$), in contrast to the behaviour of the polymeric phase for 3 other racemic components, the optical resolving ability of the cellulose derivative was much superior. An explanation for this result may be found when we consider previous work²⁴⁹ studying the circular dichromism (CD) spectra. Okamoto²⁴⁹ compared the CD of the 3,5(dimethylphenylcarbamate)s of cellobiose, cellotetraose and cellulose. The CD intensity greatly increased in the order 2-mer < 4-mer < polymer. He concluded that the degree of ordering of the structure for these derivatives also increased in that sequence, and this accounted for the low chiral recognition of the cellobiose phase and the high enantiomeric selectivity of the cellulose phase.

The oligosaccharide derivatives are much more soluble in propan-2-ol than are the polysaccharide derivatives. Therefore, only non-polar eluents such as hexane containing very low concentrations of propan-2-ol can be used. For this reason, the oligomeric stationary phases have very limited potential for practical application. The preparation of oligosaccharide derivatives chemically bonded to silica gel may improve this defect.

5.2 Preparation of Chemically Bonded Carbohydrate CSP's

The restriction in the use of certain mobile phases due to the solubility of the coated carbohydrate carbamate phases, led Okamoto⁶¹ to prepare chemically bonded carbamate phases.

In his study⁶¹ comparing the optical resolving power of coated and chemically bonded cellulose phases, it was revealed that the chiral recognition ability was not improved upon when the CSP was bonded to the silica support. It was reported that cellulose was linked to the aminopropyl support through the 6 positions on the glucoside rings and then the free hydroxyls at the 2 and 3 positions were derivatised with a large excess of isocyanate. An inherent problem with this procedure is that it is difficult to quantify the extent of polysaccharide derivatisation and no characterisation of the CSP was attempted. The uncertainty in the degree of derivatisation makes the comparison of chiral recognition of the bonded and non-bonded phases difficult to interpret. It is not possible to differentiate between a low degree of derivatisation of the polysaccharide hydroxyls and the bonding of the phase to the support as the reason for not improving the optical resolving power.

To assist in the investigation of chiral recognition by CSP's it is useful if the chiral selector is characterised before chemically bonding to the silica support. For the study of monosaccharide ester phases, König²⁹ covalently bonded 1-isothiocyanato-D-glucopyranoside to aminopropyl silica gel. This method of linkage has the advantage that the isothiocyanato-D-glucopyranoside derivative is stable and can be fully characterised. We therefore adopted this approach for the attempted preparation of a series of APS-linked oligosaccharide carbamates phases.

5.2.1.1 Derivatisation of Glucose (i) to Glucose Penta(phenylcarbamate) (ii)

Glucose penta(phenylcarbamate) was prepared by reacting glucose with phenyl isocyanate in pyridine under anhydrous conditions for 10 hours at 80°C. Elemental analysis (see Table 19) showed that all the hydroxyl groups were derivatised as carbamate moieties, which was confirmed by nmr and mass spectroscopy.

	%C	%H	%N
Experimental	63.29	4.83	8.97
Theoretical penta-substitution	63.48	4.77	9.03
Theoretical tetra-substitution	62.20	4.86	8.54

Table 19 Comparison of the elemental analysis for penta, tetra-substituted glucose

Various aspects of the nmr spectrum confirmed complete derivatisation such as the number, position, intensity and splitting of the signals. In the ^1H nmr there are 3 sets of protons (see Figure 49) N-H protons, aromatic protons on the phenyl ring and C-H protons from the monosaccharide ring.(H1-H6a,b)

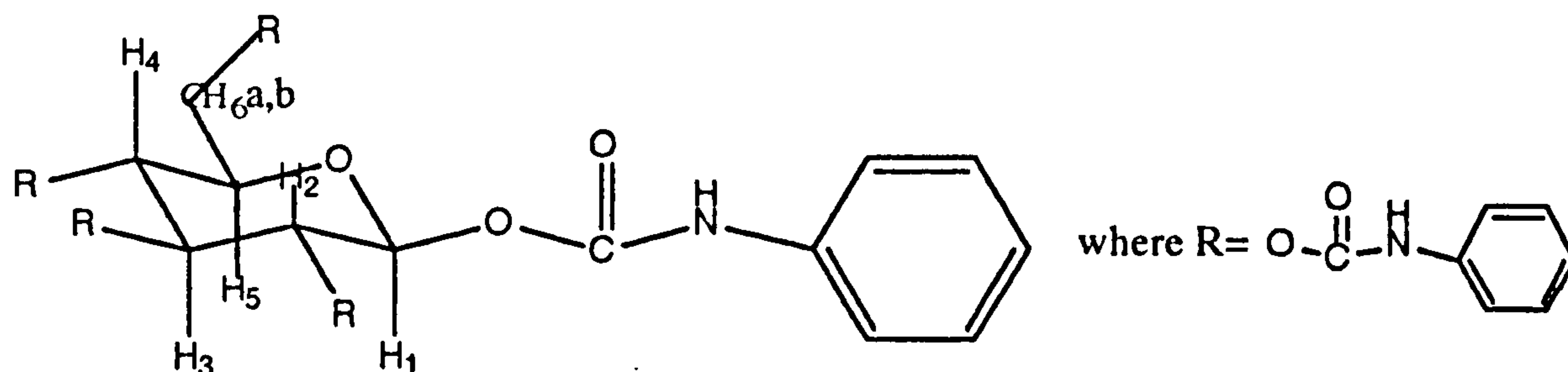


Figure 49 Glucose 1,2,3,4,6,penta(phenylcarbamate)

The peaks furthest downfield at 10.10 to 9.70 ppm are from the protons in the carbamate function. The spectrum shows an NH peak at 10.10 ppm due to the proton in the carbamate function at the C1 position on the sugar ring. The identification of this signal is important as it will give information regarding the next reaction step. The remaining 4 NH signals at different chemical shifts (δ) indicate the non-equivalence of the carbamate groups. This difference was also observed with the polysaccharide derivatives (see Chapter 3). The signals in the region 7.50-6.90 ppm are due to the aromatic protons in the phenyl ring. The protons on the sugar appear over a range of 6.20 ppm to 4.20 ppm. Due to overlapping peaks, complete assignment of the spectrum was difficult but decoupling experiments provided enough information to assign the signals. The results are shown in Figure (50), the lower spectrum i) is the normal spectrum, and the upper traces, ii)

iii) iv) the irradiated frequency in the decoupled spectra is indicated by an arrow. In spectrum ii) signal A is coupled to a signal in the multiplet at C, in iii) B is also coupled to the multiplet at C, and in figure iv) D is also coupled to C. Furthermore A is only coupled to C, to reveal (in ii) a doublet and a triplet (overlapping doublet of doublets), while signal D is a complex multiplet and remains unaffected by the decoupling in ii) and iii). Hence A is H₁, B is H₃, C is H₂ and H₄, and D is H₅ and H_{6a,6b}. The order that the sugar protons appear in the spectrum is H₁, H₃, H₂, H₄, H₅, H₆ with H₁ the furthest down field.

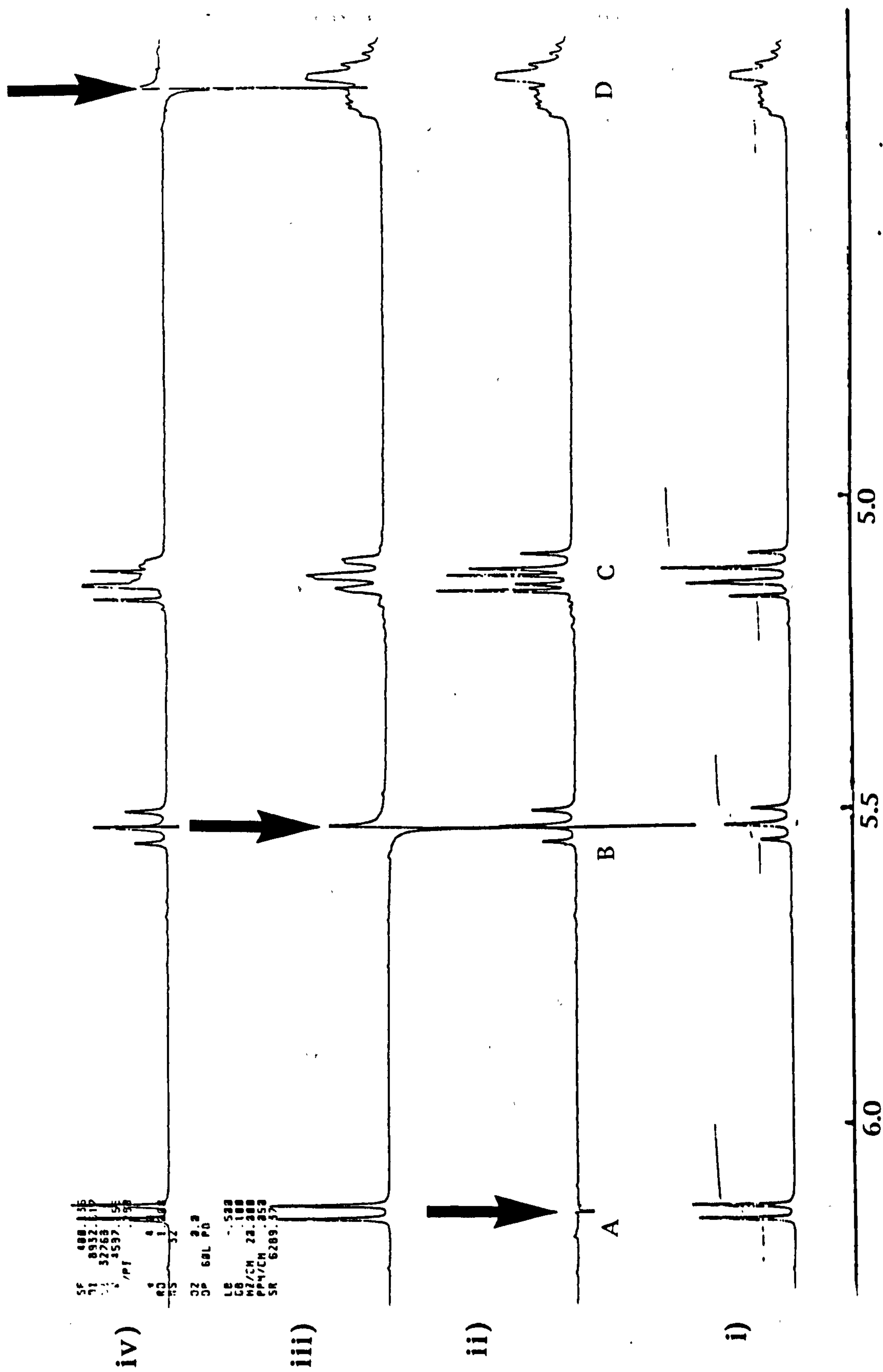


Figure 54 Proton decoupled spectra of the monosaccharide ring hydrogens

In the ^1H nmr spectra of glucose penta(phenylcarbamate) that the integrals of the NH protons are in the ratio of 5:1 with the single H_1 proton at 6.16 ppm. Quantifying the degree of derivatisation from the signals due to the aromatic region may cause erroneous results. Additional aromatic protons may be present due to the formation of the symmetrical urea and to contamination by pyridine, resulting in a higher integral. The N-H protons appear as singlets in the spectrum as the neighbouring atoms possess no hydrogens for coupling. The five protons in the aromatic group are split by each other producing a multiplet of peaks.

The proton H_1 is coupled only to H_2 to produce a doublet with a coupling constant of 8.4 Hz, which correlates to a dihedral angle of 180° , hence carbamate substitution occurred equatorially. The proton H_2 is coupled to 2 protons H_1 and H_3 (see Figure 50). The measured coupling constant for each is the same, 9.6 Hz, so the splitting pattern appears as a triplet. The dihedral angle of $\text{H}_2\text{-H}_1$ and $\text{H}_3\text{-H}_1$ is 180° , as expected for the diaxial relationships involved. H_3 is also coupled to protons H_4 and H_2 , again appearing as a triplet with coupling constants of 9.6 Hz, to both axial partners. H_4 is coupled to H_3 and H_5 and appears in the multiplet at 5.1 ppm which is attributable to both the signals H_2 and H_4 . Decoupling of H_1 simplifies the H_2 multiplet into a doublet ($d\text{H}_2\text{-3 } 9.6\text{Hz}$) and a triplet is observed for H_4 due to its coupling with H_3 and H_5 with equal J values of 9.6 Hz to both axial partners. H_5 is coupled to H_4 and the two protons at H_6 , producing a multiplet which is further complicated by the overlapping signal from $\text{H}_{6\text{a'b'}}$ and H_5 , to produce a complicated multiplet of peaks.

For the glucose penta(phenylcarbamate) (see Figure 51) analysis of the proton-decoupled ^{13}C spectrum revealed 5 carbonyl peaks in the region 153-151 ppm, four clusters of signals from the aromatic carbons at 138 ppm (A1), 128 ppm (A2 and A6), 123ppm (A3 and A5) and 118ppm (A4).

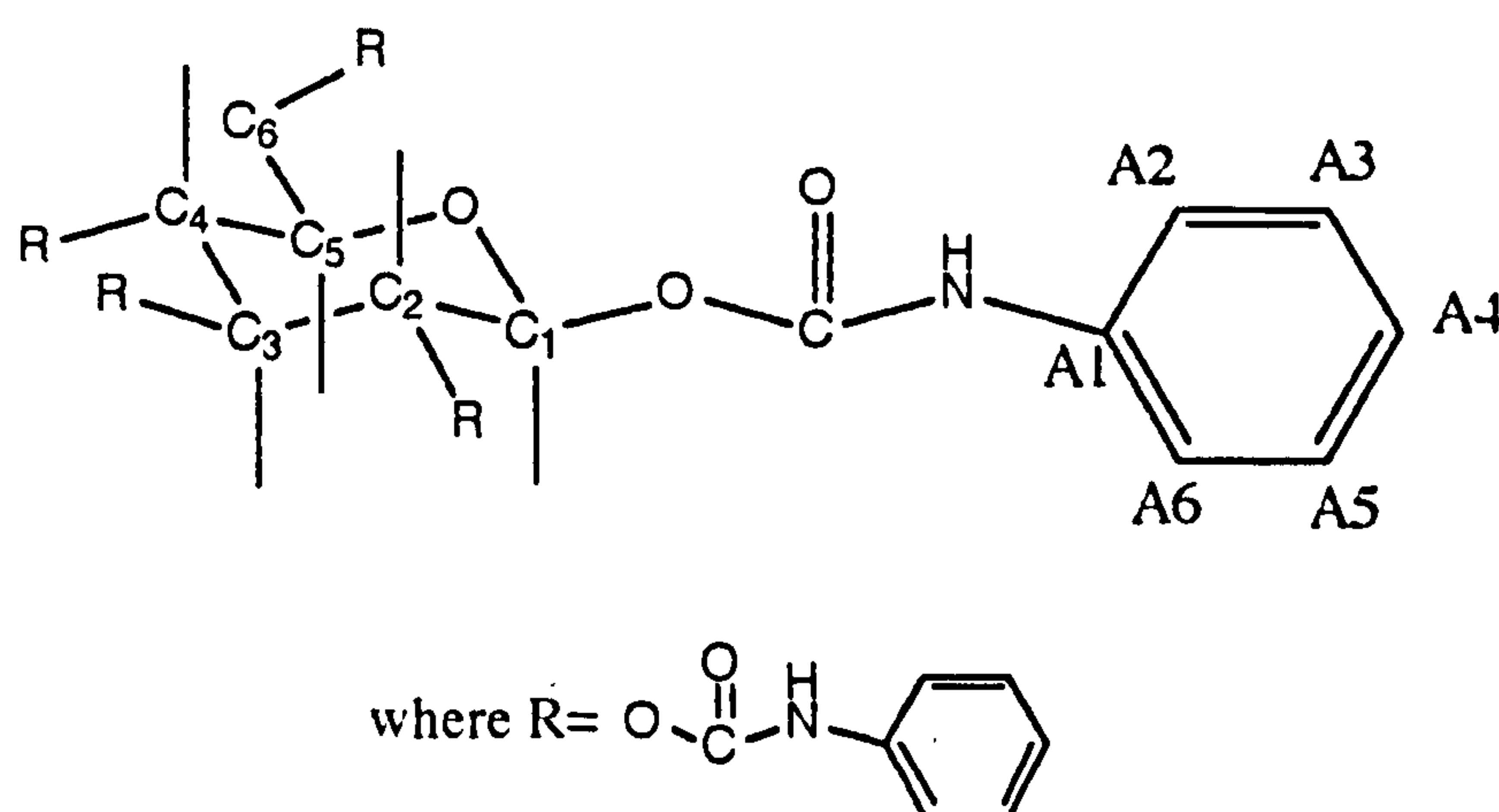


Figure 51 Different types of C atom in glucose penta(phenylcarbamate)

Assignment of the 6 sp^3 hybridised carbons of the sugar was made by considering the chemical environment and thus the distribution of surrounding electrons. C1 will be deshielded the greatest then $\text{C3} > \text{C5} > \text{C2} > \text{C4} > \text{C6}$ showing single peaks at 92.1; 79.2; 72.7; 72.4 and 68.6 ppm respectively. These values are in agreement with tables²⁵⁰.

The mass spectrum also confirmed the structure of glucose penta(phenylcarbamate). It showed the molecular ion at m/z 775; $[\text{M}]^+$, as well as the characteristic fragmentation pattern for carbamate derivatives (see Chapter 4).

5.2.1.2 Conversion of Glucose Penta(phenylcarbamate) (ii) to 1-Isothiocyanato-glucose Tetra(phenylcarbamate) (iv)

It was desired to link the carbamoylated glucose to the amino-propylated silica support through the anomeric carbon atom. To do this a suitable procedure for activation at the anomeric carbon atom was required. In addition, the activation step must occur diastereoselectively, retaining the β -linkage.

The Koenigs-Knorr Method

Protection of hydroxyl groups by derivatisation of glucose to the penta(phenylcarbamate) makes the derivative a difficult starting material for a Koenigs-Knorr synthesis. Carbamates are easy derivatives of carbohydrates to prepare, they are high melting, readily crystallised, and, more importantly, resistant to acid hydrolysis. However, they are insoluble in low polarity solvents, (e.g. chlorinated solvents) which are required for the relatively harsh conditions needed for the generation of the glycosyl halide. Many solvents were tried in the present work but were unsuccessful in their use, including (THF), 1,4-dioxan, dimethyl sulphoxide, acetic acid and chlorinated solvents. Ethyl acetate was found to be a suitable solvent in which the carbamate was slightly soluble. 1-Bromo glucose tetra(phenylcarbamate) was obtained by the reaction of glucose penta(phenylcarbamate) with HBr/acetic acid in ethyl acetate for 2.5 hours at room temperature. The ^1H nmr spectrum revealed that one N-H proton signal at 10.10ppm had disappeared leaving 4 N-H protons, and

the doublet attributed to the H_1 proton at the anomeric carbon had shifted downfield to 7.60ppm with a coupling constant of 8.4Hz. This suggested that the bromo atom was in the β configuration, and inversion at the anomeric carbon to the α conformation had not occurred. The 1H nmr spectrum also showed a doublet at 4.10ppm, which can be attributed to the hydrolysed product having C_1-OH .

The β -halide having an equatorial halogen is the product from the kinetically controlled reaction and is rather unstable and much more reactive than the α halide, which would be formed as the thermodynamically more stable form. This reactivity is attributed to the anomeric effect, i.e. a destabilisation arising from the electrostatic interaction between the parallel p orbitals of oxygen and the halogen.

The steric course of the subsequent glycosylation reaction is, however, determined not by the axial or equatorial orientation of the halogen but by the interaction of the neighbouring substituent on C_2 of the halose. The reaction of the 1-bromo glucose tetra(phenylcarbamate) with silver thiocyanate yielded 1-isothiocyanato-glucose tetra(phenylcarbamate) (v). 1H nmr studies of this compound (v) showed that the isothiocyanate group was in the β orientation ($J_{1-2} = 8.4Hz$). Irrespective of whether the β form or the α form of the pyranosyl halide (i) is used, reaction occurs via the oxo-carbenium ion (ii) (see Figure 52).

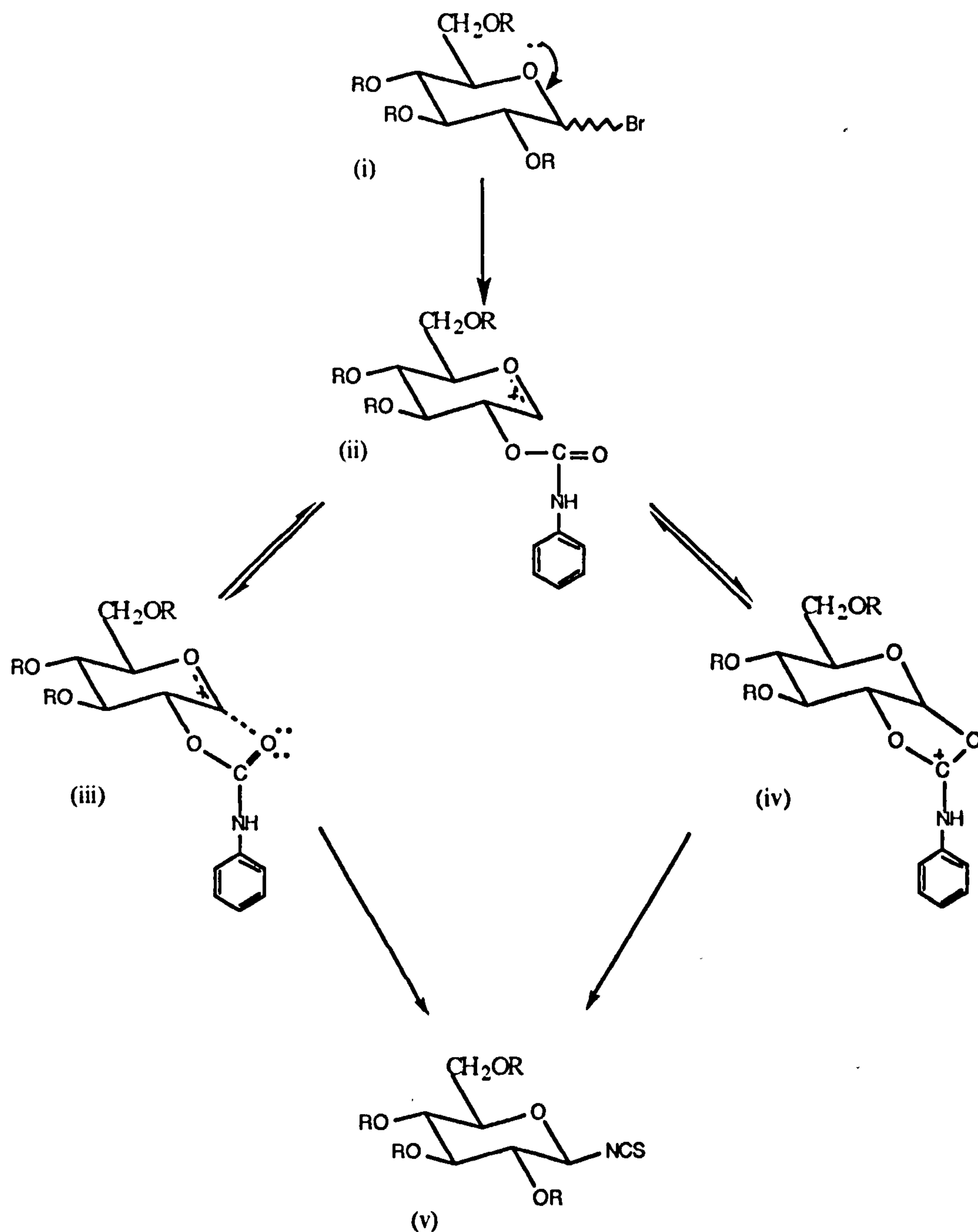


Figure 52

The neighbouring group effect involving the 2 carbamoxyl group and C1 must be responsible for stereospecificity. This effect could consist of an interaction of the p-orbitals of the carbonyl oxygen of the cation (as in iii), or the formation of an carbamoyl-oxonium ion (iv). Nucleophilic attack from above in (iii) or ring opening in

(iv) with a thiocyanate component at C1 leads, for steric reasons, only to the β glycoside (v).

Attempts were made to use a variety of solvents for the nucleophilic substitution, including pyridine, 1,4-dioxan, THF and toluene. The reaction in lone pair donor solvents (THF, pyridine) gave a mixture of product and an unknown compound, whose ^1H nmr spectrum gave a very broad singlet at 6.1ppm and had a m/z (FAB-ms) of 899. Solvent participation using nucleophilic solvents can be expected with the occurrence of oxonium (x) or ammonium ions (y) as intermediates (see Figure 53).

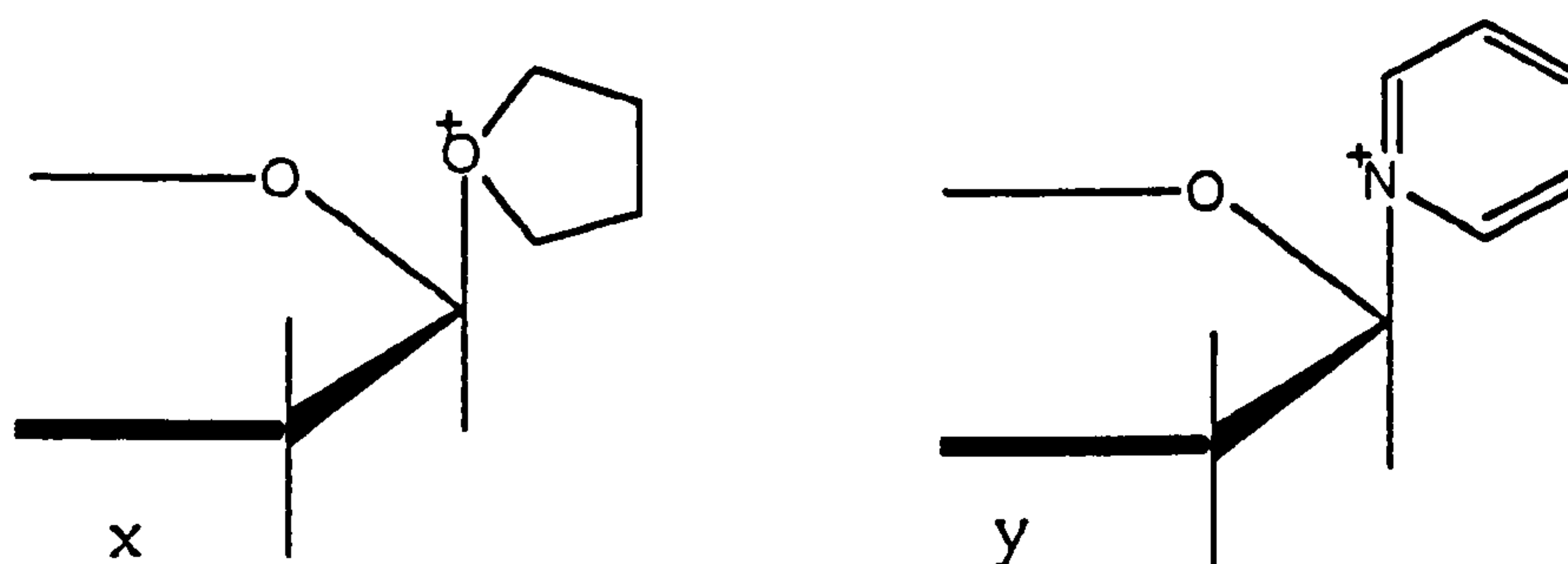


Figure 53 Oxonium and ammonium ion intermediates formed via solvent participation

The use of a non-polar solvent (toluene) gave the required product in the highest yield when the mixture was refluxed for 15 minutes. This choice of solvent is not an obvious one, as both reactants are only sparingly soluble in the solvent. The use of relatively low polarity solvents is a characteristic feature shared by glycosylation of sugar halides in the presence of Ag_2CO_3 and Ag_2O ²⁵¹.

The poor solubility of silver thiocyanate led us to examine the possible use of other thiocyanate salts to improve the yield of the reaction. Those initially considered were ammonium thiocyanate, potassium thiocyanate and lead thiocyanate.

Due to the problems experienced by Khorlin et al²¹⁹ (see page 85) the use of ammonium thiocyanate was not selected for the present reaction. The use of potassium thiocyanate with a catalyst was described by Heras²²⁰ (see page 85). Employing the same conditions the product, when analysed by infra red, gave no indication of the formation of the sugar isothiocyanate or even the thiocyanate. The procedure utilised by Ogura²¹⁷ (see page 84) was adopted for the percarbamoyleated derivatives. Yields of 45% were obtained for the isothiocyanate which is slightly less than those obtained when silver thiocyanate was used.

5.2.1.3 Reaction of 1-Isothiocyanate Glucose Tetra(phenyl-carbamate) with Amines

To model the reaction of the isothiocyanate group with the aminopropyl silica support, the glucose derivative (iv Scheme 12) was reacted with n-propylamine in THF to give N-[2,3,4,6-tetra-(O-phenylcarbamate) β -D-glucopyranosyl]-N-propyl thioureide (vi) Scheme 12). No anomerisation during the reaction was observed and consequently the coupling reaction with aminopropyl silica can be considered to proceed with retention of configuration.

5.2.1.4 Coupling of 1-Isothiocyanate Glucose Tetra(phenyl-carbamate) (iv) to Aminopropyl Silica Gel

Linkage of the sugar residue to the silica support was performed in a flask subjected to continuous automatic shaking. Stirring with a magnetic follower over prolonged periods can result in partial degradation of the silica particle and was avoided²⁹. The initial experimental procedure involves shaking 20mg of 1-isothiocyanato glucose tetra(phenylcarbamate) with 100mg of aminopropylated silica for 3 days at room temperature in 2cm³ of solvent. This procedure was optimised by studying the following experimental conditions:-

- a. *Solvent and temperature*
- b. *Concentration of chiral selector*
- c. *Reaction time*
- d. *Type of silica*
- e. *Length of spacer*

The yields of the coupling reactions were calculated from elemental analysis using Equation 5 (see page 24).

(a) Effect of Solvent and Temperature

Three solvents selected were based on their good solubility for the chiral selector: THF, 1,4-dioxan and pyridine. In order to neutralise the acidic silica surface hydroxyl groups, 2.5 μ l of pyridine was added to the non-basic solvents. The silica used for this investigation was APS Nucleosil 7 μ m (pore size 100Å) which was shown by elemental analysis to have a %C of 4.96

SOLVENT	wt of CSP mg	Experiment conditions	%C	Nº of groups reacted
THF	0	<i>refluxed</i>	4.99	<0.02
	20	<i>refluxed</i>	10.31	11.05
	20	<i>shaken</i>	10.04	10.43
PYRIDINE	0	<i>refluxed</i>	5.45	0.88
	20	<i>refluxed</i>	7.50	4.94
	20	<i>shaken</i>	7.81	5.58
1,4-DIOXAN	0	<i>refluxed</i>	4.99	<0.02
	20	<i>refluxed</i>	8.05	6.08
	20	<i>shaken</i>	8.00	5.96

Table 20 Comparison of the number of groups reacted employing different experimental conditions

The elemental analysis figures shown in Table 20 indicate 3 points:- i) Of the three solvents chosen, THF gave the overall highest percentage carbon figures and corresponding number of aminopropylated silica groups reacted; ii) It is unclear whether refluxing the reaction increases the yield. More results are needed to establish clearly the effect of temperature; iii) The

work up for the silica after reaction (i.e. washing and drying) removes all the organic impurities, so the percentage carbon is solely due to the coupling reaction on the silica surface.

(b) Profile of Percentage Loading of the Chiral Selector with Surface Coverage

To investigate the optimum concentration of chiral selector necessary for maximum surface coverage, 8 different ratios of 1-isothiocyanato glucose tetra(phenylcarbamate) to APS silica were shaken in THF for 3 days (Table 21).

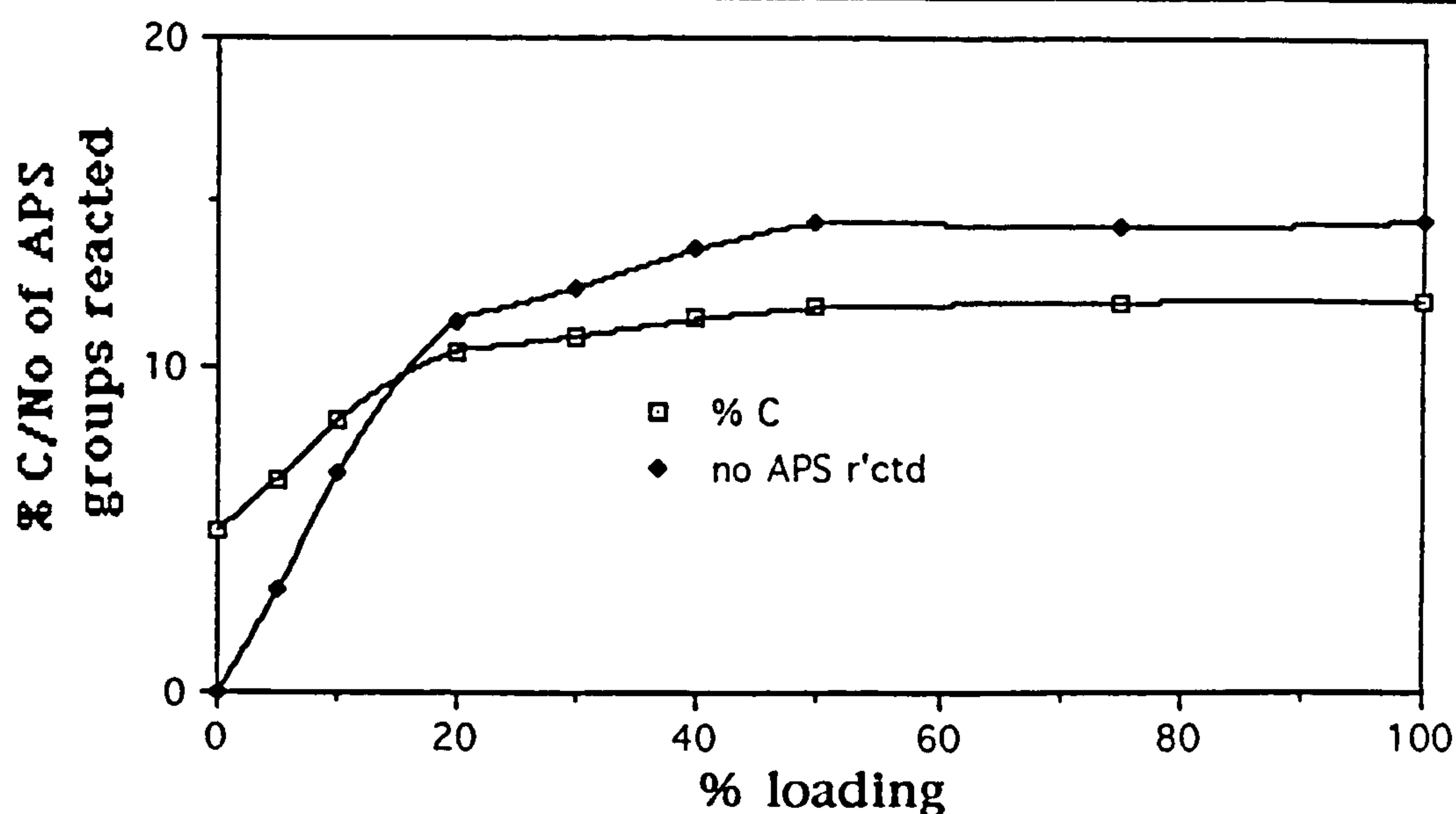
LOADING mg	wt of Hypersil APS mg	%C	% of APS groups reacted
0	100	4.96	>0.02
5	100	6.61	3.14
10	100	8.37	6.77
20	100	10.43	11.34
30	100	10.86	12.33
40	100	11.36	13.52
50	100	11.70	14.34
75	100	11.90	14.19
100	100	12.03.	14.46

Table 21 Concentration profile of CSP loading with number of APS groups reacted

It is observed from Table 20 and Graph 13 that the extent of bonding rose steeply for loading up to 20%w/w of the isothiocyanate on APS-Hypersil. On increasing the loading from 20 to 100%w/w, the overall improvement was marginal and at

concentrations above 50% no significant further improvement in coverage was obtained, even though only 14% of the APS groups had reacted. This is presumably due to the blocking of the APS sites by the large glucose tetra(phenylcarbamate) groups.

GRAPH 13 Influence loading has on the number of APS groups reacted determined from the %C analysis



The bonding profile (Graph 13) gives an insight into the amount required for the preparation of future bonded chiral phases. This is of particular importance for the higher oligomers in the malto series which are available only in small amounts due to the difficulty in their separation and purification. (See Chapter 4).

(c) Reaction Time

Once it was established that the best coverage of chiral selector was obtained in THF, the reaction time was increased. Using the same experimental conditions, the chiral selector was shaken with

a different silica Kromasil APS 7 μ m (pore size 100Å) for 3 and 5 days.

SILICA	CSP wt mg ⁻¹	reaction time hrs ⁻¹	%C	% N ^o of APS groups reacted
Kromasil	0	120	4.89	>0.02
Kromasil	20	72	9.31	10.18
Kromasil	20	120	9.35	10.28

Table 22 Effect on increasing the reaction time on N^o of APS groups reacted

On increasing the time of the reaction, there was very little increase in the number of APS groups reacted. Any variation is within the experimental error for the percentage carbon determination. One interesting observation from this experiment is that with the use of Kromasil APS, there is an apparent decrease in the number of groups reacted when compared to the coverage using Nucleosil APS. This feature prompted a further study using several different silicas of varying pore sizes.

(d) Type of Silica

Table 23 illustrates the physical properties for the 4 different types of APS silica used for this study. (Note APS Nucleosil 100Å, 500Å and Kromasil 100Å were synthesised in house, Hypersil APS

120Å was manufactured by Shandon). The same general reaction conditions were used as before, but at two temperatures.

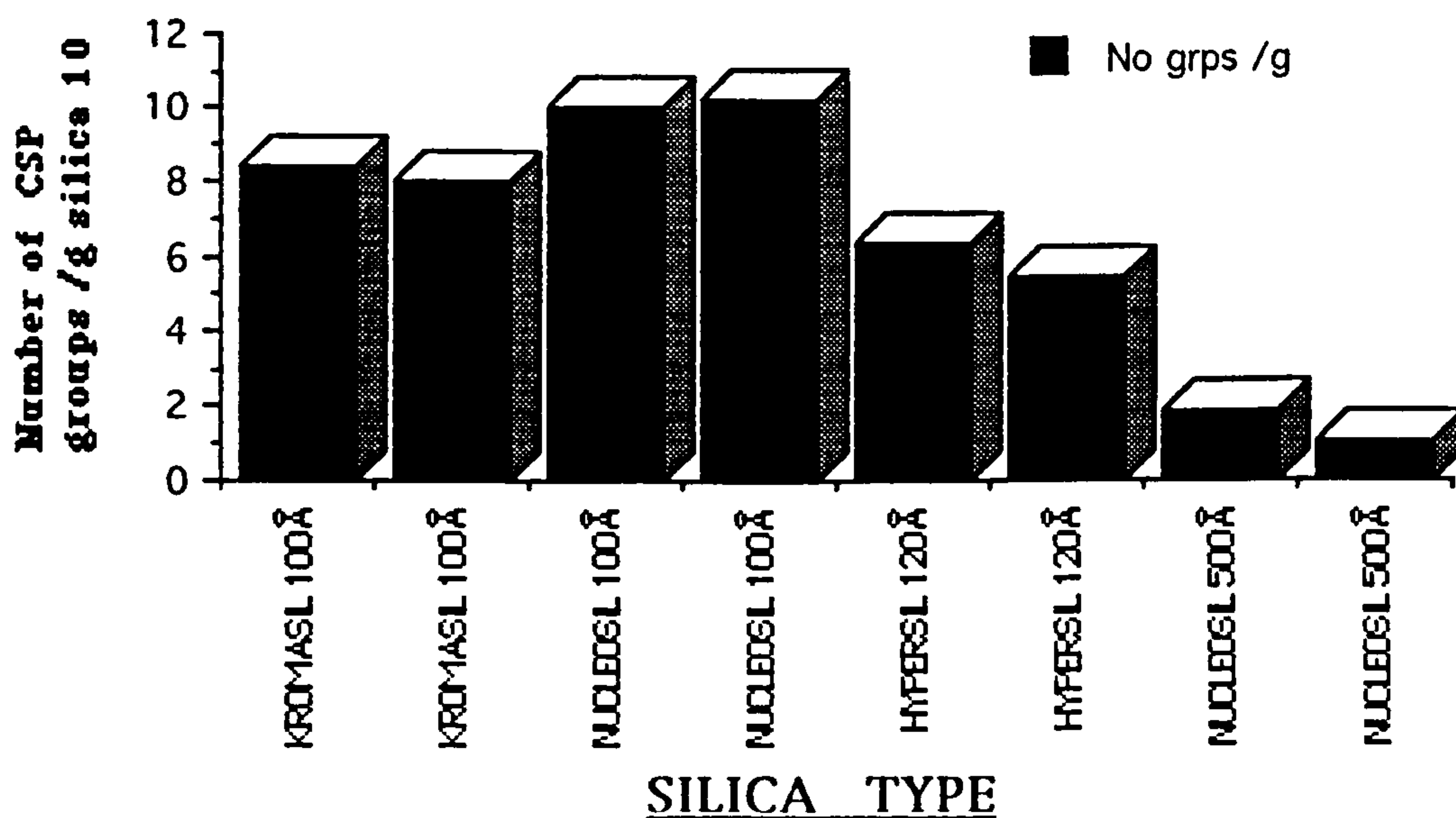
SILICA APS	PORE SIZE Å	S _{BET} m ² g	METHOD	%C	APS GRP PRIOR TO RCTION nm ²	APS GRP'S REACT'D %	N ^o BONDED GRP's/g 10 ⁸
KROMASIL 7µm	100	350	BLANK	4.37	2.24	>0.01	
			REFLUX	9.57		10.80	8.46
			SHAKEN	9.30		10.15	7.95
NUCLEOSIL 7µm	100	350	BLANK	4.99	2.59	>0.001	
			REFLUX	10.32		11.07	10.03
			SHAKEN	10.43		11.32	10.26
HYPERSIL 5µm	120	180	BLANK	2.11	2.11	>0.001	
			REFLUX	6.24		16.72	6.35
			SHAKEN	5.70		14.30	5.43
NUCLEOSIL 7µm	500	35	BLANK	1.06	4.83	0.04	
			REFLUX	2.24		10.83	1.83
			SHAKEN	1.71		6.10	1.03

Table 23 Comparison of the number of groups reacted for the different types of silica

The percentage carbon data reveals that for the smallest silica's (100Å), no clear advantage was obtained when the linkage was performed under reflux conditions. However, as the pore size is increased (120Å, 500Å), there appears to be an increasing advantage in using reflux conditions. The complexity of selecting the optimum silica as the support is revealed in Table 23. Examination of the extent of reaction in terms of % of APS groups reacted suggests that the 100Å (refluxed or shaken) and 500Å (refluxed) phases all gave about 10-11% conversion, whilst the

highest conversion of APS groups (16.72%) was seen refluxing the 120Å phase. This, however, was misleading as a true measure of coverage is best represented by the % of chiral selector groups per gram and not the number of APS groups reacted. The data calculated on this basis is shown in Graph 14 and indicates that the highest density of chiral selector is obtained from silica's of the highest surface area. The results also show that, as the surface area increases by a factor of 10, then so does the number of chiral selector groups linked to the silica support. It is also observed that when the surface area increases by 2, so does the number of organic groups per gram.

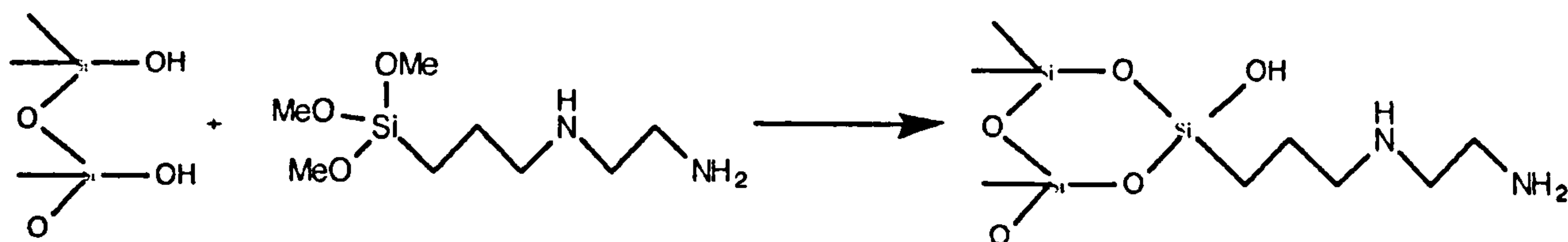
GRAPH 14 Number of CSP groups per gram of silica



(e) Length of Spacer

Modification of the support (Nucleosil 100Å) with [3-(2-aminoethyl) aminopropyl]trimethoxysilane (AEAMS), by the same procedure employed for the preparation aminopropylsilica, gave a

coverage of 2.6 AEAMS groups /nm² (%C 7.93). The introduction of this modifier onto the silica surface increases the distance between the primary amino group and the silica matrix.



Scheme 13 Preparation of AEAMS

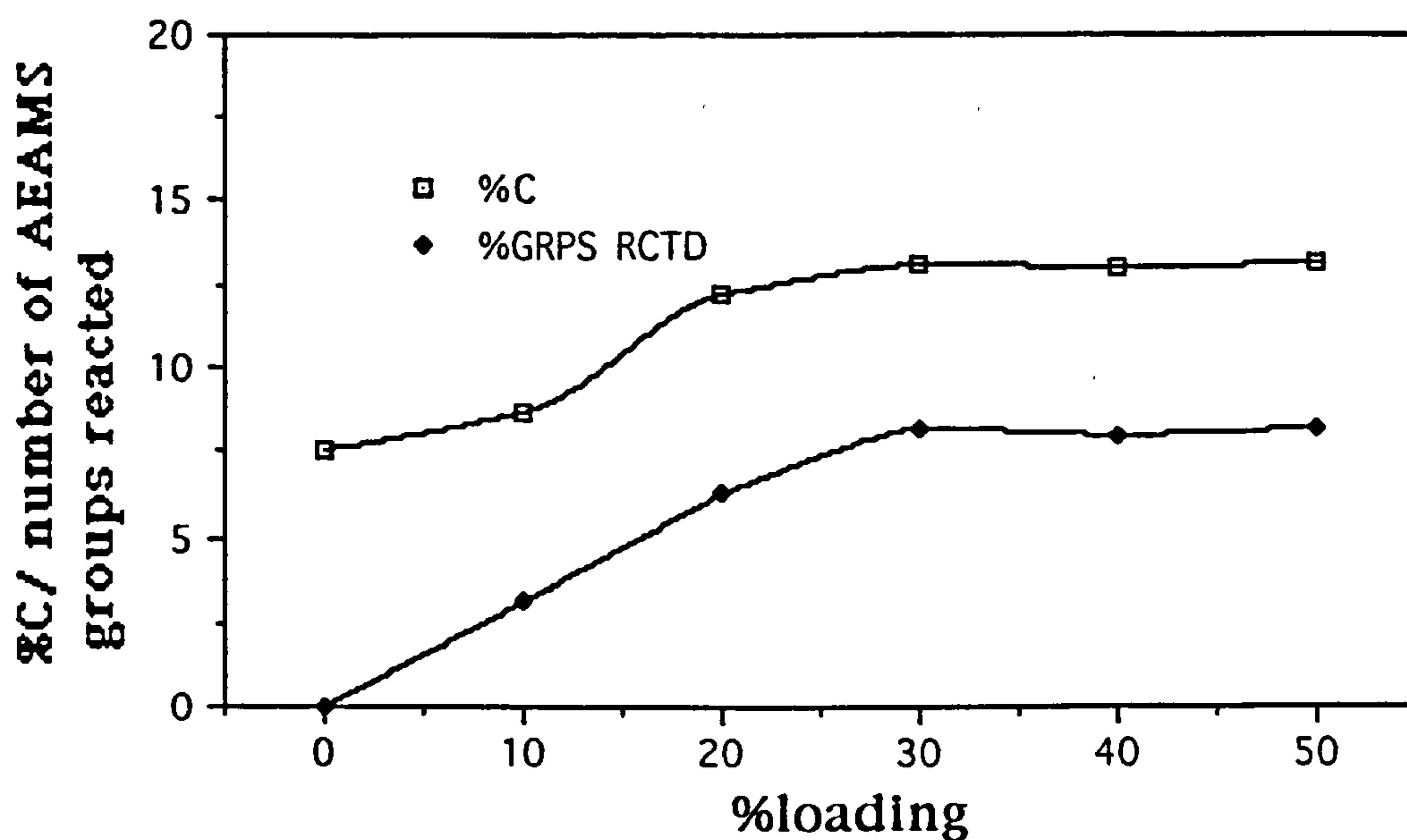
Thus, the reaction between the amino group and the isothiocyanate group will take place further away from the silica surface, which might reduce the steric effects from the support. This investigation was performed using the same conditions as for APS and different loadings of CSP were reacted with AEAMS silica (100 mg).

CSP wt mg	reaction conditions in THF	%C	% AEAMS groups reacted
0	shaken 72hr	7.97	>0.02
10	shaken 72hr	8.67	3.12
20	shaken 72hr	12.23	6.26
30	shaken 72hr	13.14	8.22
40	shaken 72hr	13.05	8.02
50	shaken 72hr	13.15	8.24

Table 24 Loading profile of CSP with the number of AEAMS groups reacted

Table 24 shows that increasing the length of spacer decreases the extent of reaction as only a maximum 8.24% of the AEAMS groups reacted. Graph 15 reveals a different rate of loading to that obtained with the aminopropyl spacer (see Graph 13) as the optimum amount of chiral selector to the AEAMS silica is 30:100^{w/w}. These results suggest that the primary amino group in AEAMS is not as reactive as the amino group in APS, which may be due to the reduction in the nucleophilicity of the terminal NH₂.

GRAPH 15 change of %C and number of AEAMS groups reacted with loading of CSP



Based on the above findings, the final procedure adopted for linkage required that at least 20% of 1-isothiocyanato-2,3,4,6, tetra(phenylcarbamate) glucopyranose was shaken for 72 hours at room temperature in THF with aminopropylated silica of pore size 100Å.

5.3 Performance of Modified Silica Gel Reacted with 1-Isothiocyanato-2,3,4,6-Tetra(phenylcarbamate)- glucopyranose

After optimising the procedure for the coupling of the monosaccharide residue to the APS surface, elemental analysis gave a percent carbon of 12.05, which corresponded to 15.20% of the original APS groups reacted and a coverage of 13.60 groups/g. The bonded phase was packed into a 15cm x 0.46 cm (i.d.) column and the test solutes 1 to 5 used to evaluate its performance.

The column retained the solutes to produce good gaussian shaped symmetrical peaks. An overall decrease in the extent of retention was observed compared to that obtained with the CPC column, but the capacity factors showed an increase compared to the data from the cellobiose octa(phenylcarbamate) coated phase. The polar solutes 2,2,2-TFAE and 1-phenylethanol were retained the longest and their k's decreased with increasing IPA modifier in the mobile phase see Table 25

SOLUTE	1-isothiocyanato -2,3,4,6,tetra(phenyl carbamate)glucopyr anose bonded to APS	20%cellobiose octa(phenyl) carbamate coated onto APS	20%cellulose tri(phenyl) carbamate coated onto APS
stilbene oxide	0.60	0.30	1.33
2,2,2TFAE	15.94	5.60	52.50
benzoin	10.00	0.40	20.30
trogers base	2.60	0.50	3.43
1-phenylethanol	5.20	0.93	8.63

Table 25 Comparison of k' values obtained on the three columns with a mobile phase composition of hexane/
propan-2-ol , 99:1

This suggests that retention is due to hydrogen bonding or dipole-dipole interaction occurring between the solutes and the chiral selector or unreacted surface hydroxyl or amino groups. However, the interactions are non-stereoselective as no chiral recognition for these compounds was observed over the range of 0-20% v/v 2-propanol in hexane.

Particularly interesting are the results obtained with stilbene oxide and trogers base. These compounds are relatively non-polar and were retained to a lesser extent than the other analytes. At very low concentrations of mobile phase modifier, (i.e. 0.25% propan-2-ol) enantiomeric selectivity was observed and on increasing the modified concentration to greater than 0.5% chiral recognition was lost. This phenomenon was also observed for trans 1,2-dimethyloxirane (see Figures 54 a, b and c). Retention was small but selectivity was high enough for separation. This

illustrates the very fine balance required for stereoselectivity in enantiomeric separation. The difference in the free energy of formation between each diastereomeric complex for the enantiomers is extremely small. In this case increasing the polarity of the mobile phase to 0.5% swamps the active polar sites necessary for the solute/phase interaction.

SOLUTE	k'1	k'2	α
stilbene oxide ^a	1.10	1.23	1.13
1,2-dimethyloxirane ^b	2.33	2.66	1.14
trogers base ^a	3.00	4.72	1.56

Table 25 Capacity factors and selectivity coefficients for solutes on the 2,3,4,6,tetra(phenyl)glucopyranose phase [conditions: a) mobile phase hexane/propan-2-ol; 99.75:0.25 . b) mobile phase hexane/propan-2-ol;99.50:0.50]

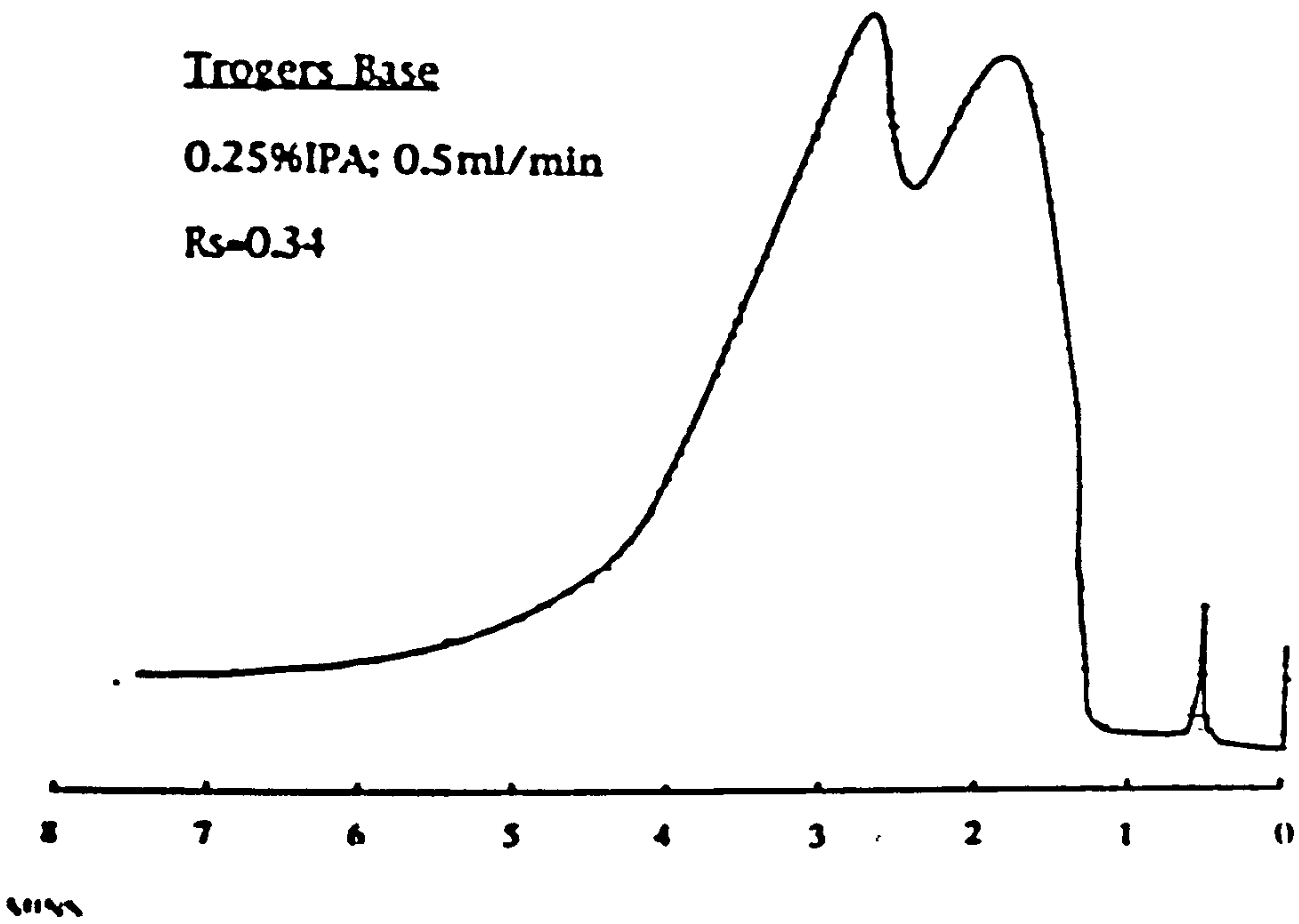
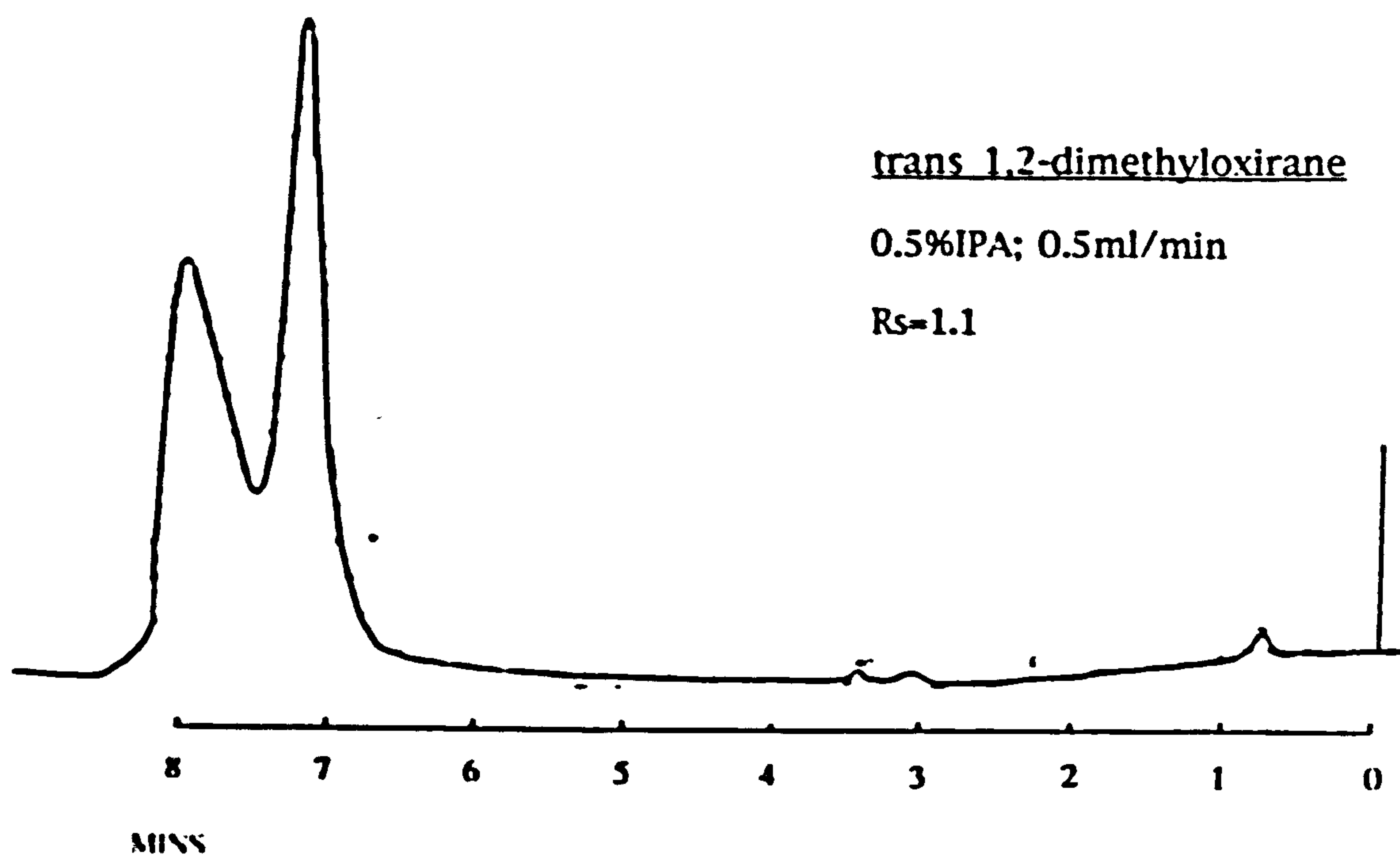


Figure 54 Chiral Recognition exhibited on bonded glucose tetra(phenylcarbamate) Isothiocyanate to APS



Sulbene Oxide
0.25%IPA; 0.5ml/min
 $R_s=1.20$

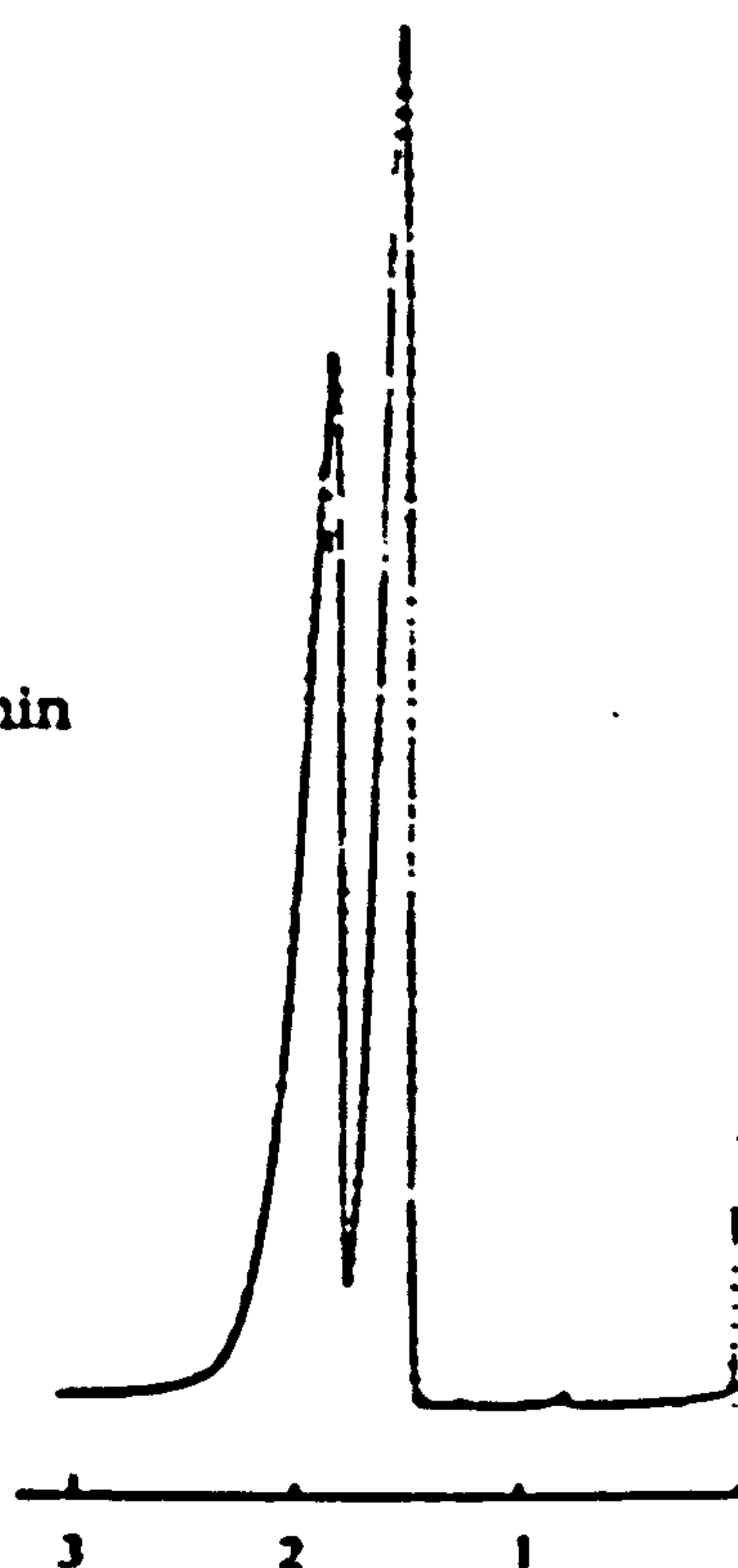


Figure 54 (continued) Chiral Recognition exhibited on bonded Glucose tetra(phenylcarbamate) isothiocyanate to APS

5.4 Linkage of Other Carbohydrate Derivatives to APS Silica

The successful synthesis (via Koenig Knorr procedure) and linkage of 1-isothiocyanato-2,3,4,6-tetra(phenylcarbamate) glucopyranose to the aminopropyl silica support led to the study of bonding the tetra(3,5-dimethylphenylcarbamate) derivative of glucose and also disaccharide and trisaccharide tris(phenylcarbamate) and tris(3,5-dimethylphenylcarbamate) derivatives.

Due to the successful application of amylose derivatives (i.e. APC and ADMPC) for chiral recognition, (see Chapter 3) and also the commercial availability of α 1,4-linked sugars, maltose (where n the number of glucose groups = 2) and maltotriose ($n=3$) were selected for study, as a preliminary to eventually bonding longer chains of glucose units in the carbohydrate, up to $n = 8$ i.e. maltooctaose, to APS silica.

5.4.1 Attempted Linkage of the Tris(3,5-dimethylphenylcarbamate) Derivatives

A) Glucose penta(3,5-dimethylphenylcarbamate) was prepared in good yield by reacting dried glucose with 3,5-dimethylphenyl isocyanate in pyridine at 80°C for 10 hours. Elemental analysis and nmr spectroscopy showed that the hydroxyl groups were fully derivatised as carbamate moieties.

Preparation of the 1-isothiocyanato compound via the 1-bromo derivative was attempted employing the same procedures as for

glucose penta(phenylcarbamate). It was found, however, that the (3,5-dimethylphenylcarbamate) derivative was less soluble than the phenyl carbamate derivative and in particular did not dissolve in ethyl acetate. To effect solubility, more polar solvents were necessary such as THF and 1,4-dioxan. Although at first these were thought not to be suitable for the relatively harsh conditions of the Koenigs-Knorr procedure, the lack of suitable alternatives meant that it was necessary to explore their possible use.

1,4-dioxan was investigated as a possible solvent and the Koenigs-Knorr reaction with a ten fold excess of HBr/acetic acid was monitored by nmr for 6 hours. After that time, no reaction had taken place, as the doublet attributed to the proton at 6.15 ppm (J 8.4 Hz) remained. After 21 hours this signal did disappear. However no doublet between 7.3 and 8.0 was observed for the bromo species. There was also no signal at 4.0ppm due to the formation of the hydrolysis product at the anomeric centre. On repeating the reaction with a larger HBr/acetic acid concentration (40 fold excess) the reaction proceeded much quicker and the doublet at 6.15 ppm disappeared after 3.5 hours. In both instances reactions of the product were carried out with silver thiocyanate, lead thiocyanate and potassium thiocyanate in toluene and 1,4-dioxan over periods ranging from 15 minutes to 24 hours. In each case ^1H nmr of the resulting products showed a broad peak at 6.0ppm and also a broad peak at 4.1ppm which may be attributed to the hydrolysis product C-OH at the anomeric carbon. Although there is no hard evidence of the formation of

the bromo derivative, the following factors indicate that a displacement had occurred at the anomeric position:-

- i) Shift of the doublet at 6.15ppm during brominolysis
- ii) Decrease in the intensity of the N-H signals at 9.9ppm after brominolysis
- iii) Emergence of a broad peak at 4.0 ppm during brominolysis
- iv) Presence of a broad peak at 6.0 ppm during the reaction with silver thiocyanate. Infra-red analysis of the product after the reaction with the thiocyanate salts revealed no adsorption characteristic of the NCS group at 2100cm^{-1} .

B) Maltose and Maltotriose (3,5-dimethylphenylcarbamates).

Maltose and maltotriose were dried thoroughly before reaction with the aryl isocyanate and the derivatives prepared in good yield. These compounds exhibited poor solubility and were only slightly soluble in 1,4 dioxan. As the conversion of the glucose homologue to the bromo derivative was proving difficult, attempts to react these compounds at the anomeric centre were left until a proven method for the glucose derivative was found.

C) Maltose and Maltotriose (phenylcarbamates)

Phenyl carbamates of maltose and maltotriose were prepared by a reaction with phenyl isocyanate.

Ethyl acetate, which was successfully used as a solvent for the formation of the 1-bromo glucose tetra(phenylcarbamate), did not dissolve the maltose octa(phenylcarbamate), so 1,4-dioxan was used as an alternative. In the formation of the 1-bromo derivative with HBr/acetic acid, the appearance of a white residue was observed, which was also formed during the corresponding reaction with the glucose derivative. Analysis of this compound showed it to have the same elemental analysis and nmr spectrum.

^1H nmr analysis of the bromo product showed that the reaction at the C1 position had occurred as the doublet had shifted from 6.2ppm to 7.6ppm. This reaction was reproducible.

The addition of silver thiocyanate and toluene gave a product which, when analysed by infra-red, showed the characteristic NCS absorption at 2068cm^{-1} . ^1H nmr showed the disappearance of the doublet at 7.6ppm from the bromo species, but confirmation of the shift of the signal to 5.8ppm was difficult to obtain as a multiplet of peaks from the other signals from the sugar protons obscured the doublet's signal. However, the integral of the multiplet showed an increase in the number of protons. ^{13}C nmr showed the presence of an NCS group (140.8ppm). FAB-MS gave an m/z of 1158, which correlates with a maltose hepta(phenylcarbamate) fragment, presumed to arise from the unstable and non-observed molecular ion which should occur at 1218. This is not unusual, due to the instability of the molecular ion under these conditions (see Chapter 4). A large signal was observed at m/z 60 but it is difficult to assign to an NCS fragment.

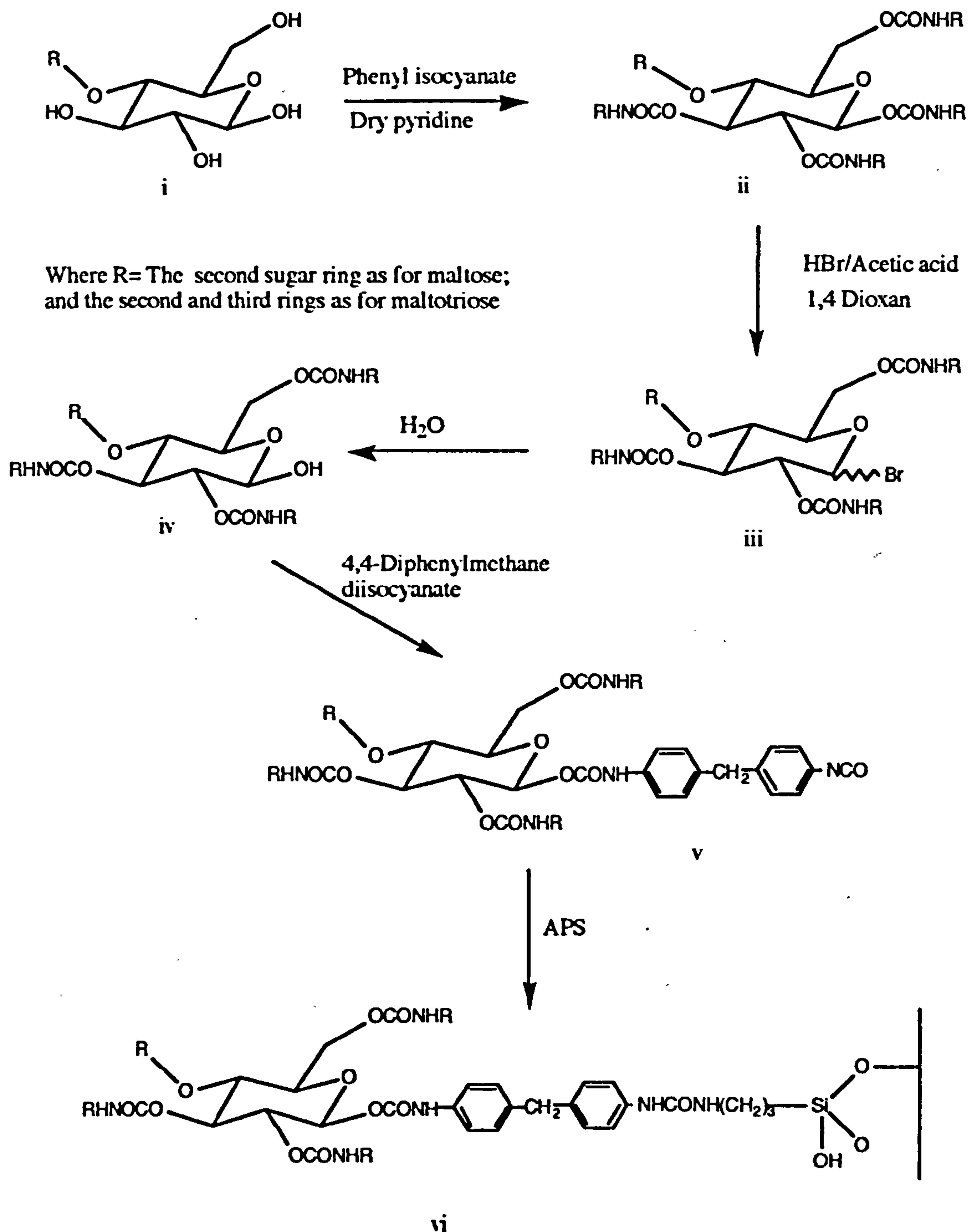
Scaling up the reaction between the bromo maltose hepta(phenyl carbamate) and silver thiocyanate did not yield the desired product and the reaction could not be reproduced.

The reaction of HBr/acetic acid with maltotriose undeca (phenylcarbamate) was performed in ethyl acetate and 1,4-dioxan. ^1H nmr analysis gave the correct indications of the displacement of the carbamate at the anomeric carbon due to the shift of the doublet at 6.2ppm to 7.6ppm in both solvents. However, nmr and infra-red studies of the product from nucleophilic substitution of the bromo derivative by the thiocyanate anion at the anomeric carbon, did not indicate that the required substitution had occurred.

Ideas for Future Work

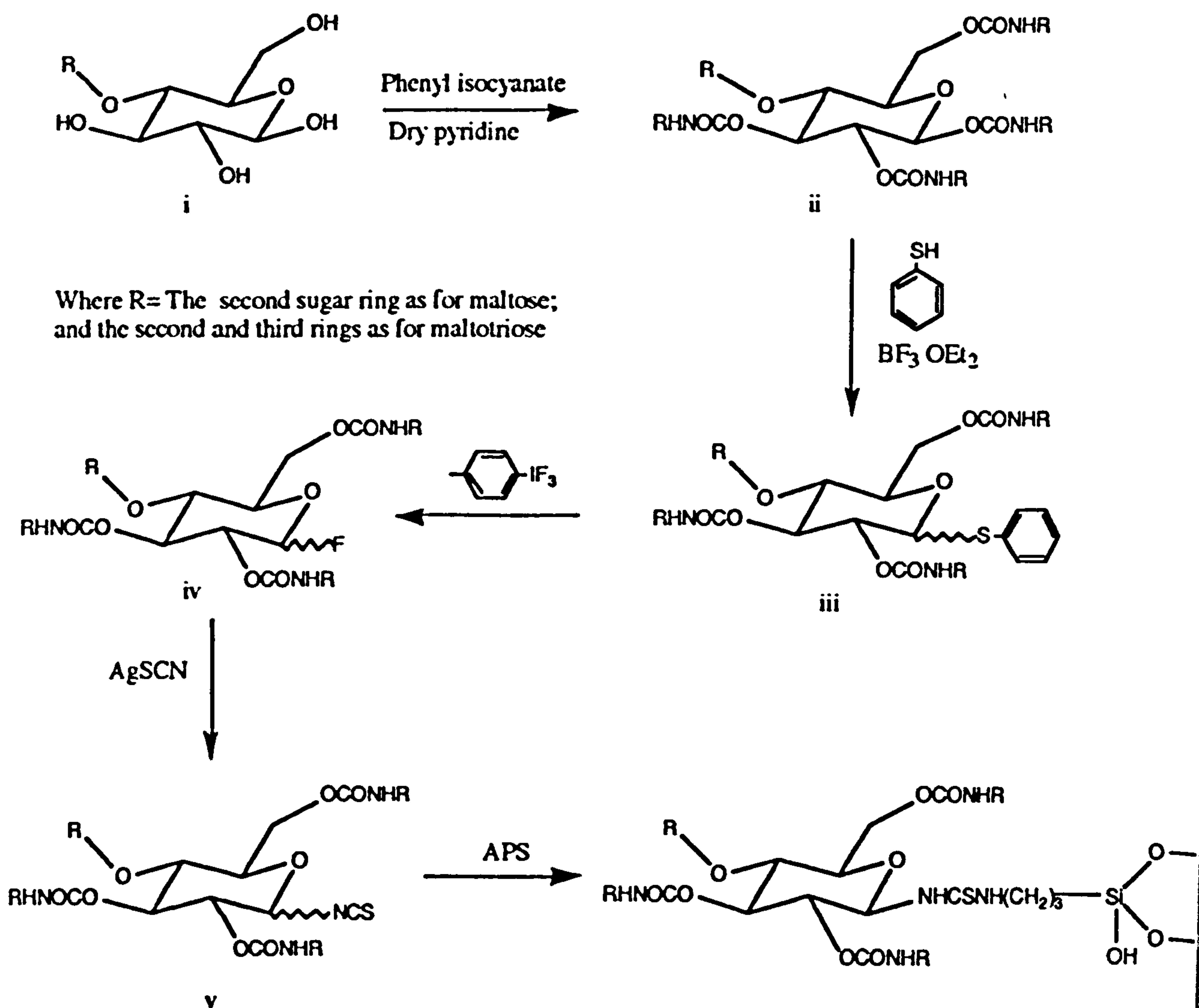
1) The glycosidation of maltose octa(phenylcarbamate) by the Koenigs-Knorr reaction appeared to have formed the 1-bromo maltose septa(phenylcarbamate) (see page 197). However, the subsequent reaction with a thiocyanate salt did not produce the desired product, 1-isothiocyanato maltose septa (phenylcarbamate). A different approach (see Scheme 14), introducing a stable and reactive group at the anomeric carbon, would be to hydrolyse the 1-bromo maltose septa(phenylcarbamate) (iii) by the addition of water, to give an hydroxyl group (iv). The hydroxyl group could then be reacted with an excess of a diisocyanate (e.g.. 4,4-diphenylmethane diisocyanate) forming a carbamate linkage at the anomeric position (v). The unreacted other half of the diisocyanate could

then be reacted with aminopropylsilica, bonding the sugar molecule to the silica surface (vi).



Scheme 14

2) A study by Motherwell ²⁵² has shown that a variety of useful functionalised 1-fluoroglycosides (iv) may be prepared under mild conditions from their corresponding arylthioglycoside derivatives (iii) by the reaction with 4-methyl (difluoroiodo) benzene (see Scheme 15).



Scheme 15

If however, the arylthioglycoside phenylcarbamate derivative (iii) is difficult to prepare, then the acetate derivative may be considered as an alternative (due to its greater solubility).

Deacetylation of the arylthioglycoside acetate derivative with sodium methoxide, followed by carbamoylation with phenyl isocyanate could give the desired product (iii).

CHAPTER 6 EXPERIMENTAL

PREPARATION OF CHIRAL STATIONARY PHASES (CSP's).

6.1 Preparation of Polysaccharide Derivatives

6.1.1 Cellulose Tris(phenylcarbamate)

Cellulose (2.0g; Avicel, Merck, 12.35 mmols, Note: the number of mmols is calculated based on the assumption the one gluco unit $C_6H_{10}O_5$ has a molecular weight of 162) previously dried for 24 hours over phosphorus pentoxide in a vacuum desiccator, was refluxed for 3 hours in pyridine (50cm³, dried over KOH) to allow for swelling to occur. After cooling, phenyl isocyanate (6.36g, 53.45 mmols) was slowly added, then the mixture refluxed with stirring for 62 hours.

After cooling, the orange-brown solution was poured into methanol (300cm³) and the precipitated white solid stirred for half an hour. The white solid was filtered off, washed well with methanol and dried under vacuum at 60°C to constant weight. Yield 6.0g 93.6% Elemental analysis %C 62.36; %H 4.40; %N 7.91.(Fully carbamoylated Avicel requires %C 62.43; %H 4.82; %N 8.09) i.r., ν max (nujol mull) 3326, 1717, 1602cm⁻¹.

6.1.2 Preparation of Cellulose Tris (3,5-dimethylphenyl-carbamate)

Cellulose (2.0g Avicel, Merck, 12.35 mmols) was treated and reacted in the same manner as for the preparation as cellulose tris(phenylcarbamate), with 3,5-dimethylphenyl isocyanate (7.48g, 50.88 mmols). Yield 6.6g; 88.65%, elemental analysis %C 65.60 %H 6.06, %N 6.93. (Fully carbamoylated Avicel requires %C 65.67; %H 6.16; %N 6.97) i.r., ν max (nujol mull) 3320, 1717, 1602 cm^{-1} .

6.1.3 Preparation of Cellulose Tris(naphthylcarbamate)

Cellulose (2.0g Avicel, Merck, 12.35 mmols) was treated and reacted in the same manner as for the preparation as cellulose tris(phenylcarbamate), with naphthyl isocyanate (9.80g, 58.00 mmols). Yield 7.1g 84.2%; elemental analysis %C 69.40 %H 4.53, %N 6.26; (Fully carbamoylated Avicel requires %C 69.95 %H4.60; %N 6.27) i.r., ν max (nujol mull) 3326, 1714, 1600 cm^{-1} .

6.1.4 Preparation of Amylose Tris(phenylcarbamate)

Amylose (2.0g, type 3, Sigma, 12.35 mmols, note: the number of mmols is calculated based on the assumption the one gluco unit $\text{C}_6\text{H}_{10}\text{O}_5$ has a molecular weight of 162) was treated with phenyl isocyanate (6.36g, 53.45 mmols) as for the preparation of cellulose tris(phenylcarbamate). Yield 5.9g 92.1%; elemental

analysis %C 61.48, %H 4.80, %N 8.08 (Fully carbamoylated amylose requires %C 62.43; %H 4.82; %N 8.09) i.r., ν max (nujol mull) 3320, 1717, 1602 cm^{-1}

6.1.5 Preparation of Amylose Tris(3,5-dimethylphenylcarbamate)

Amylose (2.0g, type 3, Sigma, 12.35 mmols) was treated with the same quantities of with 3,5-dimethylphenyl isocyanate (8.2 cm^3 , 55.78 mmols). Yield 6.6g 88.60% elemental analysis %C 65.10, %H 6.13, %N 6.90 (Fully carbamoylated amylose requires %C 65.67; %H 6.16; %N 6.97) i.r., ν max (nujol mull) 3327, 1716, 1605 cm^{-1}

6.2 Preparation of CSP's with CPC Loading of 5, 10 and 20%(wt% of silica)

In a mortar flask (50 cm^3), Hypersil APS (2.4g) was refluxed in THF (10 cm^3) for 30 minutes and then allowed to cool. CPC (0.12g, 5% w/w; 0.24g 10% w/w and 0.48g, 20% w/w: Note all the coated packing materials were prepared in accordance to the method described by Okamoto⁷⁸ in which the polysaccharide derivatives (25 wt% of silica) were adsorbed onto APS silica) was gently warmed in THF (20 cm^3) until dissolution was complete (if necessary the solution was centrifuged and the supernatant liquid decanted off). To the suspended Hypersil APS, a portion of the CPC solution(10 cm^3) was added and the solvent removed under vacuum by rotating the mortar flask very slowly at room temperature using a rotary evaporator. To the dried silica, the remaining CPC solution was added and the evaporation process repeated until dryness.

The coated silica was then dried in a vacuum oven (<50mm Hg) at 60°C for 4 hours then passed through a 35 μ m sieve to produce a fine white powder for packing.

(In the preparation of 20% w/w loading on the wider pore silica's (500Å, 1000Å, 4000Å), silica (3.0g) was coated with the CSP (0.6g).)

This procedure was employed for CDMPC and CNC. For APC and ADMPC phases, the solubility of these derivatives was enhanced by the addition of N,N-dimethylacetamide (20% v/v) to the THF solution.

6.3 Packing Procedure

To the CPC coated silica, hexane (40cm³) and propan-2-ol (40cm³) was added and the particles suspended by stirring and ultrasound for 2 minutes. The suspension was then quickly transferred to a "bomb" (80cm³ capacity) which was connected at one end to a stainless steel HPLC column (filled with hexane/propan-2-ol) fitted with a Valco end fitting and frit. After filling, the other end of the bomb was joined to a Haskel 780-3 HPLC packer. The suspension was then downward slurry packed at 4500 psi into the stainless steel column using hexane/propan-2-ol (80:20) until 250cm³ of eluent was collected.

This procedure was repeated for each of the coated silica CSP's.

6.4 Modification of the Silica Surface.

6.4.1 Aminopropylation of Silica

Silica,(Nucleosil, 7mm, 500Å, 1000Å or 4000Å, 10g) was heated under vacuum (<50mm Hg) for 16 hours at 120°C, then allowed to stand over a saturated solution of LiCl in a closed container (12% relative humidity) for 24 hours.

To a solution of toluene (75cm³, previously dried and distilled from sodium), containing γ -aminopropyltriethoxysilane (5.5cm³), the silica was added and the reaction mixture gently refluxed for 2 hours. After cooling, the product was filtered through a No 4 glass sinter, washed well with toluene (2 x 100cm³), methanol/water (1 x 25cm³) then methanol (2 x 25cm³) and dried in a vacuum oven (<50mm Hg) at 80°C to constant weight. The white powder was then submitted for elemental analysis.

This procedure was repeated for Nucleosil (7mm 100Å, 97.5g) which was added to a solution of toluene (175cm³) and γ aminopropyltriethoxysilane (63.5cm³). The suspension was refluxed with gentle stirring for 2 hours, filtered, washed and dried as previously.

Elemental analysis results:-

SILICA PORE SIZE Å	%C	%H	%N
100	4.96	1.40	1.70
500	0.79	0.17	0.30
1000	0.57	0.16	0.22
4000	0.26	0.17	0.07

Table 27

6.4.2 Modification of Silica with [3-(2-aminoethyl) aminopropyl]trimethoxysilane

Silica (Nucleosil 7µm, 100Å, 4.8g dried as above) was added to a solution of toluene (previously dried, 30cm³) containing [3-(2-aminoethyl) aminopropyl]trimethoxysilane (AEAMS) (2.8cm³) and the solution gently refluxed for two hours. The yellow powder was separated by filtering through a No 4 glass sinter, washed with methanol/water (1 x 25cm³), methanol (2 x 25cm³), dried in a vacuum oven at 60°C (<50mm Hg) to constant weight, then submitted for elemental analysis.

SILICA	%C	%H	%N
Nucleosil AEAMS	7.93	1.44	2.50

Table 28

6.5. Evaluation of CSP Phases by High Performance Liquid Chromatography

6.5.1 Hardware for Analytical Chromatography

Pump	:	Cecil CE 1100
Injector valve	:	Rheodyne model 7125
Loop size	:	20 μ l
Detector	:	Pye Unicam LC3 UV detector
Recorder	:	Servoscribe 1s, RE 541 potentiometric recorder

6.5.2 Columns

Dimensions	:	Length 10 or 15cm x 0.46cm id.
Packing materials	:	Hypersil APS 120Å 5 μ m Nucelosil APS 500Å, 1000Å, 4000Å, 7 μ m
Coating materials	:	CPC, CDMPC, CNC, APC, ADMPC.

6.5.3. Solvents

The following grades of solvents were supplied by BDH, Poole, Dorset, England:-

Propan-2-ol	:	Hypersolv, HPLC grade
Hexane	:	Hypersolv, HPLC grade
Tetrahydrofuran	:	Hypersolv, HPLC grade
Methanol	:	Hypersolv, HPLC grade

Water : Hypersolv, HPLC grade
 Acetonitrile : Hypersolv, HPLC grade (far uv)

6.5.4 Mobile Phase Preparation

Each mobile phase was degassed by ultrasonic vibration under vacuum for 10 minutes prior to use. The required mobile phase ratios were prepared using pipettes and measuring cylinders.

6.6.1 Determination of the Height Equivalent to a Theoretical Plate
HETP for an Inert Peak for the 5, 10 and 20% Loaded Phases

Hexane was pumped through the column at $0.5\text{cm}^3 \text{ min}^{-1}$. Over a 10 minute period the hexane eluting from the column was collected in a measuring cylinder and the flow rate determined. 10cm^3 of a solution of 1,3,5-tri-*tert*-butyl-benzene in the mobile phase was injected onto the column, and, with the aid of an integrator, the retention time of the eluting peak was measured.

% LOADING	$t_0 \text{ sec}^{-1}$	$w_R \text{ sec}^{-1}$	$F/\text{cm}^3\text{min}^{-1}$	HETP
5	189.0	14.55	0.54	0.133
10	189.0	13.43	0.52	0.114
20	186.6	12.87	0.49	0.107

Table 29

where w_R is the peak width at half height, chart speed 26.8 mm min^{-1} .

6.6.2 Evaluation of k' , α and R_s for Each of the CSP Columns

A solution containing the pair of enantiomers for each test compound (stilbene oxide, 2,2,2-TFAE, benzoin, trogers base and 1-phenethanol) was prepared in hexane/propan-2-ol (80:20) at a concentration of $100 \mu\text{gcm}^{-3}$. To this solution internal standard (1,3,5-tri-tert-butyl-benzene) was added ($20 \mu\text{gcm}^{-3}$). Each solution was injected onto the HPLC column ($20 \mu\text{l}$) with a range of mobile phase conditions i.e. 0.5% propan-2-ol/hexane to 20% propan-2-ol /hexane at room temperature. The k' , α and R_s values were measured from the chart recording of the chromatogram.

6.7 Preparation of Bonded Phase Chiral HPLC Columns.

6.7.1 Preparation of Glucose Penta(phenylcarbamate)

Glucose (2.0g; 11.11 mmols) previously dried over phosphorus pentoxide was dissolved in dried pyridine (50cm^3) and gently stirred with activated type 4A molecular sieves for 24 hours. The solution was decanted and phenyl isocyanate added (7.0g; 58.82 mmols) and stirred at 80°C for 16 hours.

After cooling, the pyridine was removed under reduced pressure with the aid of a rotary evaporator and the amorphous residue stirred in hexane (100cm^3) for one hour. The white solid was filtered off, washed thoroughly with hexane and recrystallised from THF/hexane producing a crystalline white solid. Yield 8.0g,

92.8% m.p. 213⁰C i.r.,_v max (nujol mull) 3326, 1714, 1602cm⁻¹. ¹H n.m.r. δ (DMSO d₆) 10.07(s) 1H N-H; 9.90-9.76(m) 4HN-H; 7.54-6.91 (m) 25H aromatic; 6.15(d, JH₁₋₂ 8.4Hz) 1H₁; 5.53 (t, JH₃₋₄;2-3 8.4Hz) 1H₃; 5.13(m) 2H H₂ and H₄; 4.32(m) 3H H₅ and H_{6a'b'}. ¹³C n.m.r. 153.1(s) C=O, 152.6(s) C=O, 152.4(s) C=O, 152.3(s) C=O, 151.4(s) C=O; 138.7 (m) (C₄ of Ph), 128.7(m) (C_{3,5} of Ph), 122.4(m) (C_{2,6} of Ph), 118.5(m) (C₁ of Ph), 92.2(s) C₁, 72.8(s) C₂, 72.47(s) C₃, 71.0(s) C₄, 68.7 C₅, 62.3 C₆; elemental analysis %C 63.29 %H 4.83 %N 8.97: (C₄₁ H₃₇ N₅ O₁₁ requires %C63.48 %H 4.77 %N9.03); FAB mass spectrum m/z 776 [M+H]⁺

6.7.2 1-Bromo-2,3,4,6-Tetra(phenylcarbamoyl)glucopyranose

To a solution of glucose penta(phenylcarbamate) (6.1g; 7.87 mmols) dissolved in dry ethyl acetate (1500cm³), HBr/acetic acid (10cm³; 40.24 mmols) and acetic anhydride (1.0cm³) was added and the solution stirred at room temperature for two and a half hours. At room temperature, the solvent was removed under vacuum on a rotary evaporator and the remaining HBr/acetic acid azeotropically removed by addition of dry toluene (3 x 175cm³) to produce a fine orange solid. Crude yield 5.8g. ¹H n.m.r. δ (DMSO d₆) 9.90-9.76(m) 4HN-H, 7.66 (d, JH₁₋₂ 8.4Hz) 1H₁; 5.32 (t, JH₃₋₄;2-3 8.4Hz) 1H₃; 5.0(m) 2H H₂ and H₄, 4.2(m); 3H H₅ and H_{6a'b'}. 4.2(dJH₁₋₂ 8.4Hz); 1H C-OH₁: ¹³C n.m.r. 153.1(s) C=O; 152.6(s) C=O; 152.4(s) C=O; 152.3(s) C=O; 138.7 (m) (C₄ of Ph); 128.7(m) (C_{3,5} of Ph); 122.4(m) (C_{2,6} of Ph); 118.5(m) (C₁ of Ph); 94.5(s) C₁; 73.2(s) C₂; 72.8(s) C₃; 71.5(s); C₄; 69.4 (s) C₅; 62.7(s) C₆.

6.7.3 Preparation of 1-isothiocyanato 2,3,4,6-Tetra(phenylcarbamate) glucopyranose (IGPC)

To a suspended solution of 2,3,4,6-tetra(phenylcarbamoyl) glucopyranosyl bromide (5.5g; 7.62mmoles) in dried toluene (200cm³), silver thiocyanate (8.0g; 48.50 mmols previously dried, over SiO₂ for 2 days) was added. The mixture was vigorously stirred and refluxed in the dark for half an hour. On cooling, the red suspension was filtered through a celite/silica bed, the eluted toluene discarded, and the celite/silica bed washed with THF (100cm³). The THF was then removed by rotary evaporation producing a yellow flaky solid which was purified by preparative TLC using SiO₂ plates, mobile phase: carbon tetrachloride 35vol, THF 15vol, R_f = 0.31, to give an off-white solid. Yield 2.4g, 48%. m.p. 197⁰C. i.r., ν max (nujol mull) 3326, 2027, 1715, 1604cm⁻¹. ¹H n.m.r. δ (DMSO d₆) 9.90-9.76(m) 4HN-H; 7.54-6.91 (m) 20 H aromatic; 5.75(d, J_{H1-2} 8.5Hz) 1H₁; 5.41 (t, J_{H3-4;2-3} 8.4Hz) 1H₃; 5.09(m) 2H H₂ and H₄; 4.32(m) 3H H₅ and H_{6a'b'}. ¹³C n.m.r. 153.0(s) C=O, 152.5(s) C=O, 152.2(s) C=O, 152.0(s) C=O, 140.9 N=C=S; 138.6 (m) (C₄ of Ph), 128.7(m) (C_{3,5} of Ph), 123.4(m) (C_{2,6} of Ph), 118.9(m) (C₁ of Ph), 82.7(s) C₁, 73.8(s) C₂, 72.1(s) C₃, 72.0(s) C₄, 68.6 C₅, 62.2 C. elemental analysis %C 59.92 %H 5.09 %N 9.75; (C₃₅ H₃₁ N₅ O₉ S requires %C60.26 %H4.45 %N10.04) FAB mass spectrum m/z 698 [M+H]⁺

6.7.4 Preparation of 1-(N,-propylureido)-2,3,4,6-Tetra(phenylcarbamate) glucopyranose

A mixture of 1-isothiocyanato-2,3,4,6,-tetra(phenylcarbamate) glucopyranose (0.3g; 0.43 mmols) and propylamine (0.3cm³ 5.88 mmols) in THF was stirred for 3 hours at room temperature, then evaporated to dryness under reduced pressure to give a residue. The reaction mixture was purified by recrystallisation from THF/hexane to give a yellow solid. Yield 0.26g; 80.0% m.p. 209 °C i.r., ν max (nujol mull) 3326, 1714, 1602 1197 cm⁻¹. ¹H n.m.r. δ (DMSO d₆) 10.07(s) 4HN-H; 7.54-6.91 (m) 20 H aromatic; 5.95(d, v. broad) 1H₁; 5.50 (t, JH₃₋₄;2-3 8.4Hz) 1H; 5.13(m) 2H H₂ and H₄, 4.32(m); 3H H₅ and H_{6a'b'}; 3.4 (s) broad 2H N-H; 1.5(m)·4H CH₂; 0.8 (m) 3H CH₃; elemental analysis %C 58.96 %H 4.88 %N 10.58 (C₃₅ H₃₄ N₆ O₉ S requires %C58.82 %H4.76 %N11.76); FAB mass spectrum m/z 715 [M+H]⁺.

6.7.5 Investigation of Coupling IGPC to Modified Silica.

6.7.5.1 Preparation of the Working Solution .

A solution containing 10,000 μ gcm⁻³ of 1-isothiocyanato,2,3,4,6-tetra(phenylcarbamate) glucopyranose (IGPC) was prepared by dissolving IGPC (1.000g) in THF (10.00cm³).

6.7.5.2. Effect of Solvent and Temperature

Performed in duplicate, the working solution (0 μ l for the blank, 100 μ l= 10mg of IGPC) was added to a suspension of silica (APS

7 μ m Nucleosil 100Å; 50mg) and solvent (THF, pyridine, 1-4 dioxan; 2cm³). (Note: to the non-basic solvents 0.25 μ l of pyridine was added.) One half of each of the prepared mixtures was refluxed for 3 days and the other half shaken for the same period. The suspensions were then filtered through a Whatman GFC filter paper, washed with THF (3x 23cm³) and dried to constant weight at 60°C in a vacuum oven. For results see Table 20.

6.7.5.3 Concentration of Chiral Selector (IGPC)

From the working solution aliquots were taken (0 μ l=blank; 50 μ l=5mg; 100 μ l=10mg; 200 μ l=20mg; 300 μ l=30mg; 400 μ l=40mg; 500 μ l=50mg; 750 μ l=75mg and 1000 μ l=100mg IGPC.) and shaken for 3 days with a suspension of silica (100mg 7 μ m APS Nucleosil), in THF (2cm³, containing 2.5 μ l of pyridine).

The suspensions were then filtered through a Whatman GFC filter paper, washed with THF (3x 23cm³) and dried to constant weight at 60°C in a vacuum oven. For results see Table 21.

6.7.5.4 Reaction time

Performed in duplicate, the working solution (100ml=10mg IGPC) was added to a suspension of silica (50mg Kromasil APS 7 μ m 100Å) in THF (2cm³, containing 2.5 μ l of pyridine). One prepared mixture was shaken for 3 days and the other shaken for 5 days. The suspensions were then filtered through a Whatman GFC filter

paper, washed with THF (3x 23cm³) and dried to constant weight at 60°C in a vacuum oven. For results see Table 22.

6.7.5.5 Type of silica

Performed in duplicate, four different silicas (all 100mg, Kromasil 100Å APS; Hypersil 120Å APS; Nucleosil 100Å APS and Nucleosil 500Å APS) were added to a solution of THF (2cm³, plus 2.5µl of pyridine) containing the working solution (0ml=blank, 200µl=20mg IGPC) One half of each of the silica's was refluxed for 3 days and the remaining half shaken for the same time period. The suspensions were then filtered through a Whatman GFC filter paper, washed with THF (3x 25cm³) and dried to constant weight at 60°C in a vacuum oven.

SILICA APS	PORE SIZE Å	SBET m ² /g	METHOD	ELEMENTAL ANALYSIS %C
KROMASIL	100	350	BLANK	4.37
			REFLUX	9.57
			SHAKEN	9.30
NUCLEOSIL	100	350	BLANK	4.99
			REFLUX	10.32
			SHAKEN	10.43
HYPERSIL	120	180	BLANK	2.11
			REFLUX	6.24
			SHAKEN	5.70
NUCLEOSIL	500	35	BLANK	1.06
			REFLUX	2.24
			SHAKEN	1.71

Table 30

6.7.5.6 Effect of the Length of Silane Modifier

From the working solution aliquots were taken (0 μ l=blank; 50 μ l=5mg; 100 μ l=10mg; 200 μ l=20mg; 300 μ l=30mg; 400 μ l=40mg; 500 μ l=50mg; 750 μ l=75mg and 1000 μ l=100mg IGPC.) and shaken for 3 days with a suspension of silica (100mg 7 μ m AEAMS Nucleosil), in THF (2cm³, containing 2.5 μ l of pyridine).

The suspensions were then filtered through a Whatman GFC filter paper, washed with THF (3x 25cm³) and dried to constant weight at 60°C in a vacuum oven.

CSP wt mg ⁻¹	Reaction conditions in THF	Elemental analysis %C
0	shaken 72hr	7.97
10	shaken 72hr	8.67
20	shaken 72hr	12.23
30	shaken 72hr	13.14
40	shaken 72hr	13.05
50	shaken 72hr	13.15

Table 31

6.8.1 Preparation of Glucose Penta(3,5-dimethylphenylcarbamate)

Glucose (2.0g; 11.11 mmols) previously dried over phosphorus pentoxide was dissolved in dried pyridine (50cm³) and gently stirred with activated type 4A molecular sieves for 24 hours. The solution was decanted, 3,5-dimethylphenyl isocyanate (8.5g 57.82 mmols) was added and the mixture stirred at 80°C for 16 hours.

After cooling, the pyridine was removed under reduced pressure with the aid of a rotary evaporator and the amorphous residue stirred in hexane (100cm³) for one hour. The white solid was filtered off, washed thoroughly with hexane and recrystallised from THF/hexane producing a crystalline white solid. Yield 8.5g, 94.0%; m.p. 243⁰C i.r., ν max (nujol mull) 3326, 1714, 1602cm⁻¹. ¹H n.m.r. δ (DMSO d₆) 9.90(s) 1H N-H, 9.67-9.56(m); 4HN-H, 7.54-6.91 (m) 15H aromatic; 6.05(d, JH₁₋₂ 8.4Hz) 1H₁; 5.44 (t, JH₃₋₄;2-3 8.4Hz) 1H₃; 5.06(m) 2H H₂ and H₄; 4.26(m) 3H H₅ and H_{6a'b'}, 2.1(m) 30 CH₃. ¹³C n.m.r. 153.1(s) C=O; 152.5(s) C=O; 152.2(s) C=O; 152.6(s) C=O; 151.1(s) C=O; 138.7 (m) (C₄ of Ph); 122.3(m) (C_{2,6} of Ph); 116.5(m) (C₁ of Ph);. 91.2(s) C₁; 72.0(s) C₂; 71.7.(s) C₃; 71.0(s) C₄; 67.7(s) C₅; 62.3 (s) C₆; 21.2 CH₃; elemental analysis %C 66.84 %H 6.31 %N 7.66 (C₅₁ H₅₇ N₅ O₁₁ requires %C66.89 %H 6.23 %N7.65); FAB mass spectrum m/z 916 [M+H]⁺.

6.8.2 Preparation of Cellobiose Octa(phenylcarbamate)

Cellobiose (2.0g, 5.84 mmols previously dried over phosphorus pentoxide in a vacuum) was dissolved in pyridine (50 cm³). To the solution phenyl isocyanate (6.0g, 50.42 mmols) was added and the reaction procedure for the preparation of glucose aryl carbamates was then repeated. m.p. 245⁰C i.r., ν max (nujol mull) 3320, 1717, 1601cm⁻¹: ¹H n.m.r. δ (DMSO d₆) 10.07(s) 1H N-H; 9.90-9.40(m)7H; N-H; 7.6-6.8 (m) aromatic 40 H; 6.06(d, JH₁₋₂ 8.4Hz) 1H₁; 5.72(d, JH_{1'-2'} 8.4Hz) 1H_{1'}; 5.50 (m) 2H_{3,3'}; 5.15-4.20(m) 10H; H_{2,2'} H_{4,4'}, H_{5,5'} and H_{6ab} 6a'b': ¹³C n.m.r. 153.1-151(m) 8 C=O; 138.7 (m) (C₄ of Ph); 128.7(m) (C_{3,5} of PH); 122.4(m) (C_{2,6} of Ph); 118.5(m) (C₁ of Ph); elemental analysis %C

62.75 %H 4.88 %N 8.74 ($C_{68}H_{62}N_8O_{19}$ requires %C63.06 %H 4.79 %N 8.66); LSIMS mass spectrum m/z 1295 $[M+H]^+$.

6.8.3 Preparation of Maltose Octa(phenylcarbamate)

Maltose monohydrate (2.0g, 5.55 mmols previously dried over phosphorus pentoxide in a vacuum) was dissolved in anhydrous pyridine and gently stirred with type 4A molecular sieve for 2 days. To the decanted solution, phenyl isocyanate (6.0g, 50.42 mmols) was added. The reaction procedure for the preparation of glucose aryl carbamates was then repeated. m.p. $248^{\circ}C$ i.r., ν max (nujol mull) 3326, 1714, 1602cm^{-1} ; 1H n.m.r. δ (DMSO d_6) 10.07(s) $\underline{1H}$ N-H; 9.90-9.40(m) $\underline{7H}$ N-H; 7.6-6.8 (m) aromatic 40 \underline{H} ; 6.06(d, J_{H1-2} 8.4Hz) $\underline{1H}$ ₁; 5.7(d, $J_{H1'-2'}$ 2.5Hz) $\underline{1H}$ _{1'}; 5.52 (m) $\underline{2H}$ _{3,3'}; 5.13-4.12(m) $\underline{10H}$ $H_{2,2'}$ $H_{4,4'}$, $H_{5,5'}$ and H_{6ab} $6a'b'$; ^{13}C n.m.r. 153.1-151(m) 8 C=O; 138.7 (m) (C4 of Ph); 128.7(m) (C 3,5 of Ph); 122.4(m) (C2,6 of Ph); 118.5(m) (C1 of Ph); elemental analysis %C 62.84 %H 4.84 %N 8.52 ($C_{68}H_{62}N_8O_{19}$ requires %C63.06 %H 4.79 %N 8.66); LSIMS mass spectra m/z 1295 $[M+H]^+$.

6.8.4 Preparation of Maltose Octa(3,5-dimethylphenylcarbamate)

Maltose monohydrate (2.0g 5.55 mmols previously dried over phosphorus pentoxide in a vacuum) was dissolved in anhydrous pyridine and gently stirred with type 4A molecular sieve for 2 days. To the decanted solution, 3,5-dimethylphenyl isocyanate (7.3g 49.65 mmols) was added. The reaction procedure for the preparation of glucose aryl carbamates was then repeated. m.p. $268^{\circ}C$ i.r., ν max (nujol mull) 3326, 1714, 1600cm^{-1} . 1H n.m.r. δ

(DMSO d_6) 9.85(s) 1H N-H; 9.85-9.60(m) 7N-H; 7.15-6.5 (m) aromatic 24 H; 6.05(d, J_{H1-2} 8.4Hz) 1H₁; 5.65(d, $J_{H1'-2'}$ 2.5Hz) 1H_{1'}; 5.50 (m) 2H_{3,3'}; 5.13-4.02(m) 10H H_{2,2'} H_{4,4'} H_{5,5'} H_{6ab} 6a'b'; 2.1(m) 48 CH₃; ¹³C n.m.r. 153.1-151.4(s) 8 C=O; elemental analysis %C 66.27 %H 6.21 %N 7.37(C₈₄ H₉₄ N₈ O₁₉ requires %C66.40 %H 6.19 %N 7.38); LSIMS .mass spectra m/z 1519 [M+H]⁺.

6.8.5 Preparation of Maltotriose Undeca(phenylcarbamate)

Maltotriose monohydrate (2.0g 3.95 mmols previously dried over phosphorus pentoxide in a vacuum) was dissolved in anhydrous pyridine and gently stirred with type 4A molecular sieve for 2 days. To the decanted solution, phenyl isocyanate (6.0g 50.42 mmols) was added. The reaction procedure for the preparation of glucose aryl carbamates was then repeated. m.p. 255°C i.r., ν max (nujol mull) 3326, 1717, 1600cm⁻¹. ¹H n.m.r. δ (DMSO d_6) 10.07(s) 1H N-H; 9.90-9.76(m) 10H H-N; 7.6-6.8Hz(m) H aromatic; 6.15(d, J_{H1-2} 8.4Hz) 1H₁; 5.73 (m) 2H_{1'1''}; 5.53 (m) 3H_{3,3'3''}; 5.13-4.10(m) 15H_{2,2'2''} H_{4,4'4''} H_{5,5'5''} and H_{6ab} 6a'b'6a''b''. ¹³C nmr 153.1-151.0 (m) 11C=O, .. elemental analysis %C 62.65 %H 4.76 %N 8.49 (C₉₅ H₈₇ N₁₁ O₂₇ requires %C 62.88 ,%H 4.80, %N 8.49); LSIMS mass spectrum m/z 1814 [M+H]⁺.

6.8.6 Preparation of Maltotriose Undeca(3,5-dimethylphenyl carbamate)

Maltotriose monohydrate (2.0g 3.95 mmols previously dried over phosphorus pentoxide in a vacuum) was dissolved in anhydrous pyridine and gently stirred with type 3A molecular sieve for 2

days. To the decanted solution, 3,5-dimethylphenyl isocyanate (7.3g 49.65 mmols) was added. The reaction procedure for the preparation of glucose aryl carbamates was then repeated. m.p. 273⁰C i.r., ν max (nujol mull) 3320, 1716, 1604cm⁻¹. ¹H n.m.r. δ (DMSO d₆) 9.85(s) 1H N-H; 9.85-9.65(m) 10H N-H; 7.15-6.5 (m) aromatic 33 H; 6.05(d, JH₁₋₂ 8.4Hz) 1H₁; 5.65 (m) 2H_{1'1''}; 5.50 (m) 3H_{3,3'3''}; 5.13-4.02(m) 15H 2,2'2'' H_{4,4'4''} H_{5,5'5''} H_{6ab} 6a'b' 6a''b''; 2.15 66CH₃. ¹³C n.m.r. 153.1-151.0 (M) 11 C=O; elemental analysis %C 66.45 %H 6.29 %N 7.41 (C₁₁₇ H₁₃₁ N₁₁ O₂₇ requires %C 66.20 ,%H 6.18, %N 7.26); LSIMS mass spectra m/z 2122 [M+H]⁺.

6.8.7 Generation of 1-Bromo Malto-Oligosaccharides

To a solution of maltose octa(phenylcarbamate) (0.30g; 0.23 mmols) dissolved in 1,4-dioxan (previously dried over LiAlH₄ ;10 cm³), HBr/acetic acid (0.6cm³; 2.20 mmols) and acetic anhydride (0.1cm³) were added and the solution stirred at room temperature for two hours. The reaction procedure for the preparation of 1-bromoglucose tetra(phenylcarbamate) was then repeated to produce a fine orange solid. Crude yield 0.28g. ¹H n.m.r. δ (DMSO d₆) 9.90-9.76(m) 4HN-H; 7.66(dJH₁₋₂ 8.4Hz)1H₁; 5.32 (t, JH₃₋₄;2-3 8.4Hz) 1H₃; 5.0(m) 2H H₂ and H₄; 4.2(m) 5H H₅ and H_{6a'b'}. C-OH₁.

This procedure was repeated for the generation of 1-bromomaltotriose deca(phenylcarbamate) Crude yield 0.29g. ¹H n.m.r. δ (DMSO d₆) 9.90-9.76(m) 10HN-H; 7.66(dJH₁₋₂ 8.4Hz)1H₁; 5.73 (m) 2H_{1'1''}; 5.53 (m) 3H_{3,3'3''}; 5.13-4.10(m) 17H_{2,2'2''} H_{4,4'4''} H_{5,5'5''} and H_{6ab} 6a'b'6a''b'', C-OH₁

6.8.8 Reaction of Bromo Oligosaccharides with Potassium Isothiocyanate

A mixture of potassium thiocyanate (0.2g, 2 mmols), tetrabutylammonium bromide (1 mmol), and molecular sieve (type 4A, 1.5g) in anhydrous acetonitrile (50cm³) was stirred at room temperature for 3 hours. Then, the sugar halide (1 mmol) was added and the mixture refluxed for 5 hours, monitored by TLC. There was no observed change. Work up by filtration and evaporation to dryness under reduced pressure afforded a residue, which gave no indication of isothiocyanate formation when analysed by i.r.

6.9 Generation of Cello- and Malto-Oligosaccharides

6.9.1 Acid Hydrolysis of Cellulose

Cellulose (powder or Whatman filter paper, 1.5g) was dissolved by stirring with hydrochloric acid (10cm³ specific gravity 1.19) at -20°C. The resulting clear viscous solution was warmed to room temperature and allowed to stand for 2 hours. After this time, the mixture was poured into water (100cm³) at 0°C and brought to pH 2-3 by the addition of sodium hydrogen carbonate (21g). The gelatinous material which separated was removed by suction filtration. The final filtrate which had a pH of 4-5 was analysed by TLC on Kieselgel(G) plates eluted with propan-2-ol/H₂O/ethyl acetate 1:2:1 v/v/v. The plates were then developed by spraying with 0.5% potassium permanganate dissolved in 1 molar sodium

hydroxide, and heated at 100°C for 1-2 minutes to reveal yellow spots on a purple background. The reaction mixture was compared with oligosaccharide standards purchased from Sigma.

OLIGOSACCHARIDE	Exp Rf value	std Rf value
Glucose	0.49	0.49
Cellobiose	0.38	0.40
Cellotriose	0.26(trace)	0.26
Cellotetraose	0.16(trace)	0.18
Cellopentaose		0.10

Table 32 Rf values for the separated oligosaccharides

6.9.2 Separation of the Malto-oligosaccharide series by HPLC

The optimum chromatographic parameters, stated below, were used for these determinations.

6.9.2.1 Analytical HPLC

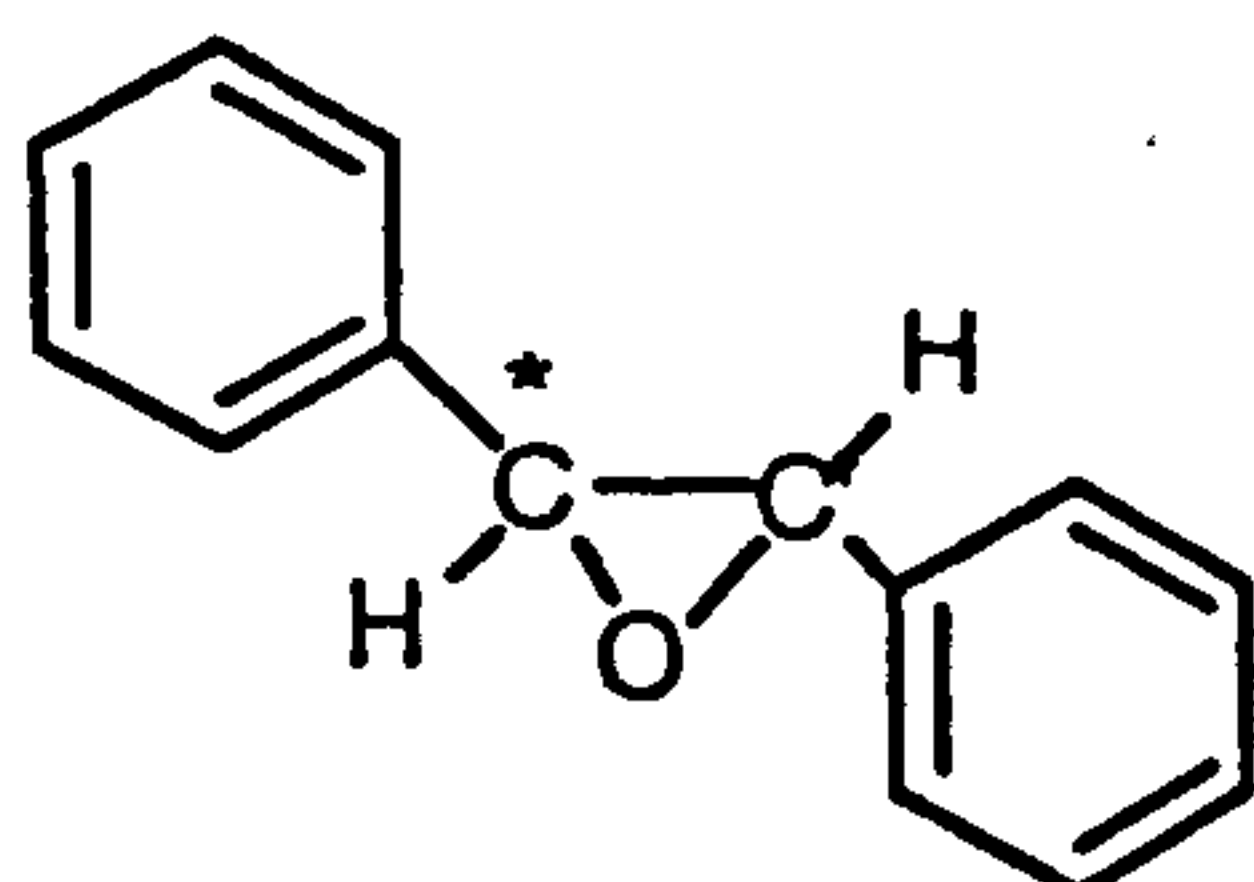
Column	:	APS Nucleosil(25cm x 0.46 i.d.)7µm pore size 100Å.
Mobile phase	:	Acetonitrile (far uv)/water 55:45
Flow rate	:	1.0cm ³ min ⁻¹
Injection volume	:	20µl,
Temperature	:	20°C
Sample	:	Malto-oligosaccharide mixture
Detection wavelength	:	190nm
Number of theoretical plates:		4056

6.9.2.2 Preparative HPLC

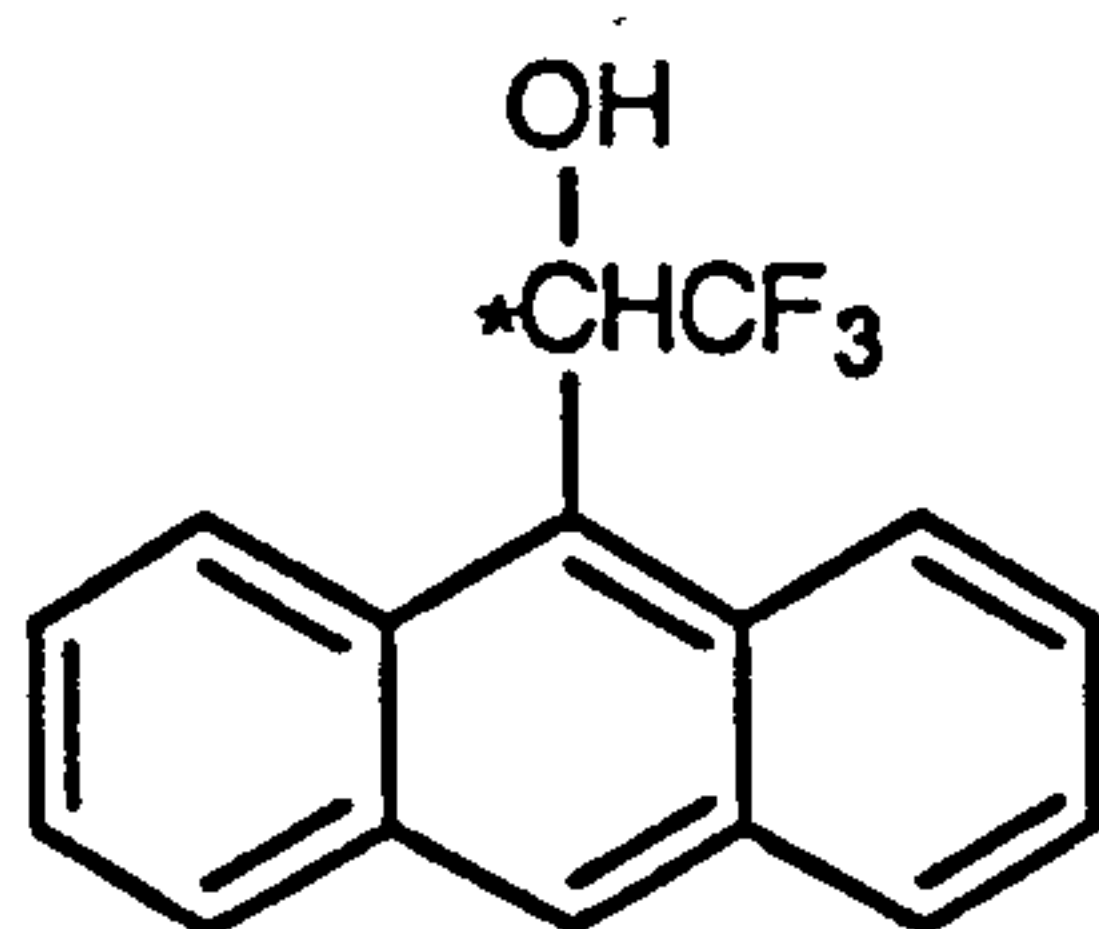
Column	:	APS Nucleosil(30 inch x 1 inch i.d.) 7μm, pore size 100Å.
Mobile phase	:	Acetonitrile (far uv)/water
Flow rate	:	15.0cm ³ min ⁻¹
Injection volume	:	2cm ³
Temperature	:	20°C
Sample	:	Malto-oligosaccharide mixture (350mg)
Detection wavelength	:	190nm
Number of theoretical plates:		3880

APPENDIX

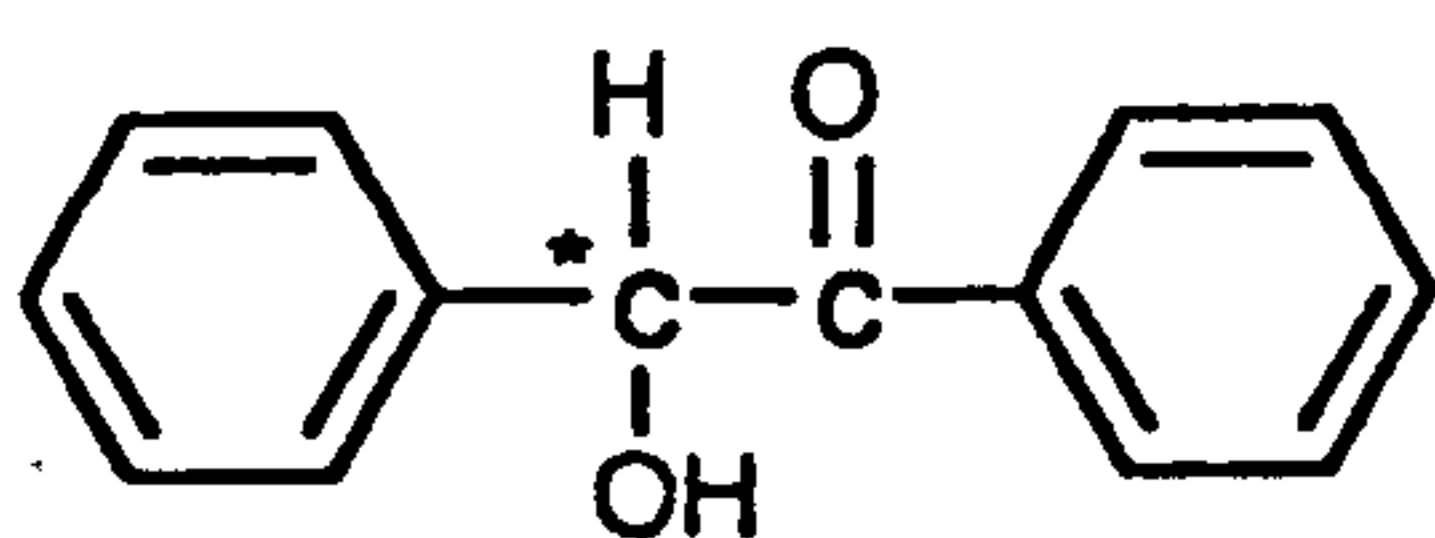
Structures of test solutes:-



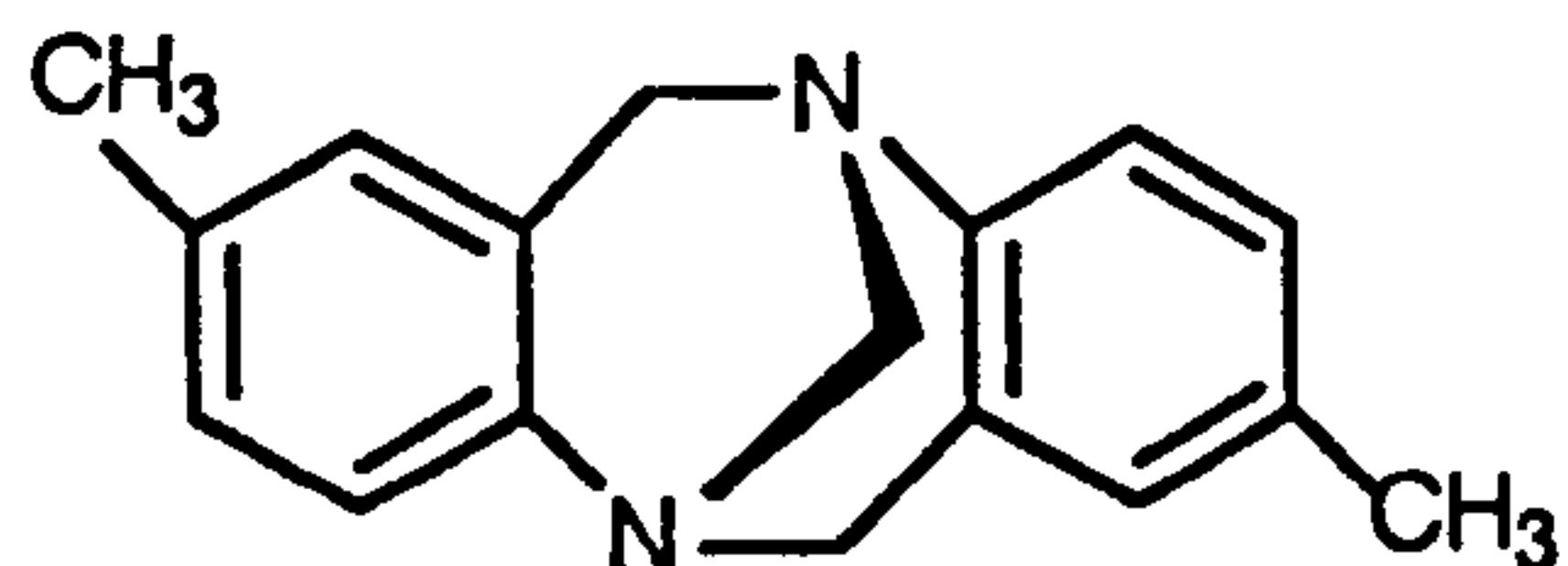
trans- Stilbene Oxide
(*trans*-1,2-Diphenyloxirane)



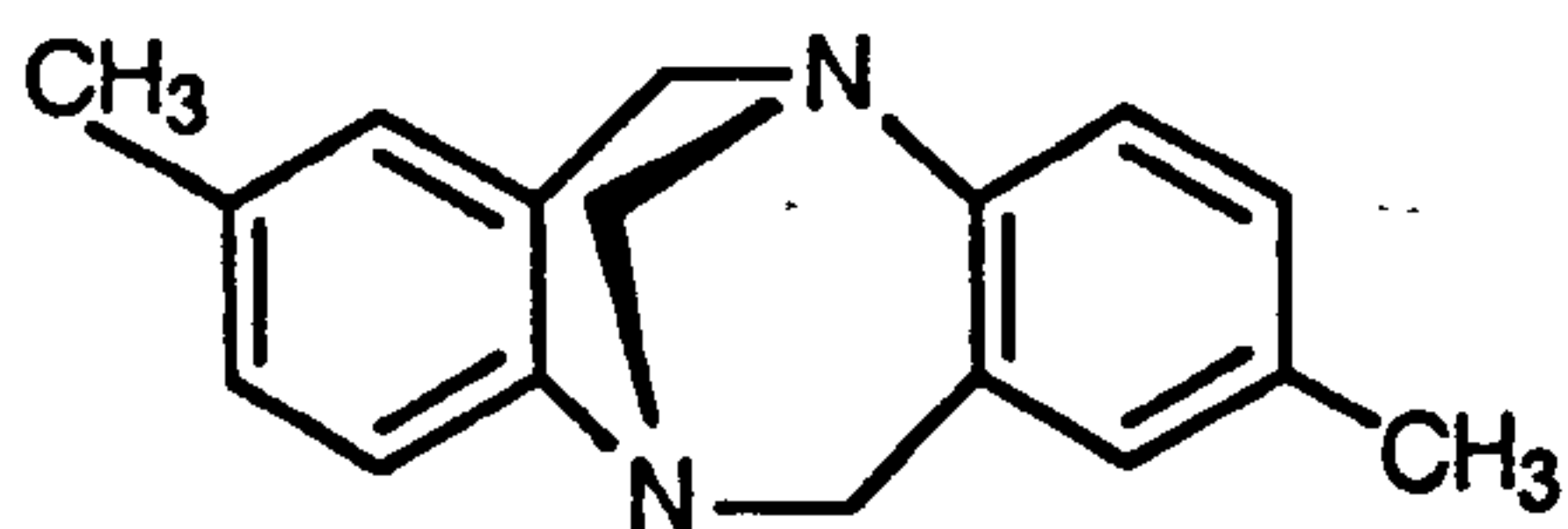
2,2,2,-Trifluoro-1-(9-anthryl)ethanol



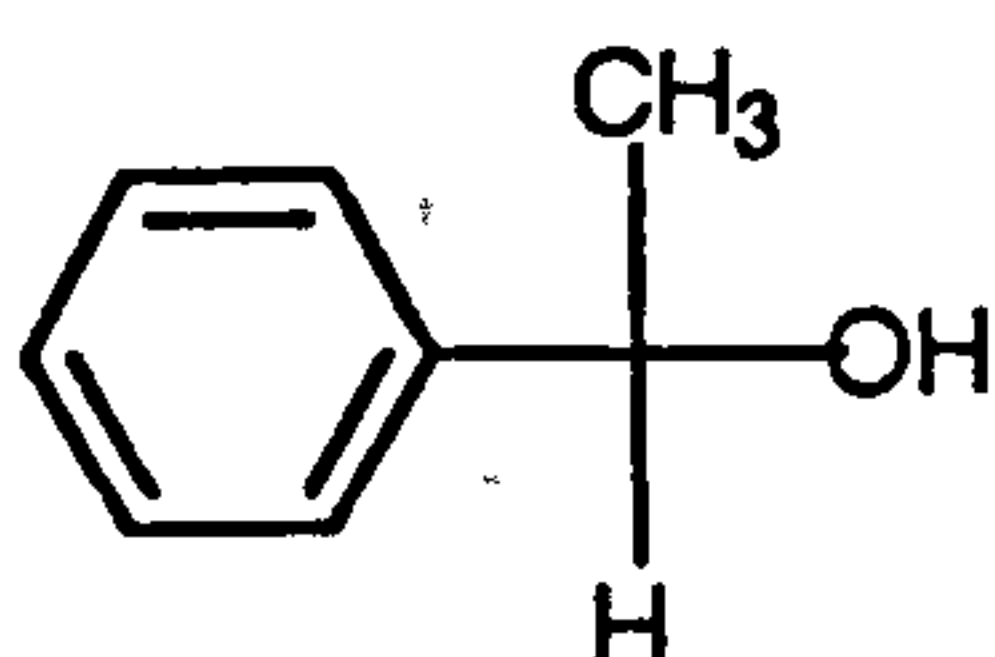
Benzoin
(2-Hydroxy-2-phenylacetophenone)



Trogers Base
(5*S*,11*S*)-(-)-2,8-Dimethyl-6*H*, 12*H*-5,
11-Methanodibenzo[*b,f*][1,5]diazocin



(5*R*,11*R*)-(+)-2,8-Dimethyl-6*H*, 12*H*-5,
11-Methanodibenzo[*b,f*][1,5]diazocin



1-Phenylethanol

where * denotes chiral center

REFERENCES

- (1) M. Tswett, *Trav. Soc. Nat. Warsovic.*, 1903, 14.
- (2) R. Kuhn, A. Winterstien and E. Lederer, *Z. Physico. Chem.*, 1931, 197, 141.
- (3) A.J.P. Martin and R.L. Synge, *J. Biol. Chem.*, 1941, 35, 1358,
- (4) D. de Vault, *J. Amer. Chem. Soc.*, 1943, 65, 532.
- (5) A.J.P. Martin, *Biochem. Soc. Symp.*, 1949, 3, 4.
- (6) A.T. James and A.J.P. Martin, *Biochem. Soc. Symp.*, 1954, 10, 170.
- (7) A.L. Le Rosen, P.H. Monaghan, C.A. Rivet and E.D. Smith, *Anal. Chem.*, 1951, 23, 730.
- (8) G.J. Pierolli, *J. Amer. Chem. Soc.*, 1950, 78, 2989.
- (9) L. Lapidus and N.R. Amundson, *J. Phys. Chem.*, 1952, 50, 984.
- (10) A.T. James and A.J.P. Martin, *J. Bio. Chem.*, 1952, 50, 679.
- (11) J.J. van Deemter, I.J. Zinderweg and A. Klinbenberg, *Chem. Eng. Sci.*, 1956, 5, 271.
- (12) J.C. Giddings, "Dynamics of Chromatography," Marcel Dekker, New York, Part 1, (1965).
- (13) J.J. Kirkland and L.R. Snyder, "Introduction to Modern Liquid Chromatography," A. Wiley-Interscience Publication, John Wiley and Sons Ltd, USA. 2nd edition, (1979).
- (14) K. Unger, *Ber. Bunsenges. Phys. Chem.*, 1975, 79, 739.
- (15) K.S.W. Sing, S. Modry and M. Svata, ed. Proceedings Of The IUPAC International Sym. on Pore Structure and Properties of Materials, vol.111, Academia, Prague. 1974, 13-15.
- (16) M.M. Dubinin, *J. Collid. Interface. Sci.*, 1967, 23, 487.
- (17) J.F.K. Huber, *Ber. Bunsenges. Phys. Chem.*, 1973, 77, 179.
- (18) J. Kirkland, *J. Chromatogr. Sci.*; 1973, 88, 10.

- (19) R.E. Majors, *Anal.Chem*, 1972, 44, 1722.
- (20) J.J. Kirkland, *J. Chromatogr.*, 1973, 83, 149.
- (21) R.E. Majors, *J.Chromatogr. Sci.*, 1973, 11, 88.
- (22) C. Rossi, S. Munari, C. Cengariand and G.T. Teaiddo, *Chim.Ind. (Milano)*; 1960, 42, 724.
- (23) I. Halasz and I. Sebastian, *Angew. Chem. Int. Ed.*, 1969, 8, 453.
- (24) E.W. Abel, G.D. Nickless, F.W. Pollard and P.C. Uden, *J. Chromatogr.*, 1966, 22, 23.
- (25) K.K. Unger, *Angew. Chem. Int. ed.*, 1972, 11, 267.
- (26) A.D Jones, I.W. Burns. S.G. Sellings and J.A. Cox, *J.Chromatogr.*, 1977, 144, 1969.
- (27) D.C. Locke, J.T. Schmermund and B. Banner, *Anal. Chem.*, 1972, 44, 90.
- (28) D.K. Gilpin, P.J. Carnillo and C.A. Janicki, *J.Chromatogr.*, 1978, 121, 13.
- (29) J. Schulze and W.A. Konig, *J. Chromatogr.*, 1986, 335, 165.
- (30) K.K. Unger, N. Becker and P. Roumeliotis, *J.Chromatogr.*, 1976, 125, 115.
- (31) K. Karch, I. Sebastian and I. Halazs, *J.Chromatogr.*, 1976, 122, 3.
- (32) K. Karch, Thesis, Univ. of Saarbrucken, (1974).
- (33) G.E. Berendsen and L.de Galan, *J. Liq. Chromatogr.*, 1978, 1, 5611.
- (34) H. Hemetsberger, M. Kellerman and H. Rickens, *Chromatographia.*, 1977, 10, 726.
- (35) J.L.M .van de Venne, J.P.M. Rindt, G.J.M.M. Coenen and C.A.M.G. Crammers, *Chromatographia.*, 1980, 13, 1.
- (36) J.J. van Deemter, I.J. Zinderweg and A. Kunkenburg, *Chem. Eng. Sci.*, 1956, 5, 271.

- (37) C. Howarth and H.J.Lin, *J. Chromatogr.*, 1977, 149, 43.
- (38) J.H. Knox, *J.Chromatogr.*, 1977, 15, 352.
- (39) L. Pasteur. "Memoire sur la relation qui pent exister entre la forme chrystaline et la composition chimique, et sur la cause de la polarisation rotatorie," competes rendues de l'Academic des Sciences, 1884, 26, 535.
- (40). E. Drayer, *Clin. Pharmacol. Theor.*, 1986, 40, 125.
- (41) E.J. Ariens, *Eur. J. Clin. Pharmacol.*, 1984, 26, 663.
- (42) G. Blaschke, H.P. Kraft, K. Flckentscher and F. Kohler, *Arzneim-Forsch.*, 1979, 29; 1640.
- (43) P.H. Boyle, *Chem. Soc. (London) Q. Rev.*, 1971, 25, 323.
- (44) U. Eriksson, Drug Level Monitoring, ed. E.T.Linn and W.Sadee, Wiley, England, Chichester, 1986, vol 2.
- (45) A.C. Menta, *J. Chromatogr.*, 1988, 426, 1.
- (46) L.H. Eassen, L.E Stedman. *J. Biochem.*, 1933, 27, 1257.
- (47) C. Dent, *J. Biochem.*, 1948, 43, 169.
- (48) M. Kotake, T. Salkan, N. Nakamura and S. Senoh, *J. Amer. Chem. Soc.*, 1951, 73, 2973.
- (49) C.E. Dalgleish, *J. Biochem.*, 1952, 52, 3.
- (50) C.E. Dalgleish, *J. Chem. Soc.*, 1952, 3940.
- (51) W.H. Pirkle and TC Pochapsky, *Chem Review.*, 1989, 89; 347.
- (52) S. Yuasa and A. Shimada, *Sci. Rep. Coll. Gen. Educ., Osaka Univ.*, 1982, 1331(1/2), 13.
- (53) The hydrolysis of natural cellulose with an aqueous mineral acid dissolves the amorphous region of the cellulose to result in powdered cellulose with a so called level degree of polymerization (ca 200) and a higher crystallinity. A Batti. Microcrystalline Polymer Science, McGraw-Hill, New York, NY 1975.
- (54) G. Hesse, R. Hagel, *Chromatographia.*, 1973, 6, 277.

- (55) R. Hesse, R. Hagel, *Chromatographia*., 1976, 9, 62.
- (56) H. Scherubal, U. Fritzsche and A. Mannschreck, *Chem. Ber.* 1984, 117, 336.
- (57) A. Mannschreck, A. Talvitie, W. Fischer and G. Snatzke, *Monatshefte fur Chemie*., 1983, 114, 101.
- (58) H. Kroller, K H. Rimbock and A. Mannschreck, *J. Chromatogr.*, 1983, 282, 89.
- (59) I. Shibata, H. Nakamura, Y. Uka and I. Okamoto, JPM. PAT. 59, 166501.
- (60) I. Shibata, H. Nakamura, I. Okamoto and H. Namikoshi, 49th National Meeting of the Chemical Soc. of Japan. Tokyo, April 1984 abstr. no 2M42, 2M43.
- (61) I. Shibata, I. Okamoto and K. Ishii, *J Liq Chromatogr.*, 1986, 9 (2 & 3), 313-340.
- (62) Y. Okamoto, S. Honda, I. Okamoto, H. Yuki, S. Murata and R. Noyroi, *J. Amer. Chem. Soc.*, 1981, 103, 6971.
- (63) A.M. Rizzi, *J. Chromatogr.*, 1990, 513, 195.
- (64) Y. Okamoto, M. Kawashima, R. Aburatani, K. Hatada, T. Nishiyama and M. Masuda, *Chem. Lett.* 1986, 1237.
- (65) A. Ichida, T. Shibata, I. Okamoto, Y. Yuki, H. Namikoshi and Y. Toga, *Chromatographia*, 1984, 19, 280.
- (66) S. Hakata, H. Namikoshi, H. Namamura, I. Okamoto, A. Ichida, Y. Yuki, K. Shimizu and Y. Toga, *Polymer preprints*, Japan, 1984, 33, 1599.
- (68) Y. Okamoto, M. Kawashima and K. Hatada. *Polymer preprints Japan*, 1984, 33, 596.
- (69) Y. Okamoto, M. Kawashima and K. Hatada. *Polymer preprints Japan*, 1984, 33, 1607.

- (70) Y. Okamoto, M. Kawashima and K. Hatada, *Chem. Lett.*, 1984, 739.
- (71) Y. Yuki, A. Ichida, I. Okamoto, H. Namikoshi, T. Shibata, H. Nakamura and Y. Toga, *Polymer Preprints, Japan*, 1983, 32, 1006.
- (72) Y. Okamoto, K. Hatano, R. Aburanti and K. Hatada, *Chem Lett*, 1989, 715.
- (73) Y. Okamoto, M. Kawashima and K. Hatada, *J. Amer. Chem. Soc.* 1984, 106, 5357.
- (74) T. Shabita, I. Okamoto, H. Namikoshi, Y. Toga and K. Shimizu. 50th National Meeting of the Chemical Society of Japan, Tokyo, April 1985, abstr no 4Z08.
- (75) T. Shabita, H. Namikoshi, H. Nakamura, I. Okamoto and K. Shimizu. The 1984 International Chemical Congress of Pacific Basin Societies, Honolulu, Hawaii, December 1984, Abstr no 09P35.
- (76) T. Shibata, H. Namikoshi, H. Nakamura, I. Okamoto, A. Ichida, Y Yuki, K. Shimizu and Y. Toga. *Polymer Preprints, Japan*, 1984, 33, 1599.
- (77) T. Shabita, H. Namikoshi, H. Nakamura, I. Okamoto, A. Ichida, Y. Yuki, K. Shimizu and Y. Toga. 7th Japanese Carb Symp., Osaka, August 1984, abstr P62.
- (78) Y. Okamoto, M. Kawashima and K. Hatada, *J. Chromatogr.*, 1986, 363, 173.
- (79) H. Ogoshi, K. Saita, K. Sakurai, T. Wataneba, H. Toi, Y. Aoyama and Y. Okamoto, *Tetrahedron Lett.*, 1986, 27, 6365.
- (80) Y. Okamoto, R. Aburantani, S. Miura and K. Hatada, *J Liq Chromatogr.*, 1987, 10, 1613.
- (81) K. Ikeda, T. Hamasaki, H. Kohno, T. Ogawa, T. Matsumoto and J. Sakai, *Chem Letts*, 1989, 1089,

- (82) H. Tessmer, *Ber*, 1885, 18, 968.
- (83) W.H. Heron, G.G.D Hiatt and C.R. Fordyce, *J. Amer. Chem.Soc.*, 1943, 65, 829.
- (84) P. Schrieibli, *Compt.Rend.*, 1952, 234, 734.
- (85) J.W. Baker, J.B. Holdsworth, *J. Chem. Soc.* 1947, 713.
- (86) L. Salem, X. Chapuisat, G. Segal, D.C. Hiberty, C. Minot, C. Leforrestier and P. Sautet, *J. Amer. Chem. Soc.*, 1987, 109, 2887.
- (87) W.H. Pirkle, M. Hyun, A. Tsipouras, B.C. Hamper and L.B. Banks, *J.Pharm. and Biomed. Anal.*, 1984, 2, 173.
- (88) R.E. Boelum, D.E. Martine and D. Armstrong. *Anal.Chem*, 1988, 60, 522.
- (89) H. Billiger and G. Keilich, *Biopolymers*, 1959, 7, 539.
- (90) A.K. Gupta, W. Barchard and E. Marchal, *Macromolecules*, 1975, 8, 843.
- (91) U. Voget and P. Zugenmaier, *Makromol. Chem. Rapid. Commun*; 1983, 4, 759.
- (92) Y. Okamoto, R. Aburatani, Y. Kaida, K. Hatada, N. Inotsume and M. Nakamo, *Chirality.*, 1989, 1, 239.
- (93) G Dotsevi, Y Sogah and D J Cram, *J. Amer. Chem. Soc.*, 1975, 97, 1259.
- (94) D.M. Vdvarhelyi, D.C. Sunter and J.C. Watkins, *J.Chromatogr.* 1990, 519, 69.
- (95) W.L. Hinze, Separation and Purification Methods, C.J. van Oss. (ed), Marcel Dekker, New York, 1981, 10, 151.
- (96) D.M. Armstrong, S.F. Yang, S.M. Han and R. Menges, *Anal.Chem.* 1987, 59; 2594.
- (97) W.L. Hinz, T.E. Richl, D.W. Armstrong, A. Alak and T.J. Ward, *Anal. Chem.* 1985, 57, 237.
- (98) C.A. Chaug, H. Ji and G. Lin, *J. Chromatogr.*, 1990, 522, 142.

- (99) W.H. Pirkle and T.C. Pochapsky, *J. Amer. Chem. Soc.*, 1986, 108, 352.
- (100) W.H. Pirkle and D.L.S Kenga, *J. Org. Chem.*, 1975, 40, 3430.
- (101) W.H. Pirkle and D W House, *J. Org. Chem.*, 1979, 44 1957.
- (102) W.H. Pirkle and R. Dappen, *J. Chromatogr.*, 1987, 404,107.
- (103) P. Macaudiere, M. Lienne, A. Tambute and M. Caude, Chiral separations by HPLC. Application to Pharmaceutical Compounds, Ellis Horwood, England, Chichester, 1989 Chapter 14.
- (104) W. Wainer and M.C. Alembik, *J Chromatogr.*, 1986, 367, 59.
- (105) W.H Pirkle, M.H. Hyun, A. Tsipouras, B.C. Hamper and B. Bank, *J. Pharm. and Biomed. Anal.*, 1984, 2(2), 173.
- (106) W.H. Pirkle, M.H. Hyun and B. Bank, *J. Chromatogr.*, 1984, 316, 585.
- (107) W.H. Pirkle and T.C. Pochapsky, *J .Amer. Chem. Soc.*, 1987, 109, 5975.
- (108) K.P. Lipokowitz, D.A. Demeter, C.A. Parish and T. Darden, *J.Comput. Chem.*, 1987, 8(6), 753.
- (109) N.Oi, M.Nagase, Y. Inda and T. Doi, *J. Chromatogr.*, 1983, 265, 111.
- (110) K.B. Lipkowitz, D. Demeter, R. Zegarra, R. Larter and T. Darden, *J.Amer. Chem. Soc.*, 1988, 110, 3346.
- (111) D.R. Taylor, D. Stevenson and I. Wilson, ed, Recent Advances in Chiral Separations. Plenum Press, New York, 1991, 5-14.
- (112) K.B. Lipkowitz, D. Demeter, R. Zegarra, R. Larter and T. Darden, *J. Comp. Chem.*, 1987, 8 (6), 753.
- (113) A. Tambute, S. Begos, M. Lienne, P. Macaudiere, M. Caude and R. Rosset, *New. J. Chem.*, 1989, 13, 625.
- (114) M. Lienne, P. Macaudiene, M. Caude, R. Rosset, *Chirality*; 1989, 1, 45.

- (115) A. Tambute, S. Begos, M. Lienne, P. Macaudiere, M. Caude and R. Rosset, *J. Chromatogr.*, 1989, 467, 357.
- (116) F. Gasparrini, D. Misiti, and C. Villani. *J. High. Res. Chrom.*, 1990, 13, 182.
- (117) W. Linder, G. Uray and U. Stiener, *J. Chromatogr.*, 1990, 553, 373.
- (118) A. Tambute, A. Begos, M. Lienne. M. Caude. and R. Rosset, *J. Chromatogr.*, 1987, 396, 65.
- (119) A. Tambute, M. Lienne. M. Caude. and R. Rosset. International Conf. On Chiral Separation. England, Guilford, 1987, Sept. 3-4th.
- (120) N.Oi. *Bunseki. Kayaku.*, 1984, 33, E401.
- (121) N.Oi and H. Kitihara, *J. Chromatogr.*, 1983, 265, 117.
- (122) W.H. Pirkle and R. Dappen, *J. Chromatogr.*, 1987, 404, 107.
- (123) W.H. Pirkle and T.J. Sowin. *J. Chromatogr.*, 1987, 396, 83.
- (124) W.H. Pirkle, 3rd International Conf. On Chiral Discrim. Germany, Tubingen, 1992, Oct 5-8th.
- (125) A. Gil Av, F. Mikes and G. Boshart. *J. Chromatogr.*, 1976, 122, 205.
- (126) F. Mikes, G.B. Bosnart and E. Gil Av, *J. Chem. Soc. Chem. Comm.*, 1976, 77, 99.
- (127) W.J.C. Prinsen and W.H. Laarhoven, *J. Chromatogr.*, 1987, 393, 3420.
- (128) F. Mikes and G. Boshart, *J. Chem. Soc. Chem. Comm.*, 1978, 173.
- (129) F. Mikes and G. Boshart, *J. Chromatogr.*, 1978, 149, 455.
- (130) S.A. Matlin, A. Tito-Lloret, W.J. Lough, D.G. Bryan, T. Browne and S. Mehani, *J. High Res. Chromatogr. Chromatogr. Commun.*, 1981, 4, 81.

- (131) C.H. Lochmuller and R.R. Ryall, *J.Chromatogr.*, 1978, 150, 511.
- (132) Y.H. Kim, A. Tishbee and E. Gil-Av, *J. Amer. Chem. Soc.*, 1980, 102, 5915.
- (133) S.A. Matlin, W.J. Lough and V.E. Stacey, *J.Chromatogr.*, 1988, 450, 157.
- (134) V.A. Davankov and S.V. Rogozhin, *J. Chromatogr.*, 1971, 60, 280.
- (135) G. Gubitz, W. Jellehz and W. Santi, *J.Chromatogr.*, 1981, 203, 377.
- (136) B. Feibush, M.J. Cohen and B.L. Karger. *J. Chromatogr.*, 1983, 282, 3.
- (137) L.R. Gelber, B.L. Karger, J.L. Neumeyer and B. Feibush, *J.Amer. Chem. Soc.*, 1984, 106, 7729.
- (138) Y. Okamoto, E. Yashima, T. Nakano and K. Hatada, *Chem. Lett.* 1987, 759.
- (139) Y. Okamoto, K. Suzuki, K. Ohta, N. Yuki and K. Hatada. *J. Amer.Chem. Soc.*, 1979, 101, 4769.
- (140) Y. Okamoto, H. Shobi and H. Yuki, *J. Polym. Sci. Polym. Lett.*, 1983, 21, 601.
- (141) Y. Okamoto and K. Hatada, *J.Liq.Chromatogr.*, 1986, 9, 369.
- (142) M.Yuki, Y. Okamoto and I. Okamoto, *J.Amer.Chem.Soc.*, 1980, 102, 6356.
- (143) Y. Okamoto, I. Okamoto, A. Yuki, S. Murata, R. Noyori and H. Takaya, *J.Amer.Chem.Soc.*, 1981, 103, 6971.
- (144) G. Schomburg, *LC-GC.*, 1988, 6, 37-40.
- (145) M.S. Allen, *Chem. Scr.*, 1982, 20, 5.
- (146) S. Allenmark, B. Bomgren, H. Boren., *J.Chromatogr.*, 1983, 264, 63.

- (147) J. Hermansson and M. Eriksson, *J. Liq. Chromatogr.*, 1986, 9, 621.
- (148) R.H. Memenany, Albumin structure function and uses. Rosenoer, U.N. Oratz and W.A. Rothschild, (ed) Pergamon Press, Oxford, 1977, 143.
- (149) Jr. Th. Peters, The plasma proteins, F.W. Putman (ed) Academic Press, New York, 1975, 1, 133.
- (150) A.M. Krstulovic and J. Lvende, *Chirality*, 1989, 1, 243-245.
- (151) K.K. Stewart and R.F. Doherty, *Proc. Natt. Acad. Sci.*, 1973, 70, 2850.
- (152) S. Allenmark, *J. Liq. Chromatogr.*, 1986, 9, 425.
- (153) A.P. Erlandson, L. Hansson and R. Isakkson, *J. Chromatogr.*, 1986, 370, 475.
- (154) B.T.B. Hsu, P.A. Shan and L.B. Rogers, *J. Chromatogr.*, 1987, 391, 145.
- (155) L.M. Aubel and L.B. Rogers, *J. Chromatogr.*, 1987, 392, 415.
- (156) Y.Q. Chu and I.W. Wainer, *Pharm. Res.*, 1988, 5, 680.
- (157) H. Lehr and P. Damm, *J. Chromatogr.*, 1980, 425, 153.
- (158) I. Wainer and R.M. Stiffen, *J. Chromatogr.*, 1990, 532, 227.
- (159) J. Hermansson, *J. Chromatogr.*, 1984, 336, 321.
- (160) J. Hermansson, J.Eur. Pat. App. No.84850169.8, Pubh.No. EPO 128886 A2.
- (161) E.D.J. Lee, S.B. Ang and T.L. Lee, *J. Chromatogr.*, 1988, 474, 257.
- (162) Y.K. Tran and S.J. Soldin, *J. Chromatogr.*, 1987, 422, 187.
- (163) G. Schill, I.W. Wainer and S. Barkan, *J. Chromatogr.*, 1986, 365, 73.
- (164) R.I. Whistler, Methods in Carbohydrate Chemistry. Academic Press, London, 1963, Vol 3, 8.

- (165) J.M. Sugihara and M.L. Wolfrom, *J. Amer. Chem. Soc.*, 1949, 71, 3357.
- (166) R.L. Whistler and J.L. Hickson, *Anal.Chem.*, 1955, 27, 1514.
- (167) M.L. Wolfrom, J.Y. Tyree, T.T. Galkowski and A.N. O'Neill, *J. Amer. Chem. Soc.*, 1951, 73, 4927.
- (168) W.J. Whelan, J.M. Bailey and P.J.P. Roberts, *J. Amer. Chem. Soc.*, 1953, 1, 293.
- (169) J.H. Pazur, *J. Biol. Chem.*, 1953, 205, 75.
- (170) H.W. Hagens. *J. Chromatogr.*, 1971, 61,169.
- (171) C. Nash A. Huber, H.D. Schbell, H. Tai, and E.E. Fischer, *Cereal Chem.*, 1966, 43, 342.
- (172) J.A. Thoma,"Starch Chemistry and Technology", R.L.Whistler and E.F.Paschall, eds, Academic Press, New York, 1965, vol1, 195.
- (173) D. French, J.L. Mancusi, M. Abdullah and G. Brammer, *J.Chromatogr*, 1965, 19, 445.
- (174) J.A. Thoma, H.B. Wright and D. French, *Arch Biochem. Biophysics.*, 1959, 85, 452.
- (175) D. French, J.F. Robyt, M. Weintraub and P. Knock, *J.Chromatogr.*, 1966, 24, 68.
- (176) H. Konodo, H. Natatani and K. Hiromi, *Agric. Biol. Chem.*, 1981, 45, 2369.
- (177) H.R. Sloan. B. Kerzner and C. Seckel, *J. Biochem.*, 1984, 14, 245.
- (178) R. Schwarzenbach, *J.Chromatgr*, 1976, 117, 206.
- (179) V.Kahle and K. Tesarik, *J.Chromatgr*,1980, 191, 121.
- (180) K. Kainuma, T. Nakakuki and T. Ogawa, *J.Chromatogr.*, 1981, 212, 126.
- (181) N.W.H. Cheetham, P. Sirimanne and W.R. Day, *J.Chromatogr*, 1981, 208, 439.

- (182) L.A.Th. Verhaar. B.F.M. Kuster and H.A. Classens, *J.Chromatogr*, 1984, 284, 1.
- (183) L.E. Fitt, W. Hassler and D.E. Just, *J.Chromatogr*, 1980, 187, 439.
- (184) H.D. Schobell and K.M. Brobst, *J.Chromatogr*, 1981, 212, 51.
- (185) J.J. Warthesen, *Cearal Chem.*, 1984, 61, 194.
- (186) N.W.H. Cheetham and P. Sirimanne, *Carbohydr. Res*, 1981, 96, 126.
- (187) W. Moody, G.N. Richards, N.W.H. Cheeetham and P. Sirimanne, *J. Carbohyr. Chem.*, 1983, 114, 306.
- (188) K.B. Hicks and S.M. Sondey, *J.Chromatogr.*, 1987, 389, 183.
- (189) G.N Ramachandran, C. Ramakrishnan and V. Sasisekharan, *Aspects of Protein Structure*, G.Nasabore (eds), Academic Press, New York 1963, 121.
- (190) H. Paulsen, *Chem. Soc.Quart Rev.*, 1984, 13, 15.
- (191) H. Paulsen, *Angew Chem. In. Ed. Engl.*, 1982, 21, 155.
- (192) R.U. Lemieux, K.B. Hendricks, R.V. Sticks and K. James, *J. Amer. Chem. Soc.*, 1975, 97, 4056.
- (193) H. Paulsen and C. Kolar, *Chem. Ber.*, 1981, 114, 306.
- (194) H. Ogura, H. Takahashi, K. Takeda, M. Sakaguchi, N. Nimura and M. Sakai, *Heterocycles*, 1975, 3, 1129.
- (195) E.L. Wagner, *J. Chem. Phys.*, 1965, 43, 2728.
- (196) E. Fischer, *Ber*, 1914, 47, 1377.
- (197) W.J.Le Noble, *Synthesis*, 1970, 1-6.
- (198) A. Fara, A. Illicete and S. Bresadila, *J. Amer. Chem. Soc.*, 1965, 87, 4790.
- (199) G.L. Caldow and H.W. Thompson, *Spectrochim Acta.*, 1958, 13, 212-215, and E. Lieber, D.N.R. Rao and J. Ramachandran, *ibid*, 296-299.

- (200) A. Mathais, *Tetrahedron*, 1965, 21, 1073.
- (201) A. Muller and A. Wilhelms, *Ber.*, 1941, 74, 698.
- (202) R.J. Ferrier and N. Vethariyasar, *Chem. Commun.*, 1970, 1385.
- (203) R.J. Ferrier and N. Vethariyasar, *J. Chem. Soc. C.*, 1971, 1907.
- (204) R.D. Guthrie and G.J. Williams, *Chem. Commun.*, 1971, 923.
- (205) R.D. Guthrie and G.J. Williams, *J. Chem. Soc. Perkin Trans.*, 1972, 1, 2619.
- (206) M. Renson, *Bull. Soc. R. Sci. Liege.*, 1960, 78. Chem. Abstr; 55, 9253f,(1961).
- (207) F. Mecheel and W. Lengsfeld, *Chem. Ber.*, 1956, 89, 1246.
- (208) U. Tonellato O. Rosseto and A. Fara, *J. Org. Chem.*, 1969, 34, 4032.
- (209) A. Fara, A. Illiceto, A. Ceccon and P. Koch, *J. Amer. Chem Soc.*, 1965, 87, 1045.
- (210) U. Billeter, *Helv. Chim. Acta.*, 1925, 8, 337.
- (211) O. Mumm and M. Richter, *Ber.*, 1940, 73, 843.
- (212) P.A.S. Smith and D.W. Emerson, *J. Amer. Chem. Soc.*, 1960, 82, 3076
- (213) F. Michael and W. Lengsfeld, *Chem. Ber.*, 1956, 89, 1246,.
- (214) E. Fischer, B. Helfrich and P. Ostmann, *Ber.*, 1920, 53, 878.
- (215) F.P. van de Kamp and F. Michael, 1956, 89, 133.
- (216) F. Michael, H. Peterson and H. Kochling, *Chem. Ber.*, 1960, 93, 1.
- (217) H. Ogura and H. Takashashi, *Heterocycles*, 1982, 17, 87.
- (218) T.B. Johnson and W. Bergmann, *J. Amer. Chem. Soc.*, 1933, 55, 395.

- (219) V.A. Kulshin, R.G. Macharadze, S.E. Zurabyan, M.L. Shulman and A.Ya Khorlin, USSR.Pat 666,182, (1979); Chem.Abstr, 91, 141,177d, (1979).
- (220) M.J.Canarasa, P. Fernandez-Resa, M.T. Garcia-Lopez, F.G. de las Heras, P.P. Mendez and A. San Felix, *Synthesis*, 1984, 509.
- (221) L. Drobica, P. Kristain, J. Augustin, *The Chemistry of Cyanates and their Derivatives*, S.Patai (ed), John Wiley and Sons, Chichester, 1974, 1014.
- (222) H. Ogura and H. Takashashi, *Heterocycles.*, 1977, 6, 1633.
- (223) H. Ogura and H. Takashashi, *Heterocycles.*, 1977, 8, 125
- (224) H.Ogura, H. Takashashi N. Nimura, *Chem. Pharm. Bull.*, 1979, 27 (5), 1130.
- (225) J. Asshauer and I. Halasz. *Anal Chem.*, 1973, 45. 1142.
- (226) J.H. Knox and D.A. Brown, *Chromatographia*, 1977,10.(6), 279.
- (227) V.R. Meyer, *Practical HPLC* ;John Wiley and sons ,Chichester 1988 p27.
- (228) L.R. Snyder, *Principles of Adsorption Chromatography*, Marcel Decker, New York, 1969.
- (229) H. Engelhardt. *HPLC*, Springer, New York, Heidelberg, Berlin,1979.
- (230) R.K. Gilpin and M.F. Burke, *Anal.Chem.*, 1973, 45, 1383.
- (231) L.R. Snyder and J.W. Ward, *J. Phys. Chem.*, 1966, 70, 3941.
- (232) L.T Zhuravlev and A.V. Kiselev, in D.H.Everett and R.H.Ottewill proceedings of IUPAC Int. Symp on Surface Area Determinations Butterworth, London, 1970, p 155.
- (233) K.K. Unger, *Ang. Chem.Int. Ed.*, 1972, 11, 267.
- (234) K.K. Unger. K. Berg, E. Gallei and G. Erdel, *Fortschr.Kolloide. Polym.*, 1971, 55, 34.

- (235) H. Engelhardt and H. Muller, *J Chromatogr.*, 1981, 218, 395.
- (236) P. Roumetiotis and K.K. Unger. *J. Chromatogr.*, 1978, 149, 221.
- (237) P.E.C. Goissedet, U.S.Patent 1,357,450, 1920, Nov 2.
- (238) W.E. Hearon *J. Amer Chem Soc.*, 1943, 65, 829.
- (239) W. Wainer *J. Chromatogr.*, 1987, 411, 139.
- (240) L.A.T. Verhaar and B.F.M. Kuster, *J. Chromatogr.*, 1982, 234, 57.
- (241) P. Orth and H. Englehardt, *Chromatographia*, 1982, 15 (2). 91
- (242) B.B. Wheals and P.C. White. *J. Chromatogr.*, 1979, 176, 421.
- (243) H.D. Beckey, "Recent Developments in Mass Spectrometry" K.Ogata and T.Hayakawa, eds, Uni. Park Press Baltimore, MD, 1970, 115.
- (244) D.J. Surman and J.C. Vickerman, *J. Chem. Res.*, 1981, 170.
- (245) M. Barber, R.S. Bordoli, R.D. Sedgwick & A.N.Taylor, *J. Chem. Soc. Chem. Comm.*, 1981, 325.
- (246) M. Linscheid, J.D. Angora, A.L. Burlingama, A. Dell & C.E.Ballou, *Proc. Natt. Acad. Sci. USA.*, 1981, 78, 1471.
- (247) T.R. Covey, R.I. Bonner, B.I. Spushan and J. Henion, *Rapid Commun. Mass. Spectrom.*, 1988, 2, 249.
- (248) A. Dell, *Methods in Enzymology*, 193, Chapter 35.
- (249) R. Aburantani, Y. Okamoto and K. Hatada, *Bull. Chem. Soc. Jpn.*, 1990, 63,3606.
- (250) K. Bock, C. Pederson and H. Pederson; *Advances Carb. Chem and Bio Chem.*, 1984, 42, 193.
- (251) G. Wulff and G. Rohle, *Angew. Chem. Internat. Ed.* 1974, 13, 157.
- (252) G.B. Motherwell, J.A. Wilkinson and S. Caddick, *J. Chem. Soc., Chem Commun.*, 1991, 694.